BRIDGE ENGINEERING

Substructure Design

EDITED BY
Wai-Fah Chen
Lian Duan

CRC PRESS

Boca Raton London New York Washington, D.C.

The material in this book was first published in *The Bridge Engineering Handbook,* CRC Press, 2000.

Library of Congress Cataloging-in-Publication Data

Bridge engineering : substructure design / edited by Wai-Fah Chen and Lian Duan.
p. cm.
Includes bibliographical references and index.
ISBN 0-8493-1681-2 (alk. paper)
1. Bridges—Foundations and piers—Design and construction. I. Chen, Wai-Fah, 1936-
II. Duan, Lian.

TG320 .B73 2003
624'.284—dc21 2002041117

International Standard Book Number 0-8493-1681-2
Library of Congress Card Number 2002041117
Printed in the United States of America 1 2 3 4 5 6 7 8 9 0
Printed on acid-free paper

Foreword

Among all engineering subjects, bridge engineering is probably the most difficult on which to compose a handbook because it encompasses various fields of arts and sciences. It not only requires knowledge and experience in bridge design and construction, but often involves social, economic, and political activities. Hence, I wish to congratulate the editors and authors for having conceived this thick volume and devoted the time and energy to complete it in such short order. Not only is it the first handbook of bridge engineering as far as I know, but it contains a wealth of information not previously available to bridge engineers. It embraces almost all facets of bridge engineering except the rudimentary analyses and actual field construction of bridge structures, members, and foundations. Of course, bridge engineering is such an immense subject that engineers will always have to go beyond a handbook for additional information and guidance.

I may be somewhat biased in commenting on the background of the two editors, who both came from China, a country rich in the pioneering and design of ancient bridges and just beginning to catch up with the modern world in the science and technology of bridge engineering. It is particularly to the editors' credit to have convinced and gathered so many internationally recognized bridge engineers to contribute chapters. At the same time, younger engineers have introduced new design and construction techniques into the treatise.

This Handbook is divided into four volumes, namely:

Superstructure Design
Substructure Design
Seismic Design
Construction and Maintenance

There are 67 chapters, beginning with bridge concepts and aesthestics, two areas only recently emphasized by bridge engineers. Some unusual features, such as rehabilitation, retrofit, and maintenance of bridges, are presented in great detail. The section devoted to seismic design includes soil-foundation-structure interaction. Another section describes and compares bridge engineering practices around the world. I am sure that these special areas will be brought up to date as the future of bridge engineering develops.

May I advise each bridge engineer to have a desk copy of this volume with which to survey and examine both the breadth and depth of bridge engineering.

T.Y. Lin
Professor Emeritus, University of California at Berkeley
Chairman, Lin Tung-Yen China, Inc.

Preface

The *Bridge Engineering Handbook* is a unique, comprehensive, and the state-of-the-art reference work and resource book covering the major areas of bridge engineering with the theme "bridge to the 21st century." It has been written with practicing bridge and structural engineers in mind. The ideal readers will be M.S.-level structural and bridge engineers with a need for a single reference source to keep abreast of new developments and the state-of-the-practice, as well as to review standard practices.

The areas of bridge engineering include planning, analysis and design, construction, maintenance, and rehabilitation. To provide engineers a well-organized and user-friendly, easy to follow resource, the Handbook is divided into four volumes: I, Superstructure Design II, Substructure Design III, Seismic Design, and IV, Construction and Maintenance.

Volume II: Substructure Design addresses the various substructure components: bearings, piers and columns, towers, abutments and retaining structures, geotechnical considerations, footing and foundations, vessel collisions, and bridge hydraulics.

The Handbook stresses professional applications and practical solutions. Emphasis has been placed on ready-to-use materials. It contains many formulas and tables that give immediate answers to questions arising from practical work. It describes the basic concepts and assumptions omitting the derivations of formulas and theories. It covers traditional and new, innovative practices. An overview of the structure, organization, and content of the book can be seen by examining the table of contents presented at the beginning of the book while an in-depth view of a particular subject can be seen by examining the individual table of contents preceding each chapter. References at the end of each chapter can be consulted for more detailed studies.

The chapters have been written by many internationally known authors from different countries covering bridge engineering practices and research and development in North America, Europe, and the Pacific Rim. This Handbook may provide a glimpse of a rapid global economy trend in recent years toward international outsourcing of practice and competition in all dimensions of engineering. In general, the Handbook is aimed toward the needs of practicing engineers, but materials may be reorganized to accommodate undergraduate and graduate level bridge courses. The book may also be used as a survey of the practice of bridge engineering around the world.

The authors acknowledge with thanks the comments, suggestions, and recommendations during the development of the Handbook, by Fritz Leonhardt, Professor Emeritus, Stuttgart University, Germany; Shouji Toma, Professor, Horrai-Gakuen University, Japan; Gerard F. Fox, Consulting Engineer; Jackson L. Kurkee, Consulting Engineer; Michael J. Abrahams, Senior Vice President; Parsons Brinckerhoff Quade & Douglas, Inc.; Ben C. Gerwick Jr., Professor Emeritus, University of California at Berkeley; Gregory F. Fenves, Professor, University of California at Berkeley; John M. Kulicki, President and Chief Engineer, Modjeski and Masters; James Chai, Supervising Transportation Engineer, California Department of Transportation; Jinron Wang, Senior Bridge Engineer, California Department of Transportation; and David W. Liu, Principal, Imbsen & Associates, Inc.

Wai-Fah Chen
Lian Duan

Editors

Wai-Fah Chen is presently Dean of the College of Engineering at the University of Hawaii. He was a George E. Goodwin Distinguished Professor of Civil Engineering and Head of the Department of Structural Engineering at Purdue University from 1976 to 1999.

He received his B.S. in civil engineering from the National Cheng-Kung University, Taiwan in 1959; M.S. in structural engineering from Lehigh University, Pennsylvania in 1963; and Ph.D. in solid mechanics from Brown University, Rhode Island in 1966. He received the Distinguished Alumnus Award from the National Cheng-Kung University in 1988 and the Distinguished Engineering Alumnus Medal from Brown University in 1999.

Dr. Chen's research interests cover several areas, including constitutive modeling of engineering materials, soil and concrete plasticity, structural connections, and structural stability. He is the recipient of several national engineering awards, including the Raymond Reese Research Prize and the Shortridge Hardesty Award, both from the American Society of Civil Engineers, and the T. R. Higgins Lectureship Award from the American Institute of Steel Construction. In 1995, he was elected to the U.S. National Academy of Engineering. In 1997, he was awarded Honorary Membership by the American Society of Civil Engineers. In 1998, he was elected to the Academia Sinica (National Academy of Science) in Taiwan.

A widely respected author, Dr. Chen authored and coauthored more than 20 engineering books and 500 technical papers. His books include several classical works such as *Limit Analysis and Soil Plasticity* (Elsevier, 1975), the two-volume *Theory of Beam-Columns* (McGraw-Hill, 1976–77), *Plasticity in Reinforced Concrete* (McGraw-Hill, 1982), and the two-volume *Constitutive Equations for Engineering Materials* (Elsevier, 1994). He currently serves on the editorial boards of more than 10 technical journals. He has been listed in more than 20 *Who's Who* publications.

Dr. Chen is the editor-in-chief for the popular 1995 *Civil Engineering Handbook* (CRC Press), the 1997 *Handbook of Structural Engineering* (CRC Press), and the 2000 *Bridge Engineering Handbook* (CRC Press). He currently serves as the consulting editor for McGraw-Hill's *Encyclopedia of Science and Technology.*

He has been a longtime member of the Executive Committee of the Structural Stability Research Council and the Specification Committee of the American Institute of Steel Construction. He has been a consultant for Exxon Production Research on offshore structures; for Skidmore, Owings & Merrill in Chicago on tall steel buildings; and for the World Bank on the Chinese University Development Projects, among many others.

Dr. Chen has taught at Lehigh University, Purdue University, and the University of Hawaii.

Lian Duan is a Senior Bridge Engineer with the California Department of Transportation (Caltrans) and Professor of Structural Engineering at Taiyuan University of Technology, China.

He received his B.S. in civil engineering in 1975 and his M.S. in structural engineering in 1981 from Taiyuan University of Technology. He received his Ph.D. in structural engineering from Purdue University, West Lafayette, Indiana in 1990. Dr. Duan worked at the Northeastern China Power Design Institute from 1975 to 1978.

His research interests include inelastic behavior of reinforced concrete and steel structures, structural stability, and seismic bridge analysis and design. Dr. Duan has authored or coauthored more than 60 papers, chapters, ad reports; his research focuses on the development of unified interaction equations for steel beam columns, flexural stiffness of reinforced concrete members, effective length factors of compression members, and design of bridge structures.

Dr. Duan is an esteemed practicing engineer and is registered as a P.E. in California. He has designed numerous building and bridge structures. He was lead engineer for the development of the seismic retrofit design criteria for the San Francisco-Oakland Bay Bridge west spans and made significant contributions to this project. He is coeditor of the *Structural Engineering Handbook* CRCnetBase 2000 (CRC Press, 2000) and *The Bridge Engineering Handbook* (CRC Press, 2000), winner of *Choice* magazine's Outstanding Academic Title Award for 2000. Dr. Duan received the ASCE 2001 Arthur M. Wellington Prize for his paper "Section Properties for Latticed Members of the San Francisco-Oakland Bay Bridge." He currently serves as Caltrans Structural Steel Committee Chairman and is a member of the Transportation Research Board A2CO2 Steel Bridge Committee.

Contributors

James Chai
California Department of Transportation
Sacramento, California

Hong Chen
J. Muller International, Inc.
San Diego, California

Wai-Fah Chen
University of Hawaii at Manoa
Honolulu, Hawaii

Nan Deng
Bechtel Corporation
San Francisco, California

Lian Duan
California Department of Transportation
Sacramento, California

Johnny Feng
J. Muller International, Inc.
Sacramento, California

Chao Gong
ICF Kaiser Engineers
Oakland, California

Michael Knott
Moffatt & Nichol Engineers
Richmond, Virginia

Youzhi Ma
Geomatrix Consultants, Inc.
Oakland, California

Thomas W. McNeilan
Fugro West, Inc.
Ventura, California

Zolan Prucz
Modjeski and Masters, Inc.
New Orleans, Louisiana

Charles Seim
T. Y. Lin International
San Francisco, California

Jim Springer
California Department of Transportation
Sacramento, California

Jinrong Wang
California Department of Transportation
Sacramento, California

Linan Wang
California Department of Transportation
Sacramento, California

Ke Zhou
California Department of Transportation
Sacramento, California

Contents

1 Bearings

Johnny Feng
J. Muller International, Inc.

Hong Chen
J. Muller International, Inc.

1.1 Introduction

Bearings are structural devices positioned between the bridge superstructure and the substructure. Their principal functions are as follows:

1. To transmit loads from the superstructure to the substructure, and
2. To accommodate relative movements between the superstructure and the substructure.

The forces applied to a bridge bearing mainly include superstructure self-weight, traffic loads, wind loads, and earthquake loads.

Movements in bearings include translations and rotations. Creep, shrinkage, and temperature effects are the most common causes of the translational movements, which can occur in both transverse and longitudinal directions. Traffic loading, construction tolerances, and uneven settlement of the foundation are the common causes of the rotations.

Usually a bearing is connected to the superstructure through the use of a steel sole plate and rests on the substructure through a steel masonry plate. The sole plate distributes the concentrated bearing reactions to the superstructure. The masonry plate distributes the reactions to the substructure. The connections between the sole plate and the superstructure, for steel girders, are by bolting or welding. For concrete girders, the sole plate is embedded into the concrete with anchor studs. The masonry plate is typically connected to the substructure with anchor bolts.

1.2 Types of Bearings

Bearings may be classified as fixed bearings and expansion bearings. Fixed bearings allow rotations but restrict translational movements. Expansion bearings allow both rotational and translational movements. There are numerous types of bearings available. The following are the principal types of bearings currently in use.

1.2.1 Sliding Bearings

A sliding bearing utilizes one plane metal plate sliding against another to accommodate translations. The sliding bearing surface produces a frictional force that is applied to the superstructure, the substructure, and the bearing itself. To reduce this friction force, PTFE (polytetrafluoroethylene) is often used as a sliding lubricating material. PTFE is sometimes referred to as Teflon, named after a widely used brand of PTFE, or TFE as appeared in AASHTO [1] and other design standards. In its common application, one steel plate coated with PTFE slides against another plate, which is usually of stainless steel.

Sliding bearings can be used alone or more often used as a component in other types of bearings. Pure sliding bearings can only be used when the rotations caused by the deflection at the supports are negligible. They are therefore limited to a span length of 15 m or less by ASHTTO [1].

A guiding system may be added to a sliding bearing to control the direction of the movement. It may also be fixed by passing anchor bolts through the plates.

1.2.2 Rocker and Pin Bearings

A rocker bearing is a type of expansion bearing that comes in a great variety. It typically consists of a pin at the top that facilitates rotations, and a curved surface at the bottom that accommodates the translational movements (Figure 1.1a). The pin at the top is composed of upper and lower semicircularly recessed surfaces with a solid circular pin placed between. Usually, there are caps at both ends of the pin to keep the pin from sliding off the seats and to resist uplift loads if required. The upper plate is connected to the sole plate by either bolting or welding. The lower curved plate sits on the masonry plate. To prevent the rocker from walking, keys are used to keep the rocker in place. A key can be a pintal which is a small trapezoidal steel bar tightly fitted into the masonry plate on one end and loosely inserted into the recessed rocker bottom plate on the other end. Or it can be an anchor bolt passing through a slotted hole in the bottom rocker plate.

A pin bearing is a type of fixed bearings that accommodates rotations through the use of a steel pin. The typical configuration of the bearing is virtually the same as the rocker described above except that the bottom curved rocker plate is now flat and directly anchored to the concrete pier (Figure 1.1b).

Rocker and pin bearings are primarily used in steel bridges. They are only suitable for the applications where the direction of the displacement is well defined since they can only accommodate translations and/or rotations in one direction. They can be designed to support relatively large loads but a high vertical clearance is usually required when the load or displacement is large. The practical limits of the load and displacement are about 1800 kN and ±100 mm, respectively, and rotations of several degrees are achievable [3].

Normally, the moment and lateral forces induced from the movement of these bearings are very small and negligible. However, metal bearings are susceptible to corrosion and deterioration. A corroded joint may induce much larger forces. Regular inspection and maintenance are, therefore, required.

1.2.3 Roller Bearings

Roller bearings are composed of one or more rollers between two parallel steel plates. Single roller bearings can facilitate both rotations and translations in the longitudinal direction, while a group of rollers would only accommodate longitudinal translations. In the latter case, the rotations are provided by combining rollers with a pin bearing (Figure 1.1c).

Roller bearings have been used in both steel and concrete bridges. Single roller bearings are relatively cheap to manufacture, but they only have a very limited vertical load capacity. Multiple roller bearings, on the other hand, may be able to support very large loads, but they are much more expensive.

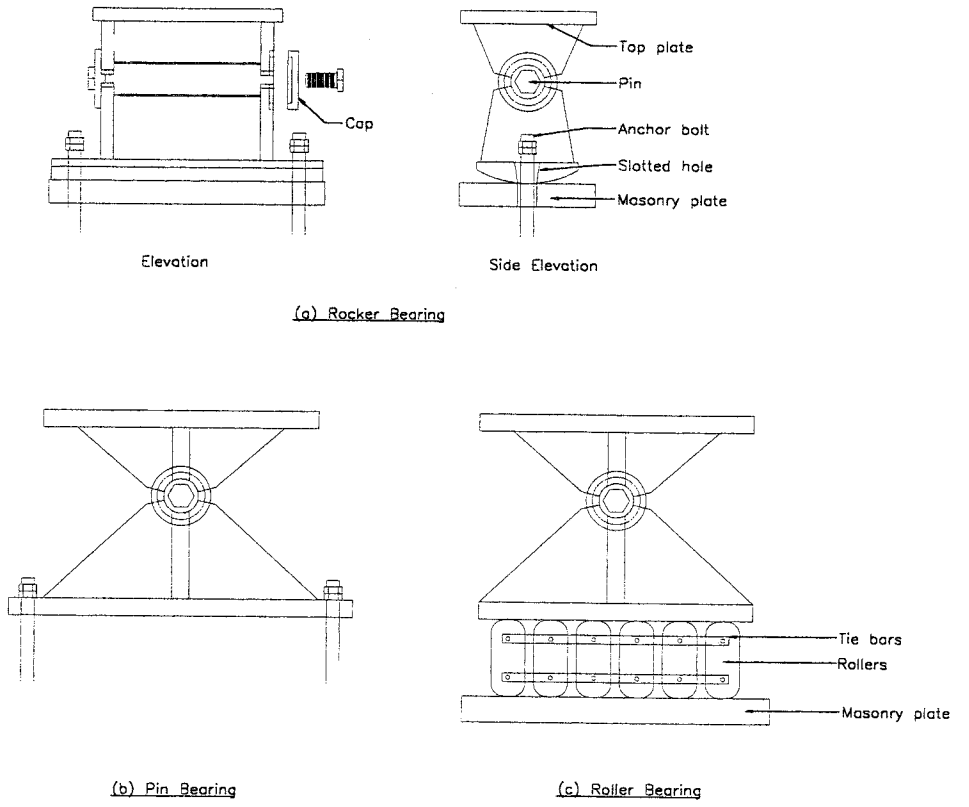

FIGURE 1.1 Typical rocker (a), pin (b), and roller bearings (c).

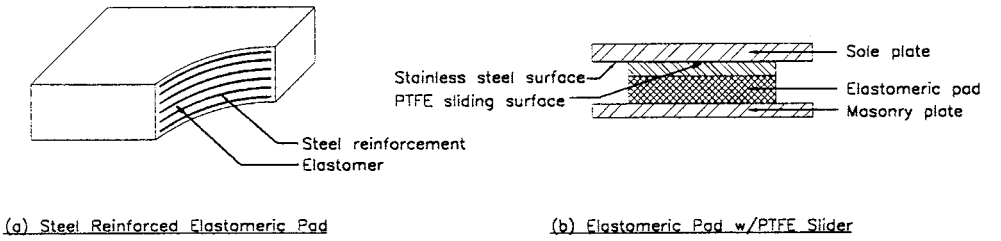

FIGURE 1.2 Elastomeric bearings. (a) Steel-reinforced elastomeric pad; (b) elastomeric pad with PTFE slider.

Like rocker and pin bearings, roller bearings are also susceptible to corrosion and deterioration. Regular inspection and maintenance are essential.

1.2.4 Elastomeric Bearings

An elastomeric bearing is made of elastomer (either natural or synthetic rubber). It accommodates both translational and rotational movements through the deformation of the elastomer.

Elastomer is flexible in shear but very stiff against volumetric change. Under compressive load, the elastomer expands laterally. To sustain large load without excessive deflection, reinforcement is used to restrain lateral bulging of the elastomer. This leads to the development of several types of elastomeric bearing pads — plain, fiberglass-reinforced, cotton duck-reinforced, and steel-reinforced elastomeric pads. Figure 1.2a shows a steel-reinforced elastomeric pad.

Plain elastomeric pads are the weakest and most flexible because they are only restrained from bulging by friction forces alone. They are typically used in short- to medium-span bridges, where bearing stress is low. Fiberglass-reinforced elastomeric pads consist of alternate layers of elastomer and fiberglass reinforcement. Fiberglass inhibits the lateral deformation of the pads under compressive loads so that larger load capacity can be achieved. Cotton-reinforced pads are elastomeric pads reinforced with closely spaced layers of cotton duck. They display high compressive stiffness and strength but have very limited rotational capacities. The thin layers also lead to high shear stiffness, which results in large forces in the bridge. So sometimes they are combined with a PTFE slider on top of the pad to accommodate translations (Figure 1.2b). Steel-reinforced elastomeric pads are constructed by vulcanizing elastomer to thin steel plates. They have the highest load capacity among the different types of elastomeric pads, which is only limited by the manufacturer's ability to vulcanize a large volume of elastomer uniformly.

All above-mentioned pads except steel-reinforced pads can be produced in a large sheet and cut to size for any particular application. Steel-reinforced pads, however, have to be custom-made for each application due to the edge cover requirement for the protection of the steel from corrosion. The steel-reinforced pads are the most expensive while the cost of the plain elastomeric pads is the lowest.

Elastomeric bearings are generally considered the preferred type of bearings because they are low cost and almost maintenance free. In addition, elastomeric bearings are extremely forgiving of loads and movements exceeding the design values.

1.2.4 Curved Bearings

A curved bearing consists of two matching curved plates with one sliding against the other to accommodate rotations. The curved surface can be either cylindrical which allows the rotation about only one axis or spherical which allows the bearing to rotate about any axis.

Lateral movements are restrained in a pure curved bearing and a limited lateral resistance may be developed through a combination of the curved geometry and the gravity loads. To accommodate lateral movements, a PTFE slider must be attached to the bearings. Keeper plates are often used to keep the superstructure moving in one direction. Large load and rotational capacities can be designed for curved bearings. The vertical capacity is only limited by its size, which depends largely on machining capabilities. Similarly, rotational capacities are only limited by the clearances between the components.

Figure 1.3a shows a typical expansion curved bearing. The lower convex steel plate that has a stainless steel mating surface is recessed in the masonry plate. The upper concave plate with a matching PTFE sliding surface sits on top of the lower convex plate for rotations. Between the sole plate and the upper concave plate there is a flat PTFE sliding surface that will accommodate lateral movements.

1.2.5 Pot Bearings

A pot bearing comprises a plain elastomeric disk that is confined in a shallow steel ring, or pot (Figure 1.3b). Vertical loads are transmitted through a steel piston that fits closely to the steel ring (pot wall). Flat sealing rings are used to contain the elastomer inside the pot. The elastomer behaves like a viscous fluid within the pot as the bearing rotates. Because the elastomeric pad is confined, much larger load can be carried this way than through conventional elastomeric pads.

Translational movements are restrained in a pure pot bearing, and the lateral loads are transmitted through the steel piston moving against the pot wall. To accommodate translational movement, a PTFE sliding surface must be used. Keeper plates are often used to keep the superstructure moving in one direction.

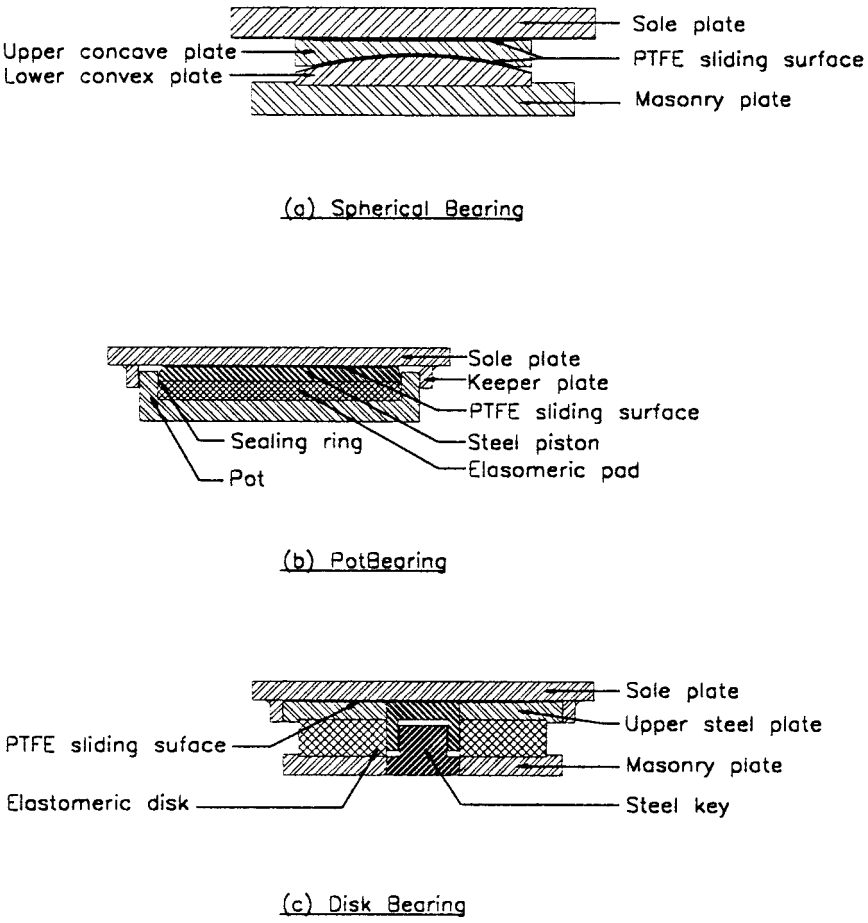

FIGURE 1.3 Typical spherical (a), pot (b), and disk (c) bearings

1.2.6 Disk Bearings

A disk bearing, as illustrated in Figure 1.3c, utilizes a hard elastomeric (polyether urethane) disk to support the vertical loads and a metal key in the center of the bearing to resist horizontal loads. The rotational movements are accommodated through the deformation of the elastomer. To accommodate translational movements, however, a PTFE slider is required. In this kind of bearings, the polyether urethane disk must be hard enough to resist large vertical load without excessive deformation and yet flexible enough to accommodate rotations easily.

1.3 Selection of Bearings

Generally the objective of bearing selection is to choose a bearing system that suits the needs with a minimum overall cost. The following procedures may be used for the selection of the bearings.

1.3.1 Determination of Functional Requirements

First, the vertical and horizontal loads, the rotational and translational movements from all sources including dead and live loads, wind loads, earthquake loads, creep and shrinkage, prestress, thermal and construction tolerances need to be calculated. Table 1.1 may be used to tabulate these requirements.

TABLE 1.1 Typical Bridge Bearing Schedule

Bridge Name of Reference					
Bearing Identification mark					
Number of bearings required					
Seating Material		Upper Surface			
		Lower Surface			
Allowable average contact pressure (PSI)		Upper Surface	Serviceability		
			Strength		
		Lower Surface	Serviceability		
			Strength		
Design Load effects (KIP)	Service limit state		Vertical	max.	
				perm	
				min.	
			Transverse		
			Longitudinal		
	Strength limit state		Vertical		
			Transverse		
			Longitudinal		
Translation	Service limit state	Irreversible	Transverse		
			Longitudinal		
		Reversible	Transverse		
			Longitudinal		
	Strength limit state	Irreversible	Transverse		
			Longitudinal		
		Reversible	Transverse		
			Longitudinal		
Rotation (RAD)	Service limit state	Irreversible	Transverse		
			Longitudinal		
		Reversible	Transverse		
			Longitudinal		
	Strength limit state	Irreversible	Transverse		
			Longitudinal		
		Reversible	Transverse		
			Longitudinal		
Maximum bearing dimensions (IN)	Upper surface		Transverse		
			Longitudinal		
	Lower surface		Transverse		
			Longitudinal		
	Overall height				
Tolerable movement of bearing under transient loads (IN)			Vertical		
			Transverse		
			Longitudinal		
Allowable resistance to translation under service limit state (KIP)			Transverse		
			Longitudinal		
Allowable resistance to rotation under service limit state (K/FT)			Transverse		
			Longitudinal		
Type of attachment to structure and substructure			Transverse		
			Longitudinal		

Source: AASHTO, *LRFD Bridge Design Scecifications,* American Association of State Highway and Transportation Officials, Washington, D.C.

TABLE 1.2 Summary of Bearing Capacities [3,5]

Bearing Type	Load		Translation		Rotation	Costs	
	Min. (KN)	Max. (KN)	Min. (mm)	Max. (mm)	Max. (rad)	Initial	Maintenance
Elastomeric pads							
Plain	0	450	0	15	0.01	Low	Low
Cotton duck reinforced	0	1,400	0	5	0.003	Low	Low
Fiberglass reinforced	0	600	0	25	0.015	Low	Low
Steel reinforced	225	3,500	0	100	0.04	Low	Low
Flat PTFE slider	0	>10,000	25	>10 0	0	Low	Moderate
Disk bearing	1,200	10,000	0	0	0.02	Moderate	Moderate
Pot bearing	1,200	10,000	0	0	0.02	Moderate	High
Pin bearing	1,200	4,500	0	0	>0.04	Moderate	High
Rocker bearing	0	1,800	0	100	>0.04	Moderate	High
Single roller	0	450	25	>10 0	>0.04	Moderate	High
Curved PTFE bearing	1,200	7,000	0	0	>0.04	High	Moderate
Multiple rollers	500	10,000	100	>10 0	>0.04	High	High

1.3.2 Evaluation of Bearings

The second step is to determine the suitable bearing types based on the above bridge functional requirements, and other factors including available clearance, environment, maintenance, cost, availability, and client's preferences. Table 1.2 summarizes the load, movement capacities, and relative costs for each bearing type and may be used for the selection of the bearings.

It should be noted that the capacity values in Table 1.2 are approximate. They are the practical limits of the most economical application for each bearing type. The costs are also relative, since the true price can only be determined by the market. At the end of this step, several qualified bearing systems with close cost ratings may be selected [5].

1.3 Preliminary Bearing Design

For the various qualified bearing alternatives, preliminary designs are performed to determine the approximate geometry and material properties in accordance with design specifications. It is likely that one or more of the previously acceptable alternatives will be eliminated in this step because of an undesirable attribute such as excessive height, oversize footprint, resistance at low temperature, sensitivity to installation tolerances, etc. [3].

At the end of this step, one or more bearing types may still be feasible and they will be included in the bid package as the final choices of the bearing types.

1.4 Design of Elastomeric Bearings

1.4.1 Design Procedure

The design procedure is according to AASHTO-LRFD [1] and is as follows:

1. Determine girder temperature movement (Art. 5.4.2.2).
2. Determine girder shortenings due to post-tensioning, concrete shrinkage, etc.
3. Select a bearing thickness based on the bearing total movement requirements (Art. 14.7.5.3.4).
4. Compute the bearing size based on bearing compressive stress (Art. 14.7.5.3.2).
5. Compute instantaneous compressive deflection (Art. 14.7.5.3.3).
6. Combine bearing maximum rotation.
7. Check bearing compression and rotation (Art. 14.7.5.3.5).
8. Check bearing stability (Art. 14.7.5.3.6).
9. Check bearing steel reinforcement (Art. 14.7.5.3.7).

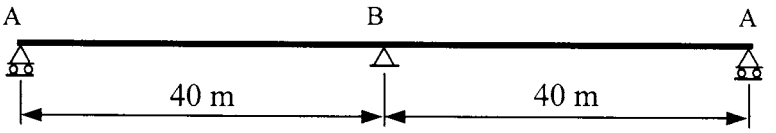

FIGURE 1.4 Bridge layout

1.4.2 Design Example (Figure 1.4)

Given

L	= expandable span length	= 40 m
R_{DL}	= DL reaction/girder	= 690 kN
R_{LL}	= LL reaction (without impact)/girder	= 220 kN
θ_s	= bearing design rotation at service limit state	= 0.025 rad
ΔT	= maximum temperature change	= 21°C
Δ_{PT}	= girder shortening due to post tensioning	= 21 mm
Δ_{SH}	= girder shortening due to concrete shrinkage	= 2 mm
G	= shear modulus of elastomer	= 0.9 ~ 1.38 MPa
γ	= load factor for uniform temperature, etc.	= 1.2
ΔF_{TH}	= constant amplitude fatigue threshold for Category A	= 165 MPa

Using 60 durometer reinforced bearing:

F_y	= yield strength of steel reinforcement	= 350 MPa

Sliding bearing used:

1. **Temperature Movement**
   From Art. 5.4.2.2, for normal density concrete, the thermal coefficient α is

$$\alpha = 10.8 \times 10^{-6}/°C$$

$$\Delta_{TEMP} = (\alpha)(\Delta T)(L) = (10.8 \times 10^{-6}/°C)(21°C)(40{,}000 \text{ mm}) = 9 \text{ mm}$$

2. **Girder Shortenings**

$$\Delta_{PT} = 21 \text{ mm and } \Delta_{SH} = 2 \text{ mm}$$

3. **Bearing Thickness**
   h_{rt} = total elastomer thickness
   h_{ri} = thickness of ith elastomeric layer
   n = number of interior layers of elastomeric layer
   Δ_S = bearing maximum longitudinal movement = $\gamma \cdot (\Delta_{TEMP} + \Delta_{PT} + \Delta_{SH})$
   $\Delta_S = 1.2 \times (9 \text{ mm} + 21 \text{ mm} + 2 \text{ mm}) = 38.4 \text{ mm}$
   h_{rt} = bearing thickness $\geq 2\Delta_S$ (AASHTO Eq. 14.7.5.3.4-1)
   $h_{rt} = 2 \times (38.4 \text{ mm}) = 76.8$

   Try $h_{rt} = 120$ mm, $h_{ri} = 20$ mm and $n = 5$

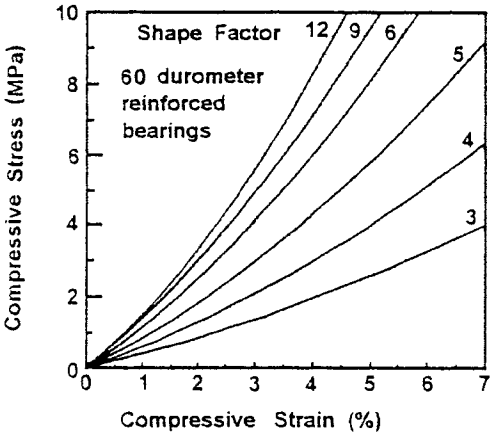

FIGURE 1.5 Stress–strain curves. (From AASHTO, Figure C14.7.5.3.3.1.)

4. Bearing Size

L = length of bearing
W = width of bearing
S_i = shape factor of thickness layer of the bearing = $\dfrac{LW}{2h_{ri}(L+W)}$

For a bearing subject to shear deformation, the compressive stresses should satisfy:

σ_S = average compressive stress due to the total load $\le 1.66GS \le 11$ (AASHTO Eq. 14.7.5.3.2-1)
σ_L = average compressive stress due to the live load $\le 0.66\ GS$ (AASHTO Eq. 14.7.5.3.2-1)

$$\sigma_s = \frac{R}{LW} = \frac{1.66GLW}{2h_{ri}(L+W)}$$

Assuming σ_S is critical, solve for L and W by error and trial.

$$L = 300 \text{ mm and } W = 460 \text{ mm}$$

$$S = \frac{LW}{2h_{ri}(L+W)} = \frac{(300 \text{ mm})(460 \text{ mm})}{2(20 \text{ mm})(300 \text{ mm} + 460 \text{ mm})} = 4.54$$

$$\sigma_L = \frac{R_L}{LW} = \frac{(200{,}000 \text{ N})}{(300 \text{ mm})(460 \text{ mm})} = 1.6 \text{ MPa} \quad \text{OK}$$
$$\le 0.66\ GS = 0.66(1.0 \text{ MPa})(4.54) = 3.0 \text{ MPa}$$

5. Instantaneous Compressive Deflection

For $\sigma_S = 6.59$ MPa and $S = 4.54$, one can determine the value of ε_i from Figure 1.5:

$$\varepsilon_i = 0.062$$

$$\delta = \sum \varepsilon_i h_{ri} \quad \text{(AASHTO Eq. 14.7.5.3.3-1)}$$
$$= 6(0.062)(20 \text{ mm}) = 7.44 \text{ mm}$$

6. Bearing Maximum Rotation

The bearing rotational capacity can be calculated as

$$\theta_{capacity} = \frac{2\delta}{L} = \frac{2(7.44\text{ mm})}{300\text{ mm}} = 0.05\text{ rad} < \theta_{design} = 0.025\text{ rad} \quad \text{OK}$$

7. Combined Bearing Compression and Rotation

a. *Uplift requirement* (AASHTO Eq. 14.7.5.3.5-1):

$$\sigma_{s,uplift} = 1.0GS\left(\frac{\theta_{design}}{n}\right)\left(\frac{L}{h_{ri}}\right)^2$$

$$= 1.0(1.2)(4.54)\left(\frac{0.025}{5}\right)\left(\frac{300}{20}\right)^2 = 6.13\text{ MPa} < \sigma_s = 6.59\text{ MPa} \quad \text{OK}$$

b. *Shear deformation requirement* (AASHTO Eq. 14.7.5.3.5-2):

$$\sigma_{s,shear} = 1.875GS\left(1 - 0.20\left(\frac{\theta_{design}}{n}\right)\left(\frac{L}{h_{ri}}\right)^2\right)$$

$$= 1.875(1.0)(4.54)\left(1 - 0.20\left(\frac{0.025}{5}\right)\left(\frac{300}{20}\right)^2\right) = 6.60\text{ MPa} > \sigma_s = 6.59\text{ MPa} \quad \text{OK}$$

8. Bearing Stability

Bearings shall be designed to prevent instability at the service limit state load combinations. The average compressive stress on the bearing is limited to half the predicted buckling stress. For this example, the bridge deck, if free to translate horizontally, the average compressive stress due to dead and live load, σ_s, must satisfy:

$$\sigma_s \le \frac{G}{2A - B} \quad \text{(AASHTO Eq. 14.7.5.3.6-1)}$$

where

$$A = \frac{1.92\frac{h_{rt}}{L}}{S\sqrt{1 + \frac{2.0\,L}{W}}} \quad \text{(AASHTO Eq. 14.7.5.3.6-3)}$$

$$= \frac{1.92\frac{(120\text{ mm})}{(300\text{ mm})}}{(4.54)\sqrt{1 + \frac{2.0(300\text{ mm})}{(460\text{ mm})}}} = 0.11$$

$$B = \frac{2.67}{S(S+2.0)\sqrt{1+\dfrac{L}{4.0W}}}$$

$$= \frac{2.67}{(4.54)(4.54+2.0)\sqrt{1+\dfrac{(300\text{ mm})}{4.0(460\text{ mm})}}} = 0.08 \qquad \text{(AASHTO Eq. 14.7.5.3.6-4)}$$

$$\frac{G}{2A-B} = \frac{(1.0\text{ MPa})}{2(0.11)-(0.08)} = 6.87 > \sigma_s \qquad \text{OK}$$

9. Bearing Steel Reinforcement

The bearing steel reinforcement must be designed to sustain the tensile stresses induced by compression of the bearing. The thickness of steel reinforcement, h_s, should satisfy:

a. *At the service limit state*:

$$h_s \geq \frac{3h_{\max}\sigma_s}{F_y} \qquad \text{(AASHTO Eq. 14.7.5.3.7-1)}$$

$$= \frac{3(20\text{ mm})(6.59\text{ MPa})}{(350\text{ MPa})} = 1.13\text{ mm} \qquad \text{(governs)}$$

b. *At the fatigue limit state*:

$$h_s \geq \frac{2h_{\max}\sigma_L}{\ddot{A}F_y} \qquad \text{(AASHTO Eq. 14.7.5.3.7-2)}$$

$$= \frac{2(20\text{ mm})(1.6\text{ MPa})}{(165\text{ MPa})} = 0.39\text{ mm}$$

where $h_{\max}$ = thickness of thickest elastomeric layer in elastomeric bearing = h_{ri}.

Elastomeric Bearings Details

Five interior lays with 20 mm thickness each layer
Two exterior lays with 10 mm thickness each layer
Six steel reinforcements with 1.2 mm each
Total thickness of bearing is 127.2 mm
Bearing size: 300 mm (longitudinal) × 460 mm (transverse)

References

1. AASHTO, *LRFD Bridge Design Specifications,* American Association of State Highway and Transportation Officials, Washington, D.C., 1994.
2. AASHTO, *Standard Specifications for the Design of Highway Bridges,* 16th ed. American Association of State Highway and Transportation Officials, Washington, D.C., 1996.
3. Stanton, J. F., Roeder, C. W., and Campbell, T. I., High Load Multi-Rotational Bridge Bearings, NCHRP Report 10-20A, Transportation Research Board, National Research Council, Washington, D.C., 1993.
4. Caltrans, Memo to Designers, California Department of Transportation, Sacramento, 1994.
5. AISI, Steel bridge bearing selection and design guide, *Highway Structures Design Handbook,* Vol. II, American Iron and Steel Institute, Washington, D.C., 1996, chap. 4.

2

Piers and Columns

Jinrong Wang
California Department of Transportation

2.1 Introduction

Piers provide vertical supports for spans at intermediate points and perform two main functions: transferring superstructure vertical loads to the foundations and resisting horizontal forces acting on the bridge. Although piers are traditionally designed to resist vertical loads, it is becoming more and more common to design piers to resist high lateral loads caused by seismic events. Even in some low seismic areas, designers are paying more attention to the ductility aspect of the design. Piers are predominantly constructed using reinforced concrete. Steel, to a lesser degree, is also used for piers. Steel tubes filled with concrete (composite) columns have gained more attention recently.

This chapter deals only with piers or columns for conventional bridges, such as grade separations, overcrossings, overheads, underpasses, and simple river crossings. Reinforced concrete columns will be discussed in detail while steel and composite columns will be briefly discussed. Substructures for arch, suspension, segmental, cable-stayed, and movable bridges are excluded from this chapter. Chapter 3 discusses the substructures for some of these special types of bridges.

2.2 Structural Types

2.2.1 General

Pier is usually used as a general term for any type of substructure located between horizontal spans and foundations. However, from time to time, it is also used particularly for a solid wall in order to distinguish it from columns or bents. From a structural point of view, a column is a member that resists the lateral force mainly by flexure action whereas a pier is a member that resists the lateral force mainly by a shear mechanism. A pier that consists of multiple columns is often called a *bent*.

There are several ways of defining pier types. One is by its structural connectivity to the superstructure: monolithic or cantilevered. Another is by its sectional shape: solid or hollow; round, octagonal, hexagonal, or rectangular. It can also be distinguished by its framing configuration: single or multiple column bent; hammerhead or pier wall.

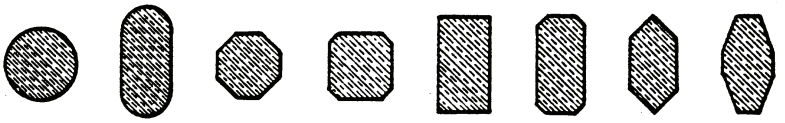

FIGURE 2.1 Typical cross-section shapes of piers for overcrossings or viaducts on land.

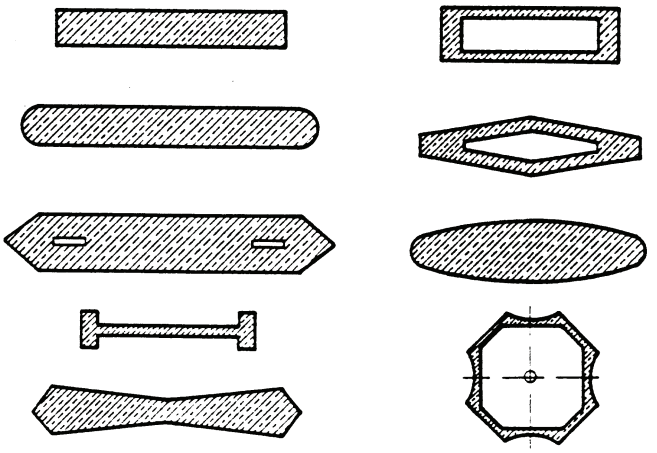

FIGURE 2.2 Typical cross-section shapes of piers for river and waterway crossings.

2.2.2 Selection Criteria

Selection of the type of piers for a bridge should be based on functional, structural, and geometric requirements. Aesthetics is also a very important factor of selection since modern highway bridges are part of a city's landscape. Figure 2.1 shows a collection of typical cross section shapes for overcrossings and viaducts on land and Figure 2.2 shows some typical cross section shapes for piers of river and waterway crossings. Often, pier types are mandated by government agencies or owners. Many state departments of transportation in the United States have their own standard column shapes.

Solid wall piers, as shown in Figures 2.3a and 2.4, are often used at water crossings since they can be constructed to proportions that are both slender and streamlined. These features lend themselves well for providing minimal resistance to flood flows.

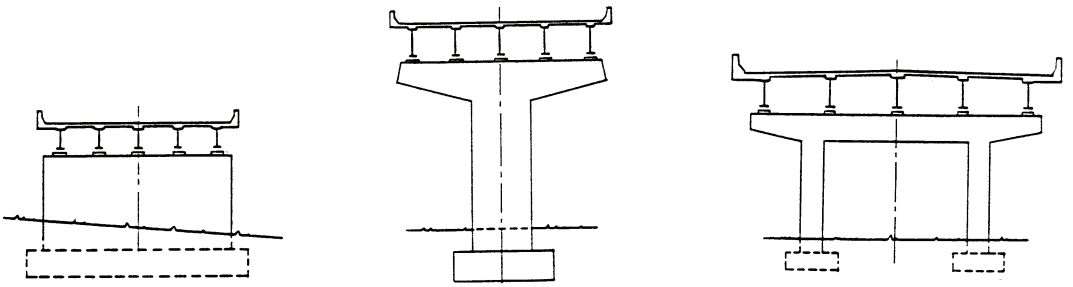

(a) Solid wall pier (b) Hammerhead pier (c) Rigid frame pier

FIGURE 2.3 Typical pier types for steel bridges.

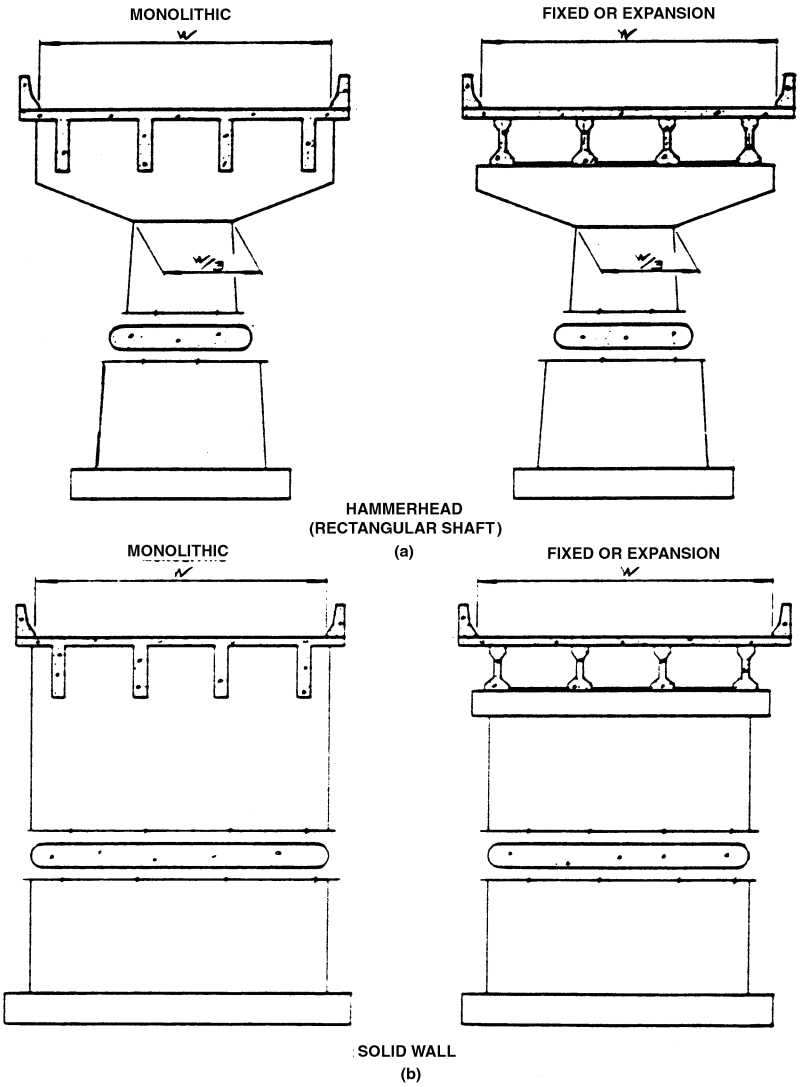

FIGURE 2.4 Typical pier types and configurations for river and waterway crossings.

Hammerhead piers, as shown in Figure 2.3b, are often found in urban areas where space limitation is a concern. They are used to support steel girder or precast prestressed concrete superstructures. They are aesthetically appealing. They generally occupy less space, thereby providing more room for the traffic underneath. Standards for the use of hammerhead piers are often maintained by individual transportation departments.

A column bent pier consists of a cap beam and supporting columns forming a frame. Column bent piers, as shown in Figure 2.3c and Figure 2.5, can either be used to support a steel girder superstructure or be used as an integral pier where the cast-in-place construction technique is used. The columns can be either circular or rectangular in cross section. They are by far the most popular forms of piers in the modern highway system.

A pile extension pier consists of a drilled shaft as the foundation and the circular column extended from the shaft to form the substructure. An obvious advantage of this type of pier is that it occupies a minimal amount of space. Widening an existing bridge in some instances may require pile extensions because limited space precludes the use of other types of foundations.

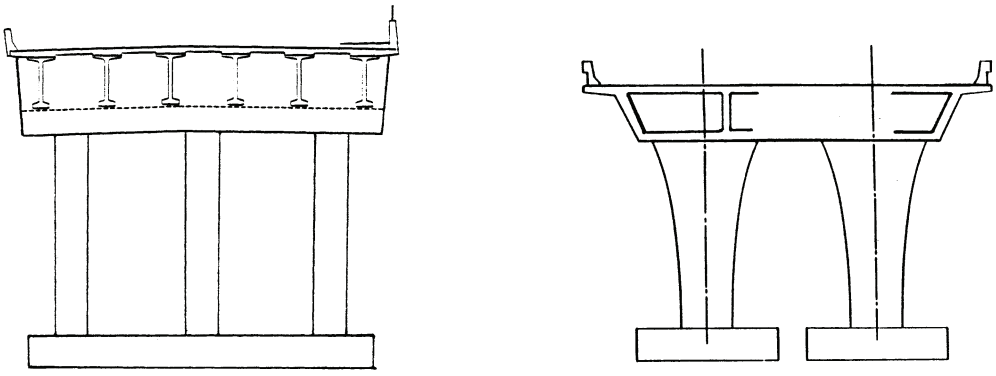

(a) Bent for precast girders

(b) Bent for cast-in-place girders

FIGURE 2.5 Typical pier types for concrete bridges.

Selections of proper pier type depend upon many factors. First of all, it depends upon the type of superstructure. For example, steel girder superstructures are normally supported by cantilevered piers, whereas the cast-in-place concrete superstructures are normally supported by monolithic bents. Second, it depends upon whether the bridges are over a waterway or not. Pier walls are preferred on river crossings, where debris is a concern and hydraulics dictates it. Multiple pile extension bents are commonly used on slab bridges. Last, the height of piers also dictates the type selection of piers. The taller piers often require hollow cross sections in order to reduce the weight of the substructure. This then reduces the load demands on the costly foundations. Table 2.1 summarizes the general type selection guidelines for different types of bridges.

2.3 Design Loads

Piers are commonly subjected to forces and loads transmitted from the superstructure, and forces acting directly on the substructure. Some of the loads and forces to be resisted by the substructure include:

- Dead loads
- Live loads and impact from the superstructure
- Wind loads on the structure and the live loads
- Centrifugal force from the superstructure
- Longitudinal force from live loads
- Drag forces due to the friction at bearings
- Earth pressure
- Stream flow pressure
- Ice pressure
- Earthquake forces
- Thermal and shrinkage forces
- Ship impact forces
- Force due to prestressing of the superstructure
- Forces due to settlement of foundations

TABLE 2.1 General Guidelines for Selecting Pier Types

		Applicable Pier Types
		Steel Superstructure
Over water	Tall piers	Pier walls or hammerheads (T-piers) (Figures 2.3a and b); hollow cross sections for most cases; cantilevered; could use combined hammerheads with pier wall base and step tapered shaft
	Short piers	Pier walls or hammerheads (T-piers) (Figures 2.3a and b); solid cross sections; cantilevered
On land	Tall piers	Hammerheads (T-piers) and possibly rigid frames (multiple column bents)(Figures 2.3b and c); hollow cross sections for single shaft and solid cross sections for rigid frames; cantilevered
	Short piers	Hammerheads and rigid frames (Figures 2.3b and c); solid cross sections; cantilevered
		Precast Prestressed Concrete Superstructure
Over water	Tall piers	Pier walls or hammerheads (Figure 2.4); hollow cross sections for most cases; cantilevered; could use combined hammerheads with pier wall base and step-tapered shaft
	Short piers	Pier walls or hammerheads; solid cross sections; cantilevered
On land	Tall piers	Hammerheads and possibly rigid frames (multiple column bents); hollow cross sections for single shafts and solid cross sections for rigid frames; cantilevered
	Short piers	Hammerheads and rigid frames (multiple column bents) (Figure 2.5a); solid cross sections; cantilevered
		Cast-in-Place Concrete Superstructure
Over water	Tall piers	Single shaft pier (Figure 2.4); superstructure will likely cast by traveled forms with balanced cantilevered construction method; hollow cross sections; monolithic; fixed at bottom
	Short piers	Pier walls (Figure 2.4); solid cross sections; monolithic; fixed at bottom
On land	Tall piers	Single or multiple column bents; solid cross sections for most cases, monolithic; fixed at bottom
	Short piers	Single or multiple column bents (Figure 2.5b); solid cross sections; monolithic; pinned at bottom

The effect of temperature changes and shrinkage of the superstructure needs to be considered when the superstructure is rigidly connected with the supports. Where expansion bearings are used, forces caused by temperature changes are limited to the frictional resistance of bearings.

In the following, two load cases, live loads and thermal forces, will be discussed in detail because they are two of the most common loads on the piers, but are often applied incorrectly.

2.3.1 Live Loads

Bridge live loads are the loads specified or approved by the contracting agencies and owners. They are usually specified in the design codes such as AASHTO LRFD Bridge Design Specifications [1]. There are other special loading conditions peculiar to the type or location of the bridge structure which should be specified in the contracting documents.

Live-load reactions obtained from the design of individual members of the superstructure should not be used directly for substructure design. These reactions are based upon maximum conditions for one beam and make no allowance for distribution of live loads across the roadway. Use of these maximum loadings would result in a pier design with an unrealistically severe loading condition and uneconomical sections.

For substructure design, a maximum design traffic lane reaction using either the standard truck load or standard lane load should be used. Design traffic lanes are determined according to AASHTO LRFD [1] Section 3.6. For the calculation of the actual beam reactions on the piers, the maximum lane reaction can be applied within the design traffic lanes as wheel loads, and then distributed to the beams assuming the slab between beams to be simply supported (Figure 2.6). Wheel loads can be positioned anywhere within the design traffic lane with a minimum distance between lane boundary and wheel load of 0.61 m (2 ft).

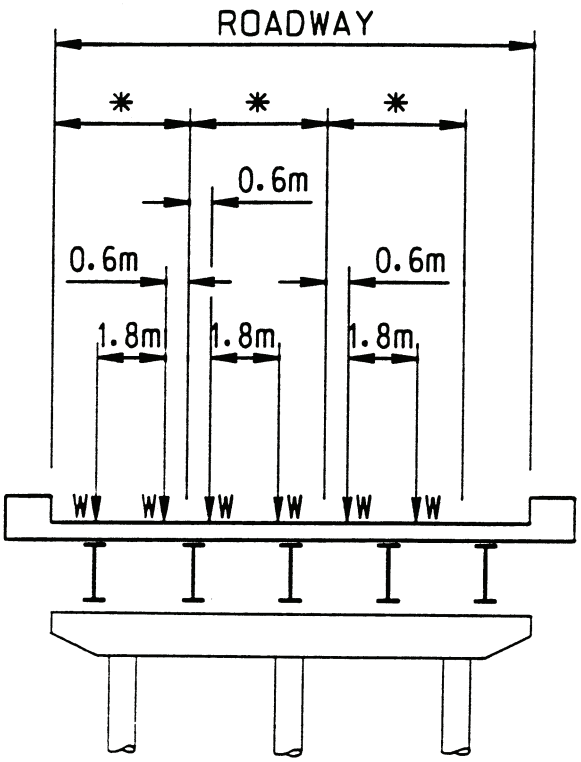

* DESIGN TRAFFIC LANE = 3.6m
NO. OF LANES = ROADWAY ÷ 3.6
REDUCED TO NEAREST WHOLE NUMBER

WHEEL LOADING $W = \frac{R_2}{2}$

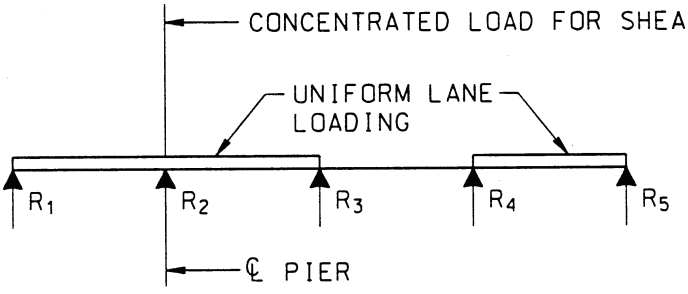

FIGURE 2.6 Wheel load arrangement to produce maximum positive moment.

The design traffic lanes and the live load within the lanes should be arranged to produce beam reactions that result in maximum loads on the piers. AASHTO LRFD Section 3.6.1.1.2 provides load reduction factors due to multiple loaded lanes.

Live-load reactions will be increased due to impact effect. AASHTO LRFD [1] refers to this as the *dynamic load allowance, IM.* and is listed here as in Table 2.2.

TABLE 2.2 Dynamic Load Allowance, IM

Component	IM
Deck joints — all limit states	75%
All other components	
• Fatigue and fracture limit state	15%
• All other limit states	33%

2.3.2 Thermal Forces

Forces on piers due to thermal movements, shrinkage, and prestressing can become large on short, stiff bents of prestressed concrete bridges with integral bents. Piers should be checked against these forces. Design codes or specifications normally specify the design temperature range. Some codes even specify temperature distribution along the depth of the superstructure member.

The first step in determining the thermal forces on the substructures for a bridge with integral bents is to determine the point of no movement. After this point is determined, the relative displacement of any point along the superstructure to this point is simply equal to the distance to this point times the temperature range and times the coefficient of expansion. With known displacement at the top and known boundary conditions at the top and bottom, the forces on the pier due to the temperature change can be calculated by using the displacement times the stiffness of the pier.

The determination of the point of no movement is best demonstrated by the following example, which is adopted from Memo to Designers issued by California Department of Transportation [2]:

Example 2.1

A 225.55-m (740-foot)-long and 23.77-m (78-foot) wide concrete box-girder superstructure is supported by five two-column bents. The size of the column is 1.52 m (5 ft) in diameter and the heights vary between 10.67 m (35 ft) and 12.80 m (42 ft). Other assumptions are listed in the calculations. The calculation is done through a table. Please refer Figure 2.7 for the calculation for determining the point of no movement.

2.4 Design Criteria

2.4.1 Overview

Like the design of any structural component, the design of a pier or column is performed to fulfill strength and serviceability requirements. A pier should be designed to withstand the overturning, sliding forces applied from superstructure as well as the forces applied to substructures. It also needs to be designed so that during an extreme event it will prevent the collapse of the structure but may sustain some damage.

A pier as a structure component is subjected to combined forces of axial, bending, and shear. For a pier, the bending strength is dependent upon the axial force. In the plastic hinge zone of a pier, the shear strength is also influenced by bending. To complicate the behavior even more, the bending moment will be magnified by the axial force due to the P-Δ effect.

In current design practice, the bridge designers are becoming increasingly aware of the adverse effects of earthquake. Therefore, ductility consideration has become a very important factor for bridge design. Failure due to scouring is also a common cause of failure of bridges. In order to prevent this type of failure, the bridge designers need to work closely with the hydraulic engineers to determine adequate depths for the piers and provide proper protection measures.

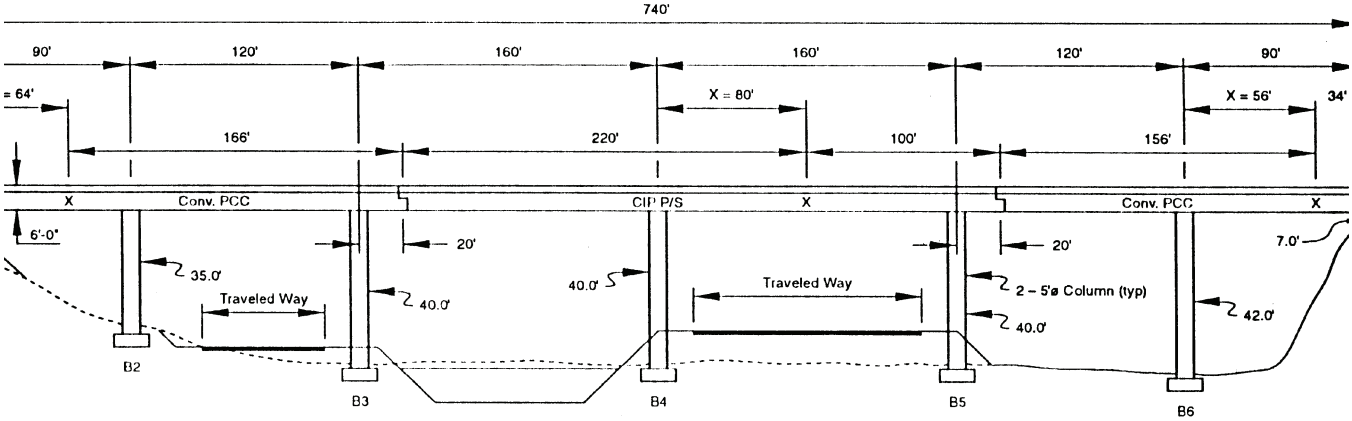

	A1		B2		B3			B4		B5			B6		A7		
$(I)^4$	1.38		61.36		61.36			61.36		61.36			61.36		102		
(Ft)	5.50		35.0		40.0		Sum	40.0		40.0		Sum	42.0		7.0		Sum
(kips) @ 1" side sway	1200	+	618	+	415	=	2,233	415	+	415	=	830	359	Will slide +	600	=	959
(distance from 1st member of frame)	0		90		210			0		160			0		90		
$\Sigma D / 100$	0	+	556	+	872	=	1,428	0	+	664	=	664	0	+	540	=	540
$X = \frac{\Sigma(P \times D) / 100}{\Sigma P} (100) = \frac{1,428}{2,233} (100) = \underline{64'}$								$\frac{664}{830} (100) = \underline{80'}$					$\frac{540}{959} (100) = \underline{56'}$				

Notes:
- Width of Structure = 78'
- Diameter of Column = 5'-0"
- K/Pile @ 1" deflection = 100 kips
- Point of No Movement = X
- Refer to Properties/Piles Table

Assumptions:
1. Super str. inf. rigid
2. Columns fixed top and bottom
3. Abutment footing will slide @ a force equal to D.W.
4. E (piles) = 4×10^6 psi
   E (columns) = 3×10^6 psi

Fixed/Fixed Condition

$P (Col.) = 12EI \frac{\Delta}{L^3}$

@ 1" defl. $= \frac{432 I}{\left(\frac{L}{10}\right)^3}$

Pinned/Fixed Condition

$P (Col.) = 3EI \frac{\Delta}{L^3}$

@ 1" defl. $= \frac{108 I}{\left(\frac{L}{10}\right)^3}$

D.W. Abut 7 = 600 k (assume linear up to 1" deflection)

$I (abut) = \frac{78}{12} (2.5)^3$

$= 102$

FIGURE 2.7 Calculation of points of no movement.

2.4.2 Slenderness and Second-Order Effect

The design of compression members must be based on forces and moments determined from an analysis of the structure. Small deflection theory is usually adequate for the analysis of beam-type members. For compression members, however, the second-order effect must be considered. According to AASHTO LRFD [1], the second-order effect is defined as follows:

> The presence of compressive axial forces amplify both out-of-straightness of a component and the deformation due to non-tangential loads acting thereon, therefore increasing the eccentricity of the axial force with respect to the centerline of the component. The synergistic effect of this interaction is the apparent softening of the component, i.e., a loss of stiffness.

To assess this effect accurately, a properly formulated large deflection nonlinear analysis can be performed. Discussions on this subject can be found in References [3,4]. However, it is impractical to expect practicing engineers to perform this type of sophisticated analysis on a regular basis. The moment magnification procedure given in AASHTO LRFD [1] is an approximate process which was selected as a compromise between accuracy and ease of use. Therefore, the AASHTO LRFD moment magnification procedure is outlined in the following.

When the cross section dimensions of a compression member are small in comparison to its length, the member is said to be slender. Whether or not a member can be considered slender is dependent on the magnitude of the slenderness ratio of the member. The slenderness ratio of a compression member is defined as, KL_u/r, where K is the effective length factor for compression members; L_u is the unsupported length of compression member; r is the radius of gyration = $\sqrt{I/A}$; I is the moment of inertia; and A is the cross-sectional area.

When a compression member is braced against side sway, the effective length factor, $K = 1.0$ can be used. However, a lower value of K can be used if further analysis demonstrates that a lower value is applicable. L_u is defined as the clear distance between slabs, girders, or other members which is capable of providing lateral support for the compression member. If haunches are present, then, the unsupported length is taken from the lower extremity of the haunch in the plane considered (AASHTO LRFD 5.7.4.3). For a detailed discussion of the K-factor, please refer to Chapter 8.

For a compression member braced against side sway, the effects of slenderness can be ignored as long as the following condition is met (AASHTO LRFD 5.7.4.3):

$$\frac{KL_u}{r} < 34 - \left(\frac{12M_{1b}}{M_{2b}}\right) \tag{2.1}$$

where

M_{1b} = smaller end moment on compression member — positive if member is bent in single curvature, negative if member is bent in double curvature

M_{2b} = larger end moment on compression member — always positive

For an unbraced compression member, the effects of slenderness can be ignored as long as the following condition is met (AASHTO LRFD 5.7.4.3):

$$\frac{KL_u}{r} < 22 \tag{2.2}$$

If the slenderness ratio exceeds the above-specified limits, the effects can be approximated through the use of the moment magnification method. If the slenderness ratio KL_u/r exceeds 100, however, a more-detailed second-order nonlinear analysis will be required. Any detailed analysis should consider the influence of axial loads and variable moment of inertia on member stiffness and forces, and the effects of the duration of the loads.

The factored moments may be increased to reflect effects of deformations as follows:

$$M_c = \delta_b M_{2b} + \delta_s M_{2s} \tag{2.3}$$

where

M_{2b} = moment on compression member due to factored gravity loads that result in no appreciable side sway calculated by conventional first-order elastic frame analysis, always positive

M_{2s} = moment on compression member due to lateral or gravity loads that result in side sway, Δ, greater than $L_u/1500$, calculated by conventional first-order elastic frame analysis, always positive

The moment magnification factors are defined as follows:

$$\delta_b = \frac{C_m}{1 - \dfrac{P_u}{\phi P_c}} \geq 1.0 \tag{2.4}$$

$$\delta_s = \frac{1}{1 - \dfrac{\sum P_u}{\phi \sum P_c}} \geq 1.0 \tag{2.5}$$

where

P_u = factored axial load

P_c = Euler buckling load, which is determined as follows:

$$P_c = \frac{\pi^2 EI}{\left(KL_u\right)^2} \tag{2.6}$$

C_m, a factor which relates the actual moment diagram to an equivalent uniform moment diagram, is typically taken as 1.0. However, in the case where the member is braced against side sway and without transverse loads between supports, it may be taken by the following expression:

$$C_m = 0.60 + 0.40\left(\frac{M_{1b}}{M_{2b}}\right) \tag{2.7}$$

The value resulting from Eq. (2.7), however, is not to be less than 0.40.

To compute the flexural rigidity *EI* for concrete columns, AASHTO offers two possible solutions, with the first being:

$$EI = \frac{\dfrac{E_c I_g}{5} + E_s I_s}{1 + \beta_d} \tag{2.8}$$

and the second, more-conservative solution being:

$$EI = \frac{\dfrac{E_c I_g}{2.5}}{1 + \beta_d} \tag{2.9}$$

where E_c is the elastic modulus of concrete, I_g is the gross moment inertia, E_s is the elastic modules of reinforcement, I_s is the moment inertia of reinforcement about centroidal axis, and β is the ratio of maximum dead-load moment to maximum total-load moment and is always positive. It is an approximation of the effects of creep, so that when larger moments are induced by loads sustained over a long period of time, the creep deformation and associated curvature will also be increased.

2.4.3 Concrete Piers and Columns

2.4.3.1 Combined Axial and Flexural Strength

A critical aspect of the design of bridge piers is the design of compression members. We will use AASHTO LRFD Bridge Design Specifications [1] as the reference source. The following discussion provides an overview of some of the major criteria governing the design of compression members.

Under the Strength Limit State Design, the factored resistance is determined with the product of nominal resistance, P_n, and the resistance factor, ϕ. Two different values of ϕ are used for the nominal resistance P_n. Thus, the factored axial load resistance ϕP_n is obtained using $\phi = 0.75$ for columns with spiral and tie confinement reinforcement. The specifications also allows for the value ϕ to be linearly increased from the value stipulated for compression members to the value specified for flexure which is equal to 0.9 as the design axial load ϕP_n decreases from $0.10 f_c' A_g$ to zero.

Interaction Diagrams

Flexural resistance of a concrete member is dependent upon the axial force acting on the member. Interaction diagrams are usually used as aids for the design of the compression members. Interaction diagrams for columns are usually created assuming a series of strain distributions, and computing the corresponding values of P and M. Once enough points have been computed, the results are plotted to produce an interaction diagram.

Figure 2.8 shows a series of strain distributions and the resulting points on the interaction diagram. In an actual design, however, a few points on the diagrams can be easily obtained and can define the diagram rather closely.

- Pure Compression:

The factored axial resistance for pure compression, ϕP_n, may be computed by:

For members with spiral reinforcement:

$$P_r = \phi P_n = \phi 0.85 P_o = \phi 0.85 \left[0.85 f_c' \left(A_g - A_{st} \right) + A_{st} f_y \right] \tag{2.10}$$

For members with tie reinforcement:

$$P_r = \phi P_n = \phi 0.80 P_o = \phi 0.80 \left[0.85 f_c' \left(A_g - A_{st} \right) + A_{st} f_y \right] \tag{2.11}$$

For design, pure compression strength is a hypothetical condition since almost always there will be moments present due to various reasons. For this reason, AASHTO LRFD 5.7.4.4 limits the nominal axial load resistance of compression members to 85 and 80% of the axial resistance at zero eccentricity, P_o, for spiral and tied columns, respectively.

- Pure Flexure:

The section in this case is only subjected to bending moment and without any axial force. The factored flexural resistance, M_r, may be computed by

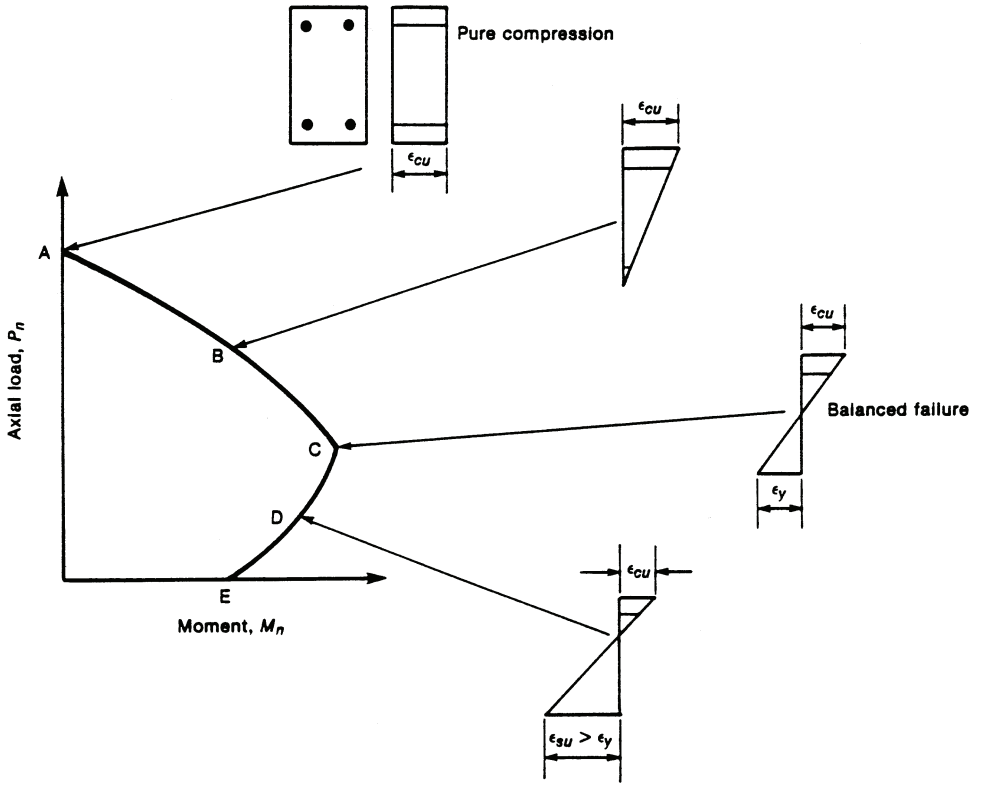

FIGURE 2.8 Strain distributions corresponding to points on interaction diagram.

$$M_r = \phi M_n = \phi\left[A_s f_y d\left(1 - 0.6\rho\frac{f_y}{f_c'}\right)\right] = \phi\left[A_s f_y\left(d - \frac{a}{2}\right)\right] \tag{2.12}$$

where

$$a = \frac{A_s f_y}{0.85 f_c' b}$$

- Balanced Strain Conditions:

Balanced strain conditions correspond to the strain distribution where the extreme concrete strain reaches 0.003 and the strain in reinforcement reaches yield at the same time. At this condition, the section has the highest moment capacity. For a rectangular section with reinforcement in one face, or located in two faces at approximately the same distance from the axis of bending, the balanced factored axial resistance, P_r, and balanced factored flexural resistance, M_r, may be computed by

$$P_r = \phi P_b = \phi\left[0.85 f_c' b a_b + A_s' f_s' - A_s f_y\right] \tag{2.13}$$

and

$$M_r = \phi M_b = \phi \left[0.85 f_c' b a_b \left(d - d'' - a_b/2 \right) + A_s' f_s' \left(d - d' - d'' \right) + A_s f_y d'' \right] \tag{2.14}$$

where

$$a_b = \left(\frac{600}{600 + f_y} \right) \beta_1 d$$

and

$$f_s' = 600 \left[1 - \left(\frac{d'}{d} \right) \left(600 + \frac{f_y}{600} \right) \right] \leq f_y$$

where f_y is in MPa.

Biaxial Bending

AASHTO LRFD 5.7.4.5 stipulates that the design strength of noncircular members subjected to biaxial bending may be computed, in lieu of a general section analysis based on stress and strain compatibility, by one of the following approximate expressions:

$$\frac{1}{P_{rxy}} = \frac{1}{P_{rx}} + \frac{1}{P_{ry}} - \frac{1}{P_o} \tag{2.15}$$

when the factored axial load, $P_u \geq 0.10 \phi f_c' A_g$

$$\frac{M_{ux}}{M_{rx}} + \frac{M_{uy}}{M_{ry}} \leq 1 \tag{2.16}$$

when the factored axial load, $P_u < 0.10 \phi f_c' A_g$

where

P_{rxy} = factored axial resistance in biaxial flexure

P_{rx}, P_{ry} = factored axial resistance corresponding to M_{rx}, M_{ry}

M_{ux}, M_{uy} = factored applied moment about the *x*-axis, *y*-axis

M_{rx}, M_{ry} = uniaxial factored flexural resistance of a section about the *x*-axis and *y*-axis corresponding to the eccentricity produced by the applied factored axial load and moment, and

P_o = $0.85 f_c' (A_g - A_s) + A_s f_y$

2.4.3.2 Shear Strength

Under the normal load conditions, the shear seldom governs the design of the column for conventional bridges since the lateral loads are usually small compared with the vertical loads. However, in a seismic design, the shear is very important. In recent years, the research effort on shear strength evaluation for columns has been increased remarkably. AASHTO LRFD provides a general shear equation that applies for both beams and columns. The concrete shear capacity component and the angle of inclination of diagonal compressive stresses are functions of the shear stress on the concrete and the strain in the reinforcement on the flexural tension side of the member. It is rather involved and hard to use.

Alternatively, the equations recommended by ATC-32 [5] can be used with acceptable accuracy. The recommendations are listed as follows.

Except for the end regions of ductile columns, the nominal shear strength provided by concrete, V_c, for members subjected to flexure and axial compression should be computed by

$$V_c = 0.165\left(1+(3.45)\left(10^{-6}\right)\frac{N_u}{A_g}\right)\sqrt{f_c'}A_e \quad \text{(MPa)} \tag{2.17}$$

If the axial force is in tension, the V_c should be computed by

$$V_c = 0.165\left(1+(1.38)\left(10^{-5}\right)\frac{N_u}{A_g}\right)\sqrt{f_c'}A_e \quad \text{(MPa)} \tag{2.18}$$

(note that N_u is negative for tension),

where
A_g = gross section area of the column (mm^2)
A_e = effective section area, can be taken as $0.8A_g$ (mm^2)
N_u = axial force applied to the column (N)
f_c' = compressive strength of concrete (MPa)

For end regions where the flexural ductility is normally high, the shear capacity should be reduced. ATC-32 [5] offers the following equations to address this interaction.

With the end region of columns extending a distance from the critical section or sections not less than $1.5D$ for circular columns or $1.5h$ for rectangular columns, the nominal shear strength provided by concrete subjected to flexure and axial compression should be computed by

$$V_c = 0.165\left(0.5+(6.9)\left(10^{-6}\right)\frac{N_u}{A_g}\right)\sqrt{f_c'}A_e \quad \text{(MPa)} \tag{2.19}$$

When axial load is tension, V_c can be calculated as

$$V_c = 0.165\left(1+(1.38)\left(10^{-5}\right)\frac{N_u}{A_g}\right)\sqrt{f_c'}A_e \quad \text{(MPa)} \tag{2.18}$$

Again, N_u should be negative in this case.

The nominal shear contribution from reinforcement is given by

$$V_s = \frac{A_v f_{yh} d}{s} \quad \text{(MPa)} \tag{2.20}$$

for tied rectangular sections, and by

$$V_s = \frac{\pi}{2}\frac{A_h f_{yh} D'}{s} \tag{2.21}$$

for spirally reinforced circular sections. In these equations, A_v is the total area of shear reinforcement parallel to the applied shear force, A_h is the area of a single hoop, f_{yh} is the yield stress of horizontal reinforcement, D' is the diameter of a circular hoop, and s is the spacing of horizontal reinforcement.

2.4.3.3 Ductility of Columns

The AASHTO LRFD [1] introduces the term *ductility* and requires that a structural system of bridge be designed to ensure the development of significant and visible inelastic deformations prior to failure.

The term *ductility* defines the ability of a structure and selected structural components to deform beyond elastic limits without excessive strength or stiffness degradation. In mathematical terms, the ductility μ is defined by the ratio of the total imposed displacement Δ at any instant to that at the onset of yield Δ_y. This is a measure of the ability for a structure, or a component of a structure, to absorb energy. The goal of seismic design is to limit the estimated maximum ductility demand to the ductility capacity of the structure during a seismic event.

For concrete columns, the confinement of concrete must be provided to ensure a ductile column. AASHTO LRFD [1] specifies the following minimum ratio of spiral reinforcement to total volume of concrete core, measured out-to-out of spirals:

$$\rho_s = 0.45\left(\frac{A_g}{A_c} - 1\right)\frac{f_c'}{f_{yh}} \tag{2.22}$$

The transverse reinforcement for confinement at the plastic hinges shall be determined as follows:

$$\rho_s = 0.16\frac{f_c'}{f_y}\left(0.5 + \frac{1.25P_u}{A_g f_c'}\right) \tag{2.23}$$

for which

$$\left(0.5 + \frac{1.25P_u}{A_g f_c'}\right) \geq 1.0$$

The total cross-sectional area (A_{sh}) of rectangular hoop (stirrup) reinforcement for a rectangular column shall be either

$$A_{sh} = 0.30ah_c\frac{f_c'}{f_{yh}}\left(\frac{A_g}{A_c} - 1\right) \tag{2.24}$$

or,

$$A_{sh} = 0.12ah_c\frac{f_c'}{f_y}\left(0.5 + \frac{1.25P_u}{A_g f_c'}\right) \tag{2.25}$$

whichever is greater,

where

a = vertical spacing of hoops (stirrups) with a maximum of 100 mm (mm)
A_c = area of column core measured to the outside of the transverse spiral reinforcement (mm^2)
A_g = gross area of column (mm^2)
A_{sh} = total cross-sectional area of hoop (stirrup) reinforcement (mm^2)
f_c' = specified compressive strength of concrete (Pa)
f_{yh} = yield strength of hoop or spiral reinforcement (Pa)
h_c = core dimension of tied column in the direction under consideration (mm)
ρ_s = ratio of volume of spiral reinforcement to total volume of concrete core (out-to-out of spiral)
P_u = factored axial load (MN)

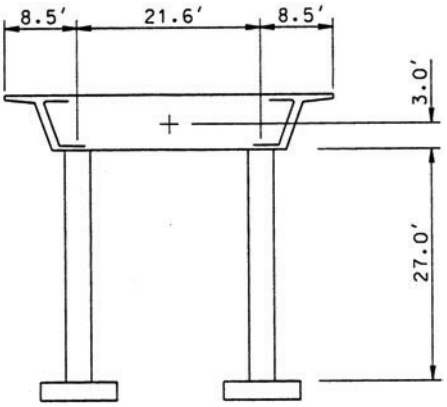

FIGURE 2.9 Example 2.2 — typical section.

TABLE 2.3 Column Group Loads — Service

		Live Load + Impact							
		Case 1	Case 2	Case 3					
	Dead Load	Trans $M_{y\text{-max}}$	Long $M_{x\text{-max}}$	Axial N-max	Wind	Wind on LL	Long Force	Centrifugal Force-M_y	Temp.
M_y (k-ft)	220	75	15	32	532	153	208	127	180
M_x (k-ft)	148	67	599	131	192	86	295	2	0
P (k)	1108	173	131	280	44	17	12	23	0

TABLE 2.4 Unreduced Seismic Loads (ARS)

	Case 1 Max. Transverse	Case 2 Max. Longitudinal
M_y — Trans (k-ft)	4855	3286
M_x — Long (k-ft)	3126	3334
P — Axial (k)	–282	–220

Example 2.2 Design of a Two-Column Bent

Design the columns of a two-span overcrossing. The typical section of the structure is shown in Figure 2.9. The concrete box girder is supported by a two-column bent and is subjected to HS20 loading. The columns are pinned at the bottom of the columns. Therefore, only the loads at the top of columns are given here. Table 2.3 lists all the forces due to live load plus impact. Table 2.4 lists the forces due to seismic loads. Note that a load reduction factor of 5.0 will be assumed for the columns.

Material Data

f_c' = 4.0 ksi (27.6 MPa) E_c = 3605 ksi (24855 MPa)

E_s = 29000 ksi (199946 MPa) f_y = 60 ksi (414 MPa)

Try a column size of 4 ft (1.22 m) in diameter. Provide 26-#9 (26-#30) longitudinal reinforcement. The reinforcement ratio is 1.44%.

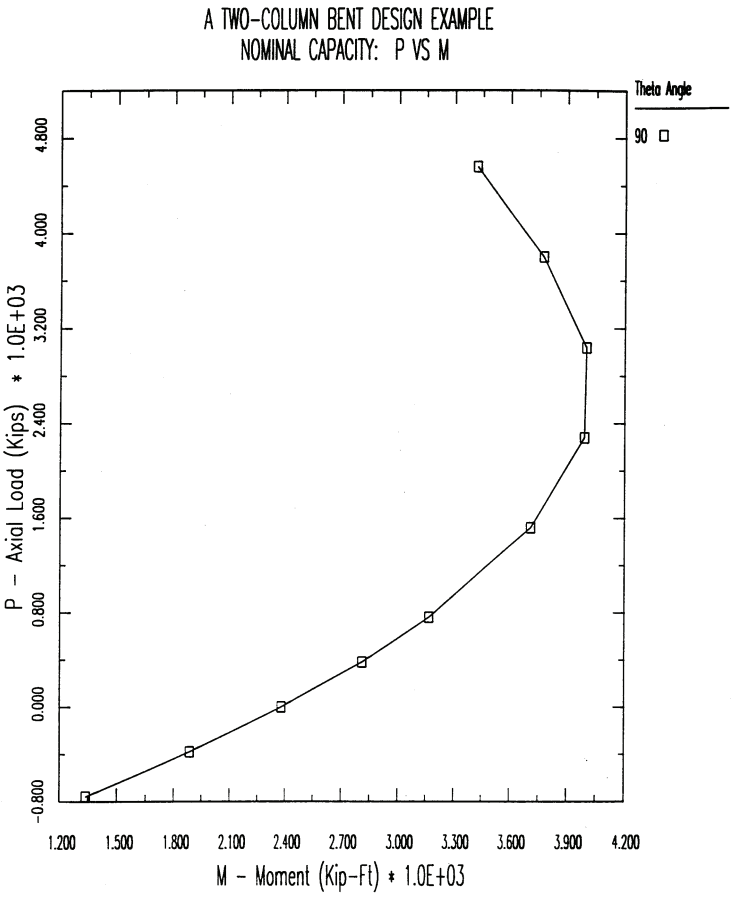

FIGURE 2.10 Example 2.2 — interaction diagram.

Section Properties

$A_g = 12.51$ ft^2 (1.16 m^2) $A_{st} = 26.0$ in^2 (16774 mm^2)

$I_{xc} = I_{yc} = 12.46$ ft^4 (0.1075 m^4) $I_{xs} = I_{ys} = 0.2712$ ft^4 (0.0023 m^4)

The analysis follows the procedure discussed in Section 2.4.3.1. The moment and axial force interaction diagram is generated and is shown in Figure 2.10.

Following the procedure outlined in Section 2.4.2, the moment magnification factors for each load group can be calculated and the results are shown in Table 2.5.

In which:

$$K_y = K_x = 2.10$$

$$K_yL/R = K_x\ L/R = 2.1 \times 27.0/(1.0) = 57$$

where R = radio of gyration = $r/2$ for a circular section.

$$22 < KL/R < 100 \quad \therefore \text{ Second-order effect should be considered.}$$

TABLE 2.5 Moment Magnification and Buckling Calculations

Load	P (k)	Moment Magnification			Cracked Transformed Section		Critical Buckling		Axial Load
Group	Case	Trans. M_{agy}	Long M_{agx}	Comb. M_{ag}	E^*I_y (k-ft^2)	E^*I_x (k-ft^2)	Trans. P_{cy} (k)	Long P_{cx} (k)	P(k)
I	1	1.571	1.640	1.587	1,738,699	1,619,399	5338	4972	1455
I	2	1.661	1.367	1.384	1,488,966	2,205,948	4571	6772	1364
I	3	2.765	2.059	2.364	1,392,713	1,728,396	4276	5306	2047
II		1.337	1.385	1.344	1,962,171	1,776,045	6024	5452	1137
III	1	1.406	1.403	1.405	2,046,281	2,056,470	6282	6313	1360
III	2	1.396	**1.344**	1.361	1,999,624	**2,212,829**	6139	**6793**	1305
III	3	1.738	1.671	1.708	1,901,005	2,011,763	5836	6176	1859
IV	1	1.437	1.611	1.455	1,864,312	1,494,630	5723	4588	1306
IV	2	1.448	1.349	1.377	1,755,985	2,098,586	5391	6443	1251
IV	3	1.920	1.978	1.936	1,635,757	1,585,579	5022	4868	1805
V		1.303	1.365	1.310	2,042,411	1,776,045	6270	5452	1094
VI	1	1.370	1.382	1.373	2,101,830	2,056,470	6453	6313	1308
VI	2	1.358	1.327	1.340	2,068,404	2,212,829	6350	6793	1256
VI	3	1.645	1.629	1.640	1,980,146	2,011,763	6079	6176	1788
VII	1	1.243	1.245	1.244	2,048,312	2,036,805	6288	6253	826
VII	2	1.296	1.275	1.286	1,940,100	2,053,651	5956	6305	888

Note: Column assumed to be unbraced against side sway.

The calculations for Loading Group III and Case 2 will be demonstrated in the following:

Bending in the longitudinal direction: M_x

$$\text{Factored load} = 1.3[\beta_D D + (L + I) + CF + 0.3W + WL + LF]$$

$\beta_D = 0.75$ when checking columns for maximum moment or maximum eccentricities and associated axial load. β_d in Eq. (2.8) = max dead-load moment, M_{DL}/max total moment, M_t.

$$M_{DL} = 148 \times 0.75 = 111 \text{ k-ft (151 kN·m)}$$

$$M_t = 0.75 \times 148 + 599 + 0.3 \times 192 + 86 + 295 + 2 = 1151 \text{ k-ft (1561 kN·m)}$$

$$\beta_d = 111/1151 = 0.0964$$

$$EI_x = \frac{\dfrac{E_c I_g}{5} + E_s I_s}{1+\beta_d} = \frac{\dfrac{3605 \times 144 \times 12.46}{5} + 29{,}000 \times 144 \times 0.2712}{1 + 0.0964} = 2{,}212{,}829 \text{ k-ft}^2$$

$$P_{cx} = \frac{\pi^2 EI_x}{(KL_u)^2} = \frac{\pi^2 \times 2{,}212{,}829}{(2.1 \times 27)^2} = 6793 \text{ kips } (30{,}229 \text{ kN})$$

$$C_m = 1.0 \text{ for frame braced against side sway}$$

$$\delta_s = \frac{1}{1 - \dfrac{\sum P_u}{\phi \sum P_c}} = \frac{1}{1 - \dfrac{1305}{0.75 \times 6793}} = 1.344$$

The magnified factored moment = $1.344 \times 1.3 \times 1151 = 2011$ k-ft (2728 kN·m)

TABLE 2.6 Comparison of Factored Loads to Factored Capacity of the Column

		Applied Factored Forces (k-ft)				Capacity (k-ft)			
Group	Case	Trans. M_y	Long M_x	Comb. M	Axial P (k)	ϕM_n	ϕ	Ratio M_u/M	Status
I	1	852	475	975	1455	2924	0.75	3.00	OK
I	2	566	1972	2051	1364	2889	0.75	1.41	OK
I	3	1065	981	1448	2047	3029	0.75	2.09	OK
II		1211	546	1328	1137	2780	0.75	2.09	OK
III	1	1622	1125	1974	1360	2886	0.75	1.46	OK
III	2	1402	**2011**	2449	1305	2861	0.75	1.17	OK
III	3	1798	1558	2379	1859	3018	0.75	1.27	OK
IV	1	1022	373	1088	1306	2865	0.75	2.63	OK
IV	2	813	1245	1487	1251	2837	0.75	1.91	OK
IV	3	1136	717	1343	1805	3012	0.75	2.24	OK
V		1429	517	1519	1094	2754	0.75	1.81	OK
VI	1	1829	1065	2116	1308	2864	0.75	1.35	OK
VI	2	1617	1905	2499	1256	2842	0.75	1.14	OK
VI	3	2007	1461	2482	1788	3008	0.75	1.21	OK
VII	1	1481	963	1766	826	2372	0.67	1.34	OK
VII	2	1136	1039	1540	888	2364	0.65	1.54	OK

Notes:
1. Applied factored moments are magnified for slenderness in accordance with AASHTO LRFD.
2. The seismic forces are reduced by the load reduction factor $R = 5.0$.

$L = 27.00$ ft, $f_c' = 4.00$ ksi, $F_y = 60.0$ ksi, $A_{st} = 26.00$ in.^{2}

The analysis results with the comparison of applied moments to capacities are summarized in Table 2.6.

Column lateral reinforcement is calculated for two cases: (1) for applied shear and (2) for confinement. Typically, the confinement requirement governs. Apply Eq. 2.22 or Eq. 2.23 to calculate the confinement reinforcement. For seismic analysis, the unreduced seismic shear forces should be compared with the shear forces due to plastic hinging of columns. The smaller should be used. The plastic hinging analysis procedure is discussed elsewhere in this handbook and will not be repeated here.

The lateral reinforcement for both columns are shown as follows.

For left column:

V_u = 148 kips (659 kN) (shear due to plastic hinging governs)

ϕV_n = 167 kips (743 kN) $\therefore$ No lateral reinforcement is required for shear.

Reinforcement for confinement = $\rho_s = 0.0057$ $\therefore$ Provide #4 at 3 in. (#15 at 76 mm)

For right column:

V_u = 180 kips (801 kN) (shear due to plastic hinging governs)

ϕV_n = 167 kips (734 kN)

ϕV_s = 13 kips (58 kN) (does not govern)

Reinforcement for confinement = $\rho_s = 0.00623$ $\therefore$ Provide #4 at 2.9 in. (#15 at 74 mm)

Summary of design:
4 ft (1.22 m) diameter of column with 26-#9 (26-#30) for main reinforcement and #4 at 2.9 in. (#15 at 74 mm) for spiral confinement.

FIGURE 2.11 Typical cross sections of composite columns.

2.4.4 Steel and Composite Columns

Steel columns are not as commonly used as concrete columns. Nevertheless, they are viable solutions for some special occasions, e.g., in space-restricted areas. Steel pipes or tubes filled with concrete known as composite columns (Figure 2.11) offer the most efficient use of the two basic materials. Steel at the perimeter of the cross section provides stiffness and triaxial confinement, and the concrete core resists compression and prohibits local elastic buckling of the steel encasement. The toughness and ductility of composite columns makes them the preferred column type for earthquake-resistant structures in Japan. In China, the composite columns were first used in Beijing subway stations as early as 1963. Over the years, the composite columns have been used extensively in building structures as well as in bridges [6–9].

In this section, the design provisions of AASHTO LRFD [1] for steel and composite columns are summarized.

Compressive Resistance

For prismatic members with at least one plane of symmetry and subjected to either axial compression or combined axial compression and flexure about an axis of symmetry, the factored resistance of components in compression, P_r, is calculated as

$$P_r = \phi_c P_n$$

where
P_n = nominal compressive resistance
ϕ_c = resistance factor for compression = 0.90

The nominal compressive resistance of a steel or composite column should be determined as

$$P_n = \begin{cases} 0.66^{\lambda} F_e A_s & \text{if} \quad \lambda \le 2.25 \\ \dfrac{0.88 F_e A_s}{\lambda} & \text{if} \quad \lambda > 2.25 \end{cases} \tag{2.26}$$

in which

For steel columns:

$$\lambda = \left(\frac{KL}{r_s} \pi \right)^2 \frac{F_y}{E_e} \tag{2.27}$$

For composite column:

$$\lambda = \left(\frac{KL}{r_s}\pi\right)^2 \frac{F_e}{E_e} \tag{2.28}$$

$$F_e = F_y + C_1 F_{yr}\left(\frac{A_r}{A_s}\right) + C_2 f_c\left(\frac{A_c}{A_s}\right) \tag{2.29}$$

$$E_e = E\left[1 + \left(\frac{C_3}{n}\right)\left(\frac{A_c}{A_s}\right)\right] \tag{2.30}$$

where
A_s = cross-sectional area of the steel section (mm^2)
A_c = cross-sectional area of the concrete (mm^2)
A_r = total cross-sectional area of the longitudinal reinforcement (mm^2)
F_y = specified minimum yield strength of steel section (MPa)
F_{yr} = specified minimum yield strength of the longitudinal reinforcement (MPa)
f_c' = specified minimum 28-day compressive strength of the concrete (MPa)
E = modules of elasticity of the steel (MPa)
L = unbraced length of the column (mm)
K = effective length factor
n = modular ratio of the concrete
r_s = radius of gyration of the steel section in the plane of bending, but not less than 0.3 times the width of the composite member in the plane of bending for composite columns, and, for filled tubes,

$$C_1 = 1.0; \quad C_2 = 0.85; \quad C_3 = 0.40$$

In order to use the above equation, the following limiting width/thickness ratios for axial compression of steel members of any shape must be satisfied:

$$\frac{b}{t} \le k\sqrt{\frac{E}{F_y}} \tag{2.31}$$

where
k = plate buckling coefficient as specified in Table 2.7
b = width of plate as specified in Table 2.7
t = plate thickness (mm)

Wall thickness of steel or composite tubes should satisfy:

For circular tubes:

$$\frac{D}{t} \le 2.8\sqrt{\frac{E}{F_y}}$$

TABLE 2.7 Limiting Width-to-Thickness Ratios

	k	b
		Plates Supported along One Edge
Flanges and projecting leg or plates	0.56	Half-flange width of I-section Full-flange width of channels Distance between free edge and first line of bolts or welds in plates Full-width of an outstanding leg for pairs of angles on continuous contact
Stems of rolled tees	0.75	Full-depth of tee
Other projecting elements	0.45	Full-width of outstanding leg for single-angle strut or double-angle strut with separator Full projecting width for others
		Plates Supported along Two Edges
Box flanges and cover plates	1.40	Clear distance between webs minus inside corner radius on each side for box flanges Distance between lines of welds or bolts for flange cover plates
Webs and other plates elements	1.49	Clear distance between flanges minus fillet radii for webs of rolled beams Clear distance between edge supports for all others
Perforated cover plates	1.86	Clear distance between edge supports

For rectangular tubes:

$$\frac{b}{t} \le 1.7\sqrt{\frac{E}{F_y}}$$

where
D = diameter of tube (mm)
b = width of face (mm)
t = thickness of tube (mm)

Flexural Resistance

The factored flexural resistance, M_r, should be determined as

$$M_r = \phi_f M_n \tag{2.32}$$

where
M_n = nominal flexural resistance
ϕ_f = resistance factor for flexure, $\phi_f = 1.0$

The nominal flexural resistance of concrete-filled pipes that satisfy the limitation

$$\frac{D}{t} \le 2.8\sqrt{\frac{E}{F_y}}$$

may be determined:

$$\text{If } \frac{D}{t} < 2.0\sqrt{\frac{E}{F_y}}, \text{ then } M_n = M_{ps} \tag{2.33}$$

$$\text{If } 2.0\sqrt{\frac{E}{F_y}} < \frac{D}{t} \le 8.8\sqrt{\frac{E}{F_y}}, \text{ then } M_n = M_{yc} \tag{2.34}$$

where
M_{ps} = plastic moment of the steel section
M_{yc} = yield moment of the composite section

Combined Axial Compression and Flexure

The axial compressive load, P_u, and concurrent moments, M_{ux} and M_{uy}, calculated for the factored loadings for both steel and composite columns should satisfy the following relationship:

$$\text{If } \frac{P_u}{P_r} < 0.2, \text{ then } \frac{P_u}{2.0P_r} + \left(\frac{M_{ux}}{M_{rx}} + \frac{M_{uy}}{M_{ry}}\right) \le 1.0 \tag{2.35}$$

$$\text{If } \frac{P_u}{P_r} \ge 0.2, \text{ then } \frac{P_u}{P_r} + \frac{8.0}{9.0}\left(\frac{M_{ux}}{M_{rx}} + \frac{M_{uy}}{M_{ry}}\right) \le 1.0 \tag{2.36}$$

where
P_r = factored compressive resistance
M_{rx}, M_{ry} = factored flexural resistances about x and y axis, respectively
M_{ux}, M_{uy} = factored flexural moments about the x and y axis, respectively

References

1. AASHTO, *LRFD Bridge Design Specifications,* 1st ed., American Association of State Highway and Transportation Officials, Washington, D.C., 1994.
2. Caltrans, Bridge Memo to Designers (7-10), California Department of Transportation, Sacramento, 1994.
3. White, D. W. and Hajjar, J. F., Application of second-order elastic analysis in LRFD: research to practice, *Eng. J.,* 28(4), 133, 1994.
4. Galambos, T. V., Ed., *Guide to Stability Design for Metal Structures*, 4th ed., the Structural Stability Research Council, John Wiley & Sons, New York, 1988.
5. ATC, Improved Seismic Design Criteria for California Bridges: Provisional Recommendations, Applied Technology Council, Report ATC-32, Redwood City, CA, 1996.
6. Cai, S.-H., Chinese standard for concrete-filled tube columns, in *Composite Construction in Steel and Concrete II,* Proc. of an Engineering Foundation Conference, Samuel Easterling, W. and Kim Roddis, W. M., Eds, Potosi, MO, 1992, 143.
7. Cai, S.-H., Ultimate strength of concrete-filled tube columns, in *Composite Construction in Steel and Concrete,* Proc. of an Engineering Foundation Conference, Dale Buckner, C. and Viest, I. M., Eds, Henniker, NH, 1987, 703.
8. Zhong, S.-T., New concept and development of research on concrete-filled steel tube (CFST) members, in *Proc. 2nd Int. Symp. on Civil Infrastructure Systems*, 1996.
9. CECS 28:90, *Specifications for the Design and Construction of Concrete-Filled Steel Tubular Structures,* China Planning Press, Beijing [in Chinese], 1990.
10. AISC, *Load and Research Factor Design Specification for Structural Steel Buildings and Commentary,* 2nd ed., American Institute of Steel Construction, Chicago, IL, 1993.
11. Galambos, T. V. and Chapuis, J., LRFD Criteria for Composite Columns and Beam Columns, Revised Draft, Washington University, Department of Civil Engineering, St. Louis, MO, December 1990.

3

Towers

Charles Seim
T. Y. Lin International

3.1 Introduction

Towers are the most visible structural elements of long-span bridges. They project above the superstructure and are seen from all directions by viewers and by users. Towers give bridges their character and a unifying theme. They project a mnemonic image that people remember as a lasting impression of the bridge itself. As examples of the powerful imagery of towers, contrast the elegant art deco towers of the Golden Gate Bridge (Figure 3.1) with the utilitarian but timeless architecture of the towers of the San Francisco–Oakland Bay Bridge (Figure 3.2). Or contrast the massive, rugged stone towers of the Brooklyn Bridge (Figure 3.3) with the awkward confusing steel towers of the Williamsburg Bridge in New York City (Figure 3.4).

Towers can be defined as vertical steel or concrete structures projecting above the deck, supporting cables and carrying the forces to which the bridge is subjected to the ground. By this definition, towers are used only for suspension bridges or for cable-stayed bridges, or hybrid suspension–cable-stayed structures. The word *pylon* is sometimes used for the towers of cable–stayed bridges. Both *pylon* and *tower* have about the same meaning — a tall and narrow structure supporting itself and the roadway. In this chapter, the word *tower* will be used for both suspension and for cabled-stayed bridges, to avoid any confusion in terms.

Both suspension and cable-stayed bridges are supported by abutments or piers at the point where these structures transition to the approach roadway or the approach structure. Abutments are discussed in Chapter 4. Piers and columns that support the superstructure for other forms of bridge structures such as girders, trusses, or arches, usually do not project above the deck. Piers and columns are discussed in Chapter 2.

The famous bridges noted above were opened in 1937, 1936, 1883, and 1903, respectively, and, if well maintained, could continue to serve for another 100 years. Bridge engineers will not design structures like these today because of changing technologies. These bridges are excellent examples of enduring structures and can serve to remind bridge engineers that well-designed and maintained structures do

FIGURE 3.1 Golden Gate Bridge, San Francisco. (Courtesy of Charles Seim.)

last for 150 years or longer. Robust designs, durable materials, provisions for access for inspection and maintenance, and a well-executed maintenance program will help ensure a long life. The appearance of the bridge, good or bad, is locked in for the life of the facility and towers are the most important visual feature leading to the viewer's impression of an aesthetic structure.

3.2 Functions

The main structural function of the towers of cable-stayed and suspension bridges is carrying the weight of the bridge, traffic loads, and the forces of nature to the foundations. The towers must perform these functions in a reliable, serviceable, aesthetic, and economical manner for the life of the bridge, as towers, unlike other bridge components, cannot be replaced. Without reliability, towers may become unsafe and the life of the entire bridge could be shortened. Without serviceability being designed into the structure, which means that it is designed for access and ease of maintenance, the bridge will not provide continuing long service to the user. The public demands that long-span bridges be attractive, aesthetic statements with long lives, so as not to be wasteful of public funds.

3.3 Aesthetics

While the main function of the towers is structural, an important secondary function is visual. The towers reveal the character or motif of the bridge. The bridges used as examples in the introduction are good illustrations of the image of the structure as revealed by the towers. Indeed, perhaps they are famous because of their towers. Most people visualize the character of the Brooklyn Bridge by the gothic, arched, masonry towers alone. The San Francisco–Oakland Bay Bridge and the Golden Gate Bridge give completely different impressions to the viewer as conveyed by the towers. Seim [7] measured the ratios of the visible components of the towers of the latter two bridges and found important, but subtle, diminution of these ratios with height above the tower base. It is the subtle changes in these ratios within the height of the towers that produce the much-admired proportions

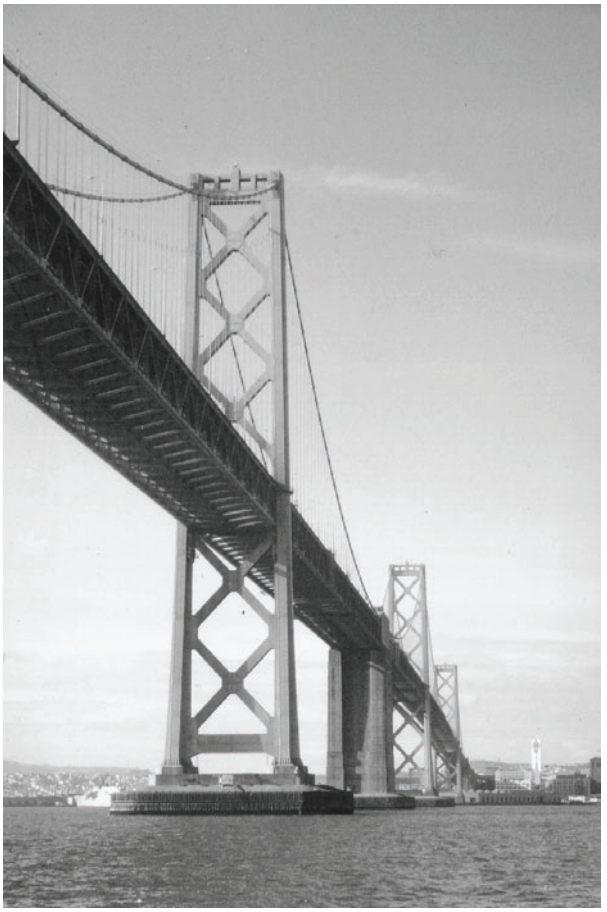

FIGURE 3.2 San Francisco–Oakland Bay Bridge. (Courtesy of Charles Seim.)

of these world-renowned bridges. The proportions of the towers for any new long-span bridge should be carefully shaped and designed to give the entire bridge a strong — even robust — graceful, and soaring visual image.

The aesthetics of the array of cables many times are of secondary importance to the aesthetics of the towers. However, the array or form of the cables must be considered in the overall aesthetic and structural evaluation of the bridge. Main cables of suspension bridges always drape in a parabolic curve that most people instinctively enjoy. The large diameter of the cables makes them stand out as an important contribution to the overall visual impression as the supporting element of the roadway.

The cables of cable-stayed bridges are usually of small diameter and do not stand out visually as strongly as do the cables of suspension bridges. However, the array of the stays, such as harp, fan, radiating star, or others, should be considered in context with the tower form. The separated, parallel cables of the harp form, for example, will not be as obtrusive to the towers as will other arrangements. However, the harp cable form may not be appropriate for very long spans or for certain tower shapes. The cables and the towers should be considered together as a visual system.

Billington [2] presents an overview of the importance of the role of aesthetics in the history of the development of modern bridge design. Leonhardt [5] presents many examples of completed bridges showing various tower shapes and cable arrangements for both suspension and cable-stayed bridges.

FIGURE 3.3 Brooklyn Bridge, New York. (Courtesy of Charles Seim.)

3.4 Conceptual Design

Perhaps the most important step in the design of a new bridge is the design concept for the structure that ultimately will be developed into a final design and then constructed. The cost, appearance, and reliability and serviceability of the facility will all be determined, for good or for ill, by the conceptual design of the structure. The cost can be increased, sometimes significantly, by a concept that is very difficult to erect. Once constructed, the structure will always be there for users to admire — or to criticize. The user ultimately pays for the cost of the facility and also usually pays for the cost of maintaining the structure. Gimsing [4] treats the concept design issues of both cable-stayed and suspension bridges very extensively and presents examples to help guide designers.

A proper bridge design that considers the four functions of reliability, serviceability, appearance, and cost together with an erectable scheme that requires low maintenance, is the ideal that the design concept should meet.

A recent trend is to employ an architect as part of the design team. Architects may view a structure in a manner different from engineers, and their roles in the project are not the same. The role of the engineer is to be involved in all four functions and, most importantly, to take responsibility for the structural adequacy of the bridge. The role of the architect generally only involves the function of aesthetics. Their roles overlap in achieving aesthetics, which may also affect the economy of the structure. Since both engineers and architects have as a common objective an elegant and economical bridge, there should be cooperation and respect between them.

Occasional differences do occur when the architect's aesthetic desires conflict with the engineer's structural calculations. Towers, as the most visible component of the bridge, seem to be a target for this type of conflict. Each professional must understand that these differences in viewpoints will occur and must be resolved for a successful and fruitful union between the two disciplines.

While economy is usually important, on occasions, cost is not an objective because the owner or the public desires a "symbolic" structure. The architect's fancy then controls and the engineer can only provide the functions of safety and serviceability.

FIGURE 3.4 Williamsburg Bridge, New York. (Courtesy of Charles Seim.)

3.4.1 Materials

Until the 1970s, steel was the predominant material used for the towers of both cable-stayed and suspension bridges. The towers were often rectangular in elevation with a cross-sectional shape of rectangular, cruciform, tee, or a similar shape easily fabricated in steel. Examples of suspension bridge steel tower design are the plain, rectangular steel towers for the two Delaware Memorial Bridges; the first constructed in 1951 and the parallel one in 1968 (Figure 3.5). An example of a cable-stayed bridge that is an exception to the rectangular tower form is the modified A-frame, weathering-steel towers of the Luling Bridge near New Orleans, 1983 (Figure 3.6).

The cross sections of steel towers are usually designed as a series of adjoining cells formed by shop-welding steel plates together in units from 6 to 12 m long. The steel towers for a suspension bridge, and for cable-stayed bridges with stays passing over the top of the tower in saddles, must be designed for the concentrated load from the saddles. The steel cellular towers for a cable-stayed bridge with cables framing in the towers must be designed for the local forces from the numerous anchorages of the cables.

Since the 1970s, reinforced concrete has been used in many forms with rectangular and other compact cross sections. Concrete towers are usually designed as hollow shafts to save weight and to reduce the amount of concrete and reinforcing bars required. As with steel towers, concrete towers must

FIGURE 3.5 Delaware Memorial Bridges. (Courtesy of D. Sailors.)

FIGURE 3.6 Luling Bridge, New Orleans, Louisiana. (Courtesy of Charles Seim.)

be designed for the concentrated load from the saddles at the top, if used, or for the local forces from the numerous anchorages of the cables framing into the tower shafts

Towers designed in steel will be lighter than towers designed in concrete, thus giving a potential for savings in foundation costs. Steel towers will generally be more flexible and more ductile and can be erected in less time than concrete towers. Steel towers will require periodic maintenance painting, although weathering steel can be used for nonmarine environments.

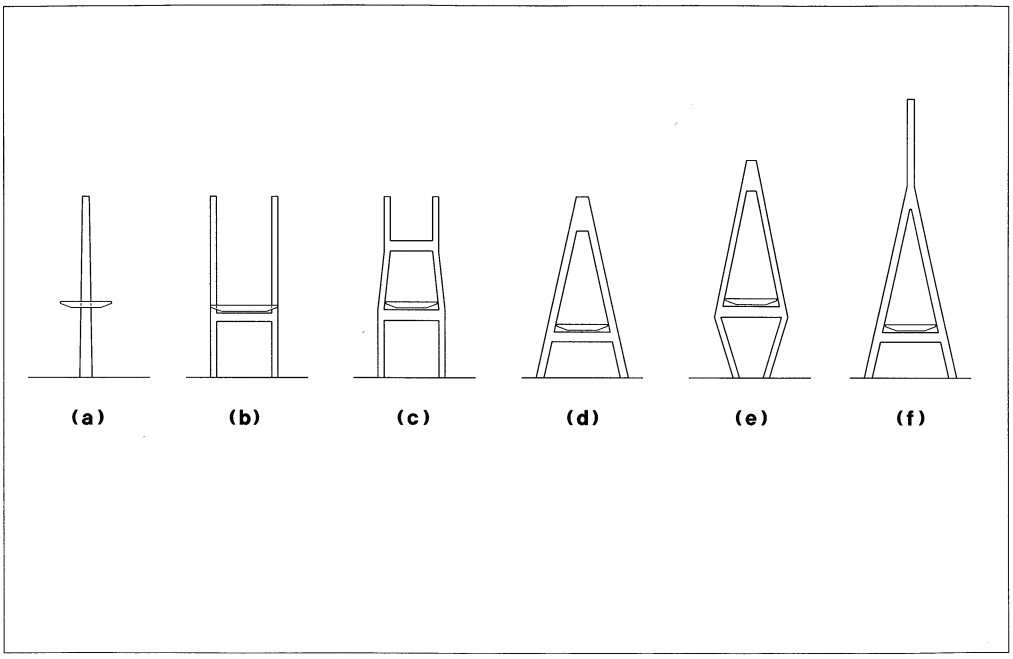

FIGURE 3.7 Generic forms for towers of cable-stayed bridges. (a) Single tower, I; (b) double vertical shafts, H; (c) double cranked shafts; (d) inclined shafts, A; (e) inclined shafts, diamond; (f) inverted Y.

The cost of steel or concrete towers can vary with a number of factors so that market conditions, contractor's experience, equipment availability, and the design details and site-specific influences will most likely determine whether steel or concrete is the most economical material. For pedestrian bridges, timber towers may be economical and aesthetically pleasing.

During the conceptual design phase of the bridge, approximate construction costs of both materials need to be developed and compared. If life-cycle cost is important, then maintenance operations and the frequencies of those operations need to be evaluated and compared, usually by a present-worth evaluation.

3.4.2 Forms and Shapes

Towers of cable-stayed bridges can have a wide variety of shapes and forms. Stay cables can also be arranged in a variety of forms. For conceptual design, the height of cable-stayed towers above the deck can be assumed to be about 20% of the main span length. To this value must be added the structural depth of the girder and the clearance to the foundation for determining the approximate total tower height. The final height of the towers will be determined during the final design phase.

The simplest tower form is a single shaft, usually vertical (Figure 3.7a). Occasionally, the single tower is inclined longitudinally. Stay cables can be arranged in a single plane to align with the tower or be splayed outward to connect with longitudinal edge beams. This form is usually employed for bridges with two-way traffic, to avoid splitting a one-way traffic flow. For roadways on curves, the single tower may be offset to the outside of the convex curve of the roadway and inclined transversely to support the curving deck more effectively.

Two vertical shafts straddling the roadway with or without cross struts above the roadway form a simple tower and are used with two planes of cables (Figure 3.7b) The stay cables would incline inward to connect to the girder, introducing a tension component across the deck support system; however, the girders are usually extended outward between the towers to align the cables vertically

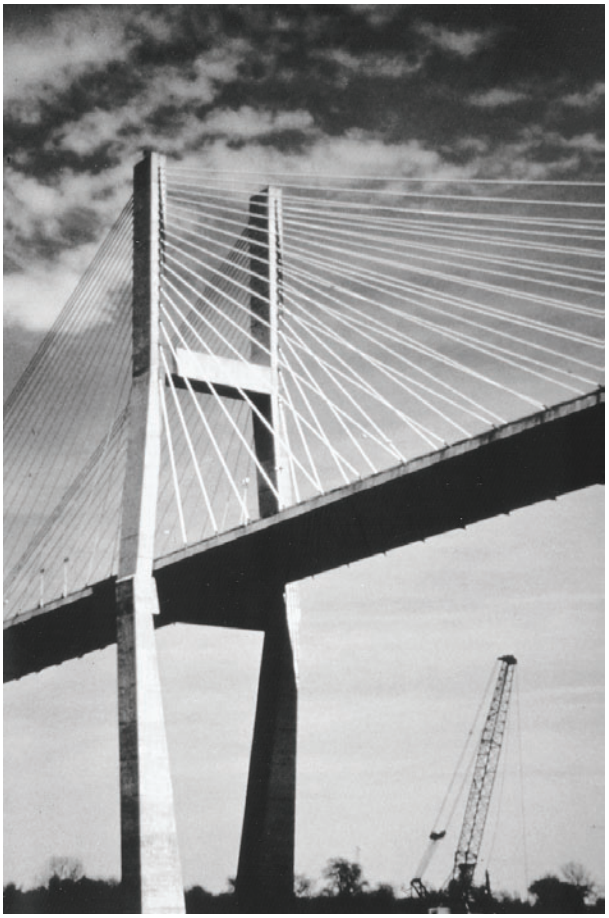

FIGURE 3.8 Talmadge Bridge, Georgia. (Courtesy of T. Y. Lin International.)

with the tower shafts. The tower shafts can also be "cranked" or offset above the roadway (Figure 3.7c). This allows the cables to be aligned in a vertical plane and to be attached to the girder, which can pass continuously through the towers as used for the Talmadge Bridge, Georgia (Figure 3.8). A horizontal strut is used between the tower shafts, offset to stabilize the towers.

The two shafts of cable-stayed bridges can be inclined inward toward each other to form a modified A-frame, similar to the Luling Bridge towers (Figure 3.6), or inclined to bring the shafts tops together to form a full A-frame (Figure 3.7d). The two planes of stay cables are inclined outward, producing a more desirable compression component across the deck support system.

The form of the towers of cable-stayed bridge below the roadway is also important for both aesthetics and costs. The shafts of the towers for a modified A-frame can be carried down to the foundations at the same slope as above the roadway, particularly for sites with low clearance. However, at high clearance locations, if the shafts of the towers for a full A-frame or for an inverted Y-frame are carried down to the foundations at the same slope as above the roadway, the foundations may become very wide and costly. The aesthetic proportions also may be affected adversely. Projecting the A-frame shafts downward vertically can give an awkward appearance. Sometimes the lower shafts are inclined inward under the roadway producing a modified diamond (Figure 3.7e), similar to the towers of the Glebe Island Bridge, Sidney, Australia (Figure 3.9). For very high roadways, the inward inclination can form a full diamond or a double diamond as in the Baytown Bridge, Texas (Figure 3.10). For very long spans requiring tall towers, the A-frame can be extended with a single vertical shaft forming an inverted Y shape (Figure 3.7f) as in the

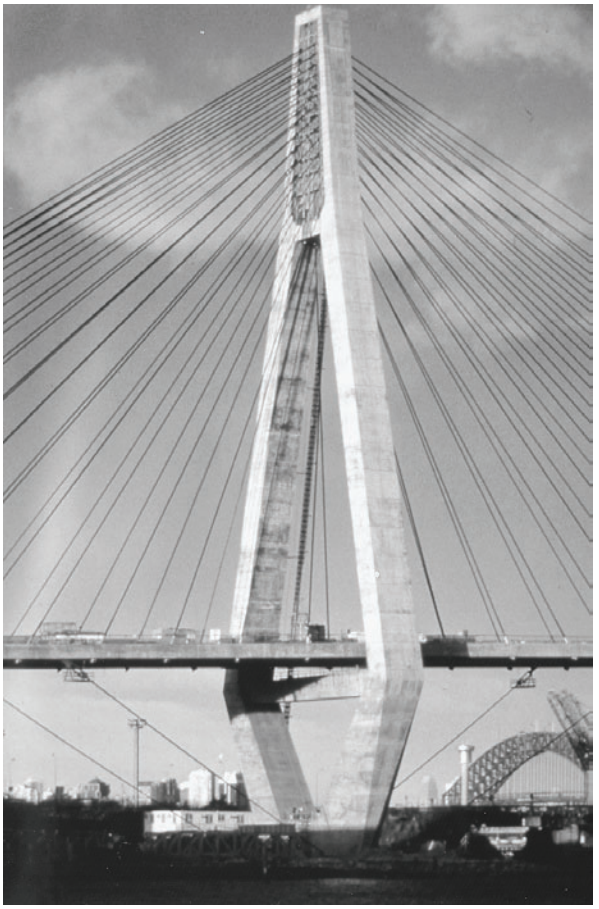

FIGURE 3.9 Glebe Island Bridge, Sidney, Australia. (Courtesy of T. Y. Lin International.)

Yang Pu Bridge, China (Figure 3.11). This form is very effective for very long spans where additional tower height is required and the inclined legs add stiffness and frame action for wind resistance.

The number of shafts or columns within the towers of cable-stayed bridges can vary from one to four. Three-shaft towers generally are not used for cable-stayed bridges except for very wide decks. Four-shaft towers can be used best to support two separate structures instead of a single wide deck. The towers could share a common foundation or each have its own foundation depending on the cost.

Suspension bridges can have from one to four cables depending on structural or architectural needs. Only a few single-cable suspension bridges have been designed with an A or inverted Y form of towers. Usually towers of suspension bridges follow a more traditional design using two vertical shafts and two planes of cables, as illustrated by the steel towers for the Delaware Memorial Bridges (see Figure 3.5). However, concrete towers have recently proved to be economical for some bridges. The very long span (1410 m) Humber Bridge, England, 1983, used uniformly spaced, multi-strut concrete towers (Figure 3.12). The crossing of the Great Belt seaway in Denmark (Figure 3.13), opening in 1999, has concrete towers 254 m high with two struts, one near the midheight and one at the top.

For conceptual designs, the height of suspension bridge towers above the deck depend on the sag-to-span ratio which can vary from about 1:8 to 1:12. A good preliminary value is about 1:10. To this value must be added the structural depth of the deck and the clearance to the foundations to obtain the approximate total tower height. The shafts are usually connected together with several

FIGURE 3.10 Baytown Bridge, Texas. (Courtesy of T. Y. Lin International.)

FIGURE 3.11 Yang Pu Bridge, China. (Courtesy of T. Y. Lin International.)

struts or cross-bracing along the height of the tower, or the shafts are connected at the top with a large single strut. Some form of strut is usually required for suspension bridges as the large cables carry lateral wind and seismic loads to the tops of the tower shafts, which then need to be braced against each other with cross struts to form a tower-frame action.

3.4.3 Erection

During the concept design phase, many different tower forms may be considered, and preliminary designs and cost estimates completed. Each alternative considered should have at least one method

FIGURE 3.12 Humber Bridge, England. (Courtesy of Charles Seim.)

of erection developed during the concept design phase to ensure that the scheme under consideration is feasible to construct. The cost of unusual tower designs can be difficult to estimate and can add significant cost to the project.

3.5 Final Design

The AASHTO Standard Specifications for Highway Bridges [1] apply to bridges 150 m or less in span. For important bridges and for long-span cable-supported bridge projects, special design criteria may have to be developed by the designer. The special design criteria may have to be also developed in cooperation with the owners of the facility to include their operations and maintenance requirements and their bridge-performance expectations after large natural events such as earthquakes. Troitsky [8], Podolny and Salzi [6], and Walter [9] present detailed design theory for cable-stayed bridges.

Design methodology for the towers should follow the same practice as the design methodology for the entire bridge. The towers should be part of a global analysis in which the entire structure is treated as a whole. From the global analyses, the towers can be modeled as a substructure unit with forces and deformations imposed as boundary conditions.

Detailed structural analyses form the basis for the final design of the tower and its components and connections. Both cabled-stayed and suspension bridges are highly indeterminate and require careful analysis in at least a geometric nonlinear program.

3.5.1 Design Loads

The towers are subject to many different loading cases. The towers, as well as the entire structure, must be analyzed, designed, and checked for the controlling loading cases.

The weight of the superstructure, including the self-weight of the towers, is obtained in the design process utilizing the unit weights of the materials used in the superstructure and distributed to the tower in accordance with a structural analysis of the completed structure or by the erection equipment during the construction phases.

Loads from traffic using the bridge such as trains, transit, trucks, or pedestrians are usually prescribed in design codes and specifications or by the owners of the facility. These are loads moving

FIGURE 3.13 Great Belt Bridge, Denmark. (Courtesy of Ben C. Gerwick, Inc.)

across the bridge and the forces imparted to the towers must be obtained from a structural analysis that considers the moving loading. These are all gravity effects that act downward on the structure, but will induce both vertical and horizontal forces on the towers.

A current trend for spanning wide widths of waterways is to design multispan bridges linked together to form a long, continuous structure. With ordinary tower designs, the multispan cable-stayed girders will deflect excessively under live loads as the towers will not be sufficiently stiffened by the cable stays anchored within the flexible adjacent spans. For multispan suspension bridges with ordinary tower designs, the same excessive live-load deflection can also occur. Towers for multispan cable-supported bridges must be designed to be sufficiently rigid to control live-load deflections.

Towers are also subject to temperature-induced displacements, both from the superstructure and cable framing into the towers, and from the temperature-induced movement of the tower itself. Towers can expand and contract differentially along the tower height from the sun shining on them from morning until sunset. These temperature effects can cause deflection and torsional twisting along the height of the tower.

Wind blowing on the towers as a bluff shape induces forces and displacements in the tower. Forces will be induced into the cables by the pressure of wind on the superstructure, as well as by the wind forces on the cables themselves. These additional forces will be carried to the towers.

For long-span bridges and for locations with known high wind speeds, wind should be treated as a dynamic loading. This usually requires a wind tunnel test on a sectional model of the super-

structure in a wind tunnel and, for important bridges, an aeroelastic model in a large wind tunnel. Under certain wind flows, the wind can also excite the tower itself, particularly if the tower is designed with light steel components. In the rare instances in which wind-induced excitation of the tower does occur, appropriate changes in the cross section of the tower can be made or a faring can be added to change the dynamic characteristics of the tower.

The seismic excitation should be treated as dynamic inertia loadings inducing response within the structure by exciting the vibrational modes of the towers. Induced seismic forces and displacement can control the design of towers in locations with high seismic activity. For locations with lower seismic activity, the tower design should be checked at least for code-prescribed seismic loadings.

A full analysis of the structure will reveal all of the forces, displacements, and other design requirements for all loading cases for the final tower design.

3.5.2 Design Considerations

Suspension bridge cables pass over cable saddles that are usually anchored to the top of the tower. A cable produces a large vertical force and smaller, but important, transverse and longitudinal forces from temperature, wind, earthquake, or from the unbalanced cable forces between main and side spans. These forces are transmitted through the cable saddle anchorage at each cable location to the top of the tower. The towers and the permanent saddle anchorages must be designed to resist these cable forces.

The erection of a suspension bridge must be analyzed and the sequence shown on the construction plans. To induce the correct loading into the cables of the side span, the erection sequence usually requires that the saddles be displaced toward the side spans. This is usually accomplished for short spans by displacing the tops of the towers by pulling with heavy cables. For long spans, the saddles can be displaced temporarily on rollers. As the stiffening deck elements are being erected into position and the cable begins to take loads, the towers or saddles are gradually brought into final vertical alignment. After the erection of the stiffening deck elements are completed, the saddles are permanently fastened into position to take the unbalanced cable loads from the center and the side spans.

At the deck level, other forces may be imposed on the tower from the box girder or stiffening truss carrying the roadway. These forces depend on the structural framing of the connection of the deck and tower. Traditional suspension bridge designs usually terminate the stiffening truss or box girder at the towers, which produces transverse, and longitudinal, forces on the tower at this point. Contemporary suspension bridge designs usually provide for passing a box girder continuously through the tower opening which may produce transverse forces but not longitudinal forces. For this arrangement, the longitudinal forces must be carried by the girder to the abutments.

The most critical area of the tower design is the tower-to-foundation connection. Both shear forces and moments are maximum at this point. Anchor bolts are generally used at the base of steel towers. The bolts must be proportioned to transfer the loads from the tower to the bolts. The bolts must be deeply embedded in the concrete footing block to transfer their loads to the footing reinforcement. Providing good drainage for the rainwater running down the tower shafts will increase the life of the steel paint system at the tower base and provide some protection to the anchor bolts.

Concrete towers must be joined to the foundations with full shear and moment connections. Lapped reinforcing bars splices are usually avoided as the lapping tends to congest the connections, the strength of the bars cannot be developed, and lapped splices cannot be used for high seismic areas. Using compact mechanical or welded splices will result in less congestion with easier placement of concrete around the reinforcement and a more robust tower-to-footing connection.

Careful coordination between the foundation designers and tower designers is required to achieve a stable, efficient, and reliable connection.

The cable arrangements for cable-stayed bridges are many and varied. Some arrangements terminate the cables in the tower, whereas other arrangements pass the cable through the tower on

cable saddles. Cables terminating in the tower can pass completely through the tower cross section and then anchor on the far side of the tower. This method of anchoring produces compression in the tower cross section at these anchorage points. Cables can also be terminated at anchors within the walls of the tower, producing tension in the tower cross section at the anchorage points. These tension forces require special designs to provide reliable, long-life support for the cables.

Just as for suspension bridges, the erection of cable-stayed bridges must be analyzed and the sequence shown on the construction plans. The girders, as they are erected outward from the towers, are very vulnerable. The critical erection sequence is just before closing the two arms of the girders at the center of the span. High winds can displace the arms and torque the towers, and heavy construction equipment can load the arms without benefit of girder continuity to distribute the loads.

3.6 Construction

Towers constructed of structural steel are usually fabricated in a shop by welding together steel plates and rolled shapes to form cells. Cells must be large enough to allow welders and welding equipment, and if the steel is to be painted, painters and cleaning and painting equipment inside each cell.

The steel tower components are transported to the bridge site and then erected by cranes and bolted together with high-strength bolts. The contractor should use a method of tensioning the high-strength bolts to give constant results and achieve the required tension. Occasionally, field welding is used, but this presents difficulties in holding the component rigidly in position while the weld is completed. Field welding can be difficult to control in poor weather conditions to achieve ductile welds, particularly for vertical and overhead welds. Full-penetration welds require backup bars that must be removed carefully if the weld is subject to fatigue loading.

Towers constructed of reinforced concrete are usually cast in forms that are removed and reused, or jumped to the next level. Concrete placing heights are usually restricted to about 6 to 12 m to limit form pressure from the freshly placed concrete. Reinforcing bar cages are usually preassembled on the ground or on a work barge, and lifted into position by crane. This requires the main load-carrying reinforcing bars to be spliced with each lift. Lapped splices are the easiest to make, but are not allowed in seismic areas.

Slip forming is an alternative method that uses forms that are pulled slowly upward, reinforcing bars positioned and the concrete placed in one continuous operation around the clock until the tower is completed. Slip forming can be economical, particularly for constant-cross-section towers. Some changes in cross section geometry can be accommodated. For shorter spans, precast concrete segments can be stacked together and steel tendons tensioned to form the towers.

Tower designers should consider the method of erection that contractors may use in constructing the towers. Often the design can reduce construction costs by incorporating more easily fabricated and assembled steel components or assembled reinforcing bar cages and tower shapes that are easily formed. Of course, the tower design cannot be compromised just to lower erection costs.

Some engineers and many architects design towers that are not vertical but are angled longitudinally toward or away from the main span. This can be done if such a design can be justified structurally and aesthetically, and the extra cost can be covered within the project budget. The difficulties of the design of longitudinally inclined towers must be carefully considered as well as the more expensive and slower erection, which will create additional costs.

Many towers of cable-stayed bridges have legs sloped toward each other to form an A, an inverted Y, a diamond, or similar shapes. These are not as difficult to construct as the longitudinally inclined tower design. The sloping concrete forms can be supported by vertical temporary supports and cross struts that tie the concrete forms together. This arrangement braces the partly cast concrete tower legs against each other for support. Some of the concrete form supports for the double-diamond towers of the Baytown Bridge are visible in Figure 3.9.

As the sloped legs are erected, the inclination may induce bending moments and lateral deflection in the plane of the slope of the legs. Both of these secondary effects must be adjusted by jacking the legs apart by a calculated amount of force or displacement to release the locked-in bending stresses. If the amount of secondary stress is small, then cambering the leg to compensate for the deflection and adding material to lower the induced stress can be used.

The jacking procedure adds cost but is an essential step in the tower erection. Neglecting this important construction detail can "lock-in" stresses and deflections that will lower the factor of safety of the tower and, in an extreme case, could cause a failure.

Tower construction usually requires special equipment to erect steel components or concrete forms to the extreme height of the tower. Suspension bridges and some cable-stayed bridges require cable saddles to be erected on the tower tops. Floating cranes rarely have the capacity to reach to the heights of towers designed for long spans. Tower cranes, connected to the tower as it is erected, can be employed for most tower designs and are a good choice for handling steel forms for the erection of concrete towers. A tower crane used to jump the forms and raise materials can be seen in Figure 3.9. Occasionally, vertical traveling cranes are used to erect steel towers by pulling themselves up the face of the tower following the erection of each new tower component.

The erection sequence for a suspension bridge may require that the towers be pulled by cables from the vertical toward the sides spans or that the cable saddles be placed on rollers and displaced toward the side spans on temporary supports. The tower restraints are gradually released or the rollers pushed toward their final position as the erection of the deck element nears completion. This operation is usually required to induce the design forces into the cables in the side spans. The cable saddles then are permanently anchored to the towers.

Because the tower erection must be done in stages, each stage must be checked for stability and for stresses and deflections. The specifications should require the tower erection to be checked by an engineer, employed by the contractor, for stability and safety at each erection stage. The construction specifications should also require the tower erection stages to be submitted to the design engineer for an evaluation. This evaluation should be thorough enough to determine if the proposed tower erection staging will meet the intent of the original design, or if it needs to be modified to bring the completed tower into compliance.

3.7 Summary

Towers provide the visible means of support of the roadway on which goods and people travel. Being the most visible elements in a bridge, they give the bridge, for good or for ill, its character, its motif, and its identifying aesthetic impression. Towers usually form structural portals through which people pass as they travel from one point to another. Of themselves, towers form an aesthetic structural statement.

Towers are the most critical structural element in the bridge as their function is to carry the forces imposed on the bridge to the ground. Unlike most other bridge components, they cannot be replaced during the life of the bridge. Towers must fulfill their function in a reliable, serviceable, economical, and aesthetic manner for the entire life of the bridge. Towers must also be practicable to erect without extraordinary expense.

Practicable tower shapes for cable-stayed bridges are many and varied. Towers can have one or several legs or shafts arrayed from vertical to inclined and forming A- or inverted Y-shaped frames. Suspension bridge towers are usually vertical, with two shafts connected with one or several struts.

The conceptual design is the most important phase in the design of a long-span bridge. This phase sets, among other items, the span length, type of deck system, and the materials and shape of the towers. It also determines the aesthetic, economics, and constructibility of the bridge. A conceptual erection scheme should be developed during this phase to ensure that the bridge can be economically constructed.

The final design phase sets the specific shape, dimensions, and materials for the bridge. A practical erection method should be developed during this phase and shown on the construction drawings. If an unusual tower design is used, the tower erection should also be shown. The specifications should allow the contractor to employ an alternative method of erection, provided that the method is designed by an engineer and submitted to the design engineer for review. It is essential that the design engineer follow the project into the construction stages. The designer must understand each erection step that is submitted by the contractor in accordance with the specifications, to ensure the construction complies with the design documents. Only by this means are owners assured that the serviceability and reliability that they are paying for are actually achieved in construction.

The successful design of a cable-stayed or a suspension bridge involves many factors and decisions that must be made during the planning, design, and construction phases of the project. Towers play an important role in that successful execution. The final judgment of a successful project is made by the people who use the facility and pay for its construction, maintenance, and long-life service to society.

References

1. AASHTO, *Standard Specifications for Highway Bridges,* American Association of State Highway and Transportation Officials, Washington, D.C., 1994.
2. Billington, D. P., *The Tower and the Bridge, The New Art of Structural Engineering,* Basic Books, New York, 1983.
3. Cerver, F. A., *New Architecture in Bridges,* Muntaner, Spain, 1992.
4. Gimsing, N. J., *Cable-Supported Bridges — Concept and Design,* John Wiley & Sons, New York, 1997.
5. Leonhardt, F., *Bridges, Aesthetics and Design,* MIT Press, Cambridge, MA, 1984.
6. Podolny, W. and Scalzi, J. B., *Construction and Design of Cable Stayed Bridges,* 2nd ed., John Wiley & Sons, New York, 1986.
7. Seim, C., San Francisco Bay's jeweled necklace, *ASCE Civil Eng.,* 66(1), 14A, 1996.
8. Troitsky, M. S., *Cable Stayed Bridges,* Van Nostrand Reinhold, 1988.
9. Walter, R., *Cable Stayed Bridges,* Thomas Telford, U.K., 1988.

4

Abutments and Retaining Structures

Linan Wang
California Transportation Department

Chao Gong
ICF Kaiser Engineers, Inc.

4.1 Introduction

As a component of a bridge, the abutment provides the vertical support to the bridge superstructure at the bridge ends, connects the bridge with the approach roadway, and retains the roadway base materials from the bridge spans. Although there are numerous types of abutments and the abutments for the important bridges may be extremely complicated, the analysis principles and design methods are very similar. In this chapter the topics related to the design of conventional highway bridge abutments are discussed and a design example is illustrated.

Unlike the bridge abutment, the earth-retaining structures are mainly designed for sustaining lateral earth pressures. Those structures have been widely used in highway construction. In this chapter several types of retaining structures are presented and a design example is also given.

4.2 Abutments

4.2.1 Abutment Types

Open-End and Closed-End Abutments

From the view of the relation between the bridge abutment and roadway or water flow that the bridge overcrosses, bridge abutments can be divided into two categories: open-end abutment and closed-end abutment, as shown in Figure 4.1.

For the open-end abutment, there are slopes between the bridge abutment face and the edge of the roadway or river canal that the bridge overcrosses. Those slopes provide a wide open area for the traffic flows or water flows under the bridge. It imposes much less impact on the environment

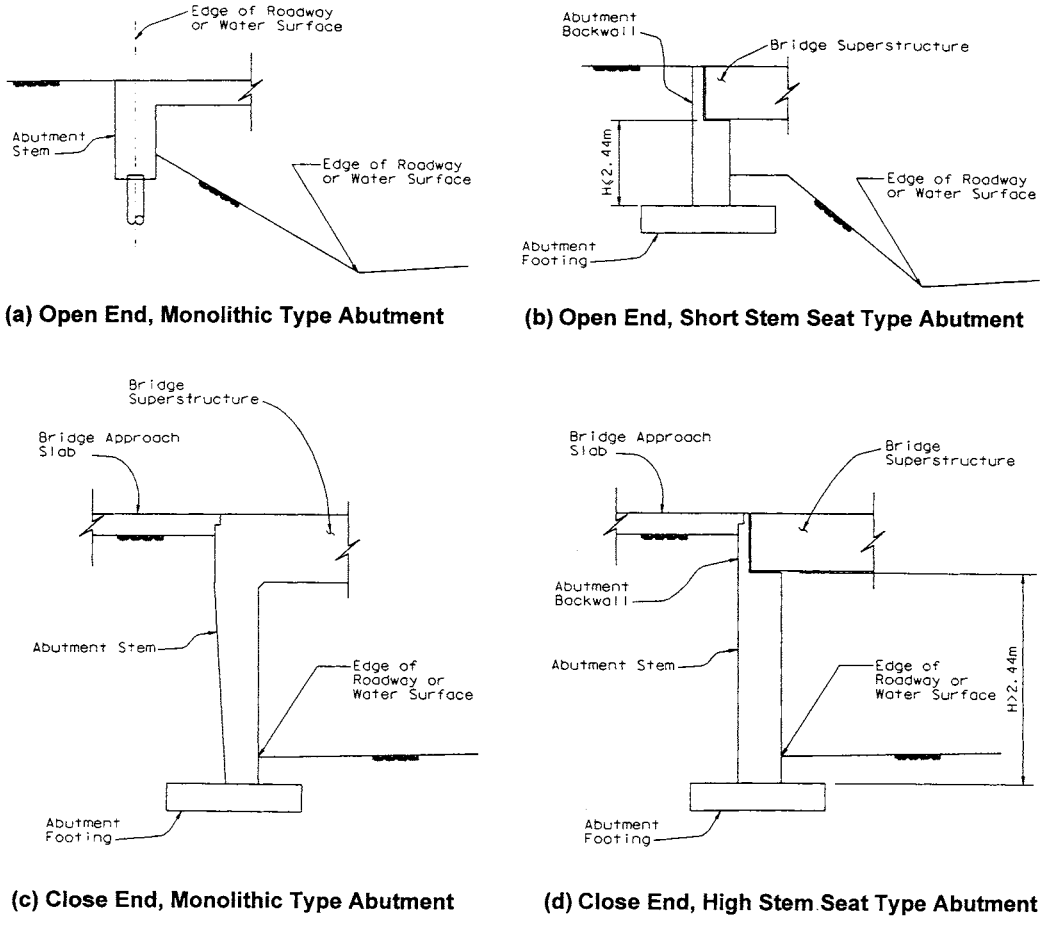

FIGURE 4.1 Typical abutment types.

and the traffic flows under the bridge than a closed-end abutment. Also, future widening of the roadway or water flow canal under the bridge by adjusting the slope ratios is easier. However, the existence of slopes usually requires longer bridge spans and some extra earthwork. This may result in an increase in the bridge construction cost.

The closed-end abutment is usually constructed close to the edge of the roadways or water canals. Because of the vertical clearance requirements and the restrictions of construction right of way, there are no slopes allowed to be constructed between the bridge abutment face and the edge of roadways or water canals, and high abutment walls must be constructed. Since there is no room or only a little room between the abutment and the edge of traffic or water flow, it is very difficult to do the future widening to the roadways and water flow under the bridge. Also, the high abutment walls and larger backfill volume often result in higher abutment construction costs and more settlement of road approaches than for the open-end abutment.

Generally, the open-end abutments are more economical, adaptable, and attractive than the closed-end abutments. However, bridges with closed-end abutments have been widely constructed in urban areas and for rail transportation systems because of the right-of-way restriction and the large scale of the live load for trains, which usually results in shorter bridge spans.

Monolithic and Seat-Type Abutments

Based on the connections between the abutment stem and the bridge superstructure, the abutments also can be grouped in two categories: the monolithic or end diaphragm abutment and the seat-type abutment, as shown in Figure 4.1.

The monolithic abutment is monolithically constructed with the bridge superstructure. There is no relative displacement allowed between the bridge superstructure and abutment. All the superstructure forces at the bridge ends are transferred to the abutment stem and then to the abutment backfill soil and footings. The advantages of this type of abutment are its initial lower construction cost and its immediate engagement of backfill soil that absorbs the energy when the bridge is subjected to transitional movement. However, the passive soil pressure induced by the backfill soil could result in a difficult-to-design abutment stem, and higher maintenance cost might be expected. In practice, this type of abutment is mainly constructed for short bridges.

The seat-type abutment is constructed separately from the bridge superstructure. The bridge superstructure seats on the abutment stem through bearing pads, rock bearings, or other devices. This type of abutment allows the bridge designer to control the superstructure forces that are to be transferred to the abutment stem and backfill soil. By adjusting the devices between the bridge superstructure and abutment, the bridge displacement can be controlled. This type of abutment may have a short stem or high stem, as shown in Figure 4.1. For a short-stem abutment, the abutment stiffness usually is much larger than the connection devices between the superstructure and the abutment. Therefore, those devices can be treated as boundary conditions in the bridge analysis. Comparatively, the high stem abutment may be subject to significant displacement under relatively less force. The stiffness of the high stem abutment and the response of the surrounding soil may have to be considered in the bridge analysis. The availability of the displacement of connection devices, the allowance of the superstructure shrinkage, and concrete shortening make this type of abutment widely selected for the long bridge constructions, especially for prestressed concrete bridges and steel bridges. However, bridge design practice shows that the relative weak connection devices between the superstructure and the abutment usually require the adjacent columns to be specially designed. Although the seat-type abutment has relatively higher initial construction cost than the monolithic abutment, its maintenance cost is relatively lower.

Abutment Type Selection

The selection of an abutment type needs to consider all available information and bridge design requirements. Those may include bridge geometry, roadway and riverbank requirements, geotechnical and right-of-way restrictions, aesthetic requirements, economic considerations, etc. Knowledge of the advantages and disadvantages for the different types of abutments will greatly benefit the bridge designer in choosing the right type of abutment for the bridge structure from the beginning stage of the bridge design.

4.2.2 General Design Considerations

Abutment design loads usually include vertical and horizontal loads from the bridge superstructure, vertical and lateral soil pressures, abutment gravity load, and the live-load surcharge on the abutment backfill materials. An abutment should be designed so as to withstand damage from the Earth pressure, the gravity loads of the bridge superstructure and abutment, live load on the superstructure or the approach fill, wind loads, and the transitional loads transferred through the connections between the superstructure and the abutment. Any possible combinations of those forces, which produce the most severe condition of loading, should be investigated in abutment design. Meanwhile, for the integral abutment or monolithic type of abutment, the effects of bridge superstructure deformations, including bridge thermal movements, to the bridge approach structures must be

TABLE 4.1 Abutment Design Loads (Service Load Design)

Abutment Design Loads	Case I	II	III	IV	V
Dead load of superstructure	X	X	—	X	X
Dead load of wall and footing	X	X	X	X	X
Dead load of earth on heel of wall including surcharge	X	X	X	X	—
Dead load of earth on toe of wall	X	X	X	X	—
Earth pressure on rear of wall including surcharge	X	X	X	X	—
Live load on superstructure	X	—	—	X	—
Temperature and shrinkage	—	—	—	X	—
Allowable pile capacity of allowable soil pressure in % or basic	100	100	150	125	150

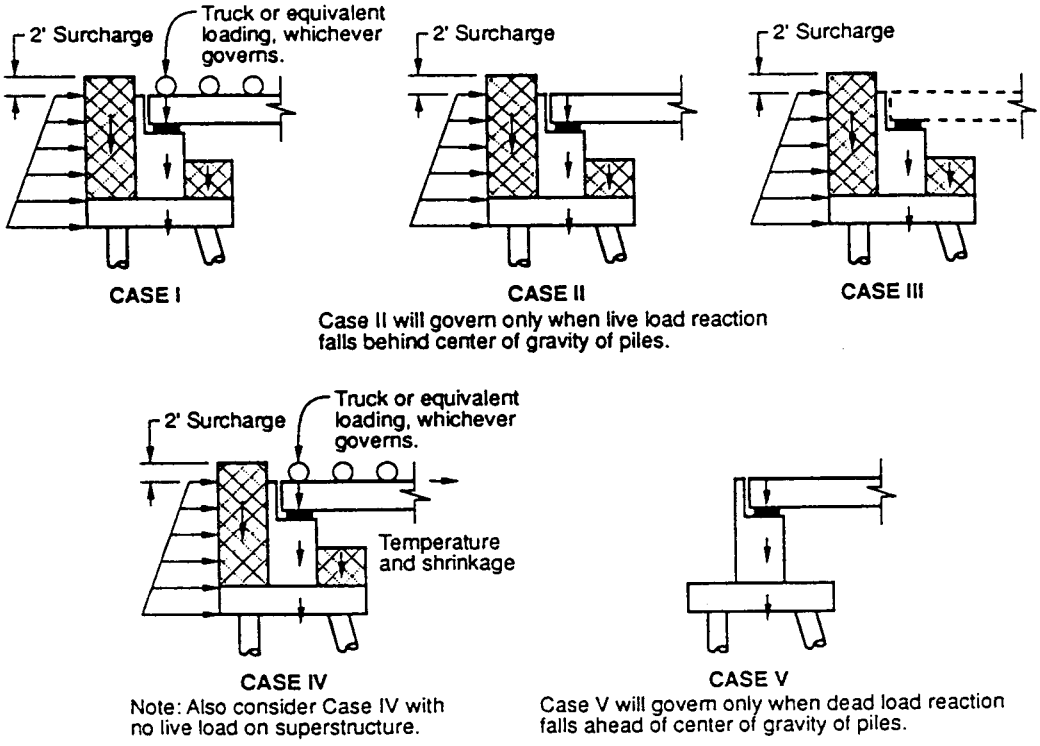

FIGURE 4.2 Configuration of abutment design load and load combinations.

considered in abutment design. Nonseismic design loads at service level and their combinations are shown in Table 4.1 and Figure 4.2. It is easy to obtain the factored abutment design loads and load combinations by multiplying the load factors to the loads at service levels. Under seismic loading, the abutment may be designed at no support loss to the bridge superstructure while the abutment may suffer some damages during a major earthquake.

The current AASHTO Bridge Design Specifications recommend that either the service load design or the load factor design method be used to perform an abutment design. However, due to the uncertainties in evaluating the soil response to static, cycling, dynamic, and seismic loading, the service load design method is usually used for abutment stability checks and the load factor method is used for the design of abutment components.

The load and load combinations listed in Table 4.1 may cause abutment sliding, overturning, and bearing failures. Those stability characteristics of abutment must be checked to satisfy certain

restrictions. For the abutment with spread footings under service load, the factor of safety to resist sliding should be greater than 1.5; the factor of safety to resist overturning should be greater than 2.0; the factor of safety against soil bearing failure should be greater than 3.0. For the abutment with pile support, the piles have to be designed to resist the forces that cause abutment sliding, overturning, and bearing failure. The pile design may utilize either the service load design method or the load factor design method.

The abutment deep shear failure also needs to be studied in abutment design. Usually, the potential of this kind of failure is pointed out in the geotechnical report to the bridge designers. Deep pilings or relocating the abutment may be used to avoid this kind of failure.

4.2.3 Seismic Design Considerations

Investigations of past earthquake damage to the bridges reveal that there are commonly two types of abutment earthquake damage — stability damage and component damage.

Abutment stability damage during an earthquake is mainly caused by foundation failure due to excessive ground deformation or the loss of bearing capacities of the foundation soil. Those foundation failures result in the abutment suffering tilting, sliding, settling, and overturning. The foundation soil failure usually occurs because of poor soil conditions, such as soft soil, and the existence of a high water table. In order to avoid these kinds of soil failures during an earthquake, borrowing backfill soil, pile foundations, a high degree of soil compaction, pervious materials, and drainage systems may be considered in the design.

Abutment component damage is generally caused by excessive soil pressure, which is mobilized by the large relative displacement between the abutment and its backfilled soil. Those excessive pressures may cause severe damage to abutment components such as abutment back walls and abutment wingwalls. However, the abutment component damages do not usually cause the bridge superstructure to lose support at the abutment and they are repairable. This may allow the bridge designer to utilize the deformation of abutment backfill soil under seismic forces to dissipate the seismic energy to avoid the bridge losing support at columns under a major earthquake strike.

The behavior of abutment backfill soil deformed under seismic load is very efficient at dissipating the seismic energy, especially for the bridges with total length of less than 300 ft (91.5 m) with no hinge, no skew, or that are only slightly skewed (i.e., <15°). The tests and analysis revealed that if the abutments are capable of mobilizing the backfill soil and are well tied into the backfill soil, a damping ratio in the range of 10 to 15% is justified. This will elongate the bridge period and may reduce the ductility demand on the bridge columns. For short bridges, a damping reduction factor, *D,* may be applied to the forces and displacement obtained from bridge elastic analysis which generally have damped ARS curves at 5% levels. This factor *D* is given in Eq. (4.1).

$$D = \frac{1.5}{40\,C + 1} + 0.5 \tag{4.1}$$

where C = damping ratio.

Based on Eq. (4.1), for 10% damping, a factor $D = 0.8$ may be applied to the elastic force and displacement. For 15% damping, a factor $D = 0.7$ may be applied. Generally, the reduction factor *D* should be applied to the forces corresponding to the bridge shake mode that shows the abutment being excited.

The responses of abutment backfill soil to the seismic load are very difficult to predict. The study and tests revealed that the soil forces, which are applied to bridge abutment under seismic load, mainly depend on the abutment movement direction and magnitude. In the design practice, the Mononobe–Okabe method usually is used to quantify those loads for the abutment with no restraints on the top. Recently, the "near full scale" abutment tests performed at the University of California at Davis show a nonlinear relationship between the abutment displacement and the

backfill soil reactions under certain seismic loading when the abutment moves toward its backfill soil. This relation was plotted as shown in Figure 4.3. It is difficult to simulate this nonlinear relationship between the abutment displacement and the backfill soil reactions while performing bridge dynamic analysis. However, the tests concluded an upper limit for the backfill soil reaction on the abutment. In design practice, a peak soil pressure acting on the abutment may be predicted corresponding to certain abutment displacements. Based on the tests and investigations of past earthquake damages, the California Transportation Department suggests guidelines for bridge analysis considering abutment damping behavior as follows.

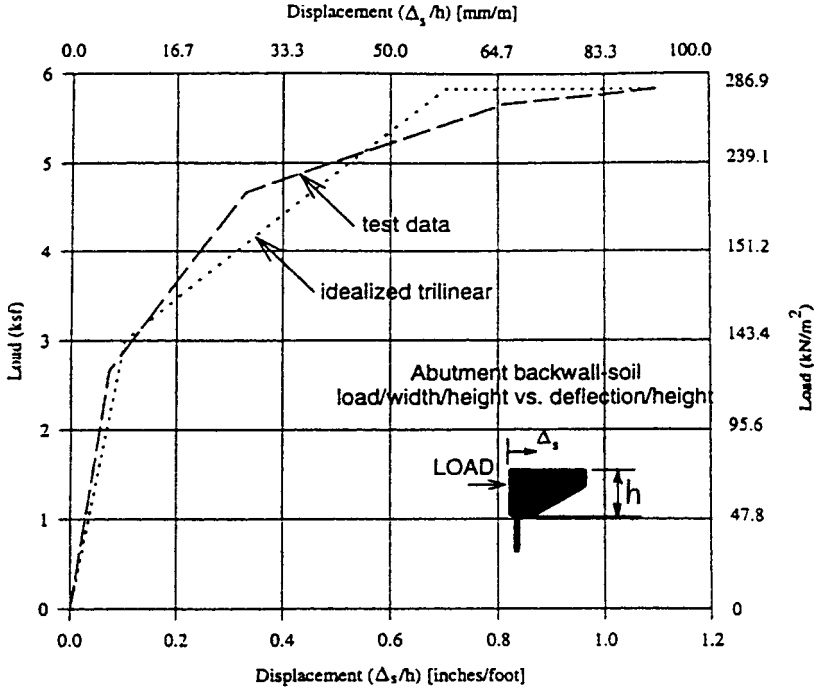

FIGURE 4.3 Proposed characteristics and experimental envelope for abutment backfill load–deformation.

By using the peak abutment force and the effective area of the mobilized soil wedge, the peak soil pressure is compared to a maximum capacity of 7.7 ksf (0.3687 MPa). If the peak soil pressure exceeds the soil capacity, the analysis should be repeated with reduced abutment stiffness. It is important to note that the 7.7 ksf (0.3687 MPa) soil pressure is based on a reliable minimum wall height of 8 ft (2.438 m). If the wall height is less than 8 ft (2.438 m), or if the wall is expected to shear off at a depth below the roadway less than 8 ft (2.438 m), the allowable passive soil pressure must be reduced by multiplying 7.7 ksf (0.3687 MPa) times the ratio of (L/8) [2], where L is the effective height of the abutment wall in feet. Furthermore, the shear capacity of the abutment wall diaphragm (the structural member mobilizing the soil wedge) should be compared with the demand shear forces to ensure the soil mobilizations. Abutment spring displacement is then evaluated against an acceptable level of displacement of 0.2 ft (61 mm). For a monolithic-type abutment this displacement is equal to the bridge superstructure displacement. For seat-type abutments this displacement usually does not equal the bridge superstructure displacement, which may include the gap between the bridge superstructure and abutment backwall. However, a net displacement of about 0.2 ft (61 mm) at the abutment should not be exceeded. Field investigations after the 1971 San Fernando earthquake revealed that the abutment, which moved up to 0.2 ft (61 mm) in the longitudinal direction into the backfill soil, appeared to survive with

little need for repair. The abutments in which the backwall breaks off before other abutment damage may also be satisfactory if a reasonable load path can be provided to adjacent bents and no collapse potential is indicated.

For seismic loads in the transverse direction, the same general principles still apply. The 0.2-ft (61-mm) displacement limit also applies in the transverse direction, if the abutment stiffness is expected to be maintained. Usually, wingwalls are tied to the abutment to stiffen the bridge transversely. The lateral resistance of the wingwall depends on the soil mass that may be mobilized by the wingwall. For a wingwall with the soil sloped away from the exterior face, little lateral resistance can be predicted. In order to increase the transverse resistance of the abutment, interior supplemental shear walls may be attached to the abutment or the wingwall thickness may be increased, as shown in Figure 4.4. In some situations larger deflection may be satisfactory if a reasonable load path can be provided to adjacent bents and no collapse potential is indicated [2].

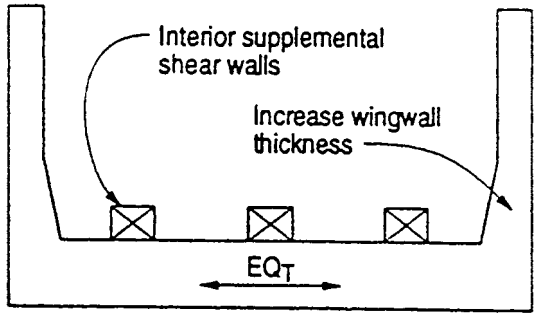

FIGURE 4.4 Abutment transverse enhancement.

Based on the above guidelines, abutment analysis can be carried out more realistically by a trial-and-error method on abutment soil springs. The criterion for abutment seismic resistance design may be set as follows.

Monolithic Abutment or Diaphragm Abutment (Figure 4.5)

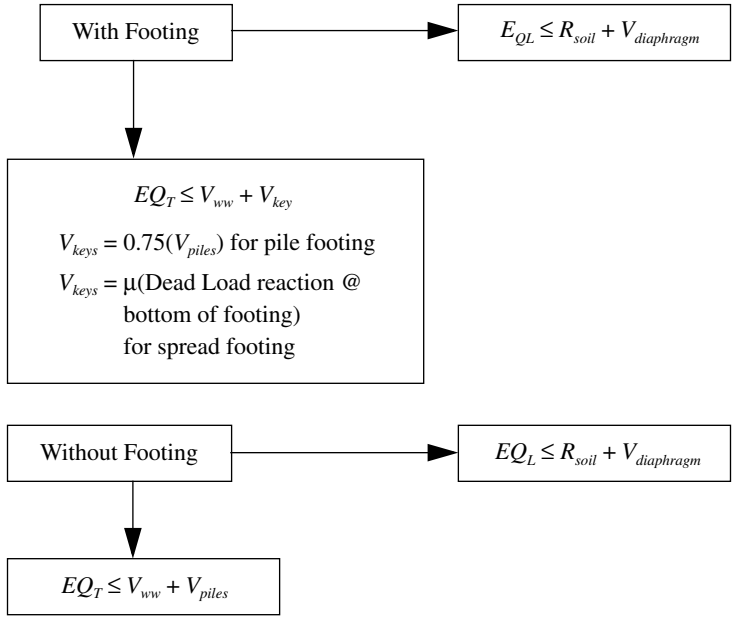

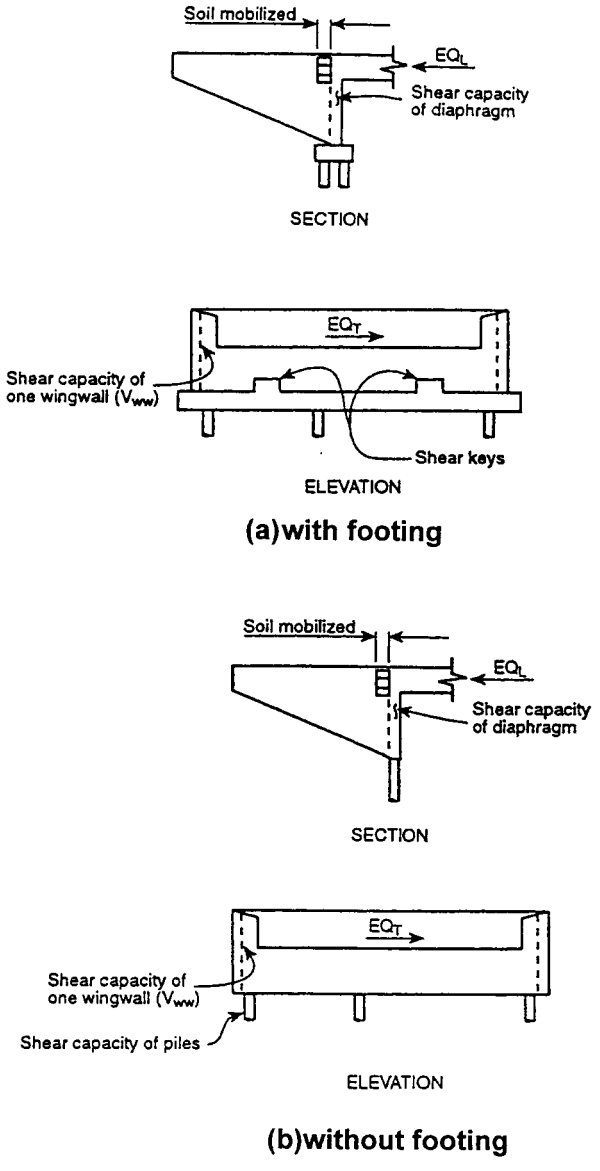

FIGURE 4.5 Seismic resistance elements for monolithic abutment.

Seat-Type Abutment (Figure 4.6)

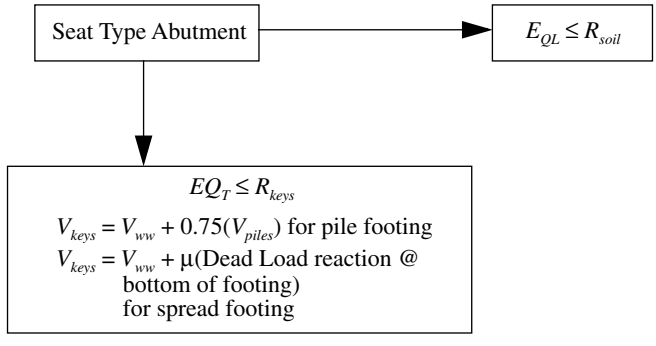

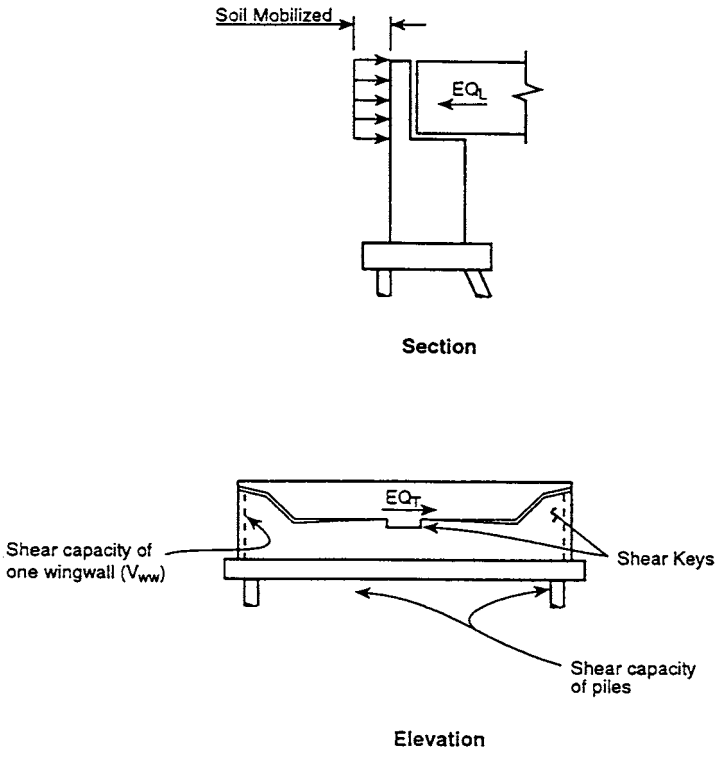

FIGURE 4.6 Seismic resistance elements for seat-type abutment.

where

EQ_L = longitudinal earthquake force from an elastic analysis
EQ_T = transverse earthquake force from an elastic analysis
R_{soil} = resistance of soil mobilized behind abutment
$R_{diaphragm}$ = φ times the nominal shear strength of the diaphragm
R_{ww} = φ times the nominal shear strength of the wingwall
R_{piles} = φ times the nominal shear strength of the piles
R_{keys} = φ times the nominal shear strength of the keys in the direction of consideration
φ = strength factor for seismic loading
μ = coefficient factor between soil and concrete face at abutment bottom

It is noted that the purpose of applying a factor of 0.75 to the design of shear keys is to reduce the possible damage to the abutment piles. For all transverse cases, if the design transverse earthquake force exceeds the sum of the capacities of the wingwalls and piles, the transverse stiffness for the analysis should equal zero ($EQ_T = 0$). Therefore, a released condition which usually results in larger lateral forces at adjacent bents should be studied.

Responding to seismic load, bridges usually accommodate a large displacement. To provide support at abutments for a bridge with large displacement, enough support width at the abutment must be designed. The minimum abutment support width, as shown in Figure 4.7, may be equal to the bridge displacement resulting from a seismic elastic analysis or be calculated as shown in Equation (29-2), whichever is larger:

$$N = (305 + 2.5L + 10H)(1 + 0.002\ S^2) \tag{4.2}$$

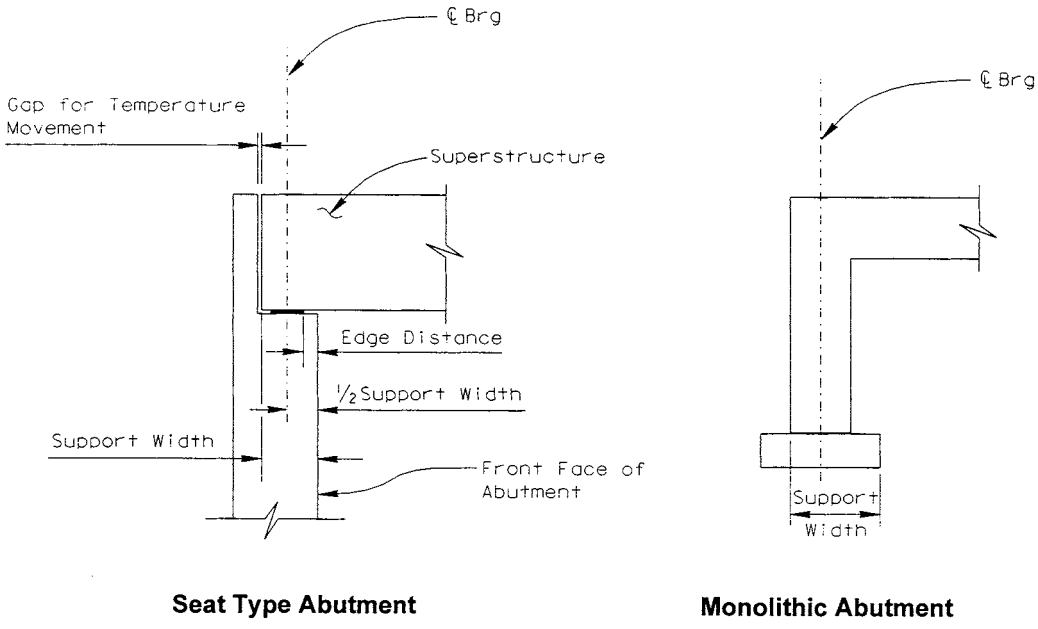

FIGURE 4.7 Abutment support width (seismic).

where

N = support width (mm)
L = length (m) of the bridge deck to the adjacent expansion joint, or to the end of bridge deck; for single-span bridges L equals the length of the bridge deck
S = angle of skew at abutment in degrees
H = average height (m) of columns or piers supporting the bridge deck from the abutment to the adjacent expansion joint, or to the end of the bridge deck; $H = 0$ for simple span bridges

4.2.4 Miscellaneous Design Considerations

Abutment Wingwall

Abutment wingwalls act as a retaining structure to prevent the abutment backfill soil and the roadway soil from sliding transversely. Several types of wingwall for highway bridges are shown in Figure 4.8. A wingwall design similar to the retaining wall design is presented in Section 4.3. However, live-load surcharge needs to be considered in wingwall design. Table 4.2 lists the live-load surcharge for different loading cases. Figure 4.9 shows the design loads for a conventional cantilever wingwall. For seismic design, the criteria in transverse direction discussed in Section 4.2.3 should be followed. Bridge wingwalls may be designed to sustain some damage in a major earthquake, as long as bridge collapse is not predicted.

Abutment Drainage

A drainage system is usually provided for the abutment construction. The drainage system embedded in the abutment backfill soil is designed to reduce the possible buildup of hydrostatic pressure, to control erosion of the roadway embankment, and to reduce the possibility of soil liquefaction during an earthquake. For a concrete-paved abutment slope, a drainage system also needs to be provided under the pavement. The drainage system may include pervious materials, PSP or PVC pipes, weep holes, etc. Figure 4.10 shows a typical drainage system for highway bridge construction.

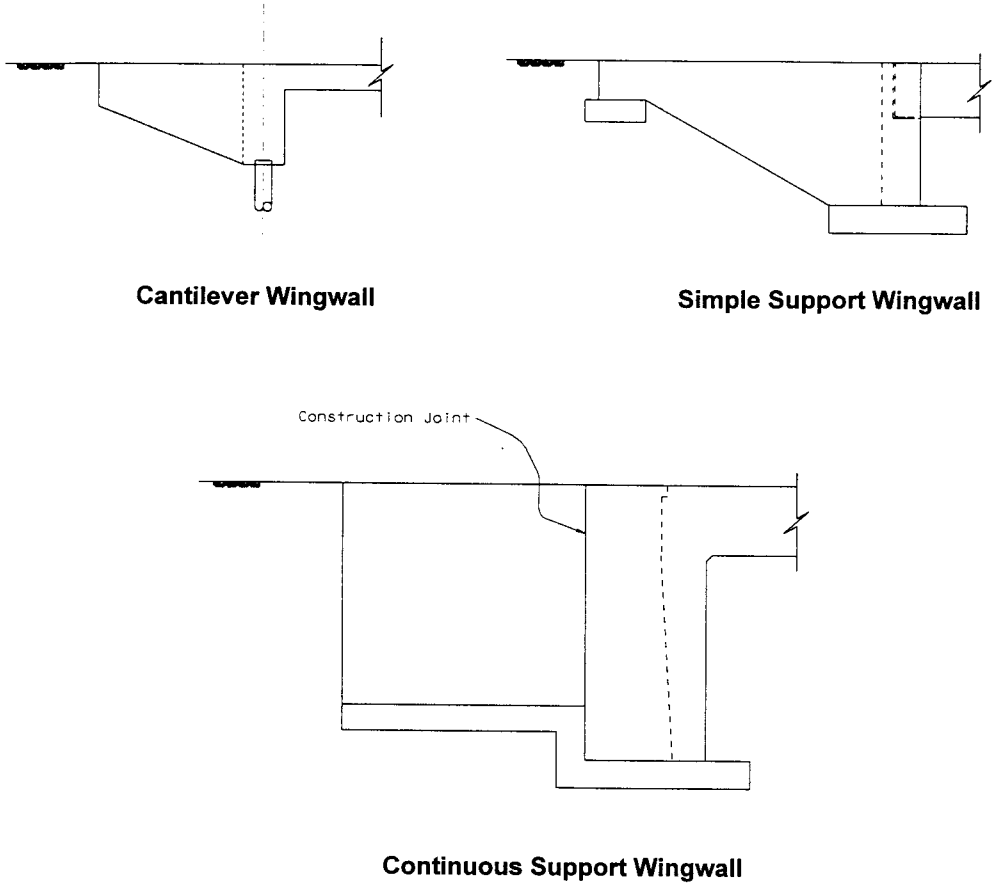

FIGURE 4.8 Typical wingwalls.

TABLE 4.2 Live Load Surcharges for Wingwall Design

Highway truck loading	2 ft 0 in. (610 mm) equivalent soil
Rail loading E-60	7 ft 6 in. (2290 mm) equivalent soil
Rail loading E-70	8 ft 9 in. (2670 mm) equivalent soil
Rail loading E-80	10 ft 0 in. (3050 mm) equivalent soil

Abutment Slope Protection

Flow water scoring may severely damage bridge structures by washing out the bridge abutment support soil. To reduce water scoring damage to the bridge abutment, pile support, rock slope protection, concrete slope paving, and gunite cement slope paving may be used. Figure 4.11 shows the actual design of rock slope protection and concrete slope paving protection for bridge abutments. The stability of the rock and concrete slope protection should be considered in the design. An enlarged block is usually designed at the toe of the protections.

Miscellaneous Details

Some details related to abutment design are given in Figure 4.12. Although they are only for regular bridge construction situations, those details present valuable references for bridge designers.

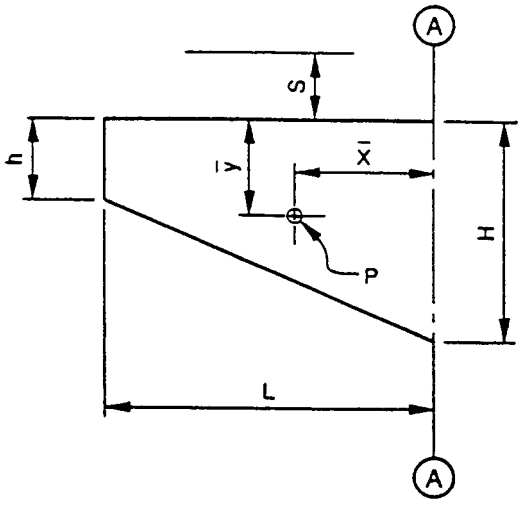

S = Surcharge, Ft.
h = End Height, Ft.
H = Section Height, Ft.
L = Length, Ft.
W =
= Equivalent Fluid Earth Pressure

$$M_{AA} = \frac{WL^2}{24}\left[3h^2 + (H + 4S)(H + 2h)\right]$$

$$P = \frac{WL}{6}\left[H^2 + (h + H)(h + 3S)\right]$$

$$\overline{X} = \frac{M_{AA}}{P}$$

FIGURE 4.9 Design loading for cantilever wingwall.

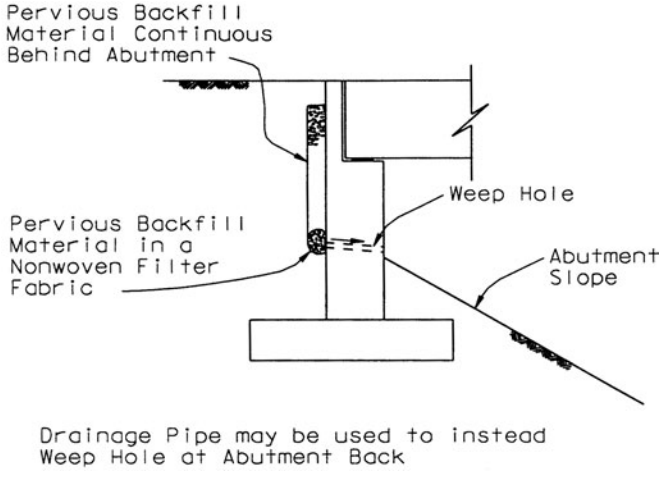

FIGURE 4.10 Typical abutment drainage system.

4.2.5 Design Example

A prestressed concrete box-girder bridge with 5° skew is proposed overcrossing a busy freeway as shown in Figure 4.13. Based on the roadway requirement, geotechnical information, and the details mentioned above, an open-end, seat-type abutment is selected. The abutment in transverse direction is 89 ft (27.13 m) wide. From the bridge analysis, the loads on abutment and bridge displacements are as listed:

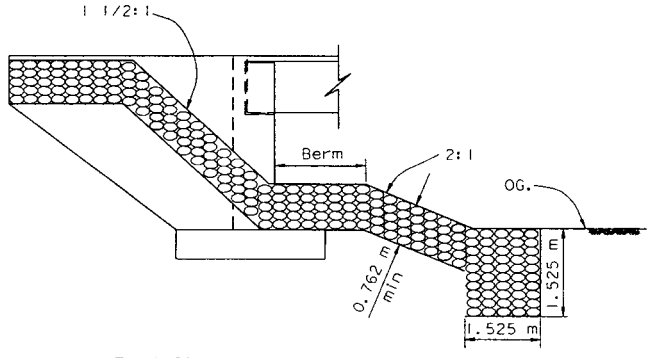

Rock Slope Protection

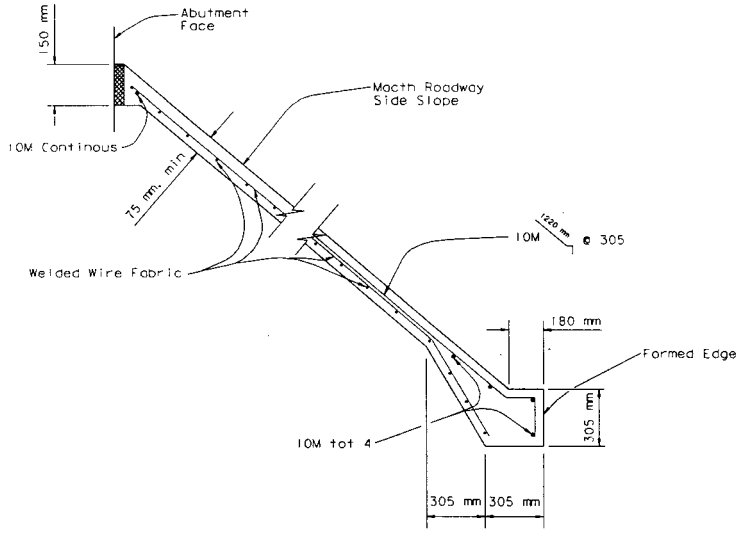

Concrete Slope Protection

FIGURE 4.11 Typical abutment slope protections.

Superstructure dead load	= 1630 kips (7251 kN)
HS20 live load	= 410 kips (1824 kN)
1.15 P-load + 1.0 HS load	= 280 kips (1245 kN)
Longitudinal live load	= 248 kips (1103 kN)
Longitudinal seismic load (bearing pad capacity)	= 326 kips (1450 kN)
Transverse seismic load	= 1241 kips (5520 kN)
Bridge temperature displacement	= 2.0 in. (75 mm)
Bridge seismic displacement	= 6.5 in. (165 mm)

Geotechnical Information

Live-load surcharge	= 2 ft (0.61 m)
Unit weight of backfill soil	= 120 pcf (1922 kg/m^3)

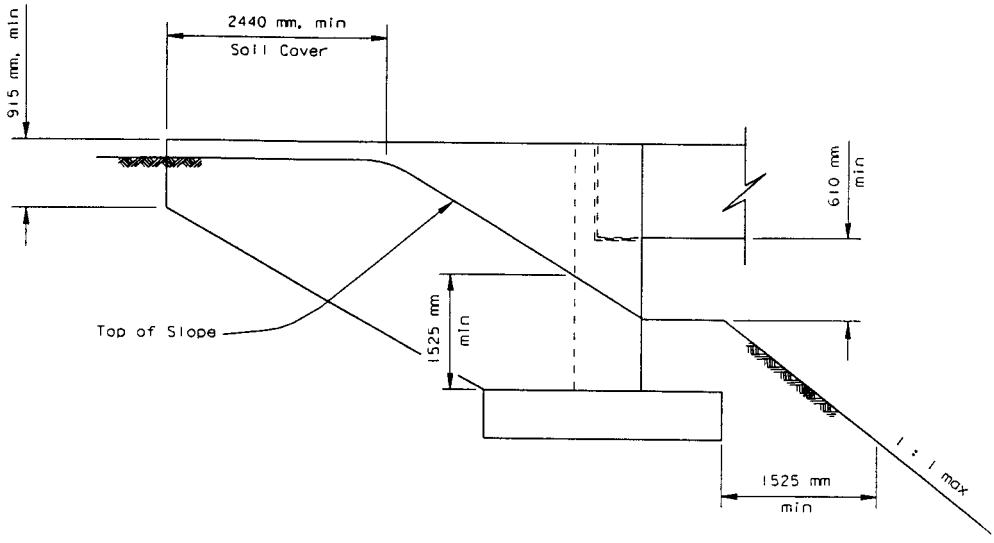

FIGURE 4.12 Abutment design miscellaneous details.

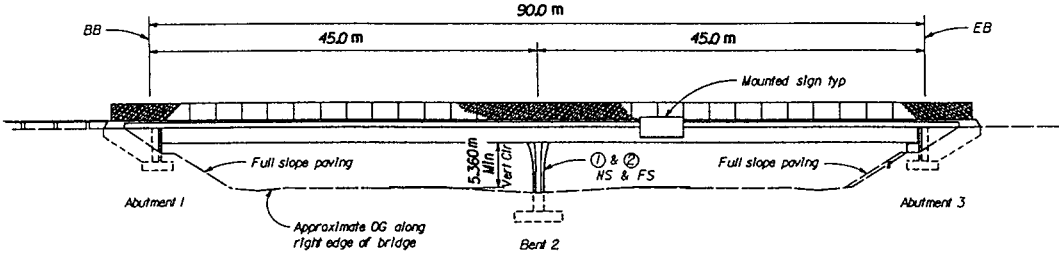

FIGURE 4.13 Bridge elevation (example).

Allowable soil bearing pressure	= 4.0 ksf (0.19 MPa)
Soil lateral pressure coefficient (Ka)	= 0.3
Friction coefficient	= tan 33°
Soil liquefaction potential	= very low
Ground acceleration	= 0.3 *g*

Design Criteria

Abutment design	Load factor method
Abutment stability	Service load method

Design Assumptions

1. Superstructure vertical loading acting on the center line of abutment footing;
2. The soil passive pressure by the soil at abutment toe is neglected;
3. 1.0 feet (0.305 m) wide of abutment is used in the design;
4. Reinforcement yield stress, f_y = 60000 psi (414 MPa);
5. Concrete strength, f_c' = 3250 psi (22.41 MPa);
6. Abutment backwall allowed damage in the design earthquake.

Solution

1. **Abutment Support Width Design**
   Applying Eq. (4.2) with

$$L = 6.5 \text{ m}$$

$$H = 90.0 \text{ m}$$

$$S = 5°$$

the support width will be $N = 600$ mm. Add 75 mm required temperature movement, the total required support width equals 675 mm. The required minimum support width for seismic case equals the sum of the bridge seismic displacement, the bridge temperature displacement, and the reserved edge displacement (usually 75 mm). In this example, this requirement equals 315 mm, not in control. Based on the 675-mm minimum requirement, the design uses 760 mm, OK. A preliminary abutment configuration is shown in Figure 4.14 based on the given information and calculated support width.

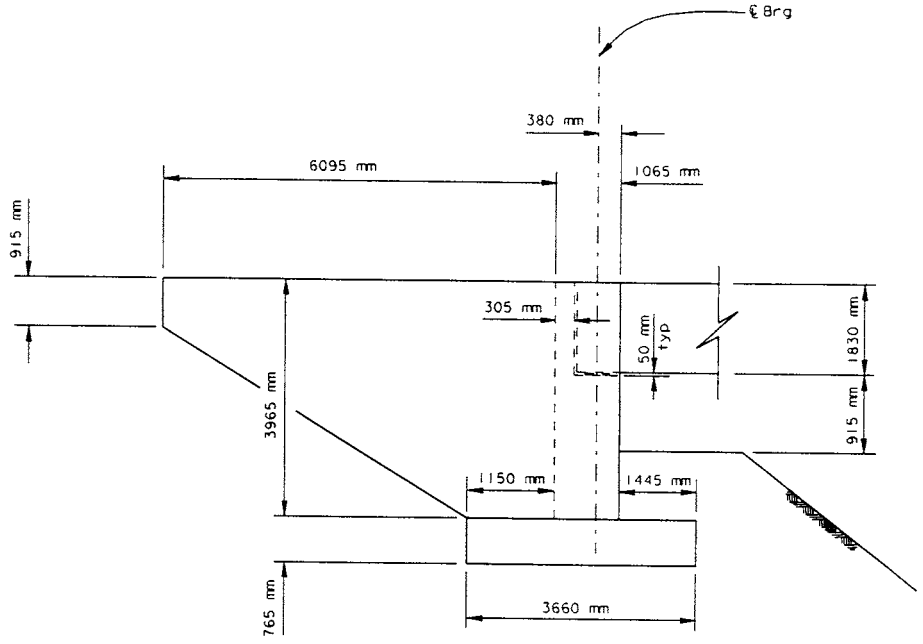

FIGURE 4.14 Abutment configuration (example).

2. **Abutment Stability Check**
   Figure 4.15 shows the abutment force diagram,

   where
   q_{sc} = soil lateral pressure by live-load surcharge
   q_e = soil lateral pressure
   q_{eq} = soil lateral apressure by seismic load
   P_{DL} = superstructure dead load
   P_{HS} = HS20 live load
   P_P = permit live load
   F = longitudinal live load

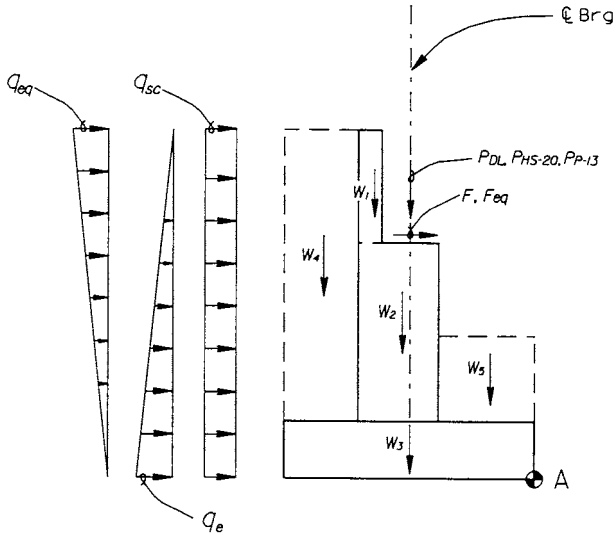

FIGURE 4.15 Abutment applying forces diagram (example).

F_{eq} = longitudinal bridge seismic load
P_{ac} = resultant of active seismic soil lateral pressure
h_{sc} = height of live-load surcharge
γ = unit weight of soil
W_i = weight of abutment component and soil block
$q_{sc} = k_a \times \gamma \times h_{sc} = 0.3 \times 0.12 \times 2 = 0.072$ ksf (0.0034 MPa)
$q_e = k_a \times \gamma \times H = 0.3 \times 0.12 \times 15.5 = 0.558$ ksf (0.0267 MPa)
$q_{eq} = k_{ae} \times \gamma \times H = 0.032 \times 0.12 \times 15.5 = 0.06$ ksf (0.003 MPa)

The calculated vertical loads, lateral loads, and moment about point *A* are listed in Table 4.3. The maximum and minimum soil pressure at abutment footing are calculated by

$$p = \frac{P}{B}\left(1 \pm \frac{6e}{B}\right) \tag{4.3}$$

where
p = soil bearing pressure
P = resultant of vertical forces
B = abutment footing width
e = eccentricity of resultant of forces and the center of footing

$$e = 2B - \frac{M}{P} \tag{4.4}$$

M = total moment to point A

Referring to the Table 4.1 and Eqs. (4.3) and (4.4) the maximum and minimum soil pressures under footing corresponding to different load cases are calculated. Since the soil bearing pressures are less than the allowable soil bearing pressure, the soil bearing stability is OK.

Load Case	p_{max}	p_{min}	$p_{allowable}$ with Allowable % of Overstress	Evaluate
I	3.81	3.10	4.00	OK
II	3.42	2.72	4.00	OK
III	1.84	1.22	6.00	OK
IV	4.86	2.15	5.00	OK
V	2.79	1.93	6.00	OK
Seismic	6.73	0.54	8.00	OK

TABLE 4.3 Vertical Forces, Lateral Forces, and Moment about Point *A* (Example)

Load Description	Vertical Load (kips)	Lateral Load (kips)	Arm to *A* (ft)	Moment to *A* (k-ft)
Backwall W_1	0.94	—	7.75	7.28
Stem W_2	3.54	—	6.00	23.01
Footing W_3	4.50	—	6.00	27.00
Backfill soil	5.85	—	10.13	59.23
	—	4.33	5.17	–22.34
Soil surcharge	—	1.16	7.75	–8.65
Front soil W_4	1.71	—	2.38	4.06
Wingwalls	0.85	—	16.12	13.70
Keys	0.17	—	6.00	1.04
P_{DL}	18.31	—	6.00	110.00
P_{HS}	4.61	—	6.00	27.64
P_P	3.15	—	6.00	18.90
F	—	2.79	9.25	–25.80
F_{eq}	—	3.66	9.25	–33.90
Soil seismic load	—	0.47	9.30	–4.37

Check for the stability resisting the overturning (load case III and IV control):

Load Case	Driving Moment	Resist Moment	Factor of Safety	Evaluate
III	31	133.55	4.3	OK
IV	56.8	262.45	4.62	OK

Checking for the stability resisting the sliding (load case III and IV control)

Load Case	Driving Force	Resist Force	Factor of Safety	Evaluation
III	5.44	11.91	2.18	OK
IV	8.23	20.7	3.26	OK

Since the structure lateral dynamic force is only combined with dead load and static soil lateral pressures, and the factor of safety FS = 1.0 can be used, the seismic case is not in control.

3. Abutment Backwall and Stem Design

Referring to AASHTO guidelines for load combinations, the maximum factored loads for abutment backwall and stem are

Location	*V* (kips)	*M* (k-ft)
Backwall level	1.95	4.67
Bottom of stem	10.36	74.85

Abutment Backwall

Try #5 at 12 in. (305 mm) with 2 in. (50 mm) clearance

d = 9.7 in. (245 mm)

$$A_s \times f_y = 0.31 \times 60 \times \frac{12}{16} = 13.95 \text{ kips } (62.05 \text{ kN})$$

$$a = \frac{A_s \cdot f_y}{\phi \cdot f_c' \cdot b_w} = \frac{13.95}{(0.85)(3.25)(12)} = 0.42 \text{ in. } (10.67 \text{ mm})$$

$$M_u = \phi \cdot M_n = \phi \cdot A_s \cdot f_y \left(d - \frac{a}{2}\right) = 0.9 \times 13.95 \times \left(9.7 - \frac{0.42}{2}\right) = 9.33 \text{ k} \cdot \text{ft } (13.46 \text{ kN} \cdot \text{m})$$

$$> 4.67 \text{ k} \cdot \text{ft } (6.33 \text{ kN} \cdot \text{m}) \quad \text{OK}$$

$$V_c = 2\sqrt{f_c'} \cdot b_w \cdot d = 2 \times \sqrt{3250} \times 12 \times 9.7 = 13.27 \text{ kips } (59.03 \text{ kN})$$

$$V_u = \phi \cdot V_c = 0.85 \times 13.27 = 11.28 \text{ kip } (50.17 \text{ kN}) > 1.95 \text{ kips } (8.67 \text{ kN}) \quad \text{OK}$$

No shear reinforcement needed.

Abutment Stem

Abutment stem could be designed based on the applying moment variations along the abutment wall height. Here only the section at the bottom of stem is designed.

Try #6 at 12 in. (305 mm) with 2 in. (50 mm) clearance.

$$A_s \times f_y = 0.44 \times 60 = 26.40 \text{ kips } (117.43 \text{ kN})$$

d = 39.4 in. (1000 mm)

$$a = \frac{A_s \cdot f_y}{\phi \cdot f_c' \cdot b_w} = \frac{26.4}{(0.85)(3.25)(12)} = 0.796 \text{ in } (20.0 \text{ mm})$$

$$M_u = \phi \cdot A_s \cdot f_y \left(d - \frac{a}{2}\right) = 0.9 \times 26.4 \times \left(39.4 - \frac{0.8}{2}\right) = 77.22 \text{ k·ft } (104.7 \text{kN·m})$$

$$> 74.85 \text{ k·ft } (101.5 \text{kN·m}) \quad \text{OK}$$

$$V_c = 2\sqrt{f_c'}\, b_w\, d = 2 \times \sqrt{3250} \times 12 \times 39.4 = 53.91 \text{ kips } (238 \text{ kN})$$

$$V_u = \phi \cdot V_c = 0.85 \times 53.91 = 45.81 \text{ kips } (202.3 \text{ kN}) > 10.36 \text{ kips } (46.08 \text{ kN}) \quad \text{OK}$$

No shear reinforcement needed.

4. Abutment Footing Design

Considering all load combinations and seismic loading cases, the soil bearing pressure diagram under the abutment footing are shown in Figure 4.16.

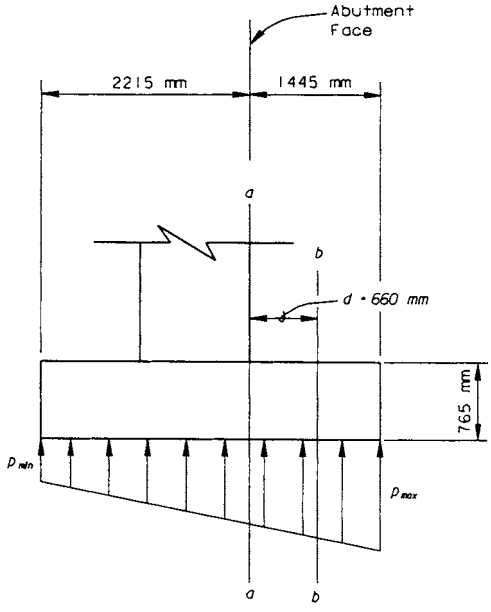

FIGURE 4.16 Bearing pressure under abutment footing (example).

a. *Design forces*:
Section at front face of abutment stem (design for flexural reinforcement):

$$q_{a\text{-}a} = 5.1263 \text{ ksf } (0.2454 \text{ MPa})$$

$$M_{a\text{-}a} = 69.4 \text{ k-ft } (94.1 \text{ kN·m})$$

Section at $d = 30 - 3 - 1 = 26$ in. (660 mm) from the front face of abutment stem (design for shear reinforcement):

$$q_{b\text{-}b} = 5.2341 \text{ ksf } (0.251 \text{ MPa})$$

$$V_{b\text{-}b} = 15.4 \text{ kips } (68.5 \text{ kN})$$

b. *Design flexural reinforcing* (*footing bottom*):
Try #8 at 12, with 3 in. (75 mm) clearance at bottom

$d = 30 - 3 - 1 = 26$ in. (660 mm)

$$A_s \times f_y = 0.79 \times 60 = 47.4 \text{ kips} \quad (211 \text{ kN})$$

$$a = \frac{A_s \cdot f_y}{\phi \cdot f_c' \cdot b_w} = \frac{47.4}{(0.85)(3.25)(12)} = 1.43 \text{ in.} \quad (36 \text{ mm})$$

$$M_n = \phi \cdot A_s \cdot f_y \left(d - \frac{a}{2} \right) = 0.9 \times 47.4 \times \left(26 - \frac{1.43}{2} \right) \quad = 89.9 \text{ k·ft} \quad (121.89 \text{ kN·m})$$

$$> 69.4 \text{ k·ft} \quad (94.1 \text{ kN·m}) \qquad \text{OK}$$

$$V_c = 2\sqrt{f_c'} \cdot b_w \cdot d = 2 \times \sqrt{3250} \times 12 \times 26 = 35.57 \text{ kips} \quad (158.24 \text{ kN})$$

$$V_u = \phi \cdot V_c = 0.85 \times 35.57 = 30.23 \text{ kips} \quad (134.5 \text{ kN}) \quad > \quad 15.5 \text{ kips} \quad (68.5 \text{ kN}) \qquad \text{OK}$$

No shear reinforcement needed.

Since the minimum soil bearing pressure under the footing is in compression, the tension at the footing top is not the case. However, the minimum temperature reinforcing, 0.308 in.^{2}/ft (652 mm^2/m) needs to be provided. Using #5 at 12 in. (305 mm) at the footing top yields

$$A_s = 0.31 \text{ in.}^2\text{/ft}, \ (656 \text{ mm}^2\text{/m}) \qquad \text{OK}$$

5. Abutment Wingwall Design

The geometry of wingwall is

h = 3.0 ft (915 mm); S = 2.0 ft (610 mm);

H = 13.0 ft (3960 mm); L = 18.25 ft (5565 mm)

Referring to the Figure 4.15, the design loads are

$$V_{A-A} = \frac{wL}{6}\left[H^2 + (h+H)(h+3S)\right]$$

$$= \frac{0.36 \times 18.25}{6}\left[13^2 + (3+13)(3+3\times 2)\right] = 34 \text{ kips} \quad (152.39 \text{ kN})$$

$$M_{A-A} = \frac{wL^2}{24}\left[3h^2 + (H+4S)(H+2h)\right]$$

$$= \frac{0.036 \times 18.25^2}{24}\left[3(3)^2 + (13+4\times 2)(12+2\times 3)\right] = 212.8 \text{ k·ft} \quad (3129 \text{ kN·m})$$

Design flexural reinforcing. Try using # 8 at 9 (225 mm).

$$A_s \times f_y = 13 \times (0.79) \times 60 \times \frac{12}{9} = 821.6 \text{ kips} \quad (3682 \text{ kN})$$

$$a = \frac{A_s \cdot f_y}{\phi \cdot f_c' \cdot b_w} = \frac{1280}{(0.85)(3.25)(13)(12)} = 2.97 \text{ in.} \quad (75 \text{ mm})$$

d = 12 – 2 – 0.5 = 9.5 in. (240 mm)

$$M_n = \phi \cdot A_s \cdot f_y\left(d - \frac{a}{2}\right) = 0.9 \times (821.6) \times \left(9.5 - \frac{2.97}{2}\right) = 493.8 \text{ k·ft} \ (7261 \text{ kN} \cdot \text{m})$$

$$> 212.8 \text{ k·ft} \quad (3129 \text{ kN} \cdot \text{m})$$

Checking for shear

$$V_c = 2\sqrt{f_c'} \cdot b_w \cdot d = 2 \times \sqrt{3250} \times 13 \times 12 \times 9.5 = 168 \text{ kips} \quad (757.3 \text{ kN})$$

$$V_u = \varphi \cdot V_c = 0.85 \times 168 = 142 \text{ kips} \quad (636 \text{ kN}) > 34 \text{ kips} \ (152.3\text{kN}) \qquad \text{OK}$$

No shear reinforcing needed.

Since the wingwall is allowed to be broken off in a major earthquake, the adjacent bridge columns have to be designed to sustain the seismic loading with no wingwall resistance. The abutment section, footing, and wingwall reinforcing details are shown in Figures 4.17a and b.

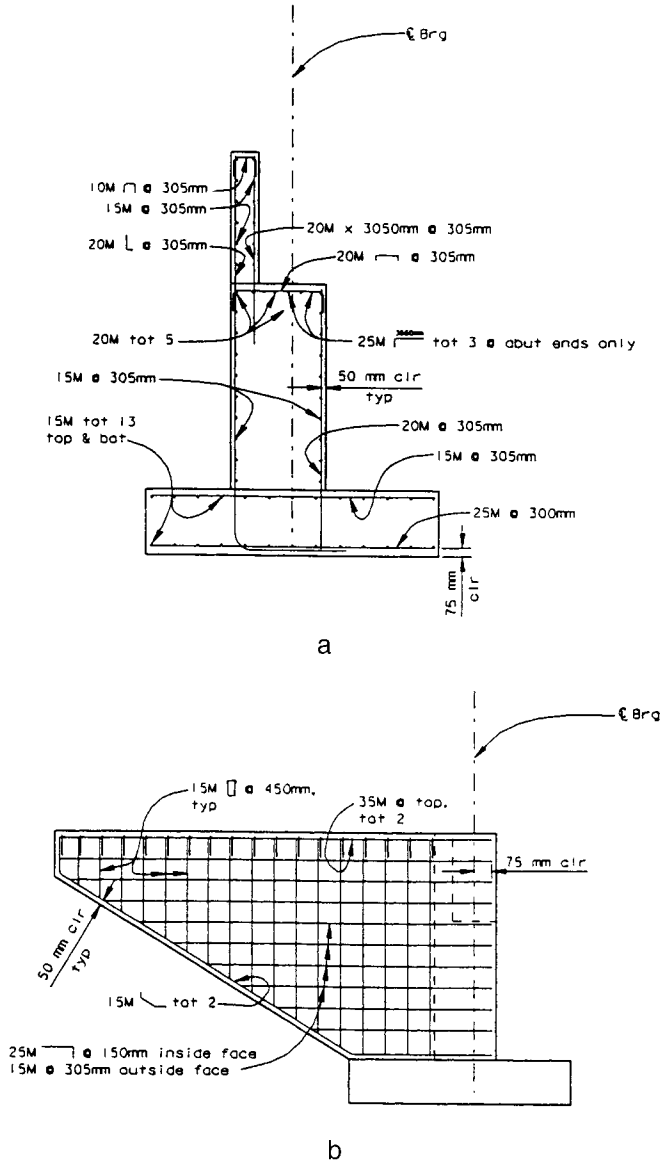

FIGURE 4.17 (a) Abutment typical section design (example). (b) Wingwall reinforcing (example).

4.3 Retaining Structures

4.3.1 Retaining Structure Types

The retaining structure, or, more specifically, the earth-retaining structure, is commonly required in a bridge design project. It is common practice that the bridge abutment itself is used as a retaining structure. The cantilever wall, tieback wall, soil nail wall and mechanically stabilized embankment (MSE) wall are the most frequently used retaining structure types. The major design function of a retaining structure is to resist lateral forces.

The cantilever retaining wall is a cantilever structure used to resist the active soil pressure in topography fill locations. Usually, the cantilever earth-retaining structure does not exceed 10 m in height. Some typical cantilever retaining wall sections are shown in Figure 4.18a.

The tieback wall can be used for topography cutting locations. High-strength tie strands are extended into the stable zone and act as anchors for the wall face elements. The tieback wall can be designed to have minimum lateral deflection. Figure 4.18d shows a tieback wall section.

The MSE wall is a kind of "reinforced earth-retaining" structure. By installing multiple layers of high-strength fibers inside of the fill section, the lateral deflection of filled soil will be restricted. There is no height limit for an MSE wall but the lateral deflection at the top of the wall needs to be considered. Figure 4.18e shows an example of an MSE wall.

The soil nail wall looks like a tieback wall but works like an MSE wall. It uses a series of soil nails built inside the soil body that resist the soil body lateral movement in the cut sections. Usually, the soil nails are constructed by pumping cement grout into predrilled holes. The nails bind the soil together and act as a gravity soil wall. A typical soil nail wall model is shown in Figure 4.18f.

4.3.2 Design Criteria

Minimum Requirements

All retaining structures must be safe from vertical settlement. They must have sufficient resistance against overturning and sliding. Retaining structures must also have adequate strength for all structural components.

1. *Bearing capacity*: Similar to any footing design, the bearing capacity factor of safety should be ≥1.0. Table 4.4 is a list of approximate bearing capacity values for some common materials. If a pile footing is used, the soil-bearing capacity between piles is not considered.
2. *Overturning resistance*: The overturning point of a typical retaining structure is located at the edge of the footing toe. The overturning factor of safety should be ≥1.50. If the retaining structure has a pile footing, the fixity of the footing will depend on the piles only.
3. *Sliding resistance*: The factor of safety for sliding should be ≥1.50. The typical retaining wall sliding capacity may include both the passive soil pressure at the toe face of the footing and the friction forces at the bottom of the footing. In most cases, friction factors of 0.3 and 0.4

TABLE 4.4 Bearing Capacity

	Bearing Capacity [N]	
Material	min, kPa	max, kPa
Alluvial soils	24	48
Clay	48	190
Sand, confined	48	190
Gravel	95	190
Cemented sand and gravel	240	480
Rock	240	—

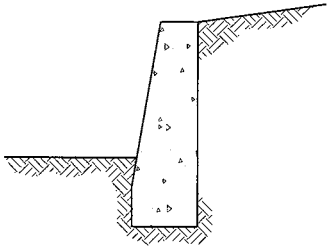

Gravity wall
(a)

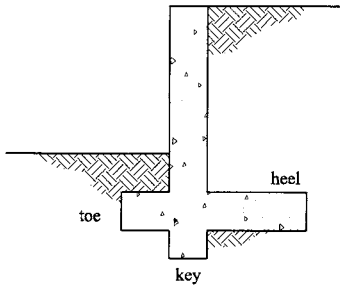

Cantilever wall
(b)

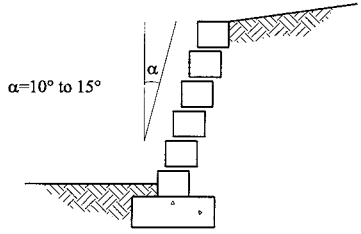

Wall With Set Back
(c)

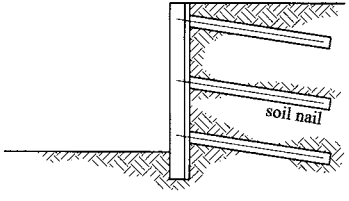

Soil Nail Wall
(f)

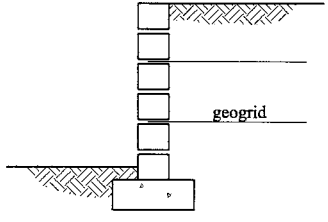

Reinforced Earth Wall
(e)

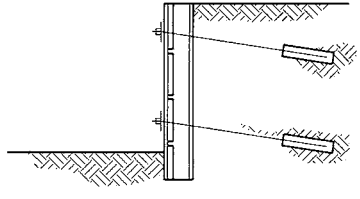

Tie Back Wall
(d)

FIGURE 4.18 Retaining wall types.

can be used for clay and sand, respectively. If battered piles are used for sliding resistance, the friction force at the bottom of the footing should be neglected.

4. Structural strength: Structural section moment and shear capacities should be designed following common strength factors of safety design procedures.

Figure 4.19 shows typical loads for cantilever retaining structure design.

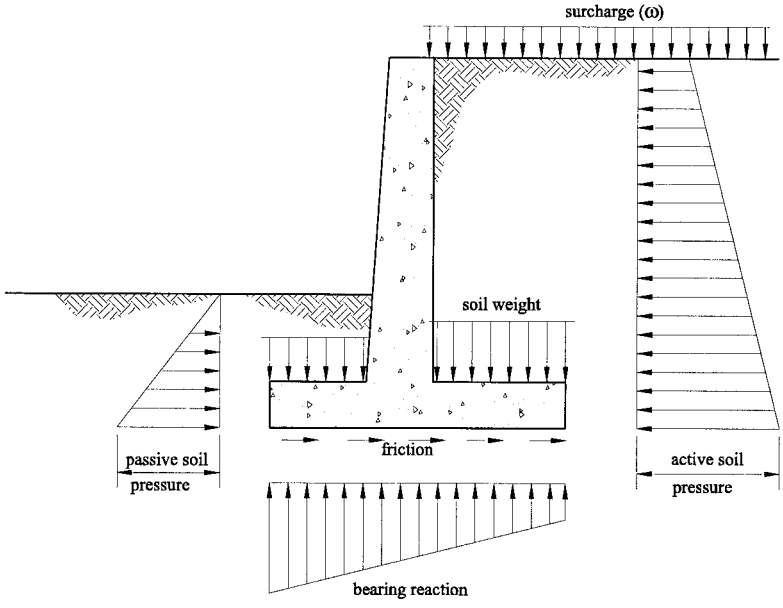

FIGURE 4 19 Typical loads on retaining wall.

Lateral Load

The unit weight of soil is typically in the range of 1.5 to 2.0 ton/m^3. For flat backfill cases, if the backfill material is dry, cohesionless sand, the lateral earth pressure (Figure 4.20a) distribution on the wall will be as follows

The active force per unit length of wall (Pa) at bottom of wall can be determined as

$$p_a = k_a \gamma H \tag{4.5}$$

The passive force per unit length of wall (Pa) at bottom of wall can be determined as

$$p_p = k_p \gamma H \tag{4.6}$$

where
H = the height of the wall (from top of the wall to bottom of the footing)
g = unit weight of the backfill material
k_a = active earth pressure coefficient
k_p = passive earth pressure coefficient

The coefficients k_a and k_p should be determined by a geologist using laboratory test data from a proper soil sample. The general formula is

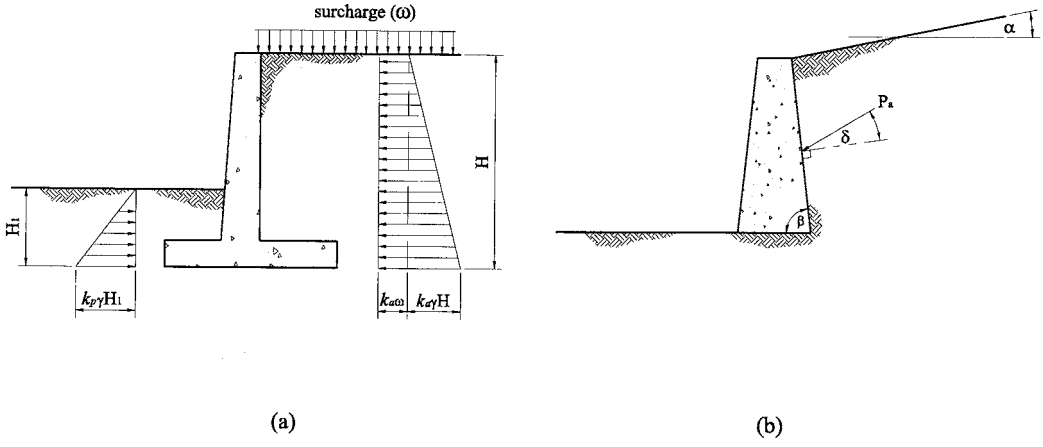

FIGURE 4.20 Lateral Earth pressure.

$$k_a = \frac{1-\sin\phi}{1+\sin\phi} \quad k_p = \frac{1}{k_a} = \frac{1+\sin\phi}{1-\sin\phi} \tag{4.7}$$

where ϕ is the internal friction angle of the soil sample.

Table 4.5 lists friction angles for some typical soil types which can be used if laboratory test data is not available. Generally, force coefficients of $k_a \geq 0.30$ and $k_p \leq 1.50$ should be used for preliminary design.

TABLE 4.5 Internal Friction Angle and Force Coefficients

Material	ϕ(*degrees*)	k_a	k_p
Earth, loam	30–45	0.33–0.17	3.00–5.83
Dry sand	25–35	0.41–0.27	2.46–3.69
Wet sand	30–45	0.33–0.17	3.00–5.83
Compact Earth	15–30	0.59–0.33	1.70–3.00
Gravel	35–40	0.27–0.22	3.69–4.60
Cinders	25–40	0.41–0.22	2.46–4.60
Coke	30–45	0.33–0.17	3.00–5.83
Coal	25–35	0.41–0.27	2.46–3.69

Based on the triangle distribution assumption, the total active lateral force per unit length of wall should be

$$P_a = \frac{1}{2} k_a \gamma H^2 \tag{4.8}$$

The resultant earth pressure always acts at distance of $H/3$ from the bottom of the wall.

When the top surface of backfill is sloped, the k_a coefficient can be determined by the Coulomb equation (see Figure 4.20):

$$k_a = \frac{\sin^2(\phi+\beta)}{\sin^2\beta\sin(\beta-\delta)\left[1+\sqrt{\dfrac{\sin(\phi+\delta)\sin(\phi-\alpha)}{\sin(\beta-\delta)\sin(\alpha+\beta)}}\right]^2} \tag{4.9}$$

Note that the above lateral earth pressure calculation formulas do not include water pressure on the wall. A drainage system behind the retaining structures is necessary; otherwise, the proper water pressure must be considered.

Table 4.6 gives values of k_a for the special case of zero wall friction.

TABLE 4.6 Active Stress Coefficient k_a Values from Coulomb Equation ($\delta = 0$)

		α					
		0.00°	18.43°	21.80°	26.57°	33.69°	45.00°
ϕ	β_o	Flat	1 to 3.0	1 to 2.5	1 to 2.0	1 to 1.5	1 to 1.0
20°	90°	0.490	0.731				
	85°	0.523	0.783				
	80°	0.559	0.842				
	75°	0.601	0.913				
	70°	0.648	0.996				
25°	90°	0.406	0.547	0.611			
	85°	0.440	0.597	0.667			
	80°	0.478	0.653	0.730			
	75°	0.521	0.718	0.804			
	70°	0.569	0.795	0.891			
30°	90°	0.333	0.427	0.460	0.536		
	85°	0.368	0.476	0.512	0.597		
	80°	0.407	0.530	0.571	0.666		
	75°	0.449	0.592	0.639	0.746		
	70°	0.498	0.664	0.718	0.841		
35°	90°	0.271	0.335	0.355	0.393	0.530	
	85°	0.306	0.381	0.404	0.448	0.602	
	80°	0.343	0.433	0.459	0.510	0.685	
	75°	0.386	0.492	0.522	0.581	0.781	
	70°	0.434	0.560	0.596	0.665	0.897	
40°	90°	0.217	0.261	0.273	0.296	0.352	
	85°	0.251	0.304	0.319	0.346	0.411	
	80°	0.287	0.353	0.370	0.402	0.479	
	75°	0.329	0.408	0.429	0.467	0.558	
	70°	0.375	0.472	0.498	0.543	0.651	
45°	90°	0.172	0.201	0.209	0.222	0.252	0.500
	85°	0.203	0.240	0.250	0.267	0.304	0.593
	80°	0.238	0.285	0.297	0.318	0.363	0.702
	75°	0.277	0.336	0.351	0.377	0.431	0.832
	70°	0.322	0.396	0.415	0.446	0.513	0.990

Any surface load near the retaining structure will generate additional lateral pressure on the wall. For highway-related design projects, the traffic load can be represented by an equivalent vertical surcharge pressure of 11.00 to 12.00 kPa. For point load and line load cases (Figure 4.21), the following formulas can be used to determine the additional pressure on the retaining wall:

For point load:

$$p_h = \frac{1.77V}{H^2}\frac{m^2n^2}{\left(m^2+n^2\right)^3} \quad (\mathrm{m} \le 0.4) \qquad p_h \frac{0.28V}{H^2}\frac{m^2n^2}{\left(0.16+n^3\right)} \quad (m > 0.4) \tag{4.10}$$

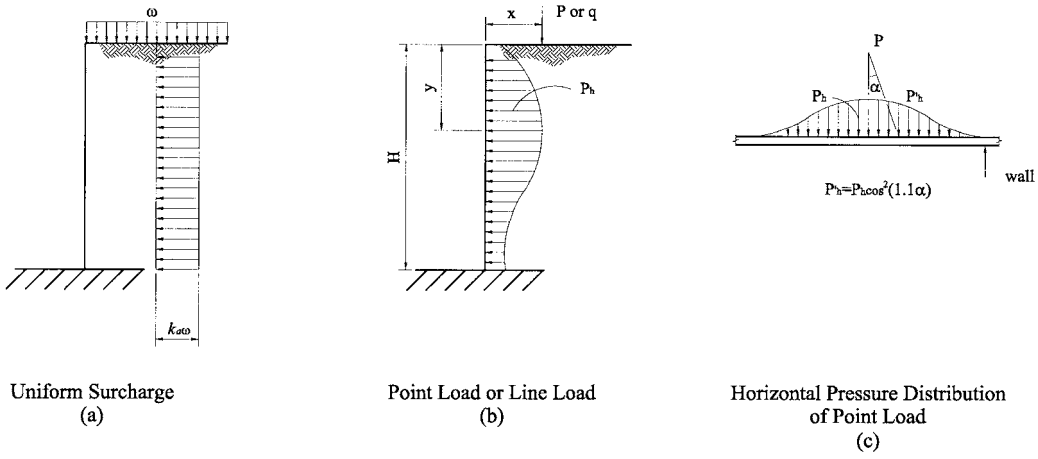

FIGURE 4.21 Additional lateral earth pressure. (a) Uniform surcharge; (b) point or line load; (c) horizontal pressure distribution of point load.

For line load:

$$p_h = \frac{\pi}{4}\frac{w}{H}\frac{m^2 n}{\left(m^2+n^2\right)^2} \quad (m \le 0.4) \quad p_h = \frac{w}{H}\frac{0.203n}{\left(0.16+n^2\right)^2} \quad (m > 0.4) \tag{4.11}$$

where

$$m = \frac{x}{H}; \quad n = \frac{y}{H}$$

Table 4.7 gives lateral force factors and wall bottom moment factors which are calculated by above formulas.

TABLE 4.7 Line Load and Point Load Lateral Force Factors

Line Load Factors			Point Load Factors		
$m = x/H$	$(f)^a$	$(m)^b$	$m = x/H$	$(f)^c$	$(m)^d$
0.40	0.548	0.335	0.40	0.788	0.466
0.50	0.510	0.287	0.50	0.597	0.316
0.60	0.469	0.245	0.60	0.458	0.220
0.70	0.429	0.211	0.70	0.356	0.157
0.80	0.390	0.182	0.80	0.279	0.114
0.90	0.353	0.158	0.90	0.220	0.085
1.00	0.320	0.138	1.00	0.175	0.064
1.50	0.197	0.076	1.50	0.061	0.019
2.00	0.128	0.047	2.00	0.025	0.007

Notes:
[a] Total lateral force along the length of wall = factor(f) × ω (force)/(unit length).
[b] Total moment along the length of wall = factor(m) × ω × H (force × length)/(unit length) (at bottom of footing).
[c] Total lateral force along the length of wall = factor(f) × V/H (force)/(unit length).
[d] Total moment along the length of wall = factor(m) × V (force × length)/(unit length) (at bottom of footing).

4.3.3 Cantilever Retaining Wall Design Example

The cantilever wall is the most commonly used retaining structure. It has a good cost-efficiency record for walls less than 10 m in height. Figure 4.22a shows a typical cross section of a cantilever retaining wall and Table 4.8 gives the active lateral force and the active moment about bottom of the cantilever retaining wall.

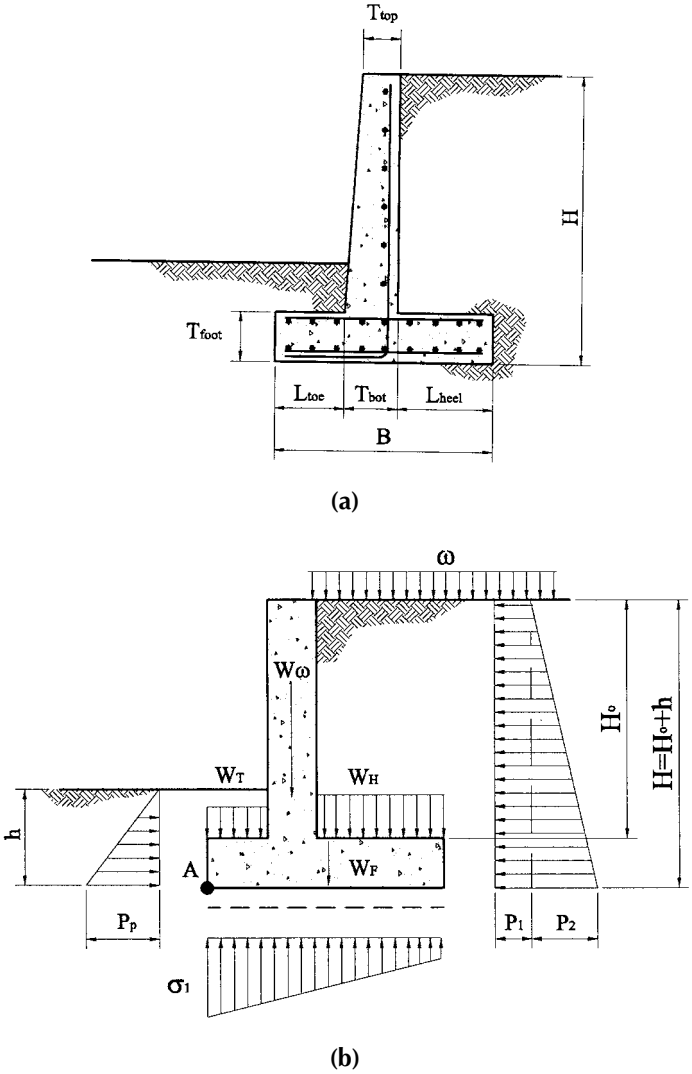

FIGURE 4.22 Design example.

For most cases, the following values can be used as the initial assumptions in the reinforced concrete retaining wall design process.

- $0.4 \le B/H \le 0.8$
- $1/12 \le t_{bot}/H \le 1/8$
- $L_{toe} \cong B/3$
- $t_{top} \ge 300$ mm
- $t_{foot} \ge t_{bot}$

TABLE 4.8 Cantilever Retaining Wall Design Data with Uniformly Distributed Surcharge Load

s	h	1.0	1.2	1.4	1.6	1.8	2.0	2.2	2.4	2.6	2.8	3.0
	p	2.94	4.24	5.77	7.53	9.53	11.77	14.24	16.94	19.89	23.06	26.48
0.00	y	0.33	0.40	0.47	0.53	0.60	0.67	0.73	0.80	0.87	0.93	1.00
	m	0.98	1.69	2.69	4.02	5.72	7.84	10.44	13.56	17.24	21.53	26.48
	p	5.30	7.06	9.06	11.30	13.77	16.47	19.42	22.59	26.01	29.65	33.54
0.40	y	0.41	0.48	0.55	0.62	0.69	0.76	0.83	0.90	0.97	1.04	1.11
	m	2.16	3.39	5.00	7.03	9.53	12.55	16.14	20.33	25.19	30.75	37.07
	p	6.47	8.47	10.71	13.18	15.89	18.83	22.00	25.42	29.06	32.95	37.07
0.60	y	0.42	0.50	0.57	0.65	0.72	0.79	0.86	0.93	1.00	1.07	1.14
	m	2.75	4.24	6.15	8.54	11.44	14.91	18.98	23.72	29.17	35.36	42.36
	p	7.65	9.88	12.36	15.06	18.00	21.18	24.59	28.24	32.12	36.24	40.60
0.80	y	0.44	0.51	0.59	0.67	0.74	0.81	0.89	0.96	1.03	1.10	1.17
	m	3.33	5.08	7.30	10.04	13.34	17.26	21.83	27.11	33.14	39.98	47.66
	p	8.83	11.30	14.00	16.94	20.12	23.53	27.18	31.07	35.18	39.54	44.13
1.00	y	0.44	0.53	0.60	0.68	0.76	0.83	0.91	0.98	1.06	1.13	1.20
	m	3.92	5.93	8.46	11.55	15.25	19.61	24.68	30.50	37.12	44.59	52.95
	p	11.77	14.83	18.12	21.65	25.42	29.42	33.65	38.13	42.83	47.77	52.95
1.50	y	0.46	0.54	0.63	0.71	0.79	0.87	0.94	1.02	1.10	1.17	1.25
	m	5.39	8.05	11.34	15.31	20.02	25.50	31.80	38.97	47.06	56.12	66.19
	p	14.71	18.36	22.24	26.36	30.71	35.30	40.13	45.19	50.48	56.01	61.78
2.00	y	0.47	0.55	0.64	0.72	0.81	0.89	0.97	1.05	1.13	1.21	1.29
	m	6.86	10.17	14.22	19.08	24.78	31.38	38.92	47.45	57.01	67.65	79.43

s	h	3.2	3.4	3.6	3.8	4.0	4.2	4.4	4.6	4.8	5.0	5.2
	p	30.12	34.01	38.13	42.48	47.07	51.89	56.95	62.25	67.78	73.55	79.55
0.00	y	1.07	1.13	1.20	1.27	1.33	1.40	1.47	1.53	1.60	1.67	1.73
	m	32.13	38.54	45.75	53.81	62.76	72.65	83.53	95.45	108.45	122.58	137.88
	p	37.66	42.01	46.60	51.42	56.48	61.78	67.31	73.07	79.08	85.31	91.78
0.40	y	1.17	1.24	1.31	1.38	1.44	1.51	1.58	1.65	1.71	1.78	1.85
	m	44.18	52.14	61.00	70.80	81.59	93.41	106.31	120.35	135.56	151.99	169.70
	p	41.42	46.01	50.83	55.89	61.19	66.72	72.49	78.49	84.72	91.20	97.90
0.60	y	1.21	1.28	1.35	1.42	1.49	1.56	1.62	1.69	1.76	1.83	1.90
	m	50.21	58.95	68.63	79.30	91.00	103.79	117.70	132.80	149.11	166.70	185.61
	p	45.19	50.01	55.07	60.37	65.90	71.66	77.66	83.90	90.37	97.08	104.02
0.80	y	1.24	1.31	1.38	1.45	1.52	1.59	1.66	1.73	1.80	1.87	1.94
	m	56.23	65.75	76.25	87.79	100.41	114.17	129.09	145.25	162.67	181.41	201.52
	p	48.95	54.01	59.31	64.84	70.60	76.60	82.84	89.31	96.02	102.96	110.14
1.00	y	1.27	1.34	1.41	1.49	1.56	1.63	1.70	1.77	1.84	1.90	1.97
	m	62.26	72.55	83.88	96.29	109.83	124.54	140.48	157.70	176.23	196.12	217.43
	p	58.37	64.01	69.90	76.02	82.37	88.96	95.79	102.85	110.14	117.67	125.44
1.50	y	1.32	1.40	1.47	1.55	1.62	1.69	1.76	1.84	1.91	1.98	2.05
	m	77.32	89.55	102.94	117.53	133.36	150.49	168.96	188.82	210.12	232.89	257.20
	p	67.78	74.02	80.49	87.19	94.14	101.32	108.73	116.38	124.26	132.38	140.74
2.00	y	1.36	1.44	1.52	1.59	1.67	1.74	1.82	1.89	1.96	2.04	2.11
	m	92.38	106.56	122.00	138.77	156.90	176.44	197.44	219.94	244.00	269.67	296.97

TABLE 4.8 Cantilever Retaining Wall Design Data with Uniformly Distributed Surcharge Load

s	h	5.4	5.6	5.8	6.0	6.2	6.4	6.6	6.8	7.0	7.2	7.4
	p	85.78	92.25	98.96	105.90	113.08	120.50	128.14	136.03	144.15	152.50	161.09
0.00	y	1.80	1.87	1.93	2.00	2.07	2.13	2.20	2.27	2.33	2.40	2.47
	m	154.41	172.21	191.33	211.81	233.70	257.06	281.92	308.33	336.35	366.01	397.36
	p	98.49	105.43	112.61	120.03	127.67	135.56	143.68	152.03	160.62	169.45	178.51
0.40	y	1.92	1.98	2.05	2.12	2.18	2.25	2.32	2.39	2.45	2.52	2.59
	m	188.72	209.11	230.91	254.17	278.94	305.26	333.18	362.74	394.01	427.01	461.80
	p	104.85	112.02	119.44	127.09	134.97	143.09	151.44	160.03	168.86	177.92	187.22
0.60	y	1.96	2.03	2.10	2.17	2.23	2.30	2.37	2.44	2.50	2.57	2.64
	m	205.88	227.56	250.70	275.35	301.55	329.36	358.81	389.95	422.83	457.51	494.02
	p	111.20	118.61	126.26	134.15	142.27	150.62	159.21	168.04	177.10	186.39	195.92
0.80	y	2.01	2.07	2.14	2.21	2.28	2.35	2.41	2.48	2.55	2.62	2.69
	m	223.04	246.01	270.50	296.53	324.17	353.46	384.43	417.16	451.66	488.01	526.24
	p	117.55	125.20	133.09	141.21	149.56	158.15	166.98	176.04	185.33	194.86	204.63
1.00	y	2.04	2.11	2.18	2.25	2.32	2.39	2.46	2.52	2.59	2.66	2.73
	m	240.19	264.46	290.29	317.71	346.79	377.55	410.06	444.36	480.49	518.51	558.46
	p	133.44	141.68	150.15	158.86	167.80	176.98	186.39	196.04	205.93	216.05	226.40
1.50	y	2.12	2.19	2.26	2.33	2.40	2.47	2.54	2.61	2.68	2.75	2.82
	m	283.08	310.59	339.77	370.67	403.33	437.80	474.14	512.38	552.57	594.76	639.00
	p	149.33	158.15	167.21	176.51	186.04	195.81	205.81	216.05	226.52	237.23	248.17
2.00	y	2.18	2.26	2.33	2.40	2.47	2.54	2.62	2.69	2.76	2.83	2.90
	m	325.97	356.72	389.25	423.62	459.87	498.05	538.21	580.39	624.64	671.01	719.55

s	h	7.6	7.8	7.0	8.2	8.4	8.6	8.8	9.0	9.2	9.5	10.0
	p	169.92	178.98	144.15	197.81	207.57	217.58	227.81	238.29	248.99	265.50	294.18
0.00	y	2.53	2.60	2.33	2.73	2.80	2.87	2.93	3.00	3.07	3.17	3.33
	m	430.46	465.35	336.35	540.67	581.21	623.72	668.25	714.86	763.58	840.74	980.60
	p	187.80	197.34	160.62	217.10	227.34	237.82	248.52	259.47	270.65	287.86	317.71
0.40	y	2.65	2.72	2.45	2.85	2.92	2.99	3.06	3.12	3.19	3.29	3.46
	m	498.43	536.94	394.01	619.79	664.23	710.75	759.38	810.17	863.18	946.94	1098.27
	p	196.75	206.51	168.86	226.75	237.23	247.93	258.88	270.06	281.47	299.03	329.48
0.60	y	2.71	2.77	2.50	2.91	2.98	3.04	3.11	3.18	3.24	3.34	3.51
	m	532.41	572.73	422.83	659.36	705.75	754.26	804.94	857.83	912.98	1000.04	1157.11
	p	205.69	215.69	177.10	236.40	247.11	258.05	269.23	280.65	292.30	310.21	341.25
0.80	y	2.75	2.82	2.55	2.96	3.02	3.09	3.16	3.23	3.29	3.39	3.56
	m	566.39	608.53	451.66	698.92	747.26	797.78	850.50	905.49	962.78	1053.14	1215.94
	p	214.63	224.87	185.33	246.05	257.00	268.17	279.59	291.24	303.12	321.39	353.02
1.00	y	2.80	2.87	2.59	3.00	3.07	3.14	3.20	3.27	3.34	3.44	3.61
	m	600.38	644.32	480.49	738.48	788.78	841.29	896.06	953.14	1012.58	1106.24	1274.78
	p	236.99	247.82	205.93	270.17	281.71	293.47	305.48	317.71	330.19	349.34	382.43
1.50	y	2.89	2.96	2.68	3.10	3.17	3.24	3.31	3.38	3.44	3.55	3.72
	m	685.34	733.81	552.57	837.38	892.57	950.08	1009.97	1072.29	1137.07	1238.99	1421.87
	p	259.35	270.76	226.52	294.30	306.42	318.77	331.36	344.19	357.25	377.29	411.85
2.00	y	2.97	3.04	2.76	3.18	3.25	3.32	3.39	3.46	3.53	3.64	3.81
	m	770.30	823.30	624.64	936.28	996.35	1058.87	1123.88	1191.43	1261.57	1371.74	1568.96

Notes:
1. s = equivalent soil thickness for uniformly distributed surcharge load (m).
2. h = wall height (m); the distance from bottom of the footing to top of the wall.
3. Assume soil density = 2.0 ton/m^3.
4. Active earth pressure factor $k_a = 0.30$.

Example

Given
A reinforced concrete retaining wall as shown in Figure 4.22b:

H_o = 3.0 m; surcharge ω = 11.00 kPa
Earth internal friction angle $\phi = 30°$
Earth unit weight $\gamma = 1.8$ *ton/m*^{3}
Bearing capacity $[\sigma]$ = 190 kPa
Friction coefficient $f = 0.30$

Solution

1. **Select Control Dimensions**
   Try h = 1.5 m, therefore, $H = H_o + h = 3.0 + 1.5 = 4.5$ m.
   Use

$$t_{bot} = 1/10H = 0.45 \text{ m} \Rightarrow 500 \text{ mm}; \; t_{top} = t_{bot} = 500 \text{ mm}$$

$$t_{foot} = 600 \text{ mm}$$

   Use

$$B = 0.6H = 2.70 \text{ m} \Rightarrow 2700 \text{ mm};$$

$$L_{toe} = 900 \text{ mm; therefore, } L_{heel} = 2.7 - 0.9 - 0.5 = 1.3 \text{ m} = 1300 \text{ mm}$$

2. **Calculate Lateral Earth Pressure**
   From Table 4.4, $k_a = 0.33$ and $k_p = 3.00$.
   Active Earth pressure:

$$\text{Part 1 (surcharge) } P_1 = k_a \omega H = 0.33(11.0)(4.5) = 16.34 \text{ kN}$$

$$\text{Part 2 } P_2 = 0.5 \, k_a \gamma \, H^2 = 0.5(0.33)(17.66)(4.5)^2 = 59.01 \text{ kN}$$

   Maximum possible passive Earth pressure:

$$P_p = 0.5 k_p \gamma h^2 = 0.5(3.00)(17.66)(1.5)^2 = 59.60 \text{ kN}$$

3. **Calculate Vertical Loads**

Surcharge	W_s (11.00)(1.3)	= 14.30 kN

   Use $\rho = 2.50$ ton/m^3 as the unit weight of reinforced concrete

Wall	W_w 0.50 (4.5 – 0.6) (24.53)	= 47.83 kN
Footing	W_f 0.60 (2.70) (24.53)	= 39.74 kN
Soil cover at toe	W_t 17.66 (1.50 – 0.60) (0.90)	= 14.30 kN
Soil cover at heel	W_h 17.66 (4.50 – 0.60) (1.30)	= 89.54 kN
		Total 205.71 kN

   Hence, the maximum possible friction force at bottom of footing

$$F = fN_{tot} = 0.30\ (205.71) = 61.71\ \text{kN}$$

4. Check Sliding

Total lateral active force (include surcharge)

$$P_1 + P_2 = 16.34 + 59.01 = 75.35\ \text{kN}$$

Total maximum possible sliding resistant capacity

$$\text{Passive} + \text{friction} = 59.60 + 61.71 = 121.31\ \text{kN}$$

Sliding safety factor = 121.31/75.35 = 1.61 > 1.50 OK

5. Check Overturning

Take point *A* as the reference point

Resistant moment (do not include passive force for conservative)

Surcharge	14.30 (1.3/2 + 0.5 + 0.9)	= 29.32 kN·m
Soil cover at heel	89.54 (1.3/2 + 0.5 + 0.9)	= 183.56 kN·m
Wall	47.83 (0.5/2 + 0.9)	= 55.00 kN·m
Soil cover at toe	14.30 (0.9/2)	= 6.44 kN·m
Footing	39.74 (2.7/2)	= 53.65 kN·m
		Total 327.97 kN·m

Overturning moment

$$P_1(H/2) + P_2(H/3) = 16.34\ (4.5)/2 + 59.01\ (4.5)/3 = 125.28\ \text{kN·m}$$

Sliding safety factor = 327.97/125.28 = 2.62 > 1.50 OK

6. Check Bearing

Total vertical load

$$N_{tot} = 205.71\ \text{kN}$$

Total moment about center line of footing:

- Clockwise (do not include passive force for conservative)

Surcharge	14.30 (2.70/2 – 1.30/2)	= 10.01 kN·m
Soil cover @ heel	89.54 (2.70/2 – 1.30/2)	= 62.68 kN·m
		72.69 kN·m

- Counterclockwise

Wall	47.83 (2.70/2 – 0.9 – 0.5/2)	= 9.57 kN·m
Soil cover at toe	14.30 (2.70/2 – 0.9/2)	= 12.87 kN·m
Active earth pressure		= 125.28 kN·m
		147.72 kN·m

Total moment at bottom of footing

$$M_{tot} = 147.72\text{-}72.69 = 75.03 \text{ kN·m (counterclockwise)}$$

Maximum bearing stress

$$\sigma = N_{tot}/A \pm M_{tot}/S$$

where
$A = 2.70\ (1.0) = 2.70\ m^2$
$S = 1.0\ (2.7)\ /6 = 1.22\ m^3$

Therefore:

$$\sigma_{max} = 205.71/2.70 + 75.03/1.22 = 137.69 \text{ kPa}$$
$$< [\sigma] = 190 \text{ kPa}$$

and

$$\sigma_{min} = 205.71/2.70 - 75.03/1.22 = 14.69 \text{ kPa}$$
$$> 0 \qquad \text{OK}$$

7. **Flexure and Shear Strength**
   Both wall and footing sections need to be designed to have enough flexure and shear capacity.

4.3.4 Tieback Wall

The tieback wall is the proper structure type for cut sections. The tiebacks are prestressed anchor cables that are used to resist the lateral soil pressure. Compared with other types of retaining structures, the tieback wall has the least lateral deflection. Figure 4.23 shows the typical components and the basic lateral soil pressure distribution on a tieback wall.

The vertical spacing of tiebacks should be between 1.5 and 2.0 m to satisfy the required clearance for construction equipment. The slope angle of drilled holes should be 10 to 15° for grouting convenience. To minimize group effects, the spacing between the tiebacks should be greater than three times the tieback hole diameter, or 1.5 m minimum.

The bond strength for tieback design depends on factors such as installation technique, hole diameter, etc. For preliminary estimates, an ultimate bound strength of 90 to 100 kPa may be assumed. Based on construction experience, most tieback hole diameters are between 150 and 300 mm, and the tieback design capacity is in the range of 150 to 250 kN. Therefore, the corresponding lateral spacing of the tieback will be 2.0 to 3.0 m. The final tieback capacity must be proof-tested by stressing the test tieback at the construction site.

A tieback wall is built from the top down in cut sections. The wall details consist of a base layer and face layer. The base layer may be constructed by using vertical soldier piles with timber or concrete lagging between piles acting as a temporary wall. Then, a final cast-in-place reinforced-concrete layer will be constructed as the finishing layer of the wall. Another type of base layer that has been used effectively is cast-in-place "shotcrete" walls.

4.3.5 Reinforced Earth-Retaining Structure

The reinforced earth-retaining structure can be used in fill sections only. There is no practical height limit for this retaining system, but there will be a certain amount of lateral movement. The essential

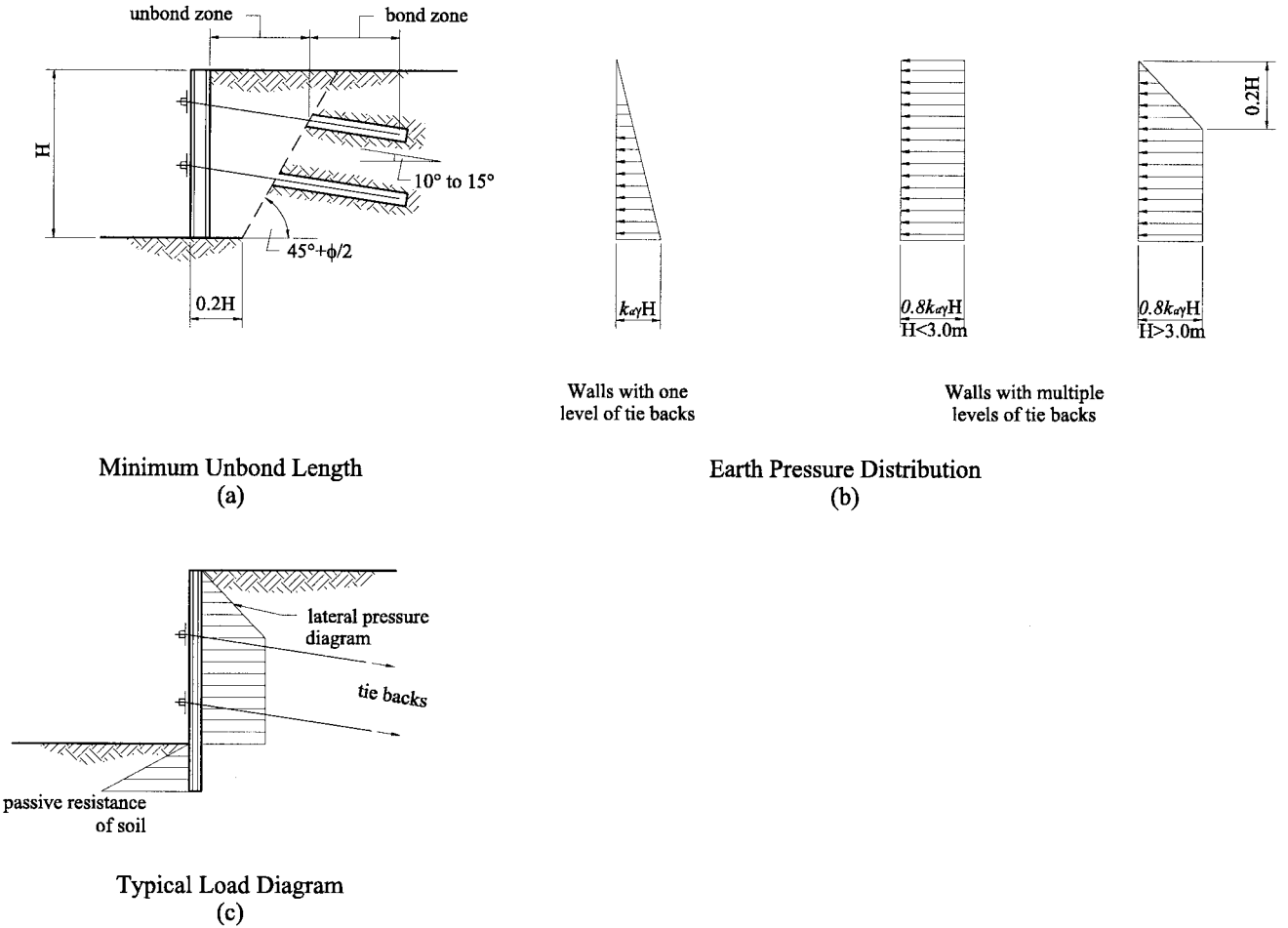

FIGURE 4.23 Tieback wall. (a) Minimum unbond length; (b) earth pressure distribution distribution; (c) typical load diagram.

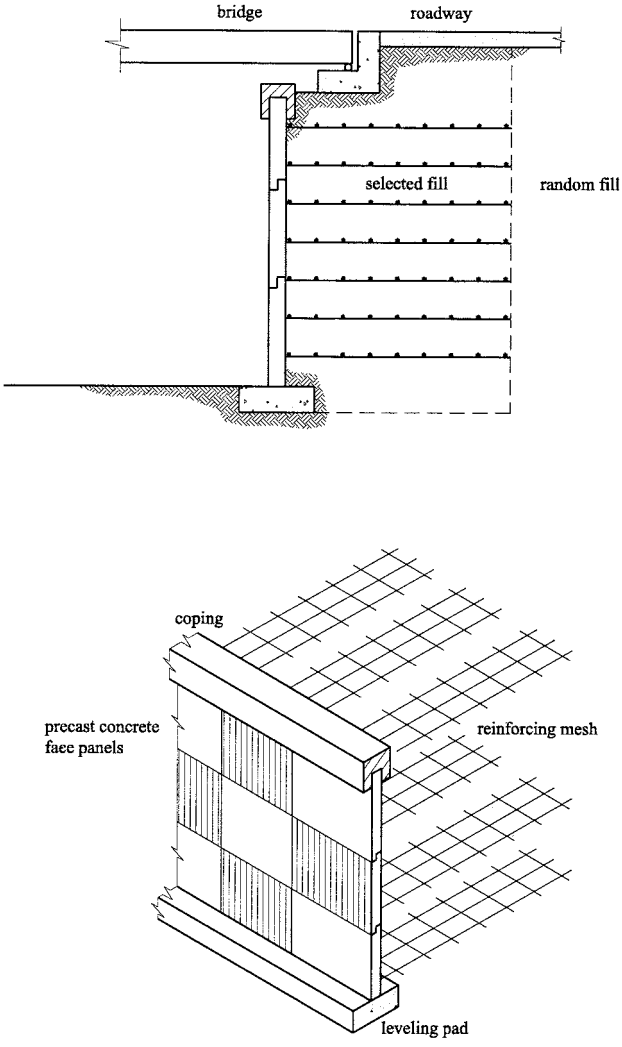

FIGURE 4.24 Mechanical Stabilized Earth (MSE).

concept is the use of multiple-layer strips or fibers to reinforce the fill material in the lateral direction so that the integrated fill material will act as a gravity retaining structure. Figure 4.24 shows the typical details of the MSE retaining structure.

Typically, the width of fill and the length of strips perpendicular to the wall face are on the order of 0.8 of the fill height. The effective life of the material used for the reinforcing must be considered. Metals or nondegradable fabrics are preferred.

Overturning and sliding need to be checked under the assumption that the reinforced soil body acts as a gravity retaining wall. The fiber strength and the friction effects between strip and fill material also need to be checked. Finally, the face panel needs to be designed as a slab which is anchored by the strips and subjected to lateral soil pressure.

4.3.6 Seismic Considerations for Retaining Structures

Seismic effects can be neglected in most retaining structure designs. For oversized retaining structures ($H > 10$ m), the seismic load on a retaining structure can be estimated by using the Mononobe–Okabe solution.

Soil Body ARS Factors

The factors k_v and k_h represent the maximum possible soil body acceleration values under seismic effects in the vertical and horizontal directions, respectively. Similar to other seismic load representations, the acceleration due to gravity will be used as the basic unit of k_v and k_h.

Unless a specific site study report is available, the maximum horizontal ARS value multiplied by 0.50 can be used as the k_h design value. Similarly, k_v will be equal to 0.5 times the maximum vertical ARS value. If the vertical ARS curve is not available, k_v can be assigned a value from $0.1k_h$ to $0.3k_h$.

Earth Pressure with Seismic Effects

Figure 4.25 shows the basic loading diagram for earth pressure with seismic effects. Similar to a static load calculation, the active force per unit length of wall (P_{ac}) can be determined as:

$$P_{ae} = \frac{1}{2} k_{ae} \gamma \left(1 - k_v\right) H^2 \tag{4.12}$$

where

$$\theta' = \tan^{-1}\left[\frac{k_h}{1 - k_v}\right] \tag{4.13}$$

$$k_{ae} = \frac{\sin^2\left(\phi + \beta - \theta'\right)}{\cos\theta' \sin^2\beta \sin\left(\beta - \theta' - \delta\right)\left[1 + \sqrt{\dfrac{\sin\left(\phi + \delta\right)\sin\left(\phi - \theta' - \alpha\right)}{\sin\left(\beta - \theta' - \delta\right)\sin\left(\alpha + \beta\right)}}\right]^2} \tag{4.14}$$

Note that with no seismic load, $k_v = k_h = \theta' = 0$. Therefore, $K_{ac} = K_a$.

The resultant total lateral force calculated above does not act at a distance of $H/3$ from the bottom of the wall. The following simplified procedure is often used in design practice:

- Calculate P_{ae} (total active lateral earth pressure per unit length of wall)
- Calculate $P_a = \frac{1}{2} k_a \gamma H^2$ (static active lateral earth pressure per unit length of wall)

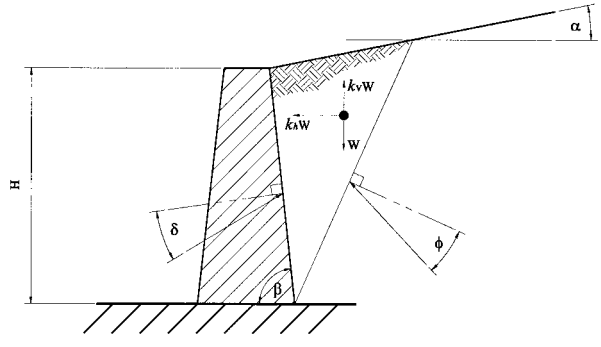

FIGURE 4.25 Load diagram for Earth pressure with seismic effects.

- Calculate $\Delta P = P_{ae} - P_a$
- Assume P_a acts at a distance of $H/3$ from the bottom of the wall
- Assume ΔP acts at a distance of $0.6H$ from the bottom of the wall

The total earth pressure, which includes seismic effects P_{ae}, should always be bigger than the static force P_a. If the calculation results indicate $\Delta P < 0$, use $k_v = 0$.

Using a procedure similar to the active Earth pressure calculation, the passive Earth pressure with seismic effects can be determined as follows:

$$P_{pe} = \frac{1}{2} k_{pe} \gamma (1 - k_v) H^2 \tag{4.15}$$

where

$$\theta' = \tan^{-1}\left[\frac{k_h}{1 - k_v}\right]$$

$$k_{pe} = \frac{\sin^2(\beta + \theta' - \phi)}{\cos\theta' \sin^2\beta \sin(\beta + \theta' + \delta - 90)\left[1 - \sqrt{\dfrac{\sin(\phi + \delta)\sin(\phi - \theta' + \alpha)}{\sin(\beta + \theta' + \delta)\sin(\alpha + \beta)}}\right]^2} \tag{4.16}$$

Note that, with no seismic load, $k_{pc} = k_p$.

References

1. AASHTO, *Standard Specifications for Highway Bridges,* 16th ed., American Association of State Highway and Transportation Officials, Washington, D.C., 1996.
2. *Bridge Memo to Designers Manual*, Department of Transportation, State of California, Sacramento.
3. Brian H. Maroney, Matt Griggs, Eric Vanderbilt, Bruce Kutter, Yuk H. Chai and Karl Romstad, Experimental measurements of bridge abutment behavior, in *Proceeding of Second Annual Seismic Research Workshop,* Division of Structures, Department of Transportation, Sacramento, CA, March 1993.
4. Brian H. Maroney and Yuk H. Chai, Bridge abutment stiffness and strength under earthquake loadings, in *Proceedings of the Second International Workshop of Seismic Design and Retroffitting of Reinforced Concrete Bridges,* Queenstown, New Zealand, August 1994.
5. Rakesh K. Goel, Earthquake behavior of bridge with integral abutment, in *Proceedings of the National Seismic Conference on Bridges and Highways,* Sacramento, CA, July 1997.
6. E. C. Sorensen, Nonlinear soil-structure interaction analysis of a 2-span bridge on soft clay foundation, in *Proceedings of the National Seismic Conference on Bridges and Highways,* Sacramento, CA, July 1997.
7. AEAR, *Manual for Railway Engineering,* 1996.
8. Braja M. Das, *Principles of Foundation Engineering*, PWS-KENT Publishing Company, Boston, MA, 1990.
9. T. William Lambe and Robert V. Whitman, *Soil Mechanics*, John Wiley & Sons, New York, 1969.
10. Gregory P. Tschebotarioff, *Foundations, Retaining and Earth Structures,* 4th ed., McGraw-Hill, New York, 1973.
11. Joseph E. Bowles, *Foundation Analysis and Design,* McGraw-Hill, New York, 1988.
12. Whitney Clark Huntington, *Earth Pressure and Retaining Walls,* John Wiley & Sons, New York.

5

Geotechnical Considerations

Thomas W. McNeilan
Fugro West, Inc.

James Chai
California Department of Transportation

5.1 Introduction

A complete geotechnical study of a site will (1) determine the subsurface stratigraphy and stratigraphic relationships (and their variability), (2) define the physical properties of the earth materials, and (3) evaluate the data generated and formulate solutions to the project-specific and site-specific geotechnical issues. Geotechnical issues that can affect a project can be broadly grouped as follows:

- *Foundation Issues* — Including the determination of the strength, stability, and deformations of the subsurface materials under the loads imposed by the structure foundations, in and beneath slopes and cuts, or surrounding the subsurface elements of the structure.
- *Earth Pressure Issues* — Including the loads and pressures imposed by the earth materials on foundations and against supporting structures, or loads and pressures created by seismic (or other) external forces.

- *Construction and Constructibility Considerations* — Including the extent and characteristics of materials to be excavated, and the conditions that affect deep foundation installation or ground improvement.
- *Groundwater Issues* — Including occurrence, hydrostatic pressures, seepage and flow, and erosion.

Site and subsurface characteristics directly affect the choice of foundation type, capacity of the foundation, foundation construction methods, and bridge cost. Subsurface and foundation conditions also frequently directly or indirectly affect the route alignment, bridge type selection, and/or foundation span lengths. Therefore, an appropriately scoped and executed foundation investigation and site characterization should:

1. Provide the required data for the design of safe, reliable, and economic foundations;
2. Provide data for contractors to use to develop appropriate construction cost estimates;
3. Reduce the potential for a "changed condition" claim during construction.

In addition, the site investigation objectives frequently may be to

1. Provide data for route selection and bridge type evaluation during planning and preliminary phase studies;
2. Provide data for as-built evaluation of foundation capacity, ground improvement, or other similar requirements.

For many projects, it is appropriate to conduct the geotechnical investigation in phases. For the first preliminary (or reconnaissance) phase, either a desktop study using only historical information or a desktop study and a limited field exploration program may be adequate. The results of the first-phase study can then be used to develop a preliminary geologic model of the site, which is used to determine the key foundation design issues and plan the design-phase site investigation.

Bridge projects may require site investigations to be conducted on land, over water, and/or on marginal land at the water's edge. Similarly, site investigations for bridge projects can range from conventional, limited-scope investigations for simple overpasses and grade separations to major state-of-the-practice investigations for large bridges over major bodies of water.

This chapter includes discussions of

- Field exploration techniques;
- Definition of the requirements for and extent of the site investigation program;
- Evaluation of the site investigation results and development/scoping of the laboratory testing program;
- Data presentation and site characterization.

The use of the site characterization results for foundation design is included in subsequent chapters.

5.2 Field Exploration Techniques

For the purpose of the following discussion, we have divided field exploration techniques into the following groupings:

- Borings (including drilling, soil sampling, and rock-coring techniques)
- Downhole geophysical logging
- *In situ* testing — including cone penetration testing (CPT) and vane shear, pressure meter and dilatometer testing
- Test pits and trenches
- Geophysical survey techniques

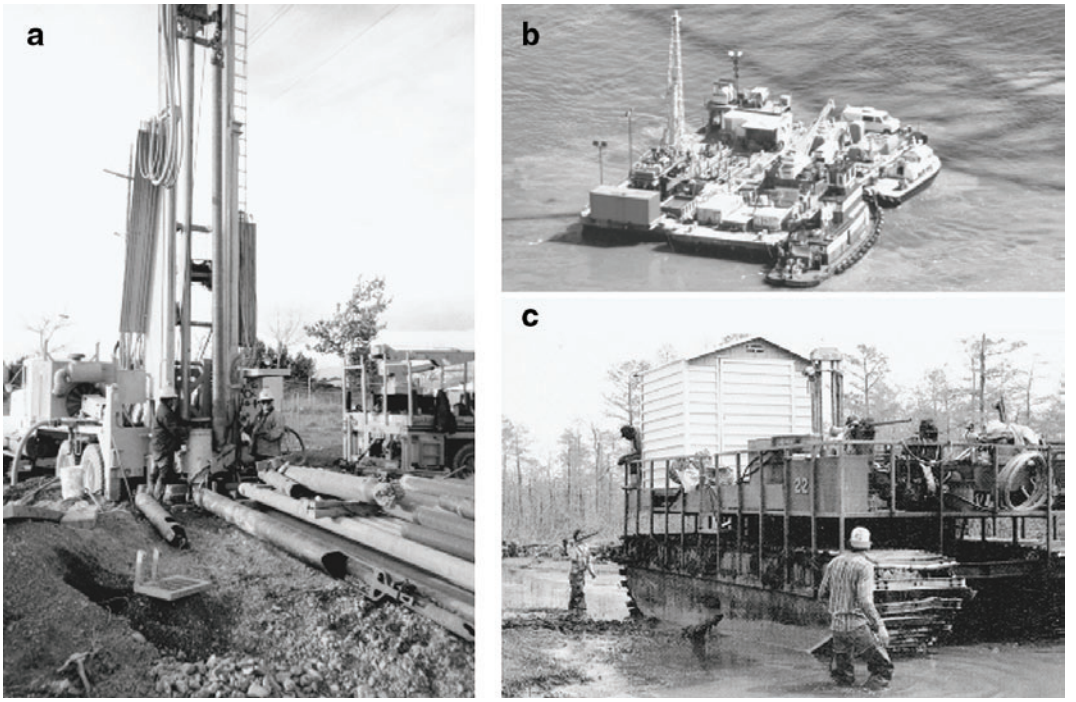

FIGURE 5.1 Drilling methods. (a) On land; (b) over water; (c) on marginal land.

5.2.1 Borings and Drilling Methods

Drilled soil (or rock) borings are the most commonly used subsurface exploration techniques. The drilled hole provides the opportunity to collect samples of the subsurface through the use of a variety of techniques and samplers. In addition to sample collection, drilling observations during the advancement of the borehole provide an important insight to the subsurface conditions. Drilling methods can be used for land, over water, and marginal land sites (Figure 5.1). It should be noted that the complexity introduced when working over water or on marginal land may require more-sophisticated and more-specialized equipment and techniques, and will significantly increase costs.

5.2.1.1 Wet (Mud) Rotary Borings

Wet rotary drilling is the most commonly used drilling method for the exploration of soil and rock, and also is used extensively for oil exploration and water well installation. It is generally the preferred method for (1) over water borings; (2) where groundwater is shallow; and (3) where the subsurface includes soft, squeezing, or flowing soils.

With this technique, the borehole is advanced by rapid rotation of the drill bit that cuts, chips, and grinds the material at the bottom of the borehole. The cuttings are removed from the borehole by circulating water or drilling fluid down through the drill string to flush the cuttings up through the annular space of the drill hole. The fluids then flow into a settling pit or solids separator. Drilling fluid is typically bentonite (a highly refined clay) and water, or one of a number of synthetic products. The drilling fluids are used to flush the cuttings from the hole, compensate the fluid pressure, and stabilize borehole sidewalls. In broken or fractured rock, coarse gravel and cobbles, or other formations with voids, it may be necessary to case the borehole to prevent loss of circulation. Wet rotary drilling is conducive to downhole geophysical testing, although the borehole must be thoroughly flushed before conducting some types of logging.

5.2.1.2 Air Rotary Borings

The air rotary drilling technology is similar to wet rotary except that the cuttings are removed with the circulation of high-pressure air rather than a fluid. Air rotary drilling techniques are typically used in hard bedrock or other conditions where drill hole stability is not an overriding issue. In very hard bedrock, a percussion hammer is often substituted for the bit. Air rotary drilling is conducive to downhole geophysical testing methods.

5.2.1.3 Bucket-Auger Borings

The rotary bucket is similar to a large- (typically 18- to 24-in.)-diameter posthole digger with a hinged bottom. The hole is advanced by rotating the bucket at the end of a kelly bar while pressing it into the soil. The bucket is removed from the hole to be emptied. Rotary-bucket-auger borings are used in alluvial soils and soft bedrock. This method is not always suitable in cobbly or rocky soils, but penetration of hard layers is sometimes possible with special coring buckets. Bucket-auger borings also may be unsuitable below the water table, although drilling fluids can be used to stabilize the borehole.

The rotary-bucket-auger drilling method allows an opportunity for continuous inspection and logging of the stratigraphic column of materials, by lowering the engineer or geologist on a platform attached to a drill rig winch. It is common in slope stability and fault hazards studies to downhole log 24-in.-diameter, rotary-bucket-auger boreholes advanced with this method.

5.2.1.4 Hollow-Stem-Auger Borings

The hollow-stem-auger drilling technique is frequently used for borings less than 20 to 30 m deep. The proliferation of the hollow-stem-auger technology in recent years occurred as the result of its use for contaminated soils and groundwater studies. The hollow-stem-auger consists of sections of steel pipe with welded helical flanges. The shoe end of the pipe has a hollow bit assembly that is plugged while rotating and advancing the auger. That plug is removed for advancement of the sampling device ahead of the bit.

Hollow-stem-auger borings are used in alluvial soils and soft bedrock. This method is not always suitable where groundwater is shallow or in cobbly and rocky soils. When attempting to sample loose, saturated sands, the sands may flow into the hollow auger and produce misleading data. The hollow-stem-auger drill hole is not conducive to downhole geophysical testing methods.

5.2.1.5 Continuous-Flight-Auger Borings

Continuous-flight-auger borings are similar to the hollow-stem-auger drilling method except that the auger must be removed for sampling. With the auger removed, the borehole is unconfined and hole instability often results. Continuous-flight-auger drill holes are used for shallow exploration above the groundwater level.

5.2.2 Soil-Sampling Methods

There are several widely used methods for recovering samples for visual classification and laboratory testing.

5.2.2.1 Driven Sampling

Driven sampling using standard penetration test (SPT) or other size samplers is the most widely used sampling method. Although this sampling method recovers a disturbed sample, the "blow count" measured with this type of procedure provides a useful index of soil density or strength. The most commonly used blow count is the SPT blow count (also referred to as the N-value). Although the N-value is an approximate and imprecise measurement (its value is affected by many operating factors that are part of the sampling process, as well as the presence of gravel or cementation), various empirical relationships have been developed to relate N-value to engineering and performance properties of the soils.

5.2.2.2 Pushed Samples

A thin-wall tube (or in some cases, other types of samplers) can be pushed into the soil using hydraulic pressure from the drill rig, the weight of the drill rod, or a fixed piston. Pushed sampling generally recovers samples that are less disturbed than those recovered using driven-sampling techniques. Thus, laboratory tests to determine strength and volume change characteristics should preferably be conducted on pushed samples rather than driven samples. Pushed sampling is the preferred sampling method in clay soils. Thin-wall samples recovered using push-sampling techniques can either be extruded in the field or sealed in the tubes.

5.2.2.3 Drilled or Cored Samplers

Drilled-in samplers also have application in some types of subsurface conditions, such as hard soil and soft rock. With these types of samplers (e.g., Denison barrel and pitcher barrel), the sample barrel is either cored into the sediment or rock or is advanced inside the drill rod while the rod is advanced.

5.2.3 Rock Coring

The two rock-coring systems most commonly used for engineering applications are the conventional core barrel and wireline (retrievable) system. At shallow depths above the water table, coring also sometimes can be performed with an air or a mist system.

Conventional core barrels consist of an inner and outer barrel with a bit assembly. To obtain a core at a discrete interval: (1) the borehole is advanced to the top of the desired interval, (2) the drill pipe is removed, (3) the core barrel/bit is placed on the bottom of the pipe, and (4) the assembly is run back to the desired depth. The selected interval is cored and the core barrel is removed to retrieve the core. Conventional systems typically are most effective at shallow depths or in cases where only discrete samples are required.

In contrast, wireline coring systems allow for continuous core retrieval without removal of the drill pipe/bit assembly. The wireline system has a retrievable inner core barrel that can be pulled to the surface on a wireline after each core run.

Variables in the coring process include the core bit type, fluid system, and drilling parameters. There are numerous bit types and compositions that are applicable to specific types of rock; however, commercial diamond or diamond-impregnated bits are usually the preferred bit from a core recovery and quality standpoint. Tungsten carbide core bits can sometimes be used in weak rock or in high-clay-content rocks. A thin bentonite mud is the typical drilling fluid used for coring. Thick mud can clog the small bit ports and is typically avoided. Drilling parameters include the revolutions per minute (RPM) and weight on bit (WOB). Typically, low RPM and WOB are used to start the core run and then both values are increased.

Rock engineering parameters include percent recovery, rock quality designation (RQD), coring rate, and rock strength. Percent recovery is a measure of the core recovery vs. the cored length, whereas RQD is a measure of the intact core pieces longer than 4 in. vs. the cored length. Both values typically increase as the rock mass becomes less weathered/fractured with depth; however, both values are highly dependent on the type of rock, amount of fracturing, etc. Rock strength (which is typically measured using unconfined triaxial compression test per ASTM guidelines) is used to evaluate bearing capacity, excavatability, etc.

5.2.4 *In Situ* Testing

There are a variety of techniques that use instrumented probes or testing devices to measure soil properties and conditions in the ground, the more widely used of which are described below. In contrast to sampling that removes a sample from its *in situ* stress conditions, *in situ* testing is used to measure soil and rock properties in the ground at their existing state of stress. The various *in*

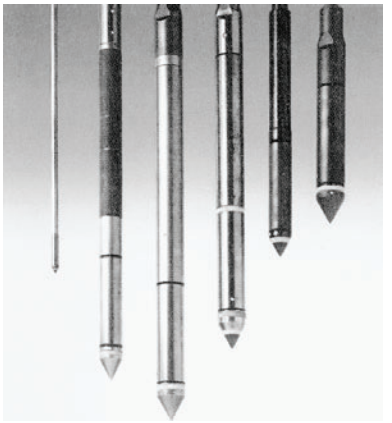

FIGURE 5.2 CPT cones.

situ tests can either be conducted in a borehole or as a continuous sounding from the ground surface. Except as noted, those techniques are not applicable to rock.

5.2.4.1 Cone Penetration Test Soundings

CPT sounding is one of the most versatile and widely used *in situ* test. The standard CPT cone consists of a 1.4-in.-diameter cone with an apex angle of 60°, although other cone sizes are available for special applications (Figure 5.2). The cone tip resistance beneath the 10-cm^2 cone tip and the friction along the 150 cm^2 friction sleeve are measured with strain gauges and recorded electronically at 1- or 2-cm intervals as the cone is advanced into the ground at a rate of about 2 cm/s. In addition to the tip and sleeve resistances, many cones also are instrumented to record pore water pressure or other parameters as the cone is advanced.

Because the CPT soundings provide continuous records of tip and sleeve resistances (and frequently pore pressure) vs. depth (Figure 5.3), they provide a continuous indicator of soil and subsurface conditions that are useful in defining soil stratification. Numerous correlations between the CPT measurements have been developed to define soil type and soil classification. In addition, empirical correlations have been published to relate the cone tip and sleeve friction resistances to engineering behavior, including undrained shear strength of clay soils and relative density and friction of granular soils.

Most land CPTs are performed as continuous soundings using large 20-ton cone trucks (Figure 5.4a), although smaller, more portable track-mounted equipment is also available. CPT soundings are commonly extended down to more than 20 to 50 m. CPT soundings also can be performed over water from a vessel using specialized equipment (Figure 5.4b) deployed by a crane or from a stern A-frame. In addition, downhole systems have been developed to conduct CPTs in boreholes during offshore site investigations. With a downhole system, CPT tests are interspersed with soil sampling to obtain CPT data to more than 100 m in depth.

5.2.4.2 *In Situ* Vane Shear Tests

The undrained shear strength of clay soils can be measured *in situ* using a vane shear test. This test is conducted by measuring the torque required to rotate a vane of known dimensions. The test can be conducted from the ground surface by attaching a vane blade onto a rod or downhole below the bottom of a borehole with a drop-in remote vane (Figure 5.5). The downhole vane is preferable, since the torque required to rotate the active rotating vane is not affected by the torque of the rod. The downhole vane is used both for land borings and over-water borings.

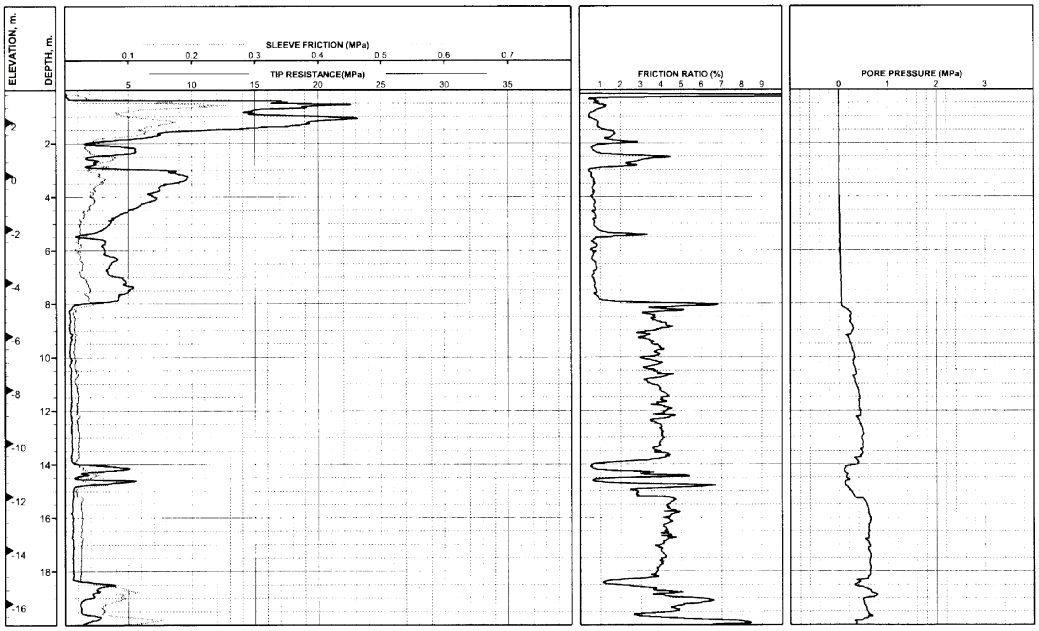

FIGURE 5.3 CPT data provide a continuous record of *in situ* conditions.

5.2.4.3 Pressure Meter and Dilatometer Tests

Pressure meter testing is used to measure the *in situ* maximum and average shear modulus of the soil or rock by inflating the pressure meter against the sidewalls of the borehole. The stresses, however, are measured in a horizontal direction, not in the vertical direction as would occur under most types of foundation loading. A test is performed by lowering the tool to the selected depth and expanding a flexible membrane through the use of hydraulic fluid. As the tool is inflated, the average displacement of the formation is measured with displacement sensors beneath the membrane, which is protected by stainless steel strips. A dilatometer is similar to a pressure meter, except that the dilatometer consists of a flat plate that is pushed into the soil below the bottom of the borehole. A dilatometer is not applicable to hard soils or rock.

5.2.5 Downhole Geophysical Logging

Geophysical logs are run to acquire data about the formation or fluid penetrated by the borehole. Each log provides a continuous record of a measured value at a specific depth in the boring, and is therefore useful for interpolating stratigraphy between sample intervals. Most downhole geophysical logs are presented as curves on grid paper or as electronic files (Figure 5.6). Some of the more prevalent geophysical tools, which are used for geotechnical investigations, are described below.

- *Electrical logs* (*E-logs*) include resistivity, induction, and spontaneous potential (SP) logs. Resistivity and induction logs are used to determine lithology and fluid type. A resistivity log is used when the borehole is filled with a conductive fluid, while an induction log is used when the borehole is filled with a non- or low-conductivity fluid. Resistivity tools typically require an open, uncased, fluid-filled borehole. Clay formations and sands with higher salinity will have low resistivity, while sands with fresh water will have higher resistivity values. Hard rock and dry formations have the highest resistivity values. An SP log is often used in suite with a resistivity or induction log to provide further information relative to formation permeability and lithology.

FIGURE 5.4 CPT sounding methods. (a) On land; (b) over water.

FIGURE 5.5 *In situ* vane shear device.

- *Suspension* (*velocity*) *logs* are used to measure the average primary, compression wave, and shear wave velocities of a 1-m-high segment of the soil and rock column surrounding the borehole. Those velocities are determined by measuring the elapsed time between arrivals of a wave propagating upward through the soil/rock column. The suspension probe includes both a shear wave source and a compression wave source, and two biaxial receivers that detect the source waves. This technique requires an open, fluid-filled hole.
- *Natural gamma logs* measure the natural radioactive decay occurring in the formation to infer soil or rock lithology. In general, clay soils will exhibit higher gamma counts than granular soils, although decomposed granitic sands are an exception to that generality. Gamma logs can be run in any salinity fluid as well as air, and also can be run in cased boreholes.
- *Caliper logs* are used to measure the diameter of a borehole to provide insight relative to caving and swelling. An accurate determination of borehole diameter also is important for the interpretation of other downhole logs.
- *Acoustic televiewer and digital borehole logs* are conducted in rock to image the rock surface within the borehole (Figure 5.7). These logs use sound in an uncased borehole to create an oriented image of the borehole surface. These logs are useful for determining rock layering, bedding, and fracture identification and orientation.
- *Crosshole, downhole, and uphole shear wave velocity measurements* are used to determine the primary and shear wave velocities either to determine the elastic soil properties of soil and rock or to calibrate seismic survey measurements. With the crosshole technique, the travel time is measured between a source in one borehole and a receiver in a second borehole. This technique can be used to measure directly the velocities of various strata. For downhole and uphole logs, the travel time is measured between the ground surface and a downhole source or receiver. Tests are conducted with the downhole source or receiver at different depths. These measurements should preferably be conducted in cased boreholes.

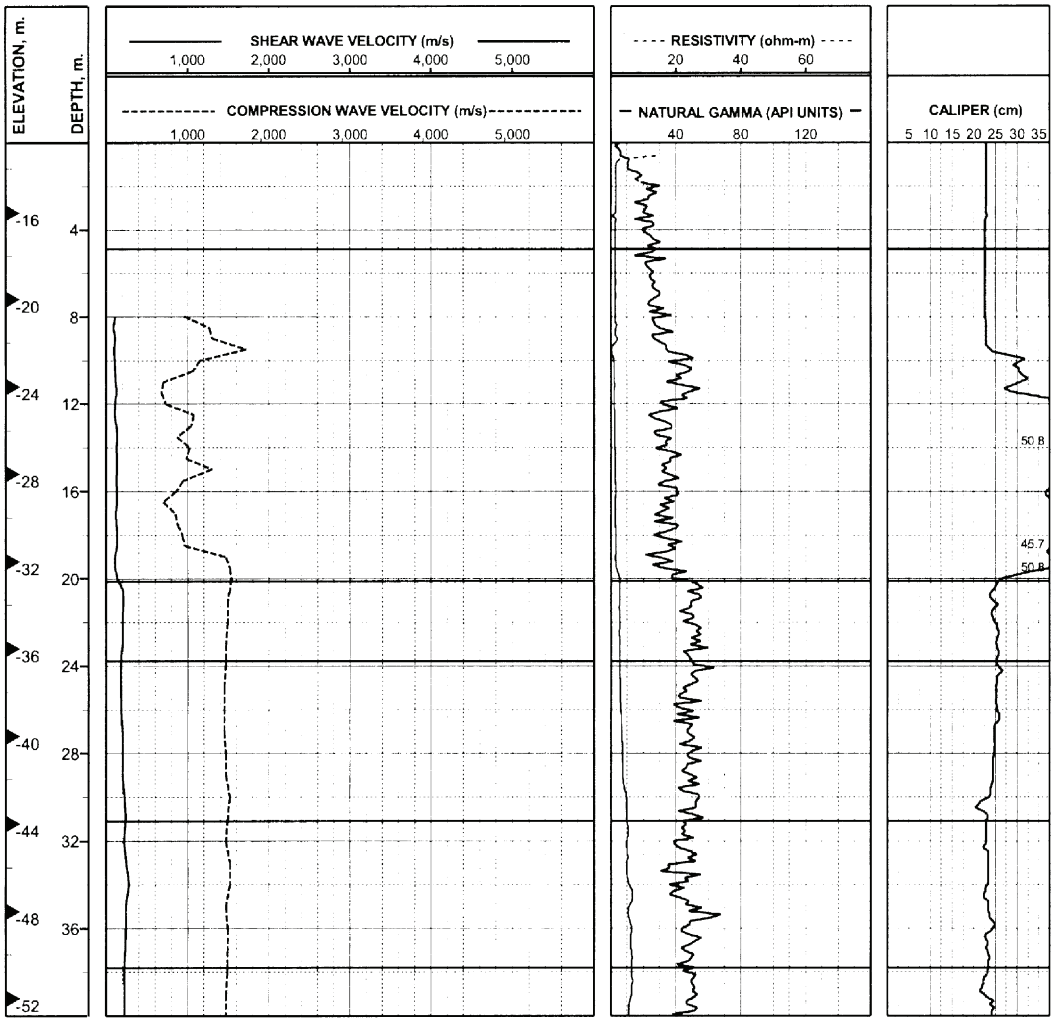

FIGURE 5.6 Example of downhole geophysical log.

5.2.6 Test Pits and Trenches

Where near-surface conditions are variable or problematic, the results of borings and *in situ* testing can be supplemented by backhoe-excavated or hand-excavated test pits or trenches. These techniques are particularly suitable for such purposes as: (1) collecting hand-cut, block samples of sensitive soils; (2) evaluating the variability of heterogeneous soils; (3) evaluating the extent of fill or rubble; (4) determining depth to groundwater; and (5) the investigation of faulting.

5.2.7 Geophysical Survey Techniques

Noninvasive (compared with drilling methods) geophysical survey techniques are available for remote sensing of the subsurface. In contrast to drilling and *in situ* testing methods, the geophysical survey methods explore large areas rapidly and economically. When integrated with boring data, these methods often are useful for extrapolating conditions between borings (Figure 5.8). Techniques are applicable either on land or below water. Some of the land techniques also are applicable for marginal land or in the shallow marine transition zone. Geophysical survey techniques can be used individually or as a group.

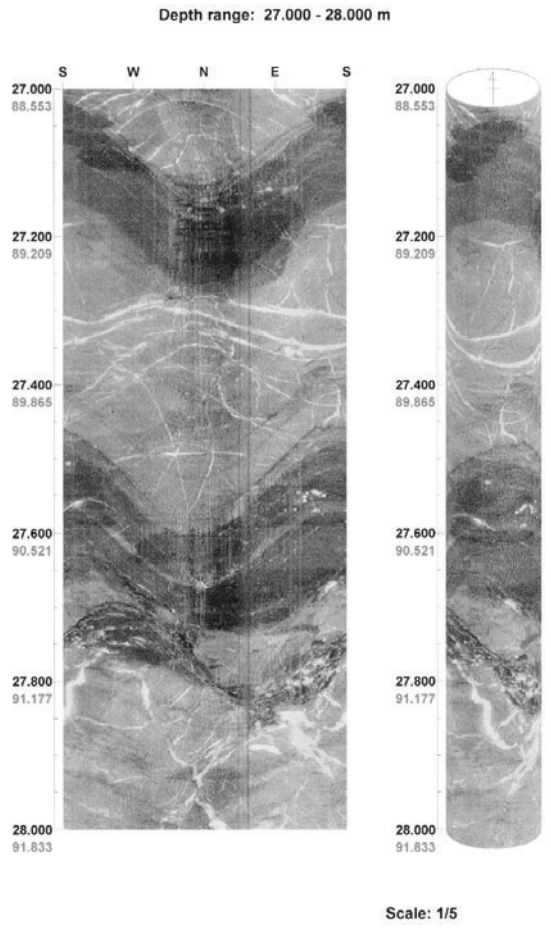

FIGURE 5.7 Example of digital borehole image in rock.

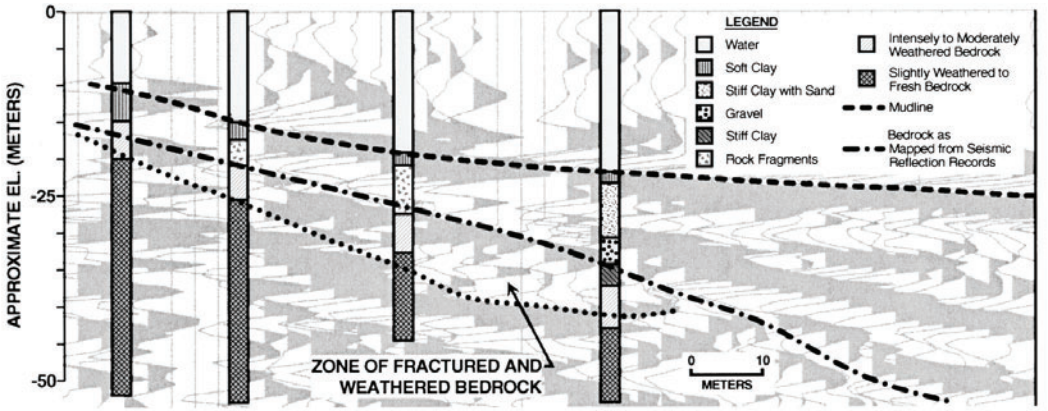

FIGURE 5.8 Example integration of seismic reflection and boring data.

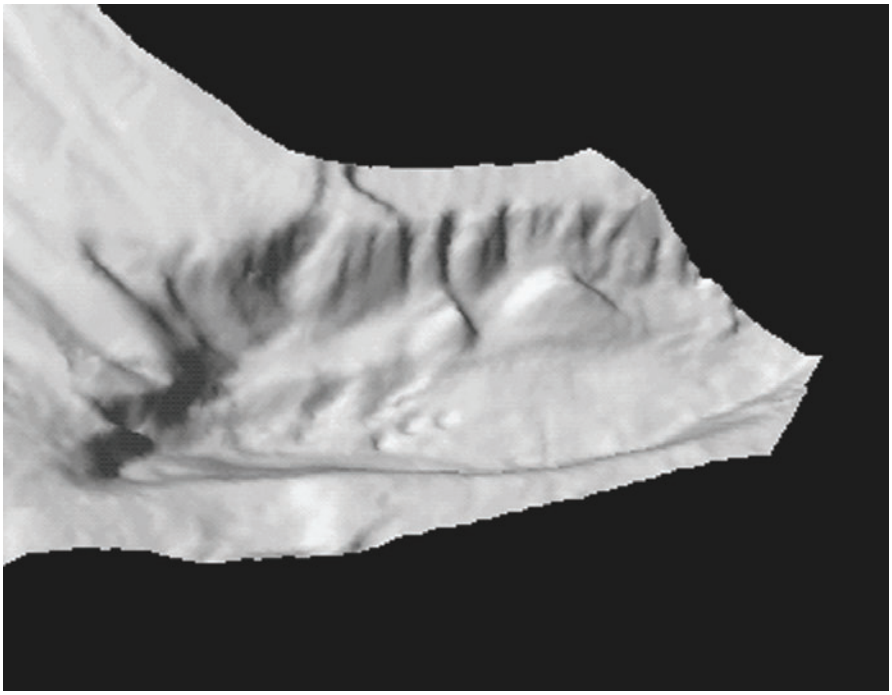

FIGURE 5.9 Multibeam image of river channel bathymetry.

5.2.7.1 Hydrographic Surveys

Hydrographic surveys provide bathymetric contour maps and/or profiles of the seafloor, lake bed, or river bottom. Water depth measurements are usually made using a high-frequency sonic pulse from a depth sounder transducer mounted on a survey vessel. The choice of depth sounder system (single-beam, multifrequency, multibeam, and swath) is dependent upon water depths, survey site conditions, and project accuracy and coverage requirements. The use and application of more sophisticated multibeam systems (Figure 5.9) have increased dramatically within the last few years.

5.2.7.2 Side-Scan Sonar

Side-scan sonar is used to locate and identify man-made objects (shipwrecks, pipelines, cables, debris, etc.) on the seafloor and determine sediment and rock characteristics of the seafloor. The side-scan sonar provides a sonogram of the seafloor that appears similar to a continuous photographic strip (Figure 5.10). A mosaic of the seafloor can be provided by overlapping the coverage of adjacent survey lines.

5.2.7.3 Magnetometer

A magnetometer measures variations in the earth's magnetic field strength that result from metallic objects (surface or buried), variations in sediment and rock mineral content, and natural (diurnal) variations. Data are used to locate and identify buried objects for cultural, environmental, and archaeological site clearances.

5.2.7.4 High-Resolution Seismic Reflection and Subbottom Profilers

Seismic images of the subsurface beneath the seafloor can be developed by inducing sonic waves into the water column from a transducer, vibrating boomer plate, sparker, or small air or gas gun. Reflections of the sonic energy from the mudline and subsurface soils horizons are recorded to provide an image of the subsurface geologic structure and stratigraphy along the path of the survey

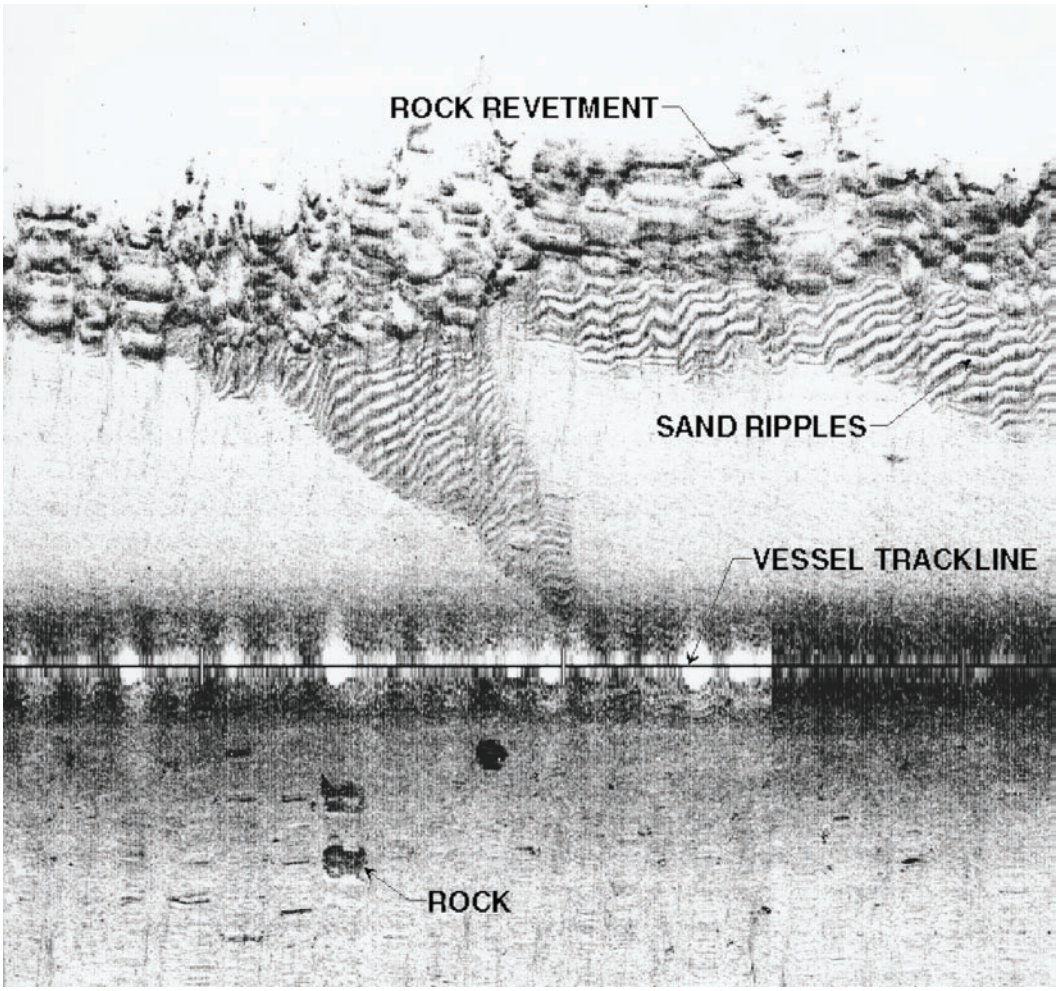

FIGURE 5.10 Side-scan sonar image of river bottom.

vessel. The effective depth of a system and resolution of subsurface horizons depend on a number of variables, including the system energy, output frequency spectrum, the nature of the seafloor, and the subsea sediments and rocks. Seismic reflection data are commonly used to determine the geologic structure (stratigraphy, depth to bedrock, folds, faults, subsea landslides, gas in sediments, seafloor seeps, etc.) and evaluate the horizon continuity between borings (Figure 5.11).

5.2.7.5 Seismic Refraction

Seismic refraction measurements are commonly used on land to estimate depth to bedrock and groundwater and to detect bedrock faulting. Measured velocities are also used for estimates of rippability and excavation characteristics. In the refraction technique, sonic energy is induced into the ground and energy refracted from subsurface soil and rock horizons is identified at a series of receivers laid out on the ground. The time–distance curves from a series of profiles are inverted to determine depths to various subsurface layers and the velocity of the layers. The data interpretation can be compromised where soft layers underlie hard layers and where the horizons are too thin to be detected by refraction arrivals at the surface. The technique also can be used in shallow water (surf zones, lakes, ponds, and river crossings) using bottom (bay) cables.

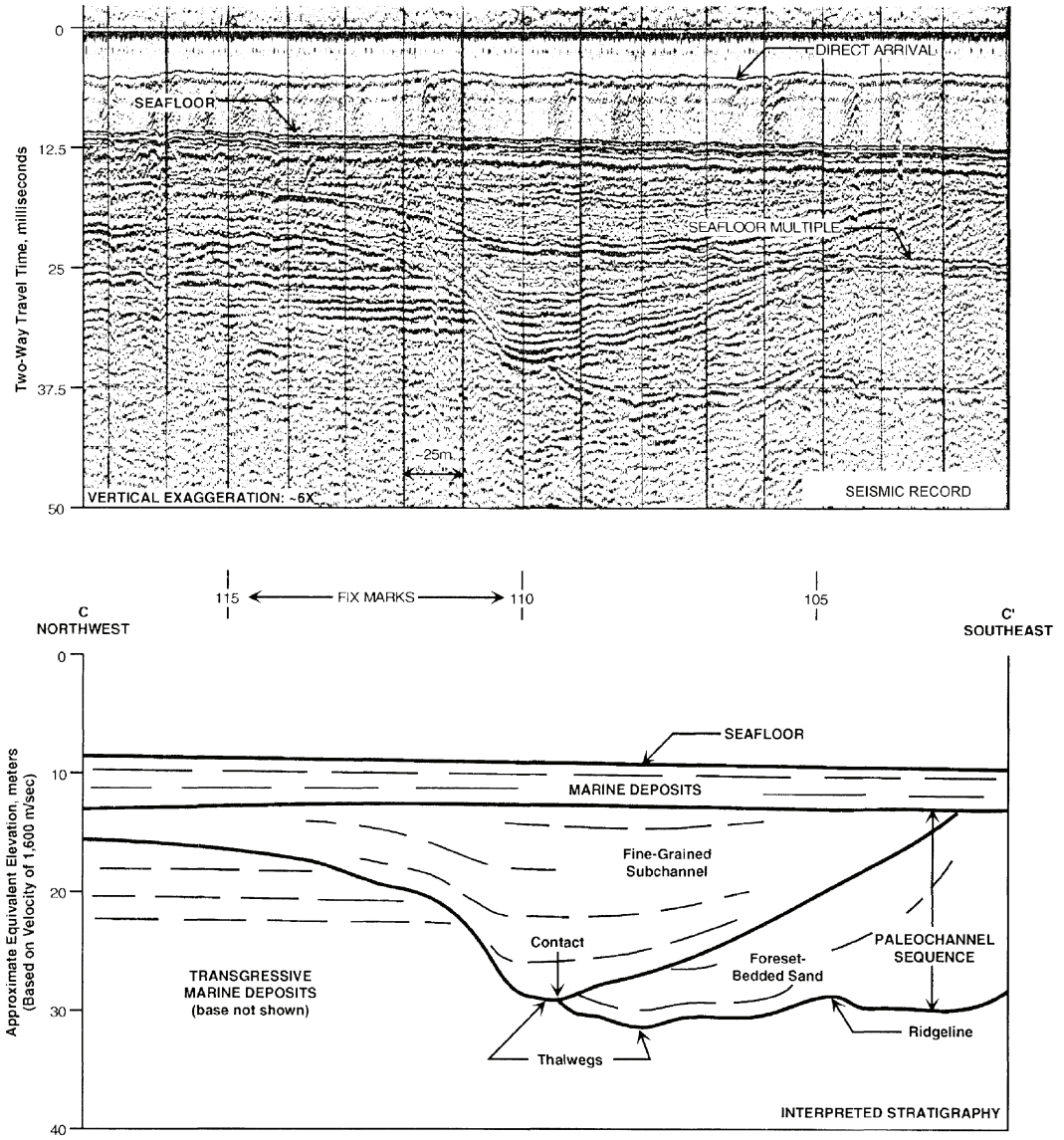

FIGURE 5.11 Interpreted stratigraphic relationships from seismic reflection data.

5.2.7.6 Ground Penetrating Radar Systems

Ground Penetrating Radar (GPR) systems measure the electromagnetic properties of the subsurface to locate buried utilities or rebar, estimate pavement thickness, interpret shallow subsurface stratigraphy, locate voids, and delineate bedrock and landslide surfaces. GPR also can be used in arctic conditions to estimate ice thickness and locate permafrost. Depths of investigation are usually limited to 50 ft or less. Where the surface soils are highly conductive, the effective depth of investigation may be limited to a few feet.

5.2.7.7 Resistivity Surveys

Resistivity surveys induce currents into the ground to locate buried objects and to investigate shallow groundwater. As electrodes are moved in specific patterns of separation, the resistivity is measured

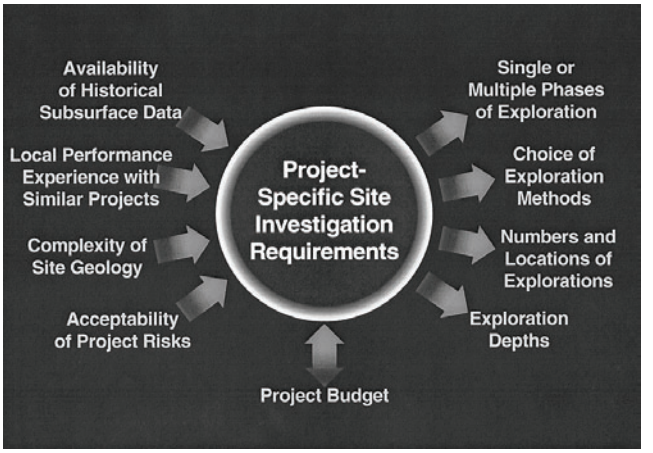

FIGURE 5.12 Key factors to consider when defining site investigation requirements.

and inverted to produce depth sections and contour maps of subsurface resistivity values. This method is used to identify and map subsurface fluids, including groundwater, surface and buried chemical plumes, and to predict corrosion potential.

5.2.8 Groundwater Measurement

Groundwater conditions have a profound effect on foundation design, construction, and performance. Thus, the measurement of groundwater depth (or depth of water when drilling over water) is one of the most fundamentally important elements of the site investigation. In addition to the measurement of the water level, the site investigation should consider and define the potential for artesian or perched groundwater. It is also important to recognize that groundwater levels may change with season, rainfall, or other temporal reasons. All groundwater and water depth measurements should document the time of measurement and, where practical, should determine variations in depth over some period of elapsed time. To determine the long-term changes in water level, it is necessary to install and monitor piezometers or monitoring wells.

5.3 Defining Site Investigation Requirements

Many factors should be considered when defining the requirements (including types, numbers, locations, and depths of explorations) for the site investigation (Figure 5.12). These factors include:

- Importance, uncertainty, or risk associated with bridge design, construction, and performance
- Geologic conditions and their potential variability
- Availability (or unavailability) of historical subsurface data
- Availability (or unavailability) of performance observations from similar nearby projects
- Investigation budget

The following factors should be considered when evaluating the project risk: (1) What are the risks? (2) How likely are the risks to be realized? (3) What are the consequences if the risks occur? Risks include:

- Certainty or uncertainty of subsurface conditions;
- Design risks (e.g., possibility that inadequate subsurface data will compromise design decisions or schedule);
- Construction risks (e.g., potential for changed conditions claims and construction delays);
- Performance risks (e.g., seismic performance).

Two additional requirements that should be considered when planning a subsurface investigation are (1) reliability of the data collected and (2) timeliness of the data generated. Unfortunately, these factors are too often ignored or underappreciated during the site investigation planning process or geotechnical consultant selection process. Because poor-quality or misleading subsurface data can lead to inappropriate selection of foundation locations, foundation types, and/or inadequate or inappropriate foundation capacities, selection of a project geotechnical consultant should be based on qualifications rather than cost. Similarly, the value of the data generated from the subsurface investigation is reduced if adequate data are not available when the design decisions, which are affected by subsurface conditions, are made. All too often, the execution of the subsurface exploration program is delayed, and major decisions relative to the general structure design and foundation locations have been cast in stone prior to the availability of the subsurface exploration results.

Frequently, the execution of the subsurface investigation is an iterative process that should be conducted in phases (i.e., desktop study, reconnaissance site investigation, detailed design-phase investigation). During each phase of site exploration, it is appropriate for data to be reviewed as they are generated so that appropriate modifications can be made as the investigation is ongoing. Appropriate adjustments in the investigation work scope can save significant expense, increase the quality and value of the investigation results, and/or reduce the potential for a remobilization of equipment to fill in missing information.

5.3.1 Choice of Exploration Methods and Consideration of Local Practice

Because many exploration techniques are suitable in some subsurface conditions, but not as suitable or economical in other conditions, the local practice for the methods of exploration vary from region to region. Therefore, the approach to the field exploration program should consider and be tailored to the local practice. Conversely, there are occasions where the requirements for a project may justify using exploration techniques that are not common in the project area. The need to use special techniques will increase with the size of the project and the uniqueness or complexity of the site conditions.

5.3.2 Exploration Depths

The depths to which subsurface exploration should be extended will depend on the structure, its size, and the subsurface conditions at the project location. The subsurface exploration for any project should extend down through unsuitable layers into materials that are competent relative to the design loads to be applied by the bridge foundations. Some of the exploration should be deep enough to verify that unsuitable materials do not exist beneath the bearing strata on which the foundations will be embedded. When the base of the foundation is underlain by layers of compressible material, the exploration should extend down through the compressible strata and into deeper strata whose compressibility will not influence foundation performance.

For lightly loaded structures, it may be adequate to terminate the exploration when rock is encountered, provided that the regional geology indicates that unsuitable strata do not underlie the rock surface. For heavily-loaded foundations or foundations bearing on rock, it is appropriate to verify that the explorations indeed have encountered rock and not a boulder. It is similarly appropriate to extend at least some of the explorations through the weathered rock into sound or fresh rock.

5.3.3 Numbers of Explorations

The basic intent of the site investigation is to determine the subsurface stratigraphy and its variations, and to define the representative soil (or rock) properties of the strata together with their lateral and vertical variations. The locations and spacing of explorations should be adequate to provide a reasonably accurate definition of the subsurface conditions, and should disclose the presence of any important irregularities in the subsurface conditions. Thus, the numbers of explorations will depend on both the project size and the geologic and depositional variability of the site location. When subsurface conditions are complex and variable, a greater number of more closely spaced explorations are

warranted. Conversely, when subsurface conditions are relatively uniform, fewer and more widely spaced explorations may be adequate.

5.3.4 The Risk of Inadequate Site Characterization

When developing a site exploration program, it is often tempting to minimize the number of explorations or defer the use of specialized techniques due to their expense. The approach of minimizing the investment in site characterization is fraught with risk. Costs saved by the execution of an inadequate site investigation, whether in terms of the numbers of explorations or the exclusion of applicable site investigation techniques, rarely reduce the project cost. Conversely, the cost saved by an inadequate investigation frequently increases the cost of construction by many times the savings achieved during the site investigation.

5.4 Development of Laboratory Testing Program

5.4.1 Purpose of Testing Program

Laboratory tests are performed on samples for the following purposes:

- Classify soil samples;
- Evaluate basic index soil properties that are useful in evaluating the engineering properties of the soil samples;
- Measure the strength, compressibility, and hydraulic properties of the soils;
- Evaluate the suitability of on-site or borrow soils for use as fill;
- Define dynamic parameters for site response and soil–structure interaction analyses during earthquakes;
- Identify unusual subsurface conditions (e.g., presence of corrosive conditions, carbonate soils, expansive soils, or potentially liquefiable soils).

The extent of laboratory testing is generally defined by the risks associated with the project.

Soil classification, index property, and fill suitability tests generally can be performed on disturbed samples, whereas tests to determine engineering properties of the soils should preferably be performed on a relatively undisturbed, intact specimen. The quality of the data obtained from the latter series of tests is significantly dependent on the magnitude of sample disturbance either during sampling or during subsequent processing and transportation.

5.4.2 Types and Uses of Tests

5.4.2.1 Soil Classification and Index Testing

Soil classification and index properties tests are generally performed for even low-risk projects. Engineering parameters often can be estimated from the available *in situ* data and basic index tests using published correlations. Site-specific correlations of these basic values may allow the results of a few relatively expensive advanced tests to be extrapolated. Index tests and their uses include the following:

- Unit weight and water content tests to evaluate the natural unit weight and water content.
- Atterberg (liquid and plastic) limit tests on cohesive soils for classification and correlation studies. Significant insight relative to strength and compressibility properties can be inferred from the natural water content and Atterberg limit test results.
- Sieve and hydrometer tests to define the grain size distribution of coarse- and fine-grained soils, respectively. Grain size data also are used for both classification and correlation studies.

Other index tests include tests for specific gravity, maximum and minimum density, expansion index, and sand equivalent.

5.4.2.2 Shear Strength Tests

Most bridge design projects require characterization of the undrained shear strength of cohesive soils and the drained strength of cohesionless soils. Strength determinations are necessary to evaluate the bearing capacity of foundations and to estimate the loads imposed on earth-retaining structures.

Undrained shear strength of cohesive soils can be estimated (often in the field) with calibrated tools such as a torvane, pocket penetrometer, fall cone, or miniature vane shear device. More definitive strength measurements are obtained in a laboratory by subjecting samples to triaxial compression (TX), direct simple shear (DSS), or torsional shear (TS) tests. Triaxial shear tests (including unconsolidated-undrained, UU, tests and consolidated-undrained, CU, tests) are the most common type of strength test. In this type of test, the sample is subject to stresses that mimic *in situ* states of stress prior to being tested to failure in compression or shear. Large and more high risk projects often warrant the performance of CU or DSS tests where samples are tested along stress paths which model the *in situ* conditions. In contrast, only less-sophisticated UU tests may be warranted for less important projects.

Drained strength parameters of cohesionless soils are generally measured in either relatively simple direct shear (DS) tests or in more-sophisticated consolidated-drained (CD) triaxial tests. In general, few laboratory strength tests are performed on *in situ* specimens of cohesionless soil because of the relative difficulty in obtaining undisturbed specimens.

5.4.2.3 Compaction Tests

Compaction tests are performed to evaluate the moisture–density relationship of potential fill material. Once the relationship has been evaluated and the minimum level of compaction of fill material to be used has been determined, strength tests may be performed on compacted specimens to evaluate design parameters for the project.

5.4.2.4 Subgrade Modulus

R-value and CBR tests are performed to determine subgrade modulus and evaluate the pavement support characteristics of the *in situ* or fill soils.

5.4.2.5 Consolidation Tests

Consolidation tests are commonly performed to (1) evaluate the compressibility of soil samples for the calculation of foundation settlement; (2) investigate the stress history of the soils at the boring locations to calculate settlement as well as to select stress paths to perform most advanced strength tests; (3) evaluate elastic properties from measured bulk modulus values; and (4) evaluate the time rate of settlement. Consolidation test procedures also can be modified to evaluate if foundation soils are susceptible to collapse or expansion, and to measure expansion pressures under various levels of confinement. Consolidation tests include incremental consolidation tests (which are performed at a number of discrete loads) and constant rate of strain (CRS) tests where load levels are constantly increased or decreased. CRS tests can generally be performed relatively quickly and provide a continuous stress–strain curve, but require more-sophisticated equipment.

5.4.2.6 Permeability Tests

In general, constant-head permeability tests are performed on relatively permeable cohesionless soils, while falling-head permeability tests are performed on relatively impermeable cohesive soils. Estimates of the permeability of cohesive soils also can be obtained from consolidation test data.

5.4.2.7 Dynamic Tests

A number of tests are possible to evaluate the behavior of soils under dynamic loads such as wave or earthquake loads. Dynamic tests generally are strength tests with the sample subjected to some sort of cyclic loading. Tests can be performed to evaluate variations of strength, modulus, and damping, with variations in rate and magnitude of cyclic stresses or strains. Small strain parameters for earthquake loading cases can be evaluated from resonant column tests.

For earthquake loading conditions, dynamic test data are often used to evaluate site response and soil–structure interaction. Cyclic testing also can provide insight into the behavior of potentially liquefiable soils, especially those which are not easily evaluated by empirical *in situ* test-based procedures.

5.4.2.8 Corrosion Tests

Corrosion tests are performed to evaluate potential impacts on steel or concrete structures due to chemical attack. Tests to evaluate corrosion potential include resistivity, pH, sulfate content, and chloride content.

5.5 Data Presentation and Site Characterization

5.5.1 Site Characterization Report

The site characterization report should contain a presentation of the site data and an interpretation and analysis of the foundation conditions at the project site. The site characterization report should:

- Present the factual data generated during the site investigation;
- Describe the procedures and equipment used to obtain the factual data;
- Describe the subsurface stratigraphic relationships at the project site;
- Define the soil and rock properties that are relevant to the planning, design, construction, and performance of the project structures;
- Formulate the solutions to the design and construction of the project.

The site data presented in the site characterization report may be developed from the current and/or past field investigations at or near the project site, as-built documents, maintenance records, and construction notes. When historic data are included or summarized, the original sources of the data should be cited.

5.5.2 Factual Data Presentation

The project report should include the accurate and appropriate documentation of the factual data collected and generated during the site investigation and testing program(s). The presentation and organization of the factual data, by necessity, will depend upon the size and complexity of the project and the types and extent of the subsurface data. Regardless of the project size or extent of exploration, all reports should include an accurate plan of exploration that includes appropriate graphical portrayal of surface features and ground surface elevation in the project area.

The boring log (Figure 5.13) is one of the most fundamental components of the data documentation. Although many styles of presentation are used, there are several basic elements that generally should be included on a boring log. Those typical components include:

- Documentation of location and ground surface elevation;
- Documentation of sampling and coring depths, types, and lengths — e.g., sample type, blow count (for driven samples), and sample length for soil samples; core run, recovery, and RQD for rock cores — as well as *in situ* test depths and lengths;
- Depths and elevations of groundwater and/or seepage encountered;
- Graphical representation of soil and rock lithology;
- Description of soil and rock types, characteristics, consistency/density, or hardness;
- Tabular or graphical representation of test data.

In addition to the boring logs, the factual data should include tabulated summaries of test types, depths, and results together with the appropriate graphical output of the tests conducted.

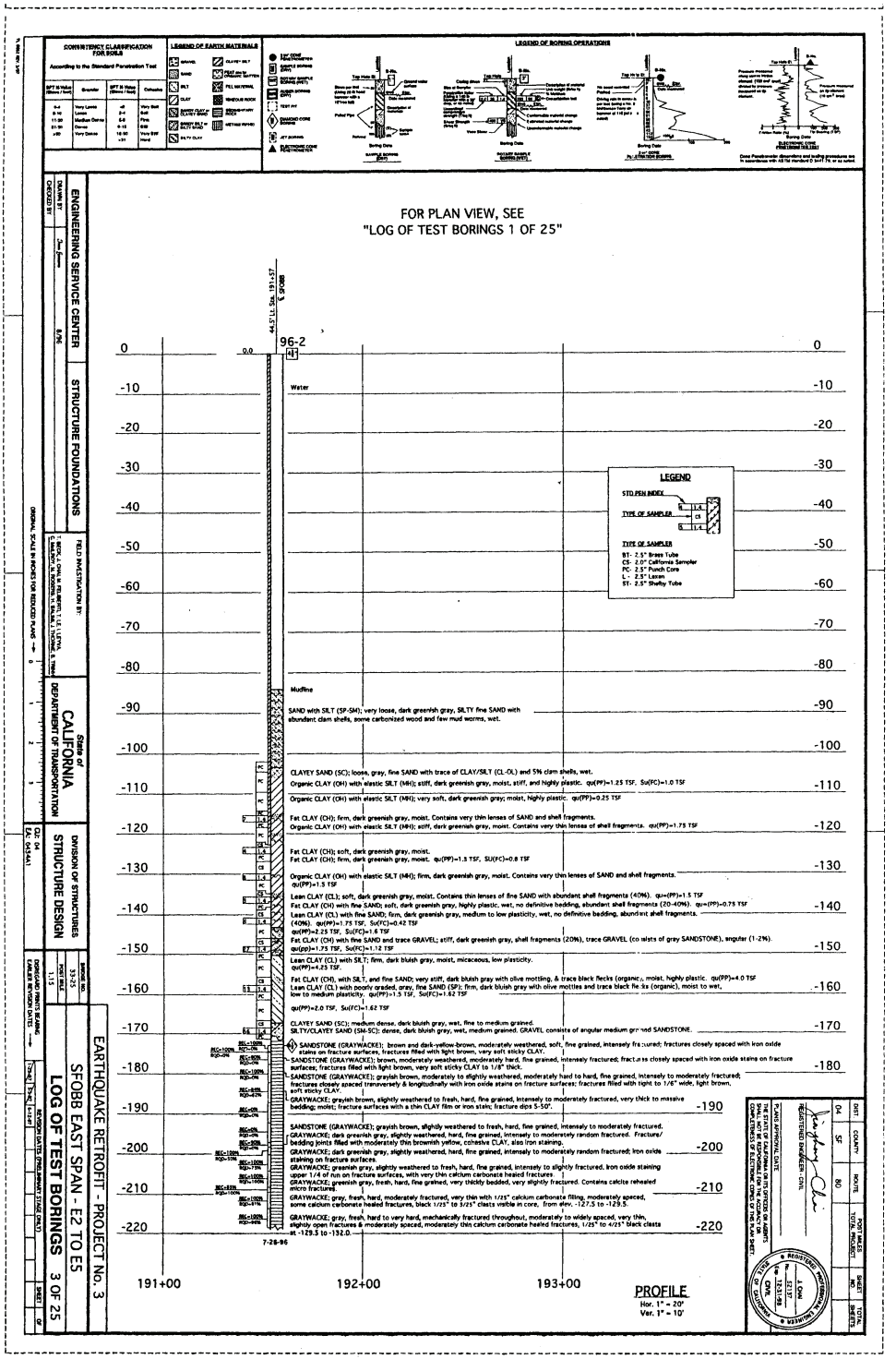

FIGURE 5.13 Typical log of test boring sheet for Caltrans project.

5.5.3 Description of Subsurface Conditions and Stratigraphy

A sound geologic interpretation of the exploration and testing data are required for any project to assess the subsurface conditions. The description of the subsurface conditions should provide users of the report with an understanding of the conditions, their possible variability, and the significance of the conditions relative to the project. The information should be presented in a useful format and terminology appropriate for the users, who usually will include design engineers and contractors who are not earth science professionals.

To achieve those objectives, the site characterization report should include descriptions of

1. Site topography and/or bathymetry,
2. Site geology,
3. Subsurface stratigraphy and stratigraphic relationships,
4. Continuity or lack of continuity of the various subsurface strata,
5. Groundwater depths and conditions, and
6. Assessment of the documented and possible undocumented variability of the subsurface conditions.

Information relative to the subsurface conditions is usually provided in text, cross sections, and maps. Subsurface cross sections, or profiles, are commonly used to illustrate the stratigraphic sequence, subsurface strata and their relationships, geologic structure, and other subsurface features across a site. The cross section can range from simple line drawings to complex illustrations that include boring logs and plotted test data (Figure 5.14).

Maps are commonly used to illustrate and define the subsurface conditions at a site. The maps can include topographic and bathymetric contour maps, maps of the structural contours of a stratigraphic surface, groundwater depth or elevation maps, isopach thickness maps of an individual stratum (or sequence of strata), and interpreted maps of geologic features (e.g., faulting, bedrock outcrops, etc.). The locations of explorations should generally be included on the interpretive maps.

The interpretive report also should describe data relative to the depths and elevations of groundwater and/or seepage encountered in the field. The potential types of groundwater surface(s) and possible seasonal fluctuation of groundwater should be described. The description of the subsurface conditions also should discuss how the groundwater conditions can affect construction.

5.5.4 Definition of Soil Properties

Soil properties generally should be interpreted in terms of stratigraphic units or geologic deposits. The interpretation of representative soil properties for design should consider lateral and vertical variability of the different soil deposits. Representative soil properties should consider the potential for possible *in situ* variations that have not been disclosed by the exploration program and laboratory testing. For large or variable sites, it should be recognized that global averages of a particular soil property may not appropriately represent the representative value at all locations. For that condition, use of average soil properties may lead to unconservative design.

Soil properties and design recommendations are usually presented with a combination of narrative text, graphs, and data presented in tabular and/or bulleted list format. It is often convenient and helpful to reference generalized subsurface profiles and boring logs in those discussions. The narrative descriptions should include such factors as depth range, general consistency or density, plasticity or grain size, occurrence of groundwater, occurrence of layers or seams, degree of weathering, and structure. For each stratigraphic unit, ranges of typical measured field and laboratory data (e.g., strength, index parameters, and blow counts) should be described.

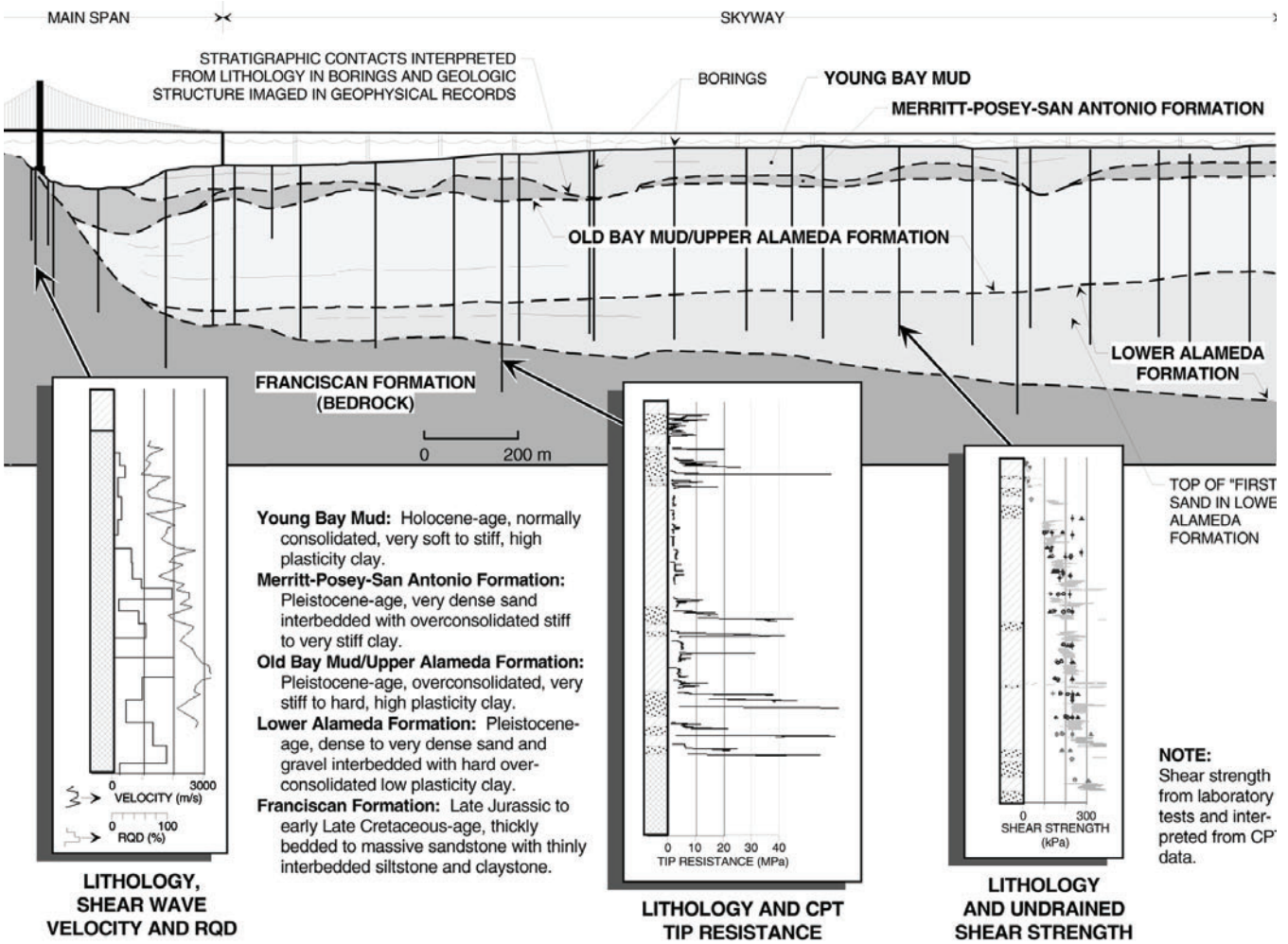

FIGURE 5.14 Subsurface cross section for San Francisco–Oakland Bay Bridge East Span alignment.

5.5.5 Geotechnical Recommendations

The site characterization report should provide solutions to the geotechnical issues and contain geotechnical recommendations that are complete, concise, and definitive. The recommended foundation and geotechnical systems should be cost-effective, performance-proven, and constructible. Where appropriate, alternative foundation types should be discussed and evaluated. When construction problems are anticipated, solutions to these problems should be described.

In addition to the standard consideration of axial and lateral foundation capacity, load–deflection characteristics, settlement, slope stability, and earth pressures, there are a number of subsurface conditions that can affect foundation design and performance:

- Liquefaction susceptibility of loose, granular soils;
- Expansive or collapsible soils;
- Mica-rich and carbonate soils;
- Corrosive soils;
- Permafrost or frozen soils;
- Perched or artesian groundwater.

When any of those conditions are present, they should be described and evaluated.

5.5.6 Application of Computerized Databases

Computerized databases provide the opportunity to compile, organize, integrate, and analyze geotechnical data efficiently. All collected data are thereby stored, in a standard format, in a central accessible location. Use of a computerized database has a number of advantages. Use of automated interactive routines allows the efficient production of boring logs, cross sections, maps, and parameter plots. Large volumes of data from multiple sources can be integrated and queried to evaluate or show trends and variability. New data from subsequent phases of study can be easily and rapidly incorporated into the existing database to update and revise the geologic model of the site.

6

Shallow Foundations

James Chai
California Department of Transportation

6.1 Introduction

A shallow foundation may be defined as one in which the foundation depth (D) is less than or on the order of its least width (B), as illustrated in Figure 6.1. Commonly used types of shallow foundations include spread footings, strap footings, combined footings, and mat or raft footings. Shallow foundations or footings provide their support entirely from their bases, whereas deep foundations derive the capacity from two parts, skin friction and base support, or one of these two. This chapter is primarily designated to the discussion of the bearing capacity and settlement of shallow foundations, although structural considerations for footing design are briefly addressed. Deep foundations for bridges are discussed in Chapter 7.

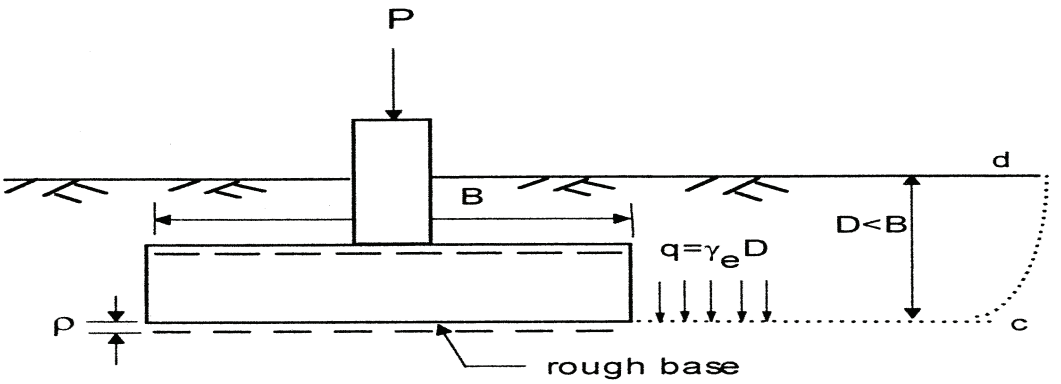

FIGURE 6.1 Definition sketch for shallow footings.

TABLE 6.1 Typical Values of Safety Factors Used in Foundation Design (after Barker et al. [9])

Failure Type	Failure Mode	Safety Factor	Remark
Shearing	Bearing capacity failure	2.0–3.0	The lower values are used when
	Overturning	2.0–2.5	uncertainty in design is small
	Overall stability	1.5–2.0	and consequences of failure are
	Sliding	1.5–2.0	minor; higher values are used
Seepage	Uplift	1.5–2.0	when uncertainty in design is
	Heave	1.5–2.0	large and consequences of failure
	Piping	2.0–3.0	are major

Source: Terzaghi, K. and Peck, R.B., *Soil Mechanics in Engineering Practice*, 2nd ed., John Wiley & Sons, New York, 1967. With permission.

6.2 Design Requirements

In general, any foundation design must meet three essential requirements: (1) providing adequate safety against structural failure of the foundation; (2) offering adequate bearing capacity of soil beneath the foundation with a specified safety against ultimate failure; and (3) achieving acceptable total or differential settlements under working loads. In addition, the overall stability of slopes in the vicinity of a footing must be regarded as part of the foundation design. For any project, it is usually necessary to investigate both the bearing capacity and the settlement of a footing. Whether footing design is controlled by the bearing capacity or the settlement limit rests on a number of factors such as soil condition, type of bridge, footing dimensions, and loads. Figure 6.2 illustrates the load–settlement relationship for a square footing subjected to a vertical load *P*. As indicated in the curve, the settlement *p* increases as load *P* increases. The ultimate load P_u is defined as a peak load (curves 1 and 2) or a load at which a constant rate of settlement (curve 3) is reached as shown in Figure 6.2. On the other hand, the ultimate load is the maximum load a foundation can support without shear failure and within an acceptable settlement. In practice, all foundations should be designed and built to ensure a certain safety against bearing capacity failure or excessive settlement. A safety factor (*SF*) can be defined as a ratio of the ultimate load P_u and allowable load P_a. Typical value of safety factors commonly used in shallow foundation design are given in Table 6.1.

6.3 Failure Modes of Shallow Foundations

Bearing capacity failure usually occurs in one of the three modes described as general shear, local shear, or punching shear failure. In general, which failure mode occurs for a shallow foundation depends on the relative compressibility of the soil, footing embedment, loading conditions, and drainage conditions. General shear failure has a well-defined rupture pattern consisting of three zones, I, II, and III, as shown in Figure 6.3a. Local shear failure generally consists of clearly defined rupture surfaces beneath the footing (zones I and II). However, the failure pattern on the sides of the footing (zone III) is not clearly defined. Punch shear failure has a poorly defined rupture pattern concentrated within zone I; it is usually associated with a large settlement and does not mobilize shear stresses in zones II and III as shown in Figure 6.3b and c. Ismael and Vesic [40] concluded that, with increasing overburden pressure (in cases of deep foundations), the failure mode changes from general shear to local or punch shear, regardless of soil compressibility. The further examination of load tests on footings by Vesic [68,69] and De Beer [29] suggested that the ultimate load occurs at the breakpoint of the load–settlement curve, as shown in Figure 6.2. Analyzing the modes of failure indicates that (1) it is possible to formulate a general bearing capacity equation for a loaded footing failing in the general shear mode, (2) it is very difficult to generalize the other two failure modes for shallow foundations because of their poorly defined rupture surfaces, and (3) it is of significance to know the magnitude of settlements of footings required to mobilize ultimate loads. In the following sections, theoretical and empirical methods for evaluating both bearing capacity and settlement for shallow foundations will be discussed.

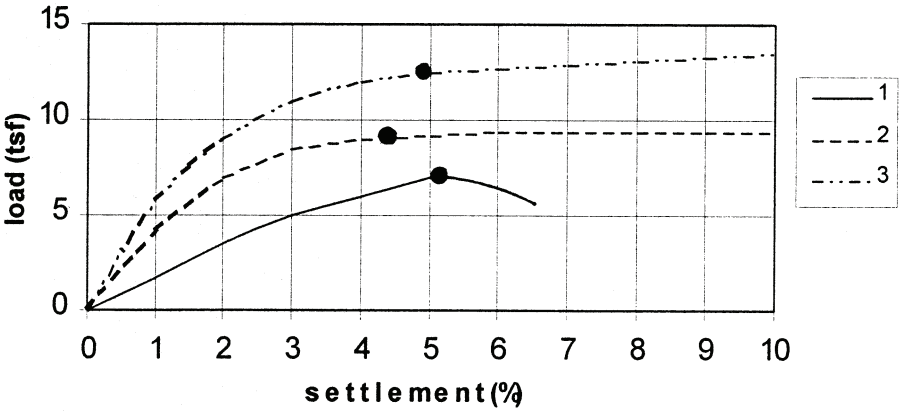

FIGURE 6.2 Load-settlement relationships of shallow footings.

6.4 Bearing Capacity for Shallow Foundations

6.4.1 Bearing Capacity Equation

The computation of ultimate bearing capacity for shallow foundations on soil can be considered as a solution to the problem of elastic–plastic equilibrium. However, what hinders us from finding closed analytical solutions rests on the difficulty in the selection of a mathematical model of soil constitutive relationships. Bearing capacity theory is still limited to solutions established for the rigid-plastic solid of the classic theory of plasticity [40,69]. Consequently, only approximate methods are currently available for the posed problem. One of them is the well-known Terzaghi's bearing capacity equation [19,63], which can be expressed as

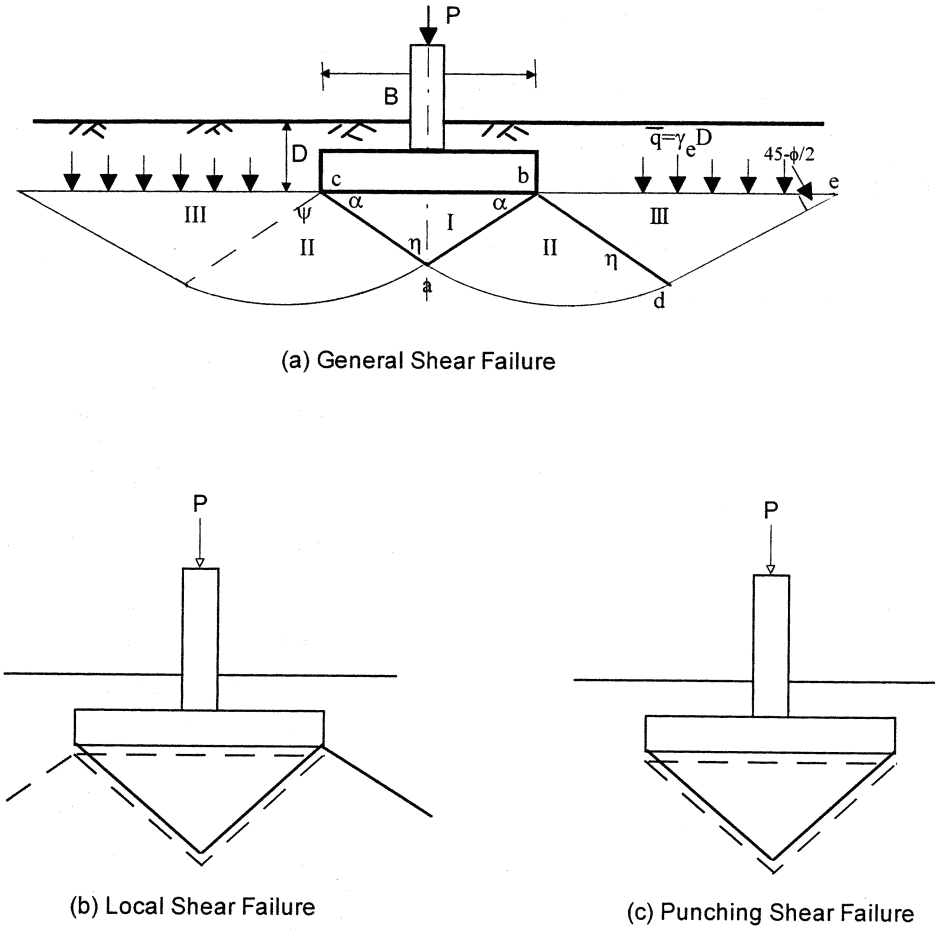

FIGURE 6.3 Three failure modes of bearing capacity.

$$q_{ult} = cN_c s_c + \bar{q}N_q + 0.5\gamma BN_\gamma s_\gamma \tag{6.1}$$

where q_{ult} is ultimate bearing capacity, c is soil cohesion, $\bar{q}$ is effective overburden pressure at base of footing ($= \gamma_1 D$), γ is effective unit weight of soil or rock, and B is minimum plan dimension of footing. N_c, N_q, and N_γ are bearing capacity factors defined as functions of friction angle of soil and their values are listed in Table 6.2. s_c and s_r are shape factors as shown in Table 6.3.

These three N factors are used to represent the influence of the cohesion (N_c), unit weight (N_γ), and overburden pressure (N_q) of the soil on bearing capacity. As shown in Figures 6.1 and 6.3(a), the assumptions used for Eq. (6.1) include

1. The footing base is rough and the soil beneath the base is incompressible, which implies that the wedge *abc* (zone I) is no longer an active Rankine zone but is in an elastic state. Consequently, zone I must move together with the footing base.
2. Zone II is an immediate zone lying on a log spiral arc *ad*.

TABLE 6.2 Bearing Capacity Factors for the Terzaghi Equation

ϕ (°)	N_c	N_q	N_γ	$K_{p\gamma}$
0	5.7[a]	1.0	0	10.8
5	7.3	1.6	0.5	12.2
10	9.6	2.7	1.2	14.7
15	12.9	4.4	2.5	18.6
20	17.7	7.4	5.0	25.0
25	25.1	12.7	9.7	35.0
30	37.2	22.5	19.7	52.0
34	52.6	36.5	36.0	—
35	57.8	41.4	42.4	82.0
40	95.7	81.3	100.4	141.0
45	172.3	173.3	297.5	298.0
48	258.3	287.9	780.1	—
50	347.5	415.1	1153.2	800.0

[a] $N_c = 1.5\pi + 1$ (Terzaghi [63], p. 127); values of N_γ for ϕ of 0, 34, and 48° are original Terzaghi values and used to backcompute $K_{p\gamma}$.

After Bowles, J.E., *Foundation Analysis and Design*, 5th ed., McGraw-Hill, New York, 1996. With permission.

TABLE 6.3 Shape Factors for the Terzaghi Equation

	Strip	Round	Square
s_c	1.0	1.3	1.3
s_γ	1.0	0.6	0.8

After Terzaghi [63].

3. Zone III is a passive Rankine zone in a plastic state bounded by a straight line *ed*.
4. The shear resistance along *bd* is neglected because the equation was intended for footings where $D < B$.

It is evident that Eq. (6.1) is only valid for the case of general shear failure because no soil compression is allowed before the failure occurs.

Meyerhof [45,48], Hansen [35], and Vesic [68,69] further extended Terzaghi's bearing capacity equation to account for footing shape (s_i), footing embedment depth (d_1), load inclination or eccentricity (i_i), sloping ground (g_i), and tilted base (b_i). Chen [26] reevaluated N factors in Terzaghi's equation using the limit analysis method. These efforts resulted in significant extensions of Terzaghi's bearing capacity equation. The general form of the bearing capacity equation [35,68,69] can be expressed as

$$q_{\text{ult}} = cN_c s_c d_c i_c g_c b_c + \bar{q} N_q s_q d_q b_q + 0.5\gamma B N_\gamma s_\gamma d_\gamma i_\gamma g_\gamma b_\gamma \tag{6.2}$$

when $\phi = 0$,

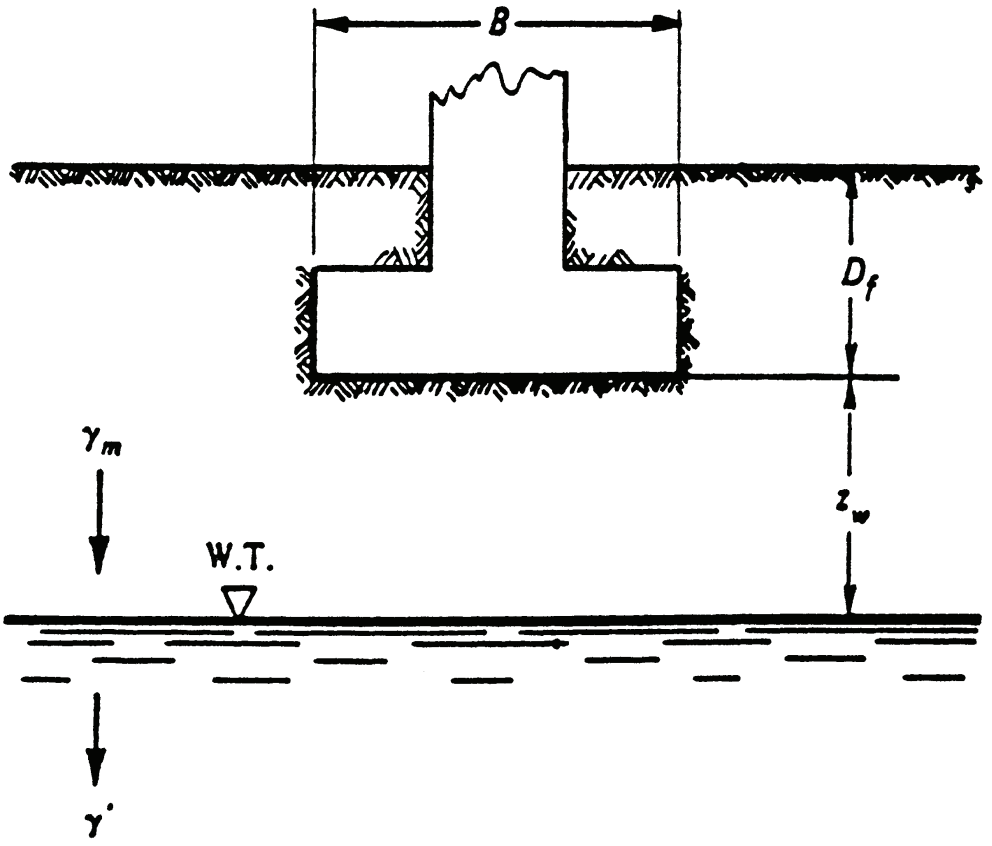

FIGURE 6.4 Influence of groundwater table on bearing capacity. (After AASHTO, 1997.)

$$q_{\text{ult}} = 5.14 s_u \left(1 + s'_c + d'_c - i'_c - b'_c - g'_c\right) + \bar{q} \tag{6.3}$$

where s_u is undrained shear strength of cohesionless. Values of bearing capacity factors N_c, N_q, and N_γ can be found in Table 6.4. Values of other factors are shown in Table 6.5. As shown in Table 6.4, N_c and N_q are the same as proposed by Meyerhof [48], Hansen [35], Vesic [68], or Chen [26]. Nevertheless, there is a wide range of values for N_γ as suggested by different authors. Meyerhof [48] and Hansen [35] use the plain-strain value of ϕ, which may be up to 10% higher than those from the conventional triaxial test. Vesic [69] argued that a shear failure in soil under the footing is a process of progressive rupture at variable stress levels and an average mean normal stress should be used for bearing capacity computations. Another reason causing the N_γ value to be unsettled is how to evaluate the impact of the soil compressibility on bearing capacity computations. The value of N_γ still remains controversial because rigorous theoretical solutions are not available. In addition, comparisons of predicted solutions against model footing test results are inconclusive.

Soil Density

Bearing capacity equations are established based on the failure mode of general shearing. In order to use the bearing capacity equation to consider the other two modes of failure, Terzaghi [63] proposed a method to reduce strength characteristics c and ϕ as follows:

$$c^* = 0.67c \quad \text{(for soft to firm clay)} \tag{6.4}$$

TABLE 6.4 Bearing Capacity Factors for Eqs. (6.2) and (6.3)

ϕ	N_c	N_q	$N_{\gamma(M)}$	$N_{\gamma(H)}$	$N_{\gamma(V)}$	$N_{\gamma(C)}$	N_q/N_c	$\tan\phi$
0	5.14	1.00	0.00	0.00	0.00	0.00	0.19	0.00
1	5.38	1.09	0.00	0.00	0.07	0.07	0.20	0.02
2	5.63	1.20	0.01	0.01	0.15	0.16	0.21	0.03
3	5.90	1.31	0.02	0.02	0.24	0.25	0.22	0.05
4	6.18	1.43	0.04	0.05	0.34	0.35	0.23	0.07
5	6.49	1.57	0.07	0.07	0.45	0.47	0.24	0.09
6	6.81	1.72	0.11	0.11	0.57	0.60	0.25	0.11
7	7.16	1.88	0.15	0.16	0.71	0.74	0.26	0.12
8	7.53	2.06	0.21	0.22	0.86	0.91	0.27	0.14
9	7.92	2.25	0.28	0.30	1.03	1.10	0.28	0.16
10	8.34	2.47	0.37	0.39	1.22	1.31	0.30	0.18
11	8.80	2.71	0.47	0.50	1.44	1.56	0.31	0.19
12	9.28	2.97	0.60	0.63	1.69	1.84	0.32	0.21
13	9.81	3.26	0.74	0.78	1.97	2.16	0.33	0.23
14	10.37	3.59	0.92	0.97	2.29	2.52	0.35	0.25
15	10.98	3.94	1.13	1.18	2.65	2.94	0.36	0.27
16	11.63	4.34	1.37	1.43	3.06	3.42	0.37	0.29
17	12.34	4.77	1.66	1.73	3.53	3.98	0.39	0.31
18	13.10	5.26	2.00	2.08	4.07	4.61	0.40	0.32
19	13.93	5.80	2.40	2.48	4.68	5.35	0.42	0.34
20	14.83	6.40	2.87	2.95	5.39	6.20	0.43	0.36
21	15.81	7.07	3.42	3.50	6.20	7.18	0.45	0.38
22	16.88	7.82	4.07	4.13	7.13	8.32	0.46	0.40
23	18.05	8.66	4.82	4.88	8.20	9.64	0.48	0.42
24	19.32	9.60	5.72	5.75	9.44	11.17	0.50	0.45
25	20.72	10.66	6.77	6.76	10.88	12.96	0.51	0.47
26	22.25	11.85	8.00	7.94	12.54	15.05	0.53	0.49
27	23.94	13.20	9.46	9.32	14.47	17.49	0.55	0.51
28	25.80	14.72	11.19	10.94	16.72	20.35	0.57	0.53
29	27.86	16.44	13.24	12.84	19.34	23.71	0.59	0.55
30	30.14	18.40	15.67	15.07	22.40	27.66	0.61	0.58
31	32.67	20.63	18.56	17.69	25.99	32.33	0.63	0.60
32	35.49	23.18	22.02	20.79	30.21	37.85	0.65	0.62
33	38.64	26.09	26.17	24.44	35.19	44.40	0.68	0.65
34	42.16	29.44	31.15	28.77	41.06	52.18	0.70	0.67
35	46.12	33.30	37.15	33.92	48.03	61.47	0.72	0.70
36	50.59	37.75	44.43	40.05	56.31	72.59	0.75	0.73
37	55.63	42.92	53.27	47.38	66.19	85.95	0.77	0.75
38	61.35	48.93	64.07	56.17	78.02	102.05	0.80	0.78
39	67.87	55.96	77.33	66.75	92.25	121.53	0.82	0.81
40	75.31	64.19	93.69	79.54	109.41	145.19	0.85	0.84
41	83.86	73.90	113.98	95.05	130.21	174.06	0.88	0.87
42	93.71	85.37	139.32	113.95	155.54	209.43	0.91	0.90
43	105.11	99.01	171.14	137.10	186.53	253.00	0.94	0.93
44	118.37	115.31	211.41	165.58	224.63	306.92	0.97	0.97
45	133.87	134.97	262.74	200.81	271.74	374.02	1.01	1.00
46	152.10	158.50	328.73	244.64	330.33	458.02	1.04	1.04
47	173.64	187.20	414.32	299.52	403.65	563.81	1.08	1.07
48	199.26	222.30	526.44	368.66	495.99	697.93	1.12	1.11
49	229.92	265.49	674.91	456.40	613.13	869.17	1.15	1.15
50	266.88	319.05	873.84	568.56	762.85	1089.46	1.20	1.19

Note: N_c and N_q are same for all four methods; subscripts identify author for N_γ: M = Meyerhof [48]; H = Hansen [35]; V = Vesic [69]; C = Chen [26].

TABLE 6.5 Shape, Depth, Inclination, Ground, and Base Factors for Eq. (6.3)

Shape Factors	Depth Factors
$s_c = 1.0 + \frac{N_q}{N_c}\ \frac{B}{L}$ $s_c = 1.0$ (for strip footing)	$d_c = 1.0 + 0.4k \begin{cases} k = \frac{D_f}{B} & \text{for } \frac{D_f}{B} \le 1 \\ k = \tan^{-1}\left(\frac{D_f}{B}\right) & \text{for } \frac{D_f}{B} > 1 \end{cases}$
$s_q = 1.0 + \frac{B}{L}\tan\phi$ (for all ϕ)	$d_q = 1 + 2\tan\phi(1-\sin\phi)^2 k$ (k defined above)
$s_\gamma = 1.0 - 0.4\frac{B}{L} \ge 0.6$	$d_\gamma = 1.00$ (for all ϕ)
Inclination Factors	**Ground Factors (base on slope)**
$i'_c = 1 - \frac{mHi}{A_f c_a N_c}$ ($\phi = 0$)	$g'_c = \frac{\beta}{5.14}$ β in radius ($\phi = 0$)
$i_c = i_q - \frac{1-i_q}{N_q - 1}$ ($\phi > 0$)	$g_c = i_q - \frac{1-i_q}{5.14\tan\phi}$ ($\phi > 0$)
$i_q = \left[1.0 - \frac{H_i}{V + A_f c_a \cot\phi}\right]^m$	$g_q = g_\gamma = (1.0 - \tan\beta)^2$ (for all ϕ)
$i_\gamma = \left[1.0 - \frac{H_i}{V + A_f c_a \cot\phi}\right]^{m+1}$	**Base Factors (tilted base)**
$m = m_B = \frac{2 + B/L}{1 + B/L}$ or	$b'_c = g'_c$ ($\phi = 0$)
$m = m_L = \frac{2 + L/B}{1 + L/B}$	$b_c = 1 - \frac{2\beta}{5.14\tan\phi}$ ($\phi > 0$)
	$b_q = b_\gamma = (1.0 - \eta\tan\phi)^2$ (for all ϕ)

Notes:
1. When $\gamma = 0$ (and $\beta \neq 0$), use $N_\gamma = 2\sin(\pm\beta)$ in N_γ term
2. Compute $m = m_B$ when $H_i = H_B$ (H parallel to B) and $m = m_L$ when $H_i = H_L$ (H parallel to L); for both H_B and H_L, use
$$m = \sqrt{m_B^2 + m_L^2}$$
3. $0 \le i_q, i_\gamma \le 1$
4. $\beta + \eta \le 90°; \beta \le \phi$

where
A_f = effective footing dimension as shown in Figure 6.6
D_f = depth from ground surface to base of footing
V = vertical load on footing
H_i = horizontal component of load on footing with $H_{max} \le V \tan\delta + c_a A_f$
c_a = adhesion to base ($0.6c \le c_a \le 1.0c$)
δ = friction angle between base and soil ($0.5\phi \le \delta \le \phi$)
β = slope of ground away from base with (+) downward
η = tilt angle of base from horizontal with (+) upward

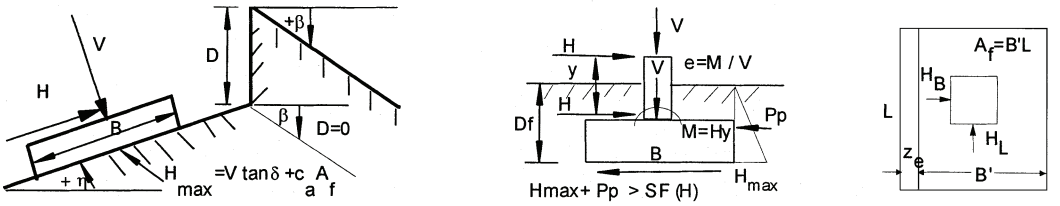

After Vesic [68,69].

$$\phi^* = \tan^{-1}\left(0.67 \tan\phi\right) \quad \left(\text{for loose sands with } \phi < 28^\circ\right) \tag{6.5}$$

Vesic [69] suggested that a flat reduction of ϕ might be too conservative in the case of local and punching shear failure. He proposed the following equation for a reduction factor varying with relative density D_r:

$$\phi^* = \tan^{-1}\left(\left(0.67 + D_r - 0.75D_r^2\right) \tan\phi\right) \quad \left(\text{for } 0 < D_r < 0.67\right) \tag{6.6}$$

Groundwater Table

Ultimate bearing capacity should always be estimated by assuming the highest anticipated groundwater table. The effective unit weight γ_e shall be used in the qN_q and $0.5\gamma B$ terms. As illustrated in Figure 6.5, the weighted average unit weight for the $0.5\gamma B$ term can be determined as follows:

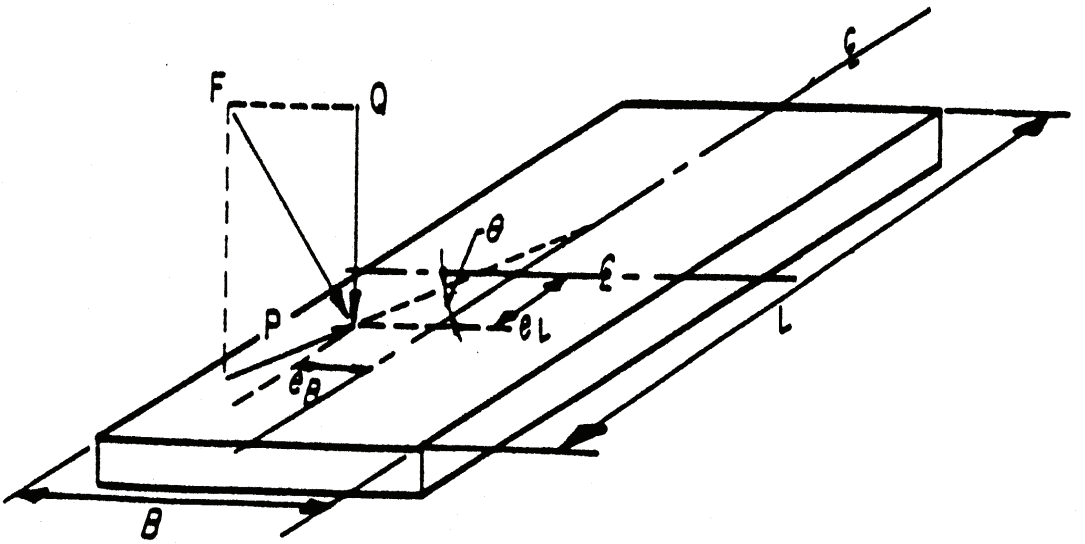

FIGURE 6.5 Definition sketch for loading and dimensions for footings subjected to eccentric or inclined loads. (After AASHTO, 1997.)

$$\gamma = \begin{cases} \gamma_{\text{avg}} & \text{for } d_w \geq B \\ \gamma' + \left(d_w/B\right)\left(\gamma_{\text{avg}} - \gamma'\right) & \text{for } 0 < d_w < B \\ \gamma' & \text{for } d \leq 0 \end{cases} \tag{6.7}$$

Eccentric Load

For footings with eccentricity, effective footing dimensions can be determined as follows:

$$A_f = B'L' \tag{6.8}$$

where $L = L - 2e_L$ and $B = B - 2e_B$. Refer to Figure 6.5 for loading definitions and footing dimensions. For example, the actual distribution of contact pressure for a rigid footing with eccentric loading in the L direction (Figure 6.6) can be obtained as follows:

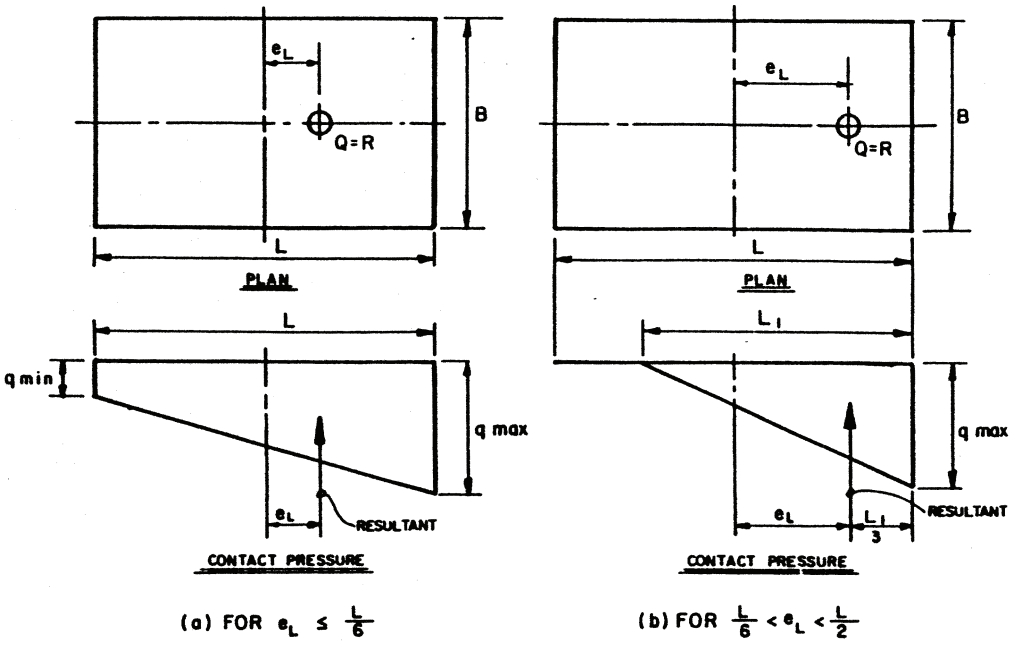

FIGURE 6.6 Contact pressure for footing loaded eccentrically about one axis. (After AASHTO 1997.)

$$q_{\substack{\max\\ \min}} = P\left[1 \pm 6e_L/L\right]/BL \quad \left(\text{for } e_L < L/6\right) \tag{6.9}$$

$$q_{\substack{\max\\ \min}} = \begin{cases} 2P/\left[3B\left(L/2 - e_L\right)\right] \\ 0 \end{cases} \quad \left(\text{for } L/6 < e_L < L/2\right) \tag{6.10}$$

Contact pressure for footings with eccentric loading in the B direction may be determined using above equations by replacing terms L with B and terms B with L. For an eccentricity in both directions, reference is available in AASHTO [2,3].

6.4.2 Bearing Capacity on Sand from Standard Penetration Tests (SPT)

Terzaghi and Peck [64, 65] proposed a method using SPT blow counts to estimate ultimate bearing capacity for footings on sand. Modified by Peck et al. [53], this method is presented in the form of the chart shown in Figure 6.7. For a given combination of footing width and SPT blow counts, the chart can be used to determine the ultimate bearing pressure associated with 25.4 mm (1.0 in.) settlement. The design chart applies to shallow footings (D_f ð B) sitting on sand with water table at great depth. Similarly, Meyerhof [46] published the following formula for estimating ultimate bearing capacity using SPT blow counts:

$$q_{\text{ult}} = N'_{\text{avg}} \frac{B}{10}\left(C_{w1} + C_{w2}\frac{D_f}{B}\right)R_I \tag{6.11}$$

where R_I is a load inclination factor shown in Table 6.6 ($R_I = 1.0$ for vertical loads). C_{w1} and C_{w2} are correction factors whose values depend on the position of the water table:

TABLE 6.6 Load Inclination Factor (R_I)

For Square Footings			
	Load Inclination Factor (R_I)		
H/V	$D_f/B = 0$	$D_f/B = 1$	$D_f/B = 3$
0.10	0.75	0.80	0.85
0.15	0.65	0.75	0.80
0.20	0.55	0.65	0.70
0.25	0.50	0.55	0.65
0.30	0.40	0.50	0.55
0.35	0.35	0.45	0.50
0.40	0.30	0.35	0.45
0.45	0.25	0.30	0.40
0.50	0.20	0.25	0.30
0.55	0.15	0.20	0.25
0.60	0.10	0.15	0.20

For Rectangular Footings						
	Load Inclination Factor (R_I)					
H/H	$D_f/B = 0$	$D_f/B = 1$	$D_f/B = 5$	$D_f/B = 0$	$D_f/B = 1$	$D_f/B = 5$
0.10	0.70	0.75	0.80	0.80	0.85	0.90
0.15	0.60	0.65	0.70	0.70	0.80	0.85
0.20	0.50	0.60	0.65	0.65	0.70	0.75
0.25	0.40	0.50	0.55	0.55	0.65	0.70
0.30	0.35	0.40	0.50	0.50	0.60	0.65
0.35	0.30	0.35	0.40	0.40	0.55	0.60
0.40	0.25	0.30	0.35	0.35	0.50	0.55
0.45	0.20	0.25	0.30	0.30	0.45	0.50
0.50	0.15	0.20	0.25	0.25	0.35	0.45
0.55	0.10	0.15	0.20	0.20	0.30	0.40
0.60	0.05	0.10	0.15	0.15	0.25	0.35

After Barker et al. [9].

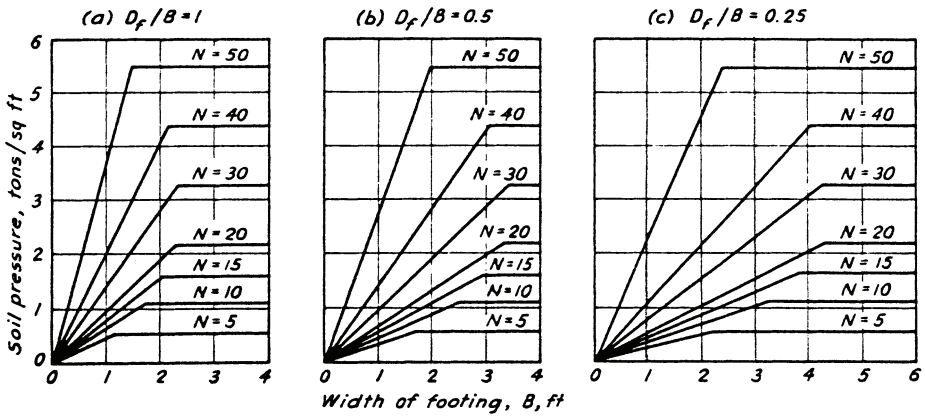

FIGURE 6.7 Design chart for proportioning shallow footings on sand. (a) Rectangular base; (b) round base. (After Peck et al. [53])

$$\begin{cases} C_{w1} = C_{w2} = 0.5 & \text{for } D_w = 0 \\ C_{w1} = C_{w2} = 1.0 & \text{for } D_w \geq D_f = 1.5B \\ C_{w1} = 0.5 \text{ and } C_{w2} = 1.0 & \text{for } D_w = D_f \end{cases} \tag{6.12}$$

N'_{avg} is an average value of the SPT blow counts, which is determined within the range of depths from footing base to 1.5B below the footing. In very fine or silty saturated sand, the measured SPT blow count (N) is corrected for submergence effect as follows:

$$N' = 15 + 0.5(N - 15) \quad \text{for } N > 15 \tag{6.13}$$

6.4.3 Bearing Capacity from Cone Penetration Tests (CPT)

Meyerhof [46] proposed a relationship between ultimate bearing capacity and cone penetration resistance in sands:

$$q_{\text{ult}} = q_c \frac{B}{40}\left(C_{w1} + C_{w2}\frac{D_f}{B}\right)R_I \tag{6.14}$$

where q_c is the average value of cone penetration resistance measured at depths from footing base to 1.5B below the footing base. C_{w1}, C_{w2}, and R_1 are the same as those as defined in Eq. (6.11).

Schmertmann [57] recommended correlated values of ultimate bearing capacity to cone penetration resistance in clays as shown in Table 6.7.

TABLE 6.7 Correlation between Ultimate Bearing Capacity (q^{ult}) and Cone Penetration Resistance (q_c)

	qult (ton/ft²)	
q_c (kg/cm² or ton/ft²)	Strip Footings	Square Footings
10	5	9
20	8	12
30	11	16
40	13	19
50	15	22

After Schmertmann [57] and Awkati, 1970.

6.4.4 Bearing Capacity from Pressure-Meter Tests (PMT)

Menard [44], Baguelin et al. [8], and Briaud [15,17] proposed using the limit pressure measured in PMT to estimate ultimate bearing capacity:

$$q_{\text{ult}} = r_0 + \kappa(p_1 - p_0) \tag{6.15}$$

where r_0 is the initial total vertical pressure at the foundation level, κ is the dimensionless bearing capacity coefficient from Figure 6.8, p_1 is limit pressure measured in PMT at depths from 1.5B above to 1.5B below foundation level, and p_0 is total horizontal pressure at the depth where the PMT is performed.

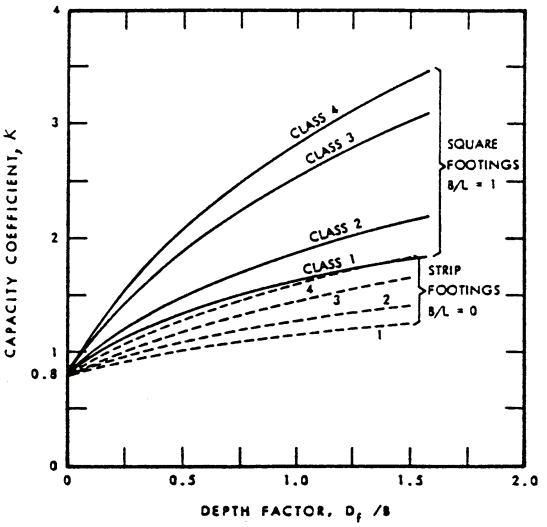

Soil Type	Consistency or Density	(P_1-P_0) (tsf)	Class
clay	soft to very firm	<12	1
	stiff	8 – 40	2
sand and gravel	loose	4-8	2
	medium to dense	10-20	3
	very dense	30-60	4
silt	loose to medium	<7	1
	dense	12-30	2
rock	very low strength	10-30	2
	low strength	30-60	3
	medium to high strength	60-100+	4

FIGURE 6.8 Values of empirical capacity coefficient, κ. (After Canadian Geotechnical Society [24].)

6.4.5 Bearing Capacity According to Building Codes

Recommendations for bearing capacity of shallow foundations are available in most building codes. Presumptive value of allowable bearing capacity for spread footings are intended for preliminary design when site-specific investigation is not justified. Presumptive bearing capacities usually do not reflect the size, shape, and depth of footing, local water table, or potential settlement. Therefore, footing design using such a procedure could be either overly conservative in some cases or unsafe in others [9]. Recommended practice is to use presumptive bearing capacity as shown in Table 6.8 for preliminary footing design and to finalize the design using reliable methods in the preceding discussion.

6.4.6 Predicted Bearing Capacity vs. Load Test Results

Obviously, the most reliable method of obtaining the ultimate bearing capacity is to conduct a full-scale footing load test at the project site. Details of the test procedure have been standardized as ASTM D1194 [5]. The load test is not usually performed since it is very costly and not practical for routine design. However, using load test results to compare with predicted bearing capacity is a vital tool to verify the accuracy and reliability of various prediction procedures. A comparison between the predicted bearing capacity and results of eight load tests conducted by Milovic [49] is summarized in Table 6.9.

Recently, load testing of five large-scale square footings (1 to 3 m) on sand was conducted on the Texas A&M University National Geotechnical Experimental Site [94]. One of the main objects of the test is to evaluate the various procedures used for estimating bearing capacities and settlements of shallow foundations. An international prediction event was organized by ASCE Geotechnical Engineering Division, which received a total of 31 predictions (16 from academics and 15 from consultants) from Israel, Australia, Japan, Canada, the United States, Hong Kong, Brazil, France, and Italy. Comparisons of predicted and measured values of bearing capacity using various procedures were summarized in Tables 6.10 through 6.12. From those comparisons, it can be argued that the most accurate settlement prediction methods are the Schmertmann-DMT (1986) and the Peck and Bazarra (1967) although they are on the unconservative side. The most conservative methods

TABLE 6.8 Presumptive Values of Allowable Bearing Capacity for Spread Foundations

Type of Bearing Material	Consistency in Place	q_{all} (ton/ft^2) Range	Recommended Value for Use
Massive crystalline igneous and metamorphic rock: granite, diorite, basalt, gneiss, thoroughly cemented conglomerate (sound condition allows minor cracks)	Hard sound rock	60–100	80
Foliated metamorphic rock: slate, schist (sound condition allows minor cracks)	Medium-hard sound rock	30–40	35
Sedimentary rock: hard cemented shales, siltstone, sandstone, limestone without cavities	Medium-hard sound rock	15–25	20
Weathered or broken bedrock of any kind except highly argillaceous rock (shale); RQD less than 25	Soft rock	8–12	10
Compaction shale or other highly argillaceous rock in sound condition	Soft rock	8–12	10
Well-graded mixture of fine and coarse-grained soil: glacial till, hardpan, boulder clay (GW-GC, GC, SC)	Very compact	8–12	10
Gravel, gravel–sand mixtures, boulder gravel mixtures (SW, SP)	Very compact	6–10	7
	Medium to compact	4–7	5
	Loose	2–5	3
Coarse to medium sand, sand with little gravel (SW, SP)	Very compact	4–6	4
	Medium to compact	2–4	3
	Loose	1–3	1.5
Fine to medium sand, silty or clayey medium to coarse sand (SW, SM, SC)	Very compact	3–5	3
	Medium to compact	2–4	2.5
	Loose	1–2	1.5
Homogeneous inorganic clay, sandy or silty clay (CL, CH)	Very stiff to hard	3–6	4
	Medium to stiff	1–3	2
	Soft	0.5–1	0.5
Inorganic silt, sandy or clayey silt, varved silt-clay-fine sand	Very stiff to hard	2–4	3
	Medium to stiff	1–3	1.5
	Soft	0.5–1	0.5

Notes:
1. Variations of allowable bearing pressure for size, depth, and arrangement of footings are given in Table 2 of NAFVAC [52].
2. Compacted fill, placed with control of moisture, density, and lift thickness, has allowable bearing pressure of equivalent natural soil.
3. Allowable bearing pressure on compressible fine-grained soils is generally limited by considerations of overall settlement of structure.
4. Allowable bearing pressure on organic soils or uncompacted fills is determined by investigation of individual case.
5. If tabulated recommended value for rock exceeds unconfined compressive strength of intact specimen, allowable pressure equals unconfined compressive strength.

After NAVFAC [52].

are Briaud [15] and Burland and Burbidge [20]. The most accurate bearing capacity prediction method was the $0.2q_c$ (CPT) method [16].

6.5 Stress Distribution Due to Footing Pressures

Elastic theory is often used to estimate the distribution of stress and settlement as well. Although soils are generally treated as elastic–plastic materials, the use of elastic theory for solving the problems is mainly due to the reasonable match between the boundary conditions for most footings and those of

TABLE 6.9 Comparison of Computed Theoretical Bearing Capacities and Milovic and Muh's Experimental Values

	Test							
Bearing Capacity Method	1	2	3	4	5	6	7	8
	D = 0.0 m	0.5	0.5	0.5	0.4	0.5	0.0	0.3
	B = 0.5 m	0.5	0.5	1.0	0.71	0.71	0.71	0.71
	L = 2.0 m	2.0	2.0	1.0	0.71	0.71	0.71	0.71
	γ = 15.69 kN/m^3	16.38	17.06	17.06	17.65	17.65	17.06	17.06
	ϕ = 37°(38.5°)	35.5 (36.25)	38.5 (40.75)	38.5	22	25	20	20
	c = 6.37 kPa	3.92	7.8	7.8	12.75	14.7	9.8	9.8
Milovic (tests)					q_{ult} (kg/cm^2) 4.1	5.5	2.2	2.6
Muh's (tests)	q_{ult} (kg/cm^2) 10.8	12.2	24.2	33.0				
Terzaghi	9.4*	9.2	22.9	19.7	4.3*	6.5*	2.5	2.9*
Meyerhof	8.2*	10.3	26.4	28.4	4.8	7.6	2.3	3.0
Hansen	7.2	9.8	23.7*	23.4	5.0	8.0	2.2*	3.1
Vesic	8.1	10.4*	25.1	24.7	5.1	8.2	2.3	3.2
Balla	14.0	15.3	35.8	33.0*	6.0	9.2	2.6	3.8

[a] After Milovic (1965), but all methods recomputed by author and Vesic added.

Notes:
1. ϕ = triaxial value ϕ_{tr}; (plane strain value) = 1.5 ϕ_{tr} - 17.
2. * = best: Terzaghi = 4; Hansen = 2; Vesic = 1; and Balla = 1.
Source: Bowles, J.E., *Foundation Analysis and Design*, 5th ed., McGraw-Hill, New York, 1996. With permission.

TABLE 6.10 Comparison of Measured vs. Predicted Load Using Settlement Prediction Method

	Predicted Load (MN) @ s = 25 mm				
Prediction Methods	1.0 m Footing	1.5 m Footing	2.5 m Footing	3.0 m(n) Footing	3.0 m(s) Footing
Briaud [15]	0.904	1.314	2.413	2.817	2.817
Burland and Burbidge [20]	0.699	1.044	1.850	2.367	2.367
De Beer (1965)	1.140	0.803	0.617	0.597	0.597
Menard and Rousseau (1962)	0.247	0.394	0.644	1.017	1.017
Meyerhof — CPT (1965)	0.288	0.446	0.738	0.918	0.918
Meyerhof — SPT (1965)	0.195	0.416	1.000	1.413	1.413
Peck and Bazarra (1967)	1.042	1.899	4.144	5.679	5.679
Peck, Hansen & Thornburn [53]	0.319	0.718	1.981	2.952	2.952
Schmertmann — CPT (1970)	0.455	0.734	1.475	1.953	1.953
Schmertmann — DMT (1970)	1.300	2.165	4.114	5.256	5.256
Schultze and Sherif (1973)	1.465	2.615	4.750	5.850	5.850
Terzaghi and Peck [65]	0.287	0.529	1.244	1.476	1.476
Measured Load @ s = 25mm	0.850	1.500	3.600	4.500	4.500

Source: FHWA, Publication No. FHWA-RD-97-068, 1997.

TABLE 6.11 Comparison of Measured vs. Predicted Load Using Bearing Capacity Prediction Method

	Predicted Bearing Capacity (MN)				
Prediction Methods	1.1 m Footing	1.5 m Footing	2.6 m Footing	3.0m(n) Footing	3.0m(s) Footing
Briaud — CPT [16]	1.394	1.287	1.389	1.513	1.513
Briaud — PMT [15]	0.872	0.779	0.781	0.783	0.783
Hansen [35]	0.772	0.814	0.769	0.730	0.730
Meyerhof [45,48]	0.832	0.991	1.058	1.034	1.034
Terzaghi [63]	0.619	0.740	0.829	0.826	0.826
Vesic [68,69]	0.825	0.896	0.885	0.855	0.855
Measured Load @ s = 150 mm					

Source: FHWA, Publication No. FHWA-RD-97-068, 1997.

TABLE 6.12 Best Prediction Method Determination

		Mean Predicted Load/ Mean Measured Load
	Settlement Prediction Method	
1	Briaud [15]	0.66
2	Burland & Burbidge [20]	0.62
3	De Beer [29]	0.24
4	Menard and Rousseau (1962)	0.21
5	Meyerhof — CPT (1965)	0.21
6	Meyerhof — SPT (1965)	0.28
7	Peck and Bazarra (1967)	1.19
8	Peck, et al. [53]	0.57
9	Schmertmann — CPT [56]	0.42
10	Schmertmann — DMT [56]	1.16
11	Shultze and Sherif (1973)	1.31
12	Terzaghi and Peck [65]	0.32
	Bearing Capacity Prediction Method	
1	Briaud — CPT [16]	1.08
2	Briaud — PMT [15]	0.61
3	Hansen [35]	0.58
4	Meyerhof [45,48]	0.76
5	Terzaghi [63]	0.59
6	Vesic [68,69]	0.66

Source: FHWA, Publication No. FHWA-RD-97-068, 1997.

elastic solutions [37]. Another reason is the lack of availability of acceptable alternatives. Observation and experience have shown that this practice provides satisfactory solutions [14,37,54,59].

6.5.1 Semi-infinite, Elastic Foundations

Bossinesq equations based on elastic theory are the most commonly used methods for obtaining subsurface stresses produced by surface loads on semi-infinite, elastic, isotropic, homogenous, weightless foundations. Formulas and plots of Bossinesq equations for common design problems are available in NAVFAC [52]. Figure 6.9 shows the isobars of pressure bulbs for square and continuous footings. For other geometry, refer to Poulos and Davis [55].

6.5.2 Layered Systems

Westergaard [70], Burmister [21–23], Sowers and Vesic [62], Poulos and Davis [55], and Perloff [54] discussed the solutions to stress distributions for layered soil strata. The reality of interlayer shear is very complicated due to *in situ* nonlinearity and material inhomogeneity [37,54]. Either zero (frictionless) or with perfect fixity is assumed for the interlayer shear to obtain possible solutions. The Westergaard method assumed that the soil being loaded is constrained by closed spaced horizontal layers that prevent horizontal displacement [52]. Figures 6.10 through 6.12 by the Westergaard method can be used for calculating vertical stresses in soils consisting of alternative layers of soft (loose) and stiff (dense) materials.

6.5.3 Simplified Method (2:1 Method)

Assuming a loaded area increasing systemically with depth, a commonly used approach for computing the stress distribution beneath a square or rectangle footing is to use the 2:1 slope method.

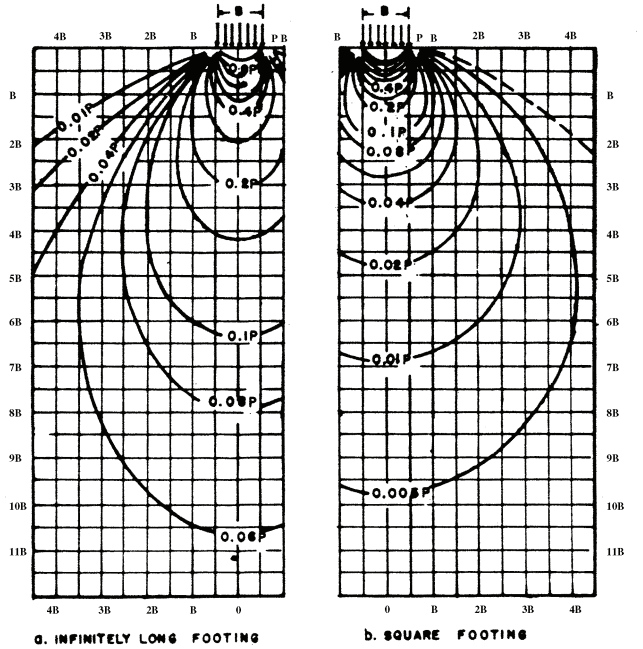

Z (FT)	Z/B	σ_z TSF
10	0.5	0.70 X 2 = 1.4
20	1	0.38 X 2 = 0.76
30	1.5	0.19 X 2 = 0.38
40	2.0	0.12 X 2 = 0.24
50	2.5	0.07 X 2 = 0.14
60	3.0	0.05 X 2 = 0.10

FIGURE 6.9 Pressure bulbs based on the Bossinesq equation for square and long footings. (After NAVFAC 7.01, 1986.)

Sometimes a 60° distribution angle (1.73-to-1 slope) may be assumed. The pressure increase Δq at a depth z beneath the loaded area due to base load P is

$$\Delta q = \begin{cases} P/(B+z)(L+z) & \text{(for a rectangle footing)} \\ P/(B+z)^2 & \text{(for a square footing)} \end{cases} \tag{6.16}$$

where symbols are referred to Figure 6.13A. The solutions by this method compare very well with those of more theoretical equations from depth z from B to about $4B$ but should not be used for depth z from 0 to B [14]. A comparison between the approximate distribution of stress calculated by a theoretical method and the 2:1 method is illustrated in Figure 6.13B.

6.6 Settlement of Shallow Foundations

The load applied on a footing changes the stress state of the soil below the footing. This stress change may produce a time-dependent accumulation of elastic compression, distortion, or consol-

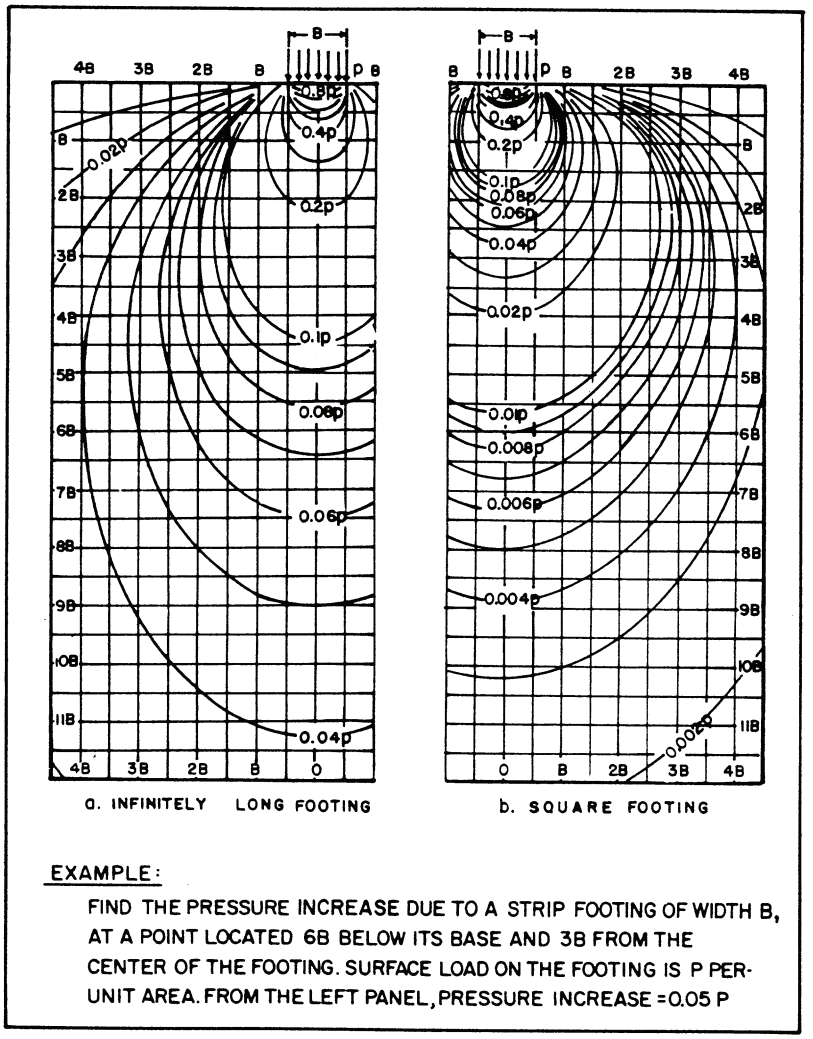

FIGURE 6.10 Vertical stress contours for square and strip footings [Westerqaard Case]. (After NAVFAC 7.01, 1986.)

idation of the soil beneath the footing. This is often termed *foundation settlement*. True elastic deformation consists of a very small portion of the settlement while the major components of the settlement are due to a change of void ratio, particle rearrangement, or crushing. Therefore, very little of the settlement will be recovered even if the applied load is removed. The irrecoverable deformation of soil reflects its inherent elastic–plastic stress–strain relationship. The reliability of settlement estimated is influenced principally by soil properties, layering, stress history, and the actual stress profile under the applied load [14,66]. The total settlement may be expressed as

$$s = s_i + s_c + s_s \tag{6.17}$$

where s is the total settlement, s_i is the immediate or distortion settlement, s_c is the primary consolidation settlement, and s_s is the secondary settlement. The time-settlement history of a shallow foundation is illustrated in Figure 6.14. Generally speaking, immediate settlement is not elastic. However, it is often referred to as elastic settlement because the elastic theory is usually used for

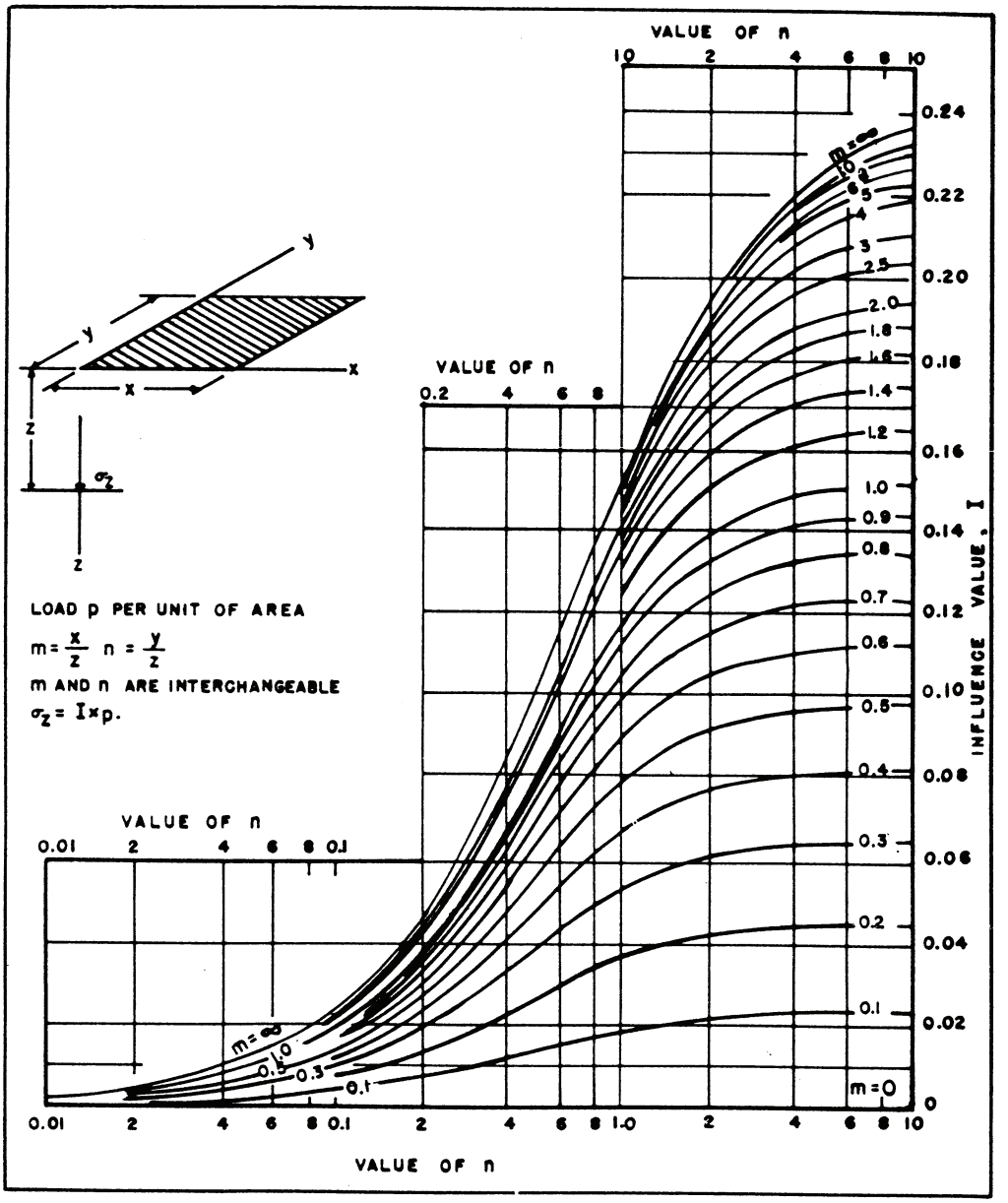

FIGURE 6.11 Influence value for vertical stress beneath a corner of a uniformly loaded rectangular area (Westerqaard Case). (After NAVFAC [52].)

computation. The immediate settlement component controls in cohesionless soils and unsaturated cohesive soils, while consolidation compression dictates in cohesive soils with a degree of saturation above 80% [3].

6.6.1 Immediate Settlement by Elastic Methods

Based on elastic theory, Steinbrenner [61] suggested that immediate settlements of footings on sands and clay could be estimated in terms of Young's modulus E of soils. A modified procedure developed

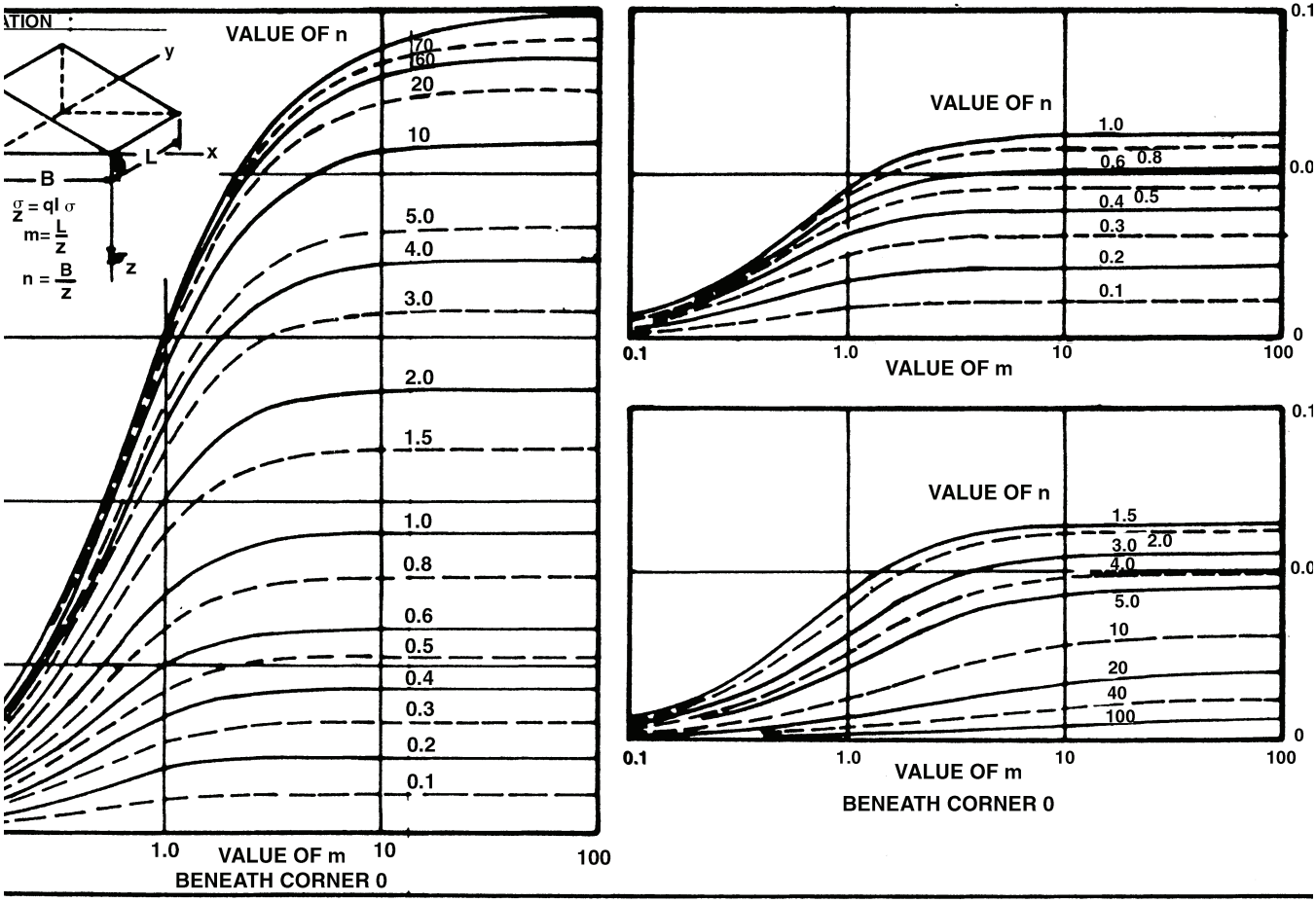

FIGURE 6.12 Influence value for vertical stress beneath triangular load (Westerqaard Case). (After NAVFAC [52].)

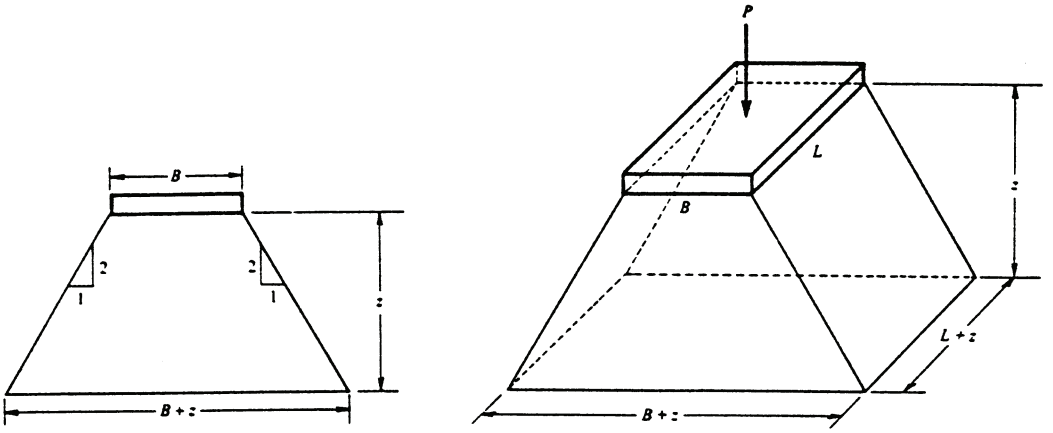

FIGURE 6.13A Approximate distribution of vertical stress due to surface load. (After Perloff [54].)

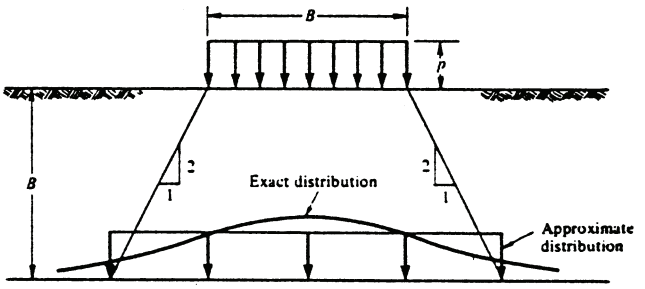

FIGURE 6.13B Relationship between vertical stress below a square uniformly loaded area as determined by approximate and exact methods. (After Perloff [54].)

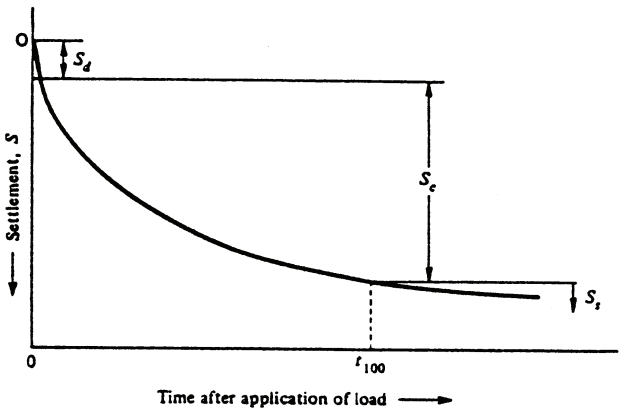

FIGURE 6.14 Schematic time–settlement history of typical point on a foundation. (After Perloff [54].)

by Bowles [14] may be used for computing settlements of footings with flexible bases on the half-space. The settlement equation can be expressed as follows:

$$s_i = q_0 B' \left(1 - \mu^2\right) m I_s I_F / E_s \tag{6.18}$$

$$I_s = n\left(I_1 + \left(1 - 2\mu\right) I_2 / \left(1 - \mu\right)\right) \tag{6.19}$$

where q_0 is contact pressure, μ and E_s are weighted average values of Poisson's ratio and Young's modulus for compressive strata, B is the least-lateral dimension of contribution base area (convert round bases to equivalent square bases; $B = 0.5B$ for center and $B = B$ for corner I_i; $L' = 0.5L$ for center and $L' = L$ for corner I_i), I_i are influence factors depending on dimension of footings, base embedment depth, thickness of soil stratum, and Poisson's ratio (I_1 and I_2 are given in Table 6.13 and I_F is given in Figure 6.15; $M = L'/B'$ and $N = H/B'$), H is the stratum depth causing settlement (see discussion below), m is number of corners contributing to settlement ($m = 4$ at the footing center; $m = 2$ at a side; and $m = 1$ at a corner), and n equals 1.0 for flexible footings and 0.93 for rigid footings.

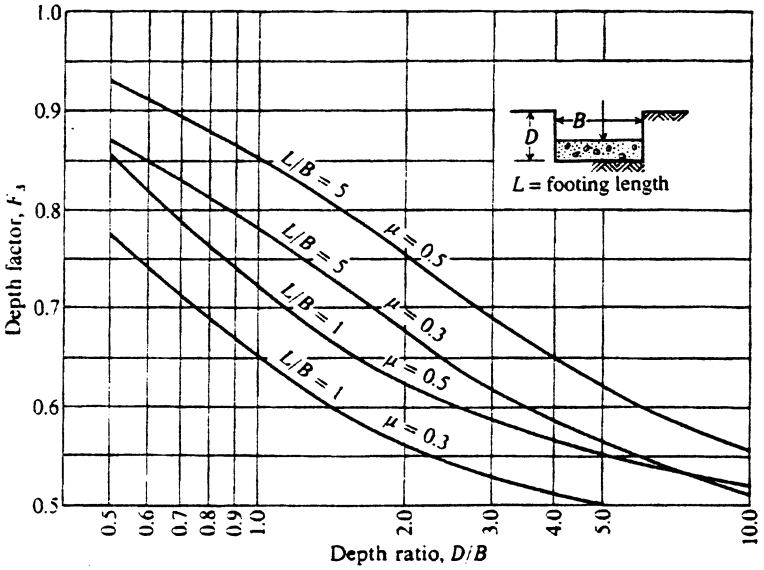

FIGURE 6.15 Influence factor I_F for footing at a depth D (use actual footing width and depth dimension for this D/B ratio). (After Bowles [14].)

This equation applies to soil strata consisting of either cohesionless soils of any water content or unsaturated cohesive soils, which may be either organic or inorganic. Highly organic soils (both E_s and μ are subject to significant changes by high organic content) will be dictated by secondary or creep compression rather than immediate settlement; therefore, the applicability of the above equation is limited.

Suggestions were made by Bowles [14] to use the equations appropriately as follows: 1. Make the best estimate of base contact pressure q_0; 2. Identify the settlement point to be calculated and divide the base (as used in the Newmark stress method) so the point is at the corner or common corner of one or up to four contributing areas; 3. Determine the stratum depth causing settlement which does not approach to infinite rather at either the depth $z = 5B$ or depth to where a hard stratum is

TABLE 6.13 Values of I_2 and I_2 to Compute Influence Factors as Used in Eq. (6.21)

N	$M = 1.0$	1.1	1.2	1.3	1.4	1.5	1.6	1.7	1.8	1.9	2.0
0.2	$I_1 = 0.009$	0.008	0.008	0.008	0.008	0.008	0.007	0.007	0.007	0.007	0.007
	$I_2 = 0.041$	0.042	0.042	0.042	0.042	0.042	0.043	0.043	0.043	0.043	0.043
0.4	0.033	0.032	0.031	0.030	0.029	0.028	0.028	0.027	0.027	0.027	0.027
	0.066	0.068	0.069	0.070	0.070	0.071	0.071	0.072	0.072	0.073	0.073
0.6	0.066	0.064	0.063	0.061	0.060	0.059	0.058	0.057	0.056	0.056	0.055
	0.079	0.081	0.083	0.085	0.087	0.088	0.089	0.090	0.091	0.091	0.092
0.8	0.104	0.102	0.100	0.098	0.096	0.095	0.093	0.092	0.091	0.090	0.089
	0.083	0.087	0.090	0.093	0.095	0.097	0.098	0.100	0.101	0.102	0.103
1.0	0.142	0.140	0.138	0.136	0.134	0.132	0.130	0.129	0.127	0.126	0.125
	0.083	0.088	0.091	0.095	0.098	0.100	0.102	0.104	0.106	0.108	0.109
1.5	0.224	0.224	0.224	0.223	0.222	0.220	0.219	0.217	0.216	0.214	0.213
	0.075	0.080	0.084	0.089	0.093	0.096	0.099	0.102	0.105	0.108	0.110
2.0	0.285	0.288	0.290	0.292	0.292	0.292	0.292	0.292	0.291	0.290	0.289
	0.064	0.069	0.074	0.078	0.083	0.086	0.090	0.094	0.097	0.100	0.102
3.0	0.363	0.372	0.379	0.384	0.389	0.393	0.396	0.398	0.400	0.401	0.402
	0.048	0.052	0.056	0.060	0.064	0.068	0.071	0.075	0.078	0.081	0.084
4.0	0.408	0.421	0.431	0.440	0.448	0.455	0.460	0.465	0.469	0.473	0.476
	0.037	0.041	0.044	0.048	0.051	0.054	0.057	0.060	0.063	0.066	0.069
5.0	0.437	0.452	0.465	0.477	0.487	0.496	0.503	0.510	0.516	0.522	0.526
	0.031	0.034	0.036	0.039	0.042	0.045	0.048	0.050	0.053	0.055	0.058
6.0	0.457	0.474	0.489	0.502	0.514	0.524	0.534	0.542	0.550	0.557	0.563
	0.026	0.028	0.031	0.033	0.036	0.038	0.040	0.043	0.045	0.047	0.050
7.0	0.471	0.490	0.506	0.520	0.533	0.545	0.556	0.566	0.575	0.583	0.590
	0.022	0.024	0.027	0.029	0.031	0.033	0.035	0.037	0.039	0.041	0.043
8.0	0.482	0.502	0.519	0.534	0.549	0.561	0.573	0.584	0.594	0.602	0.611
	0.020	0.022	0.023	0.025	0.027	0.029	0.031	0.033	0.035	0.036	0.038
9.0	0.491	0.511	0.529	0.545	0.560	0.574	0.587	0.598	0.609	0.618	0.627
	0.017	0.019	0.021	0.023	0.024	0.026	0.028	0.029	0.031	0.033	0.034
10.0	0.498	0.519	0.537	0.554	0.570	0.584	0.597	0.610	0.621	0.631	0.641
	0.016	0.017	0.019	0.020	0.022	0.023	0.025	0.027	0.028	0.030	0.031
20.0	0.529	0.553	0.575	0.595	0.614	0.631	0.647	0.662	0.677	0.690	0.702
	0.008	0.009	0.010	0.010	0.011	0.012	0.013	0.013	0.014	0.015	0.016
500	0.560	0.587	0.612	0.635	0.656	0.677	0.696	0.714	0.731	0.748	0.763
	0.000	0.000	0.000	0.000	0.000	0.000	0.001	0.001	0.001	0.001	0.001
0.2	$I_1 = 0.007$	0.006	0.006	0.006	0.006	0.006	0.006	0.006	0.006	0.006	0.006
	$I_2 = 0.043$	0.044	0.044	0.044	0.044	0.044	0.044	0.044	0.044	0.044	0.044
0.4	0.026	0.024	0.024	0.024	0.024	0.024	0.024	0.024	0.024	0.024	0.024
	0.074	0.075	0.075	0.075	0.076	0.076	0.076	0.076	0.076	0.076	0.076
0.6	0.053	0.051	0.050	0.050	0.050	0.049	0.049	0.049	0.049	0.049	0.049
	0.094	0.097	0.097	0.098	0.098	0.098	0.098	0.098	0.098	0.098	0.098
0.8	0.086	0.082	0.081	0.080	0.080	0.080	0.079	0.079	0.079	0.079	0.079
	0.107	0.111	0.112	0.113	0.113	0.113	0.113	0.114	0.114	0.014	0.014
1.0	0.121	0.115	0.113	0.112	0.112	0.112	0.111	0.111	0.110	0.110	0.110
	0.114	0.120	0.122	0.123	0.123	0.124	0.124	0.124	0.125	0.125	0.125
1.5	0.207	0.197	0.194	0.192	0.191	0.190	0.190	0.189	0.188	0.188	0.188
	0.118	0.130	0.134	0.136	0.137	0.138	0.138	0.139	0.140	0.140	0.140
2.0	0.284	0.271	0.267	0.264	0.262	0.261	0.260	0.259	0.257	0.256	0.256
	0.114	0.131	0.136	0.139	0.141	0.143	0.144	0.145	0.147	0.147	0.148
3.0	0.402	0.392	0.386	0.382	0.378	0.376	0.374	0.373	0.368	0.367	0.367
	0.097	0.122	0.131	0.137	0.141	0.144	0.145	0.147	0.152	0.153	0.154
4.0	0.484	0.484	0.479	0.474	0.470	0.466	0.464	0.462	0.453	0.451	0.451
	0.082	0.110	0.121	0.129	0.135	0.139	0.142	0.145	0.154	0.155	0.156
5.0	0.553	0.554	0.552	0.548	0.543	0.540	0.536	0.534	0.522	0.519	0.519
	0.070	0.098	0.111	0.120	0.128	0.133	0.137	0.140	0.154	0.156	0.157
6.0	0.585	0.609	0.610	0.608	0.604	0.601	0.598	0.595	0.579	0.576	0.575
	0.060	0.087	0.101	0.111	0.120	0.126	0.131	0.135	0.153	0.157	0.157
7.0	0.618	0.653	0.658	0.658	0.656	0.653	0.650	0.647	0.628	0.624	0.623

TABLE 6.13 (continued) Values of I_2 and I_2 to Compute Influence Factors as Used in Eq. (6.21)

N	$M = 1.0$	1.1	1.2	1.3	1.4	1.5	1.6	1.7	1.8	1.9	2.0
	0.053	0.078	0.092	0.103	0.112	0.119	0.125	0.129	0.152	0.157	0.158
8.0	0.643	0.688	0.697	0.700	0.700	0.698	0.695	0.692	0.672	0.666	0.665
	0.047	0.071	0.084	0.095	0.104	0.112	0.118	0.124	0.151	0.156	0.158
9.0	0.663	0.716	0.730	0.736	0.737	0.736	0.735	0.732	0.710	0.704	0.702
	0.042	0.064	0.077	0.088	0.097	0.105	0.112	0.118	0.149	0.156	0.158
10.0	0.679	0.740	0.758	0.766	0.770	0.770	0.770	0.768	0.745	0.738	0.735
	0.038	0.059	0.071	0.082	0.091	0.099	0.106	0.122	0.147	0.156	0.158
20.0	0.756	0.856	0.896	0.925	0.945	0.959	0.969	0.977	0.982	0.965	0.957
	0.020	0.031	0.039	0.046	0.053	0.059	0.065	0.071	0.124	0.148	0.156
500.0	0.832	0.977	1.046	1.102	1.150	1.191	1.227	1.259	2.532	1.721	1.879
	0.001	0.001	0.002	0.002	0.002	0.002	0.003	0.003	0.008	0.016	0.031

Source: Bowles, J.E., *Foundation Analysis and Design*, 5th ed., McGraw-Hill, New York, 1996. With permission.

encountered (where F_s in the hard layer is about $10E_s$ of the adjacent upper layer); and 4. Calculate the weighted average E_s as follows:

$$E_{s,\text{avg}} = \sum_{n}^{1} H_i E_{si} \Big/ \sum_{n}^{1} H_i \tag{6.20}$$

6.6.2 Settlement of Shallow Foundations on Sand

SPT Method

D'Appolonio et al. [28] developed the following equation to estimate settlements of footings on sand using SPT data:

$$s = \mu_0 \mu_1 \, pB/M \tag{6.21}$$

where μ_0 and μ_1 are settlement influence factors dependent on footing geometry, depth of embedment, and depth to the relative incompressible layer (Figure 6.16), p is average applied pressure under service load and M is modulus of compressibility. The correlation between M and average SPT blow count is given in Figure 6.17.

Barker et al. [9] discussed the commonly used procedure for estimating settlement of footing on sand using SPT blow count developed by Terzaghi and Peck [64,65] and Bazaraa [10].

CPT Method

Schmertmann [56,57] developed a procedure for estimating footing settlements on sand using CPT data. This CPT method uses cone penetration resistance, q_c, as a measure of the *in situ* stiffness (compressibility) soils. Schmertmann's method is expressed as follows

$$s = C_1 C_2 \Delta p \Sigma \left(I_Z / E_s \right)_i \Delta z_i \tag{6.22}$$

$$C_1 = 1 - 0.5 \left(\frac{\sigma'_{v0}}{\Delta p} \right) \geq 0.5 \tag{6.23}$$

$$C_2 = 1 + 0.2 \log \left(t_{yr} / 0.1 \right) \tag{6.24}$$

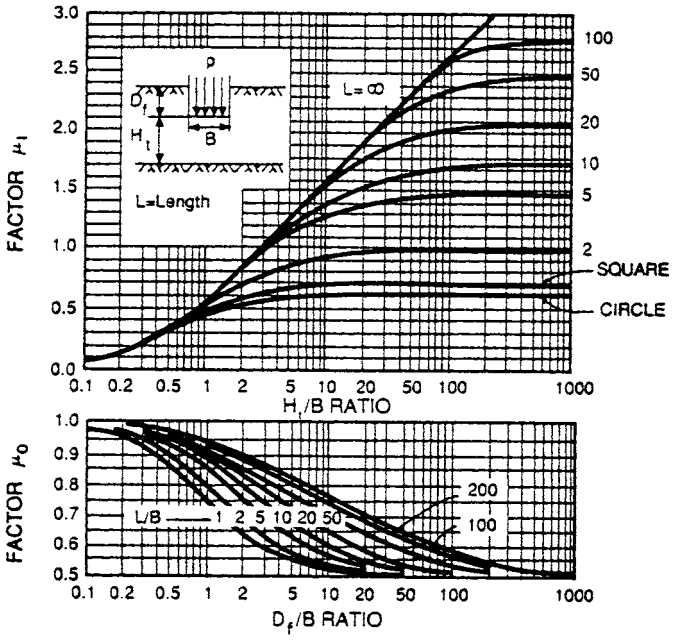

FIGURE 6.16 Settlement influence factors μ_0 and μ_1 for the D'Appolonia et al. procedure. (After D'Appolonia et al [28].)

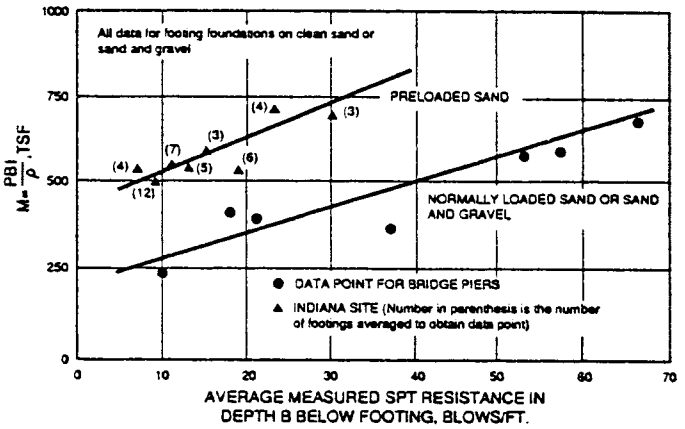

FIGURE 6.17 Correlation between modulus of compressibility and average value SPT blow count. (After D'Appolonia et al [28].)

$$E_s = \begin{cases} 2.5q_c & \text{for square footings (axisymmetric conditions)} \\ 3.5q_c & \text{for continuous footings with } L/B \geq 10 \text{ (plan strain conditions)} \\ \left[2.5 + (L/B - 1)/9\right]q_c & \text{for footings with } 1 \geq L/B \geq 10 \end{cases} \quad (6.25)$$

where $\Delta p = \sigma'_{vf} - \sigma'_{v0}$ is net load pressure at foundation level, σ'_{v0} is initial effective *in situ* overburden stress at the bottom of footings, σ'_{vf} is final effective *in situ* overburden stress at the

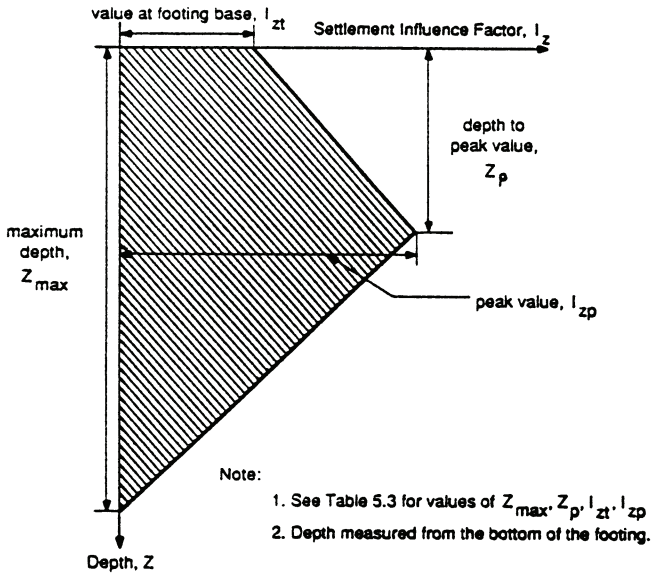

FIGURE 6.18 Variation of Schmertmann's improved settlement influence factors with depth. (After Schmertmann et al [58].)

TABLE 6.14 Coefficients to Define the Dimensions of Schmertmann's Improved Settlement Influence Factor Diagram in Figure 6.19

				Peak Value of Stress Influence Factor I_{zp}			
L/B	Max. Depth of Influence z_{max}/B	Depth to Peak Value z_p/B	Value of I_z at Top I_{zt}	$\frac{\Delta p}{\sigma'_{vp}} = 1$	$\frac{\Delta p}{\sigma'_{vp}} = 2$	$\frac{\Delta p}{\sigma'_{vp}} = 4$	$\frac{\Delta p}{\sigma'_{vp}} = 10$
1	2.00	0.50	0.10	0.60	0.64	0.70	0.82
2	2.20	0.55	0.11	0.60	0.64	0.70	0.82
4	2.65	0.65	0.13	0.60	0.64	0.70	0.82
8	3.55	0.90	0.18	0.60	0.64	0.70	0.82
Š10	4.00	1.00	0.20	0.60	0.64	0.70	0.82

Note: σ'_{vp} is the initial vertical pressure at depth of peak influence.

After Schmertmann et al. [57].

bottom of footings, I_z is strain influence factor as defined in Figure 6.18 and Table 6.14, E_s is the appropriate Young's modulus at the middle of the ith layer of thickness Δz_1, C_1 is pressure correction factor, C_2 is time rate factor (equal to 1 for immediate settlement calculation or if the lateral pressure is less than the creep pressure determined from pressure-meter tests), q_c is cone penetration resistance, in pressure units, and Δz is layer thickness.

Recent studies by Tan and Duncan [62] have compared measured settlements with settlements predicted using various procedures for footings on sand. These studies conclude that methods predicting settlements close to the average of measured settlement are likely to underestimate settlements half the time and to overestimate them half the time. The conservative methods (notably Terzaghi and Peck's) tend to overestimate settlements more than half the time and to underestimate them less often. On the other hand, there is a trade-off between accuracy and reliability. A relatively accurate method such as the D'Appolonia et al. method calculates settlements that are about equal to the average value of actual settlements, but it underestimates settlements half the time (a reliability of 50%). To ensure that the calculated settlements equal or exceed the measured settlements about

TABLE 6.15 Value of Adjustment Factor for 50 and 90% Reliability in Displacement Estimates

Method	Soil Type	Adjustment Factor	
		For 50% Reliability	For 90% Reliability
Terzaghi and Peck [65]	Sand	0.45	1.05
Schmertmann	Sand	0.60	1.25
D'Appolonia et al. [28]	Sand	1.00	2.00

TABLE 6.16 Some Empirical Equations for C_c and C_α

Compression Index	Source	Comment
$C_c = 0.009(LL - 10)$	Terzaghi and Peck [65]	S_t ð 5, $LL < 100$
$C_c = 0.2343e_0$	Nagaraj and Murthy [51]	
$C_c = 0.5G_s(PI/100)$	Worth and Wood [71]	Modified cam clay model
$C_c = 0PI/74$	EPRI (1990)	
$C_c = 0.37(e_0 + 0.003w_L + 0.0004w_N - 0.34)$	Azzouz et al. [7]	Statistical analysis
Recompression Index	**Source**	
$C_r = 0.0463w_LG_s$	Nagaraj and Murthy [50]	

90% of the time (a reliability of 90%), an adjustment factor of two should be applied to the settlements predicted by the D'Appolonia et al. method. Table 6.15 shows values of the adjustment factor for 50 and 90% reliability in settlement predicted using Terzaghi and Peck, D'Appolonia et al., and Schmertmann methods.

6.6.3 Settlement of Shallow Foundations on Clay

Immediate Settlement

Immediate settlement of shallow foundations on clay can be estimated using the approach described in Section 6.6.1.

Consolidation Settlement

Consolidation settlement is time dependent and may be estimated using one-dimensional consolidation theory [43,53,66]. The consolidation settlement can be calculated as follows

$$s_c \begin{cases} \dfrac{H_c}{1+e_0}\left[C_r \log\left(\dfrac{\sigma'_p}{\sigma''_{vo}}\right) + C_c \log\left(\dfrac{\sigma'_{vf}}{\sigma'_p}\right)\right] & \left(\text{for OC soils, i.e., } \sigma'_p > \sigma'_{v0}\right) \\ \dfrac{H_c}{1+e_0} C_c \log\left(\dfrac{\sigma'_{vf}}{\sigma'_p}\right) & \left(\text{for NC soils, i.e., } \sigma'_p = \sigma'_{v0}\right) \end{cases} \tag{6.26}$$

where H_c is height of compressible layer, e_0 is void ratio at initial vertical effective stress, C_γ is recompression index (see Table 6.16), C_c is compression index (see Table 6.16), σ'_p is maximum past vertical effective stress, σ'_{v0} is initial vertical effective stress, σ'_{vf} is final vertical effective stress. Highly compressible cohesive soils are rarely chosen to place footings for bridges where tolerable amount of settlement is relatively small. Preloading or surcharging to produce more rapid consolidation has been extensively used for foundations on compressible soils [54]. Alternative foundation systems would be appropriate if large consolidation settlement is expected to occur.

TABLE 6.17 Secondary Compression Index

C_α/C_c	Material
0.02 ± 0.01	Granular soils including rockfill
0.03 ± 0.01	Shale and mudstone
0.04 ± 0.01	Inorganic clays and silts
0.05 ± 0.01	Organic clays and silts
0.06 ± 0.01	Peat and muskeg

Source: Terzaghi, I. et al., *Soil Mechanics in Engineering Practice,* 3rd ed., John Wiley & Sons, New York, 1996. With permission.

Secondary Settlement

Settlements of footings on cohesive soils continuing beyond primary consolidation are called secondary settlement. Secondary settlement develops at a slow and continually decreasing rate and may be estimated as follows:

$$s_s = C_\alpha H_t \log \frac{t_{sc}}{t_p} \tag{6.27}$$

where C_α is coefficient of secondary settlement (Table 6.17), H_t is total thickness of layers undergoing secondary settlement, t_{sc} is time for which secondary settlement is calculated (in years), and t_p is time for primary settlement (>1 year).

6.6.4 Tolerable Settlement

Tolerable movement criteria for foundation settlement should be established consistent with the function and type of structure, anticipated service life, and consequences of unacceptable movements on structure performance as outlined by AASHTO [3]. The criteria adopted by AASHTO considering the angular distortion (δ/l) between adjacent footings is as follows:

$$\frac{\delta}{l} \leq \begin{cases} 0.008 & \text{for simple - span bridge} \\ 0.004 & \text{for continuous - span bridge} \end{cases} \tag{6.28}$$

where δ is differential settlement of adjacent footings and l is center–center spacing between adjacent footings. These (δ/l) limits are not applicable to rigid frame structures, which shall be designed for anticipated differential settlement using special analysis.

6.7 Shallow Foundations on Rock

Wyllie [72] outlines the following examinations which are necessary for designing shallow foundations on rock:

1. The bearing capacity of the rock to ensure that there will be no crushing or creep of material within the loaded zone;
2. Settlement of the foundation which will result from elastic strain of the rock, and possibly inelastic compression of weak seams within the volume of rock compressed by the applied load;
3. Sliding and shear failure of blocks of rock formed by intersecting fractures within the foundation.

TABLE 6.18 Presumptive Bearing Pressures (tsf) for Foundations on Rock after Putnam, 1981

Code	Year[1]	Bedrock[2]	Sound Foliated Rock	Sound Sedimentary Rock	Soft Rock[3]	Soft Shale	Broken Shale
Baltimore	1962	100	35		10		
BOCA	1970	100	40	25	10	4	(4)
Boston	1970	100	50	10	10		1.5
Chicago	1970	100	100				(4)
Cleveland	1951/1969			25			
Dallas	1968	$0.2q_u$	$2q_u$	$0.2q_u$	$0.2q_u$	$0.2q_u$	$0.2q_u$
Detroit	1956	100	100	9600	12	12	
Indiana	1967	$0.2q_u$	$2q_u$	$0.2q_u$	$0.2q_u$	$0.2q_u$	$0.2q_u$
Kansas	1961/1969	$0.2q_u$	$2q_u$	$0.2q_u$	$0.2q_u$	$0.2q_u$	$0.2q_u$
Los Angeles	1970	10	4	3	1	1	1
New York City	1970	60	60	60	8		
New York State		100	40	15			
Ohio	1970	100	40	15	10	4	
Philadelphia	1969	50	15	10–15	8		
Pittsburgh	1959/1969	25	25	25	8	8	
Richmond	1968	100	40	25	10	4	1.5
St. Louis	1960/1970	100	40	25	10	1.5	1.5
San Francisco	1969	3–5	3–5	3–5			
UBC	1970	$0.2q_u$	$2q_u$	$0.2q_u$	$0.2q_u$	$0.2q_u$	$0.2q_u$
NBC Canada	1970			100			
New South Wales, Australia	1974		33	13	4.5		

Notes:
1. Year of code or original year and date of revision.
2. Massive crystalline bedrock.
3. Soft and broken rock, not including shale.
4. Allowable bearing pressure to be determined by appropriate city official.
5. q_u = unconfined compressive strength.

This condition usually occurs where the foundation is located on a steep slope and the orientation of the fractures is such that the blocks can slide out of the free face.

6.7.1 Bearing Capacity According to Building Codes

It is common to use allowable bearing capacity for various rock types listed in building codes for footing design. As provided in Table 6.18, the bearing capacities have been developed based on rock strength from case histories and include a substantial factor of safety to minimize settlement.

6.7.2 Bearing Capacity of Fractured Rock

Various empirical procedures for estimating allowable bearing capacity of foundations on fractured rock are available in the literature. Peck et al. [53] suggested an empirical procedure for estimating allowable bearing pressures of foundations on jointed rock based on the RQD index. The predicted bearing capacities by this method shall be used with the assumption that the foundation settlement does not exceed 12.7 mm (0.5 in.) [53]. Carter and Kulhawy [25] proposed an empirical approach for estimating ultimate bearing capacity of fractured rock. Their method is based on the unconfined compressive strength of the intact rock core sample and rock mass quality.

Wyllie [72] detailed an analytical procedure for computing bearing capacity of fractured rock mass using Hoek–Brown strength criterion. Details of rational methods for the topic can also be found in Kulhawy and Goodman [42] and Goodman [32].

6.7.3 Settlements of Foundations on Rock

Wyllie [72] summarizes settlements of foundations on rock as following three different types: (1) Elastic settlements result from a combination of strain of the intact rock, slight closure and movement of fractures and compression of any minor clay seams (less than a few millimeters). Elastic theory can be used to calculate this type of settlement. Detailed information can be found in Wyllie [72], Kulhawy, and AASHTO [3]. (2) Settlements result from the movement of blocks of rock due to shearing of fracture surfaces. This occurs when foundations are sitting at the top of a steep slope and unstable blocks of rocks are formed in the face. The stability of foundations on rock is influenced by the geologic characterization of rock blocks. The information required on structural geology consists of the orientation, length and spacing of fractures, and their surface and infilling materials. Procedures have been developed for identifying and analyzing the stability of sliding blocks [72], stability of wedge blocks [36], stability of toppling blocks [33], or three-dimensional stability of rock blocks [34]. (3) Time-dependent settlement occurs when foundations found on rock mass that consists of substantial seams of clay or other compressible materials. This type of settlement can be estimated using the procedures described in Section 6.6.3. Also time-dependent settlement can occur if foundations found on ductile rocks, such as salt where strains develop continuously at any stress level, or on brittle rocks when the applied stress exceeds the yield stress.

6.8 Structural Design of Spread Footings

The plan dimensions (B and L) of a spread footing are controlled by the allowable soil pressure beneath the footing. The pressure distribution beneath footings is influenced by the interaction of the footing rigidity with the soil type, stress–state, and time response to stress as shown in Figure 6.19 (a) (b). However, it is common practice to use the linear pressure distribution beneath rigid footings as shown in Figure 6.19 (c). The depth (D) for spread footings is usually controlled by shear stresses. Two-way action shear always controls the depth for centrally loaded square footings. However, wide-beam shear may control the depth for rectangular footings when the L/B ratio is greater than about 1.2 and may control for other L/B ratios when there is overturning or eccentric loading (Figure 6.20a). In addition, footing depth should be designed to satisfy diagonal (punching) shear requirement (Figure 6.20b). Recent studies by Duan and McBride [30] indicate that when the length-to-thickness ratio of cantilever (L/D as defined in Figure 6.21) of a footing (or pile-cap) is greater than 2.2, a nonlinear distribution of reaction should be used for footing or pile-cap design. The specifications and procedures for footing design can be found in AASHTO [2], ACI [4], or Bowles [12, 13].

Acknowledgment

I would like to take this opportunity to thank Bruce Kutter, who reviewed the early version of the chapter and provided many thoughtful suggestions. Advice and support from Prof. Kutter are greatly appreciated.

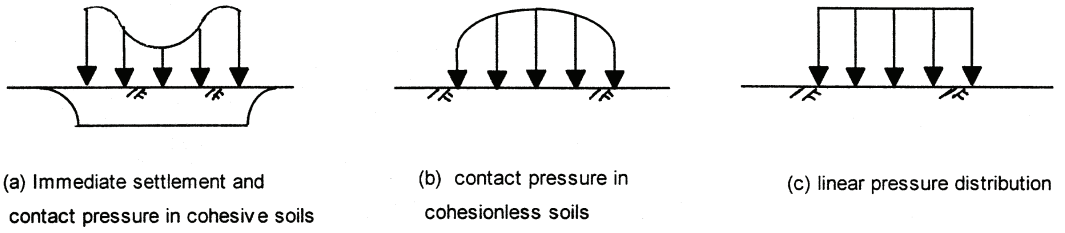

FIGURE 6.19 Contact pressure distribution for a rigid footing. (a) On cohesionless soils; (b) on cohesive soils; (c) usual assumed linear distribution.

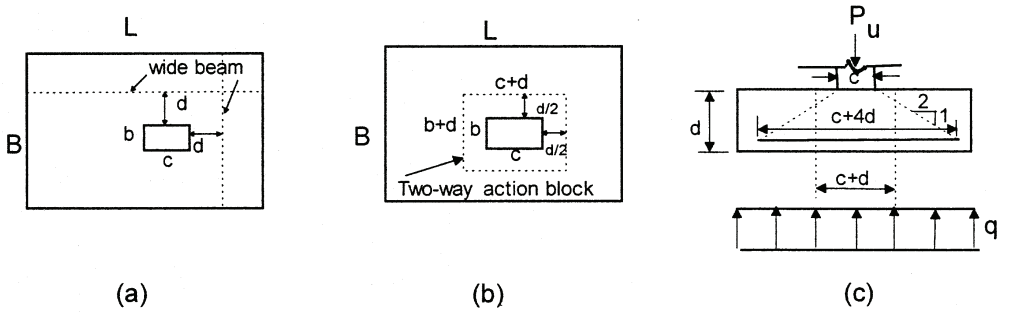

FIGURE 6.20 (a) Section for wide-beam shear; (b) section for diagonal-tension shear; (c) method of computing area for allowable column bearing stress.

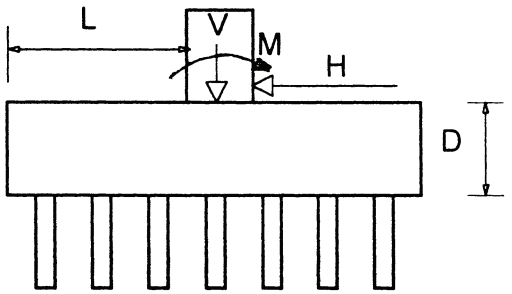

FIGURE 6.21 Illustration of the length-to-thickness ratio of cantilever of a footing or pile cap.

References

1. AASHTO, *LRFD Bridge Design Specifications*, American Association of State Highway and Transportation Officials, Washington, D.C., 1994.
2. AASHTO, *Standard Specifications for Highway Bridges (Interim Revisions)*, 16th ed., American Association of State Highway and Transportation Officials, Washington, D.C., 1997.
3. AASHTO, *LRFD Bridge System Design Specification (Interim Revisions)*, American Association of State Highway and Transportation Officials, Washington, D.C., 1997.
4. ACI, *Building Code Requirements for Reinforced Concrete* (ACI 318-89), American Concrete Institute, Detroit, MI, 1989, 353 pp. (with commentary).
5. ASTM, Section 4 Construction, 04.08 Soil and Rock (I): D420–D4914, American Society for Testing and Materials, Philadelphia, PA, 1997.

6. ATC-32, *Improved Seismic Design Criteria for California Bridges: Provisional Recommendations*, Applied Technology Council, Redwood City, CA, 1996.
7. Azzouz, A.S., Krizek, R.J., and Corotis, R.B., Regression of analysis of soil compressibility, *JSSMFE Soils and Foundations*, 16(2), 19–29, 1976.
8. Baguelin, F., Jezequel, J.F., and Shields, D.H., *The Pressuremeter and Foundation Engineering*, Transportation Technical Publications, Clausthal, 1978, 617 pp.
9. Barker, R.M., Duncan, J.M., Rojiani, K.B., Ooi, P.S.K., Tan, C.K., and Kim, S.G., Manuals for the Design of Bridge Foundations, National Cooperative Highway Research Program Report 343, Transportation Research Board, National Research Council, Washington, D.C., 1991.
10. Bazaraa, A.R.S.S., Use of Standard Penetration Test for Estimating Settlements of Shallow Foundations on Sands, Ph.D. dissertation, Department of Civil Engineering, University of Illinois, Urbana, 1967, 380 pp.
11. Bowles, J.E., *Analytical and Computer Methods in Foundation Engineering*, McGraw-Hill, New York, 1974.
12. Bowles, J.E., Spread footings, Chapter 15, in *Foundation Engineering Handbook*, Winterkorn, H.F. and Fang, H.Y., Eds., Van Nostrand Reinhold, New York, 1975.
13. Bowles, J.E., *Foundation Analysis and Design*, 5th ed., McGraw-Hill, New York, 1996.
14. Briaud, J.L., *The Pressuremeter*, A.A. Balkema Publishers, Brookfield, VT, 1992.
15. Briaud, J.L., Spread footing design and performance, FHWA Workshop at the Tenth Annual International Bridge Conference and Exhibition, 1993.
16. Briaud, J.L., Pressuremeter and foundation design, in *Proceedings of the Conference on Use of* in situ *tests in Geotechnical Engineering*, ASCE Geotechnical Publication No. 6, 74–116, 1986.
17. Briaud, J.L. and Gibben, R., Predicted and measured behavior of five spread footings on sand, Geotechnical Special Publication No. 41, ASCE Specialty Conference: Settlement 1994, ASCE, New York, 1994.
18. Buisman, A.S.K., *Grondmechanica*, Waltman, Delft, 190, 1940.
19. Burland, J.B. and Burbidge, M.C., Settlement of foundations on sand and gravel, *Proc. Inst. Civil Eng.*, Tokyo, 2, 517, 1984.
20. Burmister, D.M., The theory of stresses and displacements in layered systems and application to the design of airport runways, *Proc. Highway Res. Board*, 23, 126–148, 1943.
21. Burmister, D.M., Evaluation of pavement systems of WASHO road test layered system methods, Highway Research Board Bull. No. 177, 1958.
22. Burmister, D.M., Applications of dimensional analyses in the evaluation of asphalt pavement performances, paper presented at Fifth Paving Conference, Albuquerque, NM, 1967.
23. Canadian Geotechnical Society, *Canadian Foundation Engineering Manual*, 2nd ed., 1985, 456.
24. Carter. J.P. and Kulhawy, F.H., Analysis and Design of Drilled Shaft Foundations Socketed into Rock, Report No. EL-5918, Empire State Electric Engineering Research Corporation and Electric Power Research Institute, 1988.
25. Chen, W.F., *Limit Analysis and Soil Plasticity*, Elsevier, Amsterdam, 1975.
26. Chen, W.F. and Mccarron, W.O., Bearing capacity of shallow foundations, Chap. 4, in *Foundation Engineering Handbook*, 2nd ed., Fang, H.Y., Ed., Chapman & Hall, 1990.
27. D'Appolonia, D.J., D'Appolonia, E., and Brisette, R.F., Settlement of spread footings on sand (closure), *ASCE J. Soil Mech. Foundation Div.*, 96(SM2), 754–761, 1970.
28. De Beer, E.E., Bearing capacity and settlement of shallow foundations on sand, *Proc. Symposium on Bearing Capacity and Settlement of Foundations*, Duke University, Durham, NC, 315–355, 1965.
29. De Beer, E.E., Proefondervindelijke bijdrage tot de studie van het gransdraagvermogen van zand onder funderingen p staal, Bepaling von der vormfactor sb, *Ann. Trav. Publics Belg.*, 1967.
30. Duan, L. and McBride, S.B., The effects of cap stiffness on pile reactions, *Concrete International*, American Concrete Institue, 1995.
31. FHWA, Large-Scale Load Tests and Data Base of Spread Footings on Sand, Publication No. FHWA-RD-97-068, 1997.

32. Goodman, R.E. and Bray, J.W., Toppling of rock slopes, in *Proceedings of the Specialty Conference on Rock Engineering for Foundations and Slopes*, Vol. 2, ASCE, Boulder, CO, 1976, 201–234.
33. Goodman, R.E. and Shi, G., *Block Theory and Its Application to Rock Engineering*, Prentice-Hall, Englewood Cliffs, NJ, 1985.
34. Hansen, B.J., A Revised and Extended Formula for Bearing Capacity, Bull. No. 28, Danish Geotechnical Institute, Copenhagen, 1970, 5–11.
35. Hoek, E. and Bray, J., *Rock Slope Engineering*, 2nd ed., IMM, London, 1981.
36. Holtz, R.D., Stress distribution and settlement of shallow foundations, Chap. 5, in *Foundation Engineering Handbook*, 2nd ed., Fang, H.Y., Ed., Chapman & Hall, 1990.
37. Ismael, N.F. and Vesic, A.S., Compressibility and bearing capacity, *ASCE J. Geotech. Foundation Eng. Div.* 107(GT12), 1677–1691, 1981.
38. Kulhawy, F.H. and Mayne, P.W., Manual on Estimating Soil Properties for Foundation Design, Electric Power Research Institute, EPRI EL-6800, Project 1493-6, Final Report, August, 1990.
39. Kulhawy, F.H. and Goodman, R.E., Foundation in rock, Chap. 55, in *Ground Engineering Reference Manual*, F.G. Bell, Ed., Butterworths, 1987.
40. Lambe, T.W. and Whitman, R.V., *Soil Mechanics*, John Wiley & Sons, New York, 1969.
41. Menard, L., Regle pour le calcul de la force portante et du tassement des fondations en fonction des resultats pressionmetriques, in *Proceedings of the Sixth International Conference on Soil Mechanics and Foundation Engineering*, Vol. 2, Montreal, 1965, 295–299.
42. Meyerhof, G.G., The ultimate bearing capacity of foundations, *Geotechnique*, 2(4), 301–331, 1951.
43. Meyerhof, G.G., Penetration tests and bearing capacity of cohesionless soils, *ASCE J. Soil Mech. Foundation Div.*, 82(SM1), 1–19, 1956.
44. Meyerhof, G.G., Some recent research on the bearing capacity of foundations, *Can. Geotech. J.*, 1(1), 16–36, 1963.
45. Meyerhof, G.G., Shallow foundations, *ASCE J. Soil Mech. and Foundations Div.,* 91, No. SM2, 21–31, 1965.
46. Milovic, D.M., Comparison between the calculated and experimental values of the ultimate bearing capacity, in *Proceedings of the Sixth International Conference on Soil Mechanics and Foundation Engineering*, Vol. 2, Montreal, 142–144, 1965.
47. Nagaraj, T.S. and Srinivasa Murthy, B.R., Prediction of preconsolidation pressure and recompression index of soils, *ASTMA Geotech. Testing J.*, 8(4), 199–202, 1985.
48. Nagaraj. T.S. and Srinivasa Murthy, B.R., A critical reappraisal of compression index, *Geotechnique*, 36(1), 27–32, 1986.
49. NAVFAC, Design Manual 7.02, *Foundations & Earth Structures*, Naval Facilities Engineering Command, Department of the Navy, Washington, D.C., 1986.
50. NAVFAC, Design Manual 7.01, Soil Mechanics, Naval Facilities Engineering Command, Department of the Navy, Washington, D.C., 1986.
51. Peck, R.B., Hanson, W.E., and Thornburn, T.H., *Foundation Engineering*, 2nd ed., John Wiley & Sons, New York, 1974.
52. Perloff, W.H., Pressure distribution and settlement, Chap. 4, in *Foundation Engineering Handbook*, 2nd ed., Fang, H.Y., Ed., Chapman & Hall, 1975.
53. Poulos, H.G. and Davis, E.H., *Elastic Solutions for Soil and Rock Mechanics*, John Wiley & Sons, New York, 1974.
54. Schmertmann, J.H., Static cone to compute static settlement over sand, *ASCE J. Soil Mech. Foundation Div.*, 96(SM3), 1011–1043, 1970.
55. Schmertmann, J.H., Guidelines for cone penetration test performance and design, Federal Highway Administration, Report FHWA-TS-78-209, 1978.
56. Schmertmann, J.H., Dilatometer to Computer Foundation Settlement, *Proc.* In Situ *'86, Specialty Conference on the Use of* In Situ *Tests and Geotechnical Engineering*, ASCE, New York, 303–321, 1986.
57. Schmertmann, J.H., Hartman, J.P., and Brown, P.R., Improved strain influence factor diagrams, *ASCE J. Geotech. Eng. Div.*, 104(GT8), 1131–1135, 1978.

58. Schultze, E. and Sherif, G. Prediction of settlements from evaluated settlement observations on sand, *Proc. 8th Int. Conference on Soil Mechanics and Foundation Engineering,* Moscow, 225–230, 1973.
59. Scott, R.F., *Foundation Analysis*, Prentice-Hall, Englewood Cliffs, NJ, 1981.
60. Sowers, G.F. and Vesic, A.B., Vertical stresses in subgrades beneath statically loaded flexible pavements, Highway Research Board Bulletin, No. 342, 1962.
61. Steinbrenner, W., *Tafeln zur Setzungberechnung*, Die Strasse, 1943, 121–124.
62. Tan, C.K. and Duncan, J.M., Settlement of footings on sand—accuracy and reliability, in *Proceedings of Geotechnical Congress*, Boulder, CO, 1991.
63. Terzaghi, J., *Theoretical Soil Mechanics*, John Wiley & Sons, New York, 1943.
64. Terzaghi, K. and Peck, R.B., *Soil Mechanics in Engineering Practice*, John Wiley & Sons, New York, 1948.
65. Terzaghi, K. and Peck, R.B., *Soil Mechanics in Engineering Practice*, 2nd ed., John Wiley & Sons, New York, 1967.
66. Terzaghi, K., Peck, R.B., and Mesri, G., *Soil Mechanics in Engineering Practice*, 3rd ed., John Wiley & Sons, New York, 1996.
67. Vesic, A.S., Bearing capacity of deep foundations in sand, National Academy of Sciences, National Research Council, Highway Research Record, 39, 112–153, 1963.
68. Vesic, A.S., Analysis of ultimate loads of shallow foundations, *ASCE J. Soil Mech. Foundation Eng. Div.*, 99(SM1), 45–73, 1973.
69. Vesic, A.S., Bearing capacity of shallow foundations, Chap. 3, in *Foundation Engineering Handbook*, Winterkorn, H.F. and Fang, H.Y., Ed., Van Nostrand Reinhold, New York, 1975.
70. Westergaard, H.M., A problem of elasticity suggested by a problem in soil mechanics: soft material reinforced by numerous strong horizontal sheets, in *Contributions to the Mechanics of Solids*, Stephen Timoshenko Sixtieth Anniversary Volume, Macmillan, New York, 1938.
71. Wroth, C.P. and Wood, D.M., The correlation of index properties with some basic engineering properties of soils, *Can. Geotech. J.*, 15(2), 137–145, 1978.
72. Wyllie, D.C., *Foundations on Rock*, E & FN SPON, 1992.

7

Deep Foundations

Youzhi Ma
Geomatrix Consultants, Inc.

Nan Deng
Bechtel Corporation

7.1 Introduction

A bridge foundation is part of the bridge substructure connecting the bridge to the ground. A foundation consists of man-made structural elements that are constructed either on top of or within existing geologic materials. The function of a foundation is to provide support for the bridge and to transfer loads or energy between the bridge structure and the ground.

A deep foundation is a type of foundation where the embedment is larger than its maximum plane dimension. The foundation is designed to be supported on deeper geologic materials because either the soil or rock near the ground surface is not competent enough to take the design loads or it is more economical to do so.

The merit of a deep foundation over a shallow foundation is manifold. By involving deeper geologic materials, a deep foundation occupies a relatively smaller area of the ground surface. Deep foundations can usually take larger loads than shallow foundations that occupy the same area of the ground surface. Deep foundations can reach deeper competent layers of bearing soil or rock, whereas shallow foundations cannot. Deep foundations can also take large uplift and lateral loads, whereas shallow foundations usually cannot.

The purpose of this chapter is to give a brief but comprehensive review to the design procedure of deep foundations for structural engineers and other bridge design engineers. Considerations of selection of foundation types and various design issues are first discussed. Typical procedures to calculate the axial and lateral capacities of an individual pile are then presented. Typical procedures to analyze pile groups are also discussed. A brief discussion regarding seismic design is also presented for its uniqueness and importance in the foundation design.

7.2 Classification and Selection

7.2.1 Typical Foundations

Typical foundations are shown on Figure 7.1 and are listed as follows:

A *pile* usually represents a slender structural element that is driven into the ground. However, a pile is often used as a generic term to represent all types of deep foundations, including a (driven) pile, (drilled) shaft, caisson, or an anchor. A *pile group* is used to represent various grouped deep foundations.

A *shaft* is a type of foundation that is constructed with cast-in-place concrete after a hole is first drilled or excavated. A *rock socket* is a shaft foundation installed in rock. A shaft foundation also is called a *drilled pier* foundation.

A *caisson* is a type of large foundation that is constructed by lowering preconstructed foundation elements through excavation of soil or rock at the bottom of the foundation. The bottom of the caisson is usually sealed with concrete after the construction is completed.

An *anchor* is a type of foundation designed to take tensile loading. An anchor is a slender, small-diameter element consisting of a reinforcement bar that is fixed in a drilled hole by grout concrete. Multistrain high-strength cables are often used as reinforcement for large-capacity anchors. An *anchor for suspension bridge* is, however, a foundation that sustains the pulling loads located at the ends of a bridge; the foundation can be a deadman, a massive tunnel, or a composite foundation system including normal anchors, piles, and drilled shafts.

A *spread footing* is a type of foundation that the embedment is usually less than its smallest width. Normal spread footing foundation is discussed in detail in Chapter 6.

7.2.2 Typical Bridge Foundations

Bridge foundations can be individual, grouped, or combination foundations. Individual bridge foundations usually include individual footings, large-diameter drilled shafts, caissons, rock sockets, and deadman foundations. Grouped foundations include groups of caissons, driven piles, drilled shafts, and rock sockets. Combination foundations include caisson with driven piles, caisson with drilled shafts, large-diameter pipe piles with rock socket, spread footings with anchors, deadman with piles and anchors, etc.

For small bridges, small-scale foundations such as individual footings or drilled shaft foundations, or a small group of driven piles may be sufficient. For larger bridges, large-diameter shaft foundations, grouped foundations, caissons, or combination foundations may be required. Caissons, large-diameter steel pipe pile foundations, or other types of foundations constructed by using the cofferdam method may be necessary for foundations constructed over water.

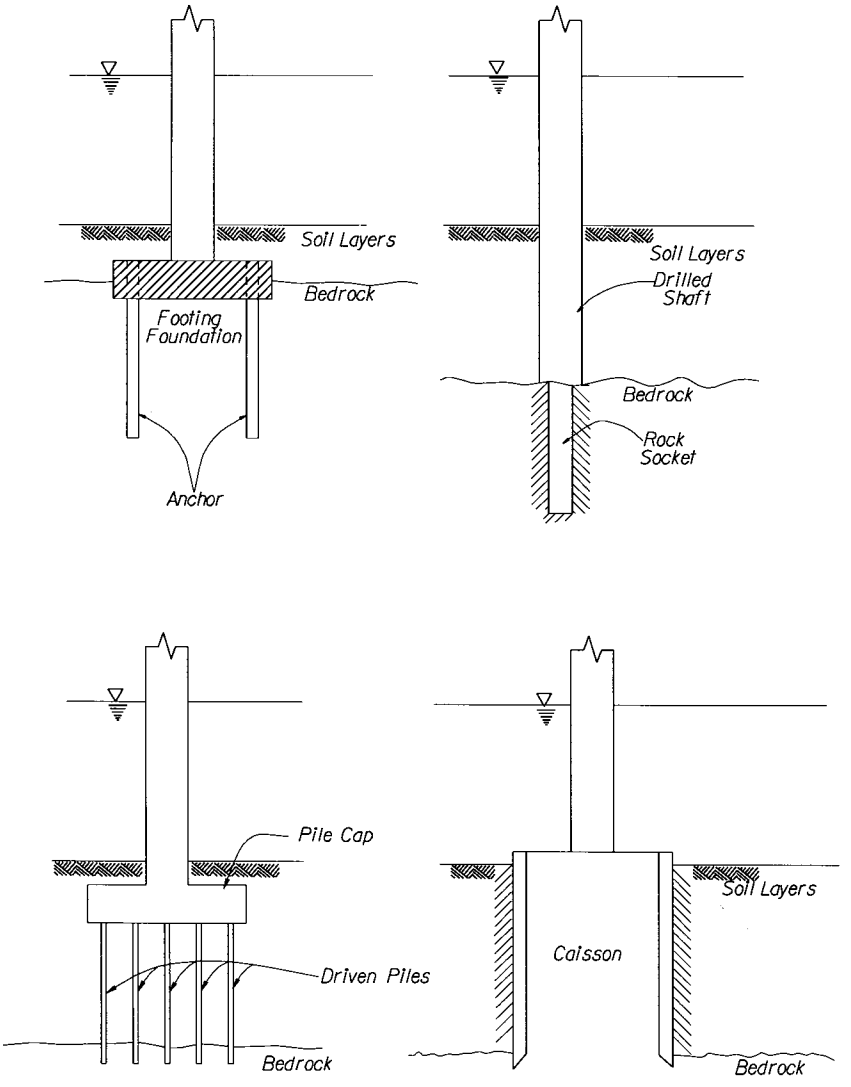

FIGURE 7.1 Typical foundations.

Bridge foundations are often constructed in difficult ground conditions such as landslide areas, liquefiable soil, collapsible soil, soft and highly compressible soil, swelling soil, coral deposits, and underground caves. Special foundation types and designs may be needed under these circumstances.

7.2.3 Classification

Deep foundations are of many different types and are classified according to different aspects of a foundation as listed below:

Geologic conditions — Geologic materials surrounding the foundations can be soil and rock. Soil can be fine grained or coarse grained; from soft to stiff and hard for fine-grained soil, or from loose to dense and very dense for coarse-grained soil. Rock can be sedimentary, igneous, or metamorphic; and from very soft to medium strong and hard. Soil and rock mass may possess predefined weaknesses and

TABLE 7.1 Range of Maximum Capacity of Individual Deep Foundations

Type of Foundation	Size of Cross Section	Maximum Compressive Working Capacity
Driven concrete piles	Up to 45 cm	100 to 250 tons (900 to 2200 kN)
Driven steel pipe piles	Up to 45 cm	50 to 250 tons (450 to 2200 kN)
Driven steel H-piles	Up to 45 cm	50 to 250 tons (450 to 2200 kN)
Drilled shafts	Up to 60 cm	Up to 400 tons (3500 kN)
Large steel pipe piles, concrete-filled; large-diameter drilled shafts; rock rocket	0.6 to 3 m	300 to 5,000 tons or more (2700 to 45000 kN)

discontinuities, such as rock joints, beddings, sliding planes, and faults. Water conditions can be different, including over river, lake, bay, ocean, or land with groundwater. Ice or wave action may be of concern in some regions.

Installation methods — Installation methods can be piles (driven, cast-in-place, vibrated, torqued, and jacked); shafts (excavated, drilled and cast-in-drilled-hole); anchor (drilled); caissons (Chicago, shored, benoto, open, pneumatic, floating, closed-box, Potomac, etc.); cofferdams (sheet pile, sand or gravel island, slurry wall, deep mixing wall, etc.); or combined.

Structural materials — Materials for foundations can be timber, precast concrete, cast-in-place concrete, compacted dry concrete, grouted concrete, post-tension steel, H-beam steel, steel pipe, composite, etc.

Ground effect — Depending on disturbance to the surrounding ground, piles can be displacement piles, low displacement, or nondisplacement piles. Driven precast concrete piles and steel pipes with end plugs are displacement piles; H-beam and unplugged steel pipes are low-displacement piles; and drilled shafts are nondisplacement piles.

Function — Depending on the portion of load carried by the side, toe, or a combination of the side and toe, piles are classified as frictional, end bearing, and combination piles, respectively.

Embedment and relative rigidity — Piles can be divided into long piles and short piles. A long pile, simply called a pile, is embedded deep enough that fixity at its bottom is established, and the pile is treated as a slender and flexible element. A short pile is a relatively rigid element that the bottom of the pile moves significantly. A caisson is often a short pile because of its large cross section and stiffness. An extreme case for short piles is a spread-footing foundation.

Cross section — The cross section of a pile can be square, rectangular, circular, hexagonal, octagonal, H-section; either hollow or solid. A pile cap is usually square, rectangular, circular, or bell-shaped. Piles can have different cross sections at different depths, such as uniform, uniform taper, step-taper, or enlarged end (either grouted or excavated).

Size — Depending on the diameter of a pile, piles are classified as pin piles and anchors (100 to 300 mm), normal-size piles and shafts (250 to 600 mm), large-diameter piles and shafts (600 to 3000 mm), caissons (600 mm and up to 3000 mm or larger), and cofferdams or other shoring construction method (very large).

Loading — Loads applied to foundations are compression, tension, moment, and lateral loads. Depending on time characteristics, loads are further classified as static, cyclic, and transient loads. The magnitude and type of loading also are major factors in determining the size and type of a foundation (Table 7.1).

Isolation — Piles can be isolated at a certain depth to avoid loading utility lines or other construction, or to avoid being loaded by them.

Inclination — Piles can be vertical or inclined. Inclined piles are often called battered or raked piles.

Multiple Piles — Foundation can be an individual pile, or a pile group. Within a pile group, piles can be of uniform or different sizes and types. The connection between the piles and the pile cap can be fixed, pinned, or restrained.

7.2.4 Advantages/Disadvantages of Different Types of Foundations

Different types of foundations have their unique features and are more applicable to certain conditions than others. The advantages and disadvantages for different types of foundations are listed as follows.

Driven Precast Concrete Pile Foundations

Driven concrete pile foundations are applicable under most ground conditions. Concrete piles are usually inexpensive compared with other types of deep foundations. The procedure of pile installation is straightforward; piles can be produced in mass production either on site or in a manufacture factory, and the cost for materials is usually much less than steel piles. Proxy coating can be applied to reduce negative skin friction along the pile. Pile driving can densify loose sand and reduce liquefaction potential within a range of up to three diameters surrounding the pile.

However, driven concrete piles are not suitable if boulders exist below the ground surface where piles may break easily and pile penetration may be terminated prematurely. Piles in dense sand, dense gravel, or bedrock usually have limited penetration; consequently, the uplift capacity of this type of piles is very small.

Pile driving produces noise pollution and causes disturbance to the adjacent structures. Driving of concrete piles also requires large overhead space. Piles may break during driving and impose a safety hazard. Piles that break underground cannot take their design loads, and will cause damage to the structures if the broken pile is not detected and replaced. Piles could often be driven out of their designed alignment and inclination and, as a result, additional piles may be needed. A special hardened steel shoe is often required to prevent pile tips from being smashed when encountering hard rock. End-bearing capacity of a pile is not reliable if the end of a pile is smashed.

Driven piles may not be a good option when subsurface conditions are unclear or vary considerably over the site. Splicing and cutting of piles are necessary when the estimated length is different from the manufactured length. Splicing is usually difficult and time-consuming for concrete piles. Cutting of a pile would change the pattern of reinforcement along the pile, especially where extra reinforcement is needed at the top of a pile for lateral capacity. A pilot program is usually needed to determine the length and capacity prior to mass production and installation of production piles.

The maximum pile length is usually up to 36 to 38 m because of restrictions during transportation on highways. Although longer piles can be produced on site, slender and long piles may buckle easily during handling and driving. Precast concrete piles with diameters greater than 45 cm are rarely used.

Driven Steel Piles

Driven steel piles, such as steel pipe and H-beam piles, are extensively used as bridge foundations, especially in seismic retrofit projects. Having the advantage and disadvantage of driven piles as discussed above, driven steel piles have their uniqueness.

Steel piles are usually more expensive than concrete piles. They are more ductile and flexible and can be spliced more conveniently. The required overhead is much smaller compared with driven concrete piles. Pipe piles with an open end can penetrate through layers of dense sand. If necessary, the soil inside the pipe can be taken out before further driving; small boulders may also be crushed and taken out. H-piles with a pointed tip can usually penetrate onto soft bedrock and establish enough end-bearing capacity.

Large-Diameter Driven, Vibrated, or Torqued Steel Pipe Piles

Large-diameter pipe piles are widely used as foundations for large bridges. The advantage of this type of foundation is manifold. Large-diameter pipe piles can be built over water from a barge, a trestle, or a temporary island. They can be used in almost all ground conditions and penetrate to a great depth to reach bedrock. Length of the pile can be adjusted by welding. Large-diameter pipe

piles can also be used as casings to support soil above bedrock from caving in; rock sockets or rock anchors can then be constructed below the tip of the pipe. Concrete or reinforced concrete can be placed inside the pipe after it is cleaned. Another advantage is that no workers are required to work below water or the ground surface. Construction is usually safer and faster than other types of foundations, such as caissons or cofferdam construction.

Large-diameter pipe piles can be installed by methods of driving, vibrating, or torque. Driven piles usually have higher capacity than piles installed through vibration or torque. However, driven piles are hard to control in terms of location and inclination of the piles. Moreover, once a pile is out of location or installed with unwanted inclination, no corrective measures can be applied. Piles installed with vibration or torque, on the other hand, can be controlled more easily. If a pile is out of position or inclination, the pile can even be lifted up and reinstalled.

Drilled Shaft Foundations

Drilled shaft foundations are the most versatile types of foundations. The length and size of the foundations can be tailored easily. Disturbance to the nearby structures is small compared with other types of deep foundations. Drilled shafts can be constructed very close to existing structures and can be constructed under low overhead conditions. Therefore, drilled shafts are often used in many seismic retrofit projects. However, drilled shafts may be difficult to install under certain ground conditions such as soft soil, loose sand, sand under water, and soils with boulders. Drilled shafts will generate a large volume of soil cuttings and fluid and can be a mess. Disposal of the cuttings is usually a concern for sites with contaminated soils.

Drilled shaft foundations are usually comparable with or more expensive than driven piles. For large bridge foundations, their cost is at the same level of caisson foundations and spread footing foundations combined with cofferdam construction. Drilled shaft foundations can be constructed very rapidly under normal conditions compared with caisson and cofferdam construction.

Anchors

Anchors are special foundation elements that are designed to take uplift loads. Anchors can be added if an existing foundation lacks uplift capacity, and competent layers of soil or rock are shallow and easy to reach. Anchors, however, cannot take lateral loads and may be sheared off if combined lateral capacity of a foundation is not enough.

Anchors are, in many cases, pretensioned in order to limit the deformation to activate the anchor. The anchor system is therefore very stiff. Structural failure resulting from anchor rupture often occurs very quickly and catastrophically. Pretension may also be lost over time because of creep in some types of rock and soil. Anchors should be tested carefully for their design capacity and creep performance.

Caissons

Caissons are large structures that are mainly used for construction of large bridge foundations. Caisson foundations can take large compressive and lateral loads. They are used primarily for over-water construction and sometimes used in soft or loose soil conditions, with a purpose to sink or excavate down to a depth where bedrock or firm soil can be reached. During construction, large boulders can be removed.

Caisson construction requires special techniques and experience. Caisson foundations are usually very costly, and comparable to the cost of cofferdam construction. Therefore, caissons are usually not the first option unless other types of foundation are not favored.

Cofferdam and Shoring

Cofferdams or other types of shoring systems are a method of foundation construction to retain water and soil. A dry bottom deep into water or ground can be created as a working platform. Foundations of essentially any of the types discussed above can be built from the platform on top of firm soil or rock at a great depth, which otherwise can only be reached by deep foundations.

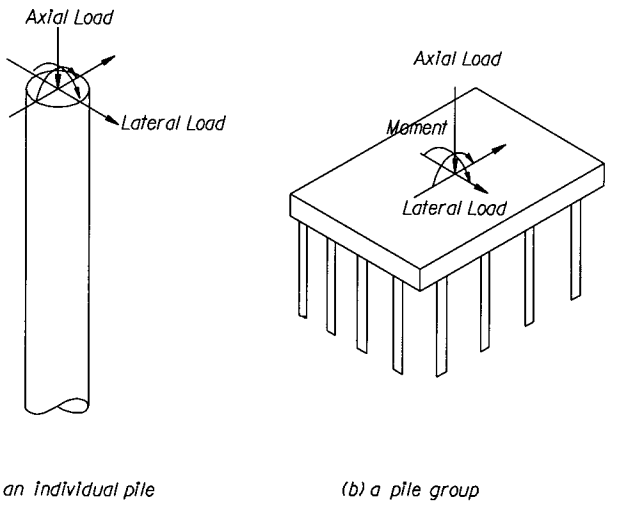

FIGURE 7.2 Acting loads on top of a pile or a pile group. (a) Individual pile; (b) pile group.

A spread footing type of foundation can be built from the platform. Pile foundations also can be constructed from the platform, and the pile length can be reduced substantially. Without cofferdam or shoring, a foundation may not be possible if constructed from the water or ground surface, or it may be too costly.

Cofferdam construction is often very expensive and should only be chosen if it is favorable compared with other foundation options in terms of cost and construction conditions.

7.2.5 Characteristics of Different Types of Foundations

In this section, the mechanisms of resistance of an individual foundation and a pile group are discussed. The function of different types of foundations is also addressed.

Complex loadings on top of a foundation from the bridge structures above can be simplified into forces and moments in the longitudinal, transverse, and vertical directions, respectively (Figure 7.2). Longitudinal and transverse loads are also called horizontal loads; longitudinal and transverse moments are called overturning moments, moment about the vertical axis is called torsional moment. The resistance provided by an individual foundation is categorized in the following (also see Figure 7.3).

End-bearing: Vertical compressive resistance at the base of a foundation; distributed end-bearing pressures can provide resistance to overturning moments;
Base shear: Horizontal resistance of friction and cohesion at the base of a foundation;
Side resistance: Shear resistance from friction and cohesion along the side of a foundation;
Earth pressure: Mainly horizontal resistance from lateral Earth pressures perpendicular to the side of the foundation;
Self-weight: Effective weight of the foundation.

Both base shear and lateral earth pressures provide lateral resistance of a foundation, and the contribution of lateral earth pressures decreases as the embedment of a pile increases. For long piles, lateral earth pressures are the main source of lateral resistance. For short piles, base shear and end-bearing pressures can also contribute part of the lateral resistance. Table 7.2 lists various types of resistance of an individual pile.

For a pile group, through the action of the pile cap, the coupled axial compressive and uplift resistance of individual piles provides the majority of the resistance to the overturning moment loading. Horizontal (or lateral) resistance can at the same time provide torsional moment resistance.

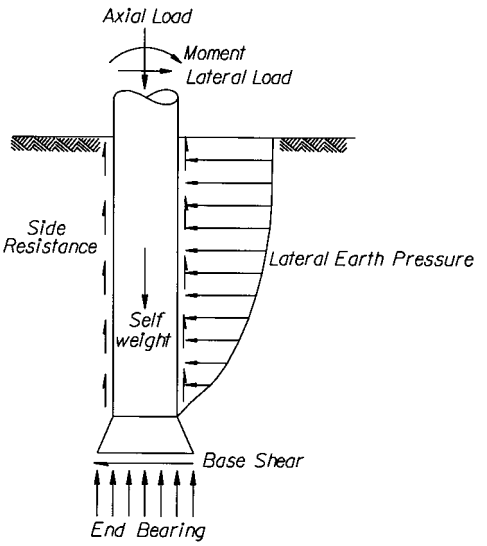

FIGURE 7.3 Resistances of an individual foundation.

TABLE 7.2 Resistance of an Individual Foundation

	Type of Resistance				
Type of Foundation	Vertical Compressive Load (Axial)	Vertical Uplift Load (Axial)	Horizontal Load (Lateral)	Overturning Moment (Lateral)	Torsional Moment (Torsional)
Spread footing (also see Chapter 31)	End bearing	—	Base shear, lateral earth pressure	End bearing, lateral earth pressure	Base shear, lateral earth pressure
Individual short pile foundation	End bearing; side friction	Side friction	Lateral earth pressure, base shear	Lateral earth pressure, end bearing	Side friction, lateral earth pressure, base shear
Individual end-bearing long pile foundation	End bearing	—	Lateral earth pressure	Lateral earth pressure	—
Individual frictional long pile foundation	Side friction	Side friction	Lateral earth pressure	Lateral earth pressure	Side friction
Individual long pile foundation	End bearing; side friction	Side friction	Lateral earth pressure	Lateral earth pressure	Side friction
Anchor	—	Side friction	—	—	—

TABLE 7.3 Additional Functions of Pile Group Foundations

	Type of Resistance	
Type of Foundation	Overturning moment (Lateral)	Torsional moment (Torsional)
Grouped spread footings	Vertical compressive resistance	Horizontal resistance
Grouped piles, foundations	Vertical compressive and uplift resistance	Horizontal resistance
Grouped anchors	Vertical uplift resistance	—

A pile group is more efficient in resisting overturning and torsional moment than an individual foundation. Table 7.3 summarizes functions of a pile group in addition to those of individual piles.

7.2.6 Selection of Foundations

The two predominant factors in determining the type of foundations are bridge types and ground conditions.

The bridge type, including dimensions, type of bridge, and construction materials, dictates the design magnitude of loads and the allowable displacements and other performance criteria for the foundations, and therefore determines the dimensions and type of its foundations. For example, a suspension bridge requires large lateral capacity for its end anchorage which can be a huge deadman, a high capacity soil or rock anchor system, a group of driven piles, or a group of large-diameter drilled shafts. Tower foundations of an over-water bridge require large compressive, uplift, lateral, and overturning moment capacities. The likely foundations are deep, large-size footings using cofferdam construction, caissons, groups of large-diameter drilled shafts, or groups of a large number of steel piles.

Surface and subsurface geologic and geotechnical conditions are another main factor in determining the type of bridge foundations. Subsurface conditions, especially the depths to the load-bearing soil layer or bedrock, are the most crucial factor. Seismicity over the region usually dictates the design level of seismic loads, which is often the critical and dominant loading condition. A bridge that crosses a deep valley or river certainly determines the minimum span required. Over-water bridges have limited options to chose in terms of the type of foundations.

The final choice of the type of foundation usually depends on cost after considering some other factors, such as construction conditions, space and overhead conditions, local practice, environmental conditions, schedule constraints, etc. In the process of selection, several types of foundations would be evaluated as candidates once the type of bridge and the preliminary ground conditions are known. Certain types of foundations are excluded in the early stage of study. For example, from the geotechnical point of view, shallow foundations are not an acceptable option if a thick layer of soft clay or liquefiable sand is near the ground surface. Deep foundations are used in cases where shallow foundations would be excessively large and costly. From a constructibility point of view, driven pile foundations are not suitable if boulders exist at depths above the intended firm bearing soil/rock layer.

For small bridges such as roadway overpasses, for example, foundations with driven concrete or steel piles, drilled shafts, or shallow spread footing foundations may be the suitable choices. For large over-water bridge foundations, single or grouped large-diameter pipe piles, large-diameter rock sockets, large-diameter drilled shafts, caissons, or foundations constructed with cofferdams are the most likely choice. Caissons or cofferdam construction with a large number of driven pile groups were widely used in the past. Large-diameter pipe piles or drilled shafts, in combination with rock sockets, have been preferred for bridge foundations recently.

Deformation compatibility of the foundations and bridge structure is an important consideration. Different types of foundation may behave differently; therefore, the same type of foundations should be used for one section of bridge structure. Diameters of the piles and inclined piles are two important factors to considere in terms of deformation compatibility and are discussed in the following.

Small-diameter piles are more “brittle” in the sense that the ultimate settlement and lateral deflection are relatively small compared with large-diameter piles. For example, 20 small piles can have the same ultimate load capacity as two large-diameter piles. However, the small piles reach the ultimate state at a lateral deflection of 50 mm, whereas the large piles do at 150 mm. The smaller piles would have failed before the larger piles are activated to a substantial degree. In other words, larger piles will be more flexible and ductile than smaller piles before reaching the ultimate state. Since ductility usually provides more seismic safety, larger-diameter piles are preferred from the point of view of seismic design.

Inclined or battered piles should not be used together with vertical piles unless the inclined piles alone have enough lateral capacity. Inclined piles provide partial lateral resistance from their axial capacity, and, since the stiffness in the axial direction of a pile is much larger than in the perpendicular directions, inclined piles tend to attract most of the lateral seismic loading. Inclined piles will fail or reach their ultimate axial capacity before the vertical piles are activated to take substantial lateral loads.

7.3 Design Considerations

7.3.1 Design Concept

The current practice of foundation design mainly employs two types of design concepts, i.e., the permissible stress approach and the limit state approach.

By using the permissible stress approach, both the demanded stresses from loading and the ultimate stress capacity of the foundation are evaluated. The foundation is considered to be safe as long as the demanded stresses are less than the ultimate stress capacity of the foundation. A factor of safety of 2 to 3 is usually applied to the ultimate capacity to obtain various allowable levels of loading in order to limit the displacements of a foundation. A separate displacement analysis is usually performed to determine the allowable displacements for a foundation, and for the bridge structures. Design based on the permissible concept is still the most popular practice in foundation design.

Starting to be adopted in the design of large critical bridges, the limit state approach requires that the foundation and its supported bridge should not fail to meet performance requirements when exceeding various limit states. Collapse of the bridge is the ultimate limit state, and design is aimed at applying various factors to loading and resistance to ensure that this state is highly improbable. A design needs to ensure the structural integrity of the critical foundations before reaching the ultimate limit state, such that the bridge can be repaired a relatively short time after a major loading incident without reconstruction of the time-consuming foundations.

7.3.2 Design Procedures

Under normal conditions, the design procedures of a bridge foundation should involve the following steps:

1. Evaluate the site and subsurface geologic and geotechnical conditions, perform borings or other field exploratory programs, and conduct field and laboratory tests to obtain design parameters for subsurface materials;
2. Review the foundation requirements including design loads and allowable displacements, regulatory provisions, space, or other constraints;
3. Evaluate the anticipated construction conditions and procedures;
4. Select appropriate foundation type(s);
5. Determine the allowable and ultimate axial and lateral foundation design capacity, load vs. deflection relationship, and load vs. settlement relationship;
6. Design various elements of the foundation structure; and
7. Specify requirements for construction inspection and/or load test procedures, and incorporate the requirements into construction specifications.

7.3.3 Design Capacities

Capacity in Long-Term and Short-Term Conditions

Depending on the loading types, foundations are designed for two different stress conditions. Capacity in total stress is used where loading is relatively quick and corresponds to an undrained

condition. Capacity in effective stress is adopted where loading is slow and corresponds to a drained condition. For many types of granular soil, such as clean gravel and sand, drained capacity is very close to undrained capacity under most loading conditions. Pile capacity under seismic loading is usually taken 30% higher than capacity under static loading.

Axial, Lateral, and Moment Capacity

Deep foundations can provide lateral resistance to overturning moment and lateral loads and axial resistance to axial loads. Part or most of the moment capacity of a pile group are provided by the axial capacity of individual piles through pile cap action. The moment capacity depends on the axial capacity of the individual piles, the geometry arrangement of the piles, the rigidity of the pile cap, and the rigidity of the connection between the piles and the pile cap. Design and analysis is often concentrated on the axial and lateral capacity of individual piles. Axial capacity of an individual pile will be addressed in detail in Section 7.4 and lateral capacity in Section 7.5. Pile groups will be addressed in Section 7.6.

Structural Capacity

Deep foundations may fail because of structural failure of the foundation elements. These elements should be designed to take moment, shear, column action or buckling, corrosion, fatigue, etc. under various design loading and environmental conditions.

Determination of Capacities

In the previous sections, the general procedure and concept for the design of deep foundations are discussed. Detailed design includes the determination of axial and lateral capacity of individual foundations, and capacity of pile groups. Many methods are available to estimate these capacities, and they can be categorized into three types of methodology as listed in the following:

- Theoretical analysis utilizing soil or rock strength;
- Empirical methods including empirical analysis utilizing standard field tests, code requirements, and local experience; and
- Load tests, including full-scale load tests, and dynamic driving and restriking resistance analysis.

The choice of methods depends on the availability of data, economy, and other constraints. Usually, several methods are used; the capacity of the foundation is then obtained through a comprehensive evaluation and judgment.

In applying the above methods, the designers need to keep in mind that the capacity of a foundation is the sum of capacities of all elements. Deformation should be compatible in the foundation elements, in the surrounding soil, and in the soil–foundation interface. Settlement or other movements of a foundation should be restricted within an acceptable range and usually is a controlling factor for large foundations.

7.3.4 Summary of Design Methods

Table 7.4 presents a partial list of design methods available in the literature.

7.3.5 Other Design Issues

Proper foundation design should consider many factors regarding the environmental conditions, type of loading conditions, soil and rock conditions, construction, and engineering analyses, including:

- Various loading and loading combinations, including the impact loads of ships or vehicles
- Earthquake shaking
- Liquefaction

TABLE 7.4 Summary of Design Methods for Deep Foundations

Type	Design For	Soil Condition	Method and Author
Driven pile	End bearing	Clay	N_c method [67]
			N_c method [23]
			CPT methods [37,59,63]
			CPT [8,10]
		Sand	N_q method with critical depth concept [38]
			N_q method [3]
			N_q method [23]
			N_q by others [26,71,76]
			Limiting N_q values [1,13]
			Value of ϕ [27,30,39]
			SPT [37,38]
			CPT methods [37,59,63]
			CPT [8,10]
		Rock	[10]
	Side resistance	Clay	α-method [72,73]
			α-method [1]
			β-method [23]
			λ-method [28,80]
			CPT methods [37,59,63]
			CPT [8,10]
			SPT [14]
		Sand	α-method [72,73]
			β-method [7]
			β-method [23]
			CPT method [37,59,63]
			CPT [8,10]
			SPT [37,38]
	Side and end	All	Load test: ASTM D 1143, static axial compressive test
			Load test: ASTM D 3689, static axial tensile test
			Sanders' pile driving formula (1850) [50]
			Danish pile driving formula [68]
			Engineering News formula (Wellingotn, 1988)
			Dynamic formula — WEAP Analysis
			Strike and restrike dynamic analysis
			Interlayer influence [38]
			No critical depth [20,31]
	Load-settlement	Sand	[77]
			[41,81]
		All	Theory of elasticity, Mindlin's solutions [50]
			Finite-element method [15]
			Load test: ASTM D 1143, static axial compressive test
			Load test: ASTM D 3689, static axial tensile test
Drilled shaft	End bearing	Clay	N_c method [66]
			Large base [45,57]
			CPT [8,10]
		Sand	[74]
			[38]
			[55]
			[52]
			[37,38]
			[8,10]
		Rock	[10]
		Rock	Pressure meter [10]

TABLE 7.4 (continued) Summary of Design Methods for Deep Foundations

Type	Design For	Soil Condition	Method and Author
	Side resistance	Clay	α-method [52]
			α-method [67]
			α-method [83]
			CPT [8,10]
		Sand	[74]
			[38]
			[55]
			β-method [44,52]
			SPT [52]
			CPT [8,10]
		Rock	Coulombic [34]
			Coulombic [75]
			SPT [12]
			[24]
			[58]
			[11,32]
			[25]
	Side and end	Rock	[46]
			[84]
			[60]
			[48]
			[61,62]
			FHWA [57]
		All	Load test [47]
	Load-settlement	Sand	[57]
		Clay	[57]
			[85]
		All	Load test [47]
All	Lateral resistance	Clay	Broms' method [5]
		Sand	Broms' method [6]
		All	*p–y* method [56]
		Clay	*p–y* response [35]
		Clay (w/water)	*p–y* response [53]
		Clay (w/o water)	*p–y* response [82]
		Sand	*p–y* response [53]
		All	*p–y* response [1]
			p–y response for inclined piles [2,29]
			p–y response in layered soil
			p–y response [42]
		Rock	*p–y* response [86]
	Load-settlement	All	Theory of elasticity method [50]
			Finite-difference method [64]
			General finite-element method (FEM)
			FEM dynamic
	End bearing		Pressure meter method [36,78]
	Lateral resistance		Pressure meter method [36]
			Load test: ASTM D 3966
Group	Theory		Elasticity approach [50]
			Elasticity approach [21]
			Two-dimensional group [51]
			Three-dimensional group [52]
	Lateral g-factor		[10]
			[16]

- Rupture of active fault and shear zone
- Landslide or ground instability
- Difficult ground conditions such as underlying weak and compressible soils
- Debris flow
- Scour and erosion
- Chemical corrosion of foundation materials
- Weathering and strength reduction of foundation materials
- Freezing
- Water conditions including flooding, water table change, dewatering
- Environmental change due to construction of the bridge
- Site contamination condition of hazardous materials
- Effects of human or animal activities
- Influence upon and by nearby structures
- Governmental and community regulatory requirements
- Local practice

7.3.6 Uncertainty of Foundation Design

Foundation design is as much an art as a science. Although most foundation structures are man-made, the surrounding geomaterials are created, deposited, and altered in nature over the geologic times. The composition and engineering properties of engineering materials such as steel and concrete are well controlled within a variation of uncertainty of between 5 to 30%. However, the uncertainty of engineering properties for natural geomaterials can be up to several times, even within relatively uniform layers and formations. The introduction of faults and other discontinuities make generalization of material properties very hard, if not impossible.

Detailed geologic and geotechnical information is usually difficult and expensive to obtain. Foundation engineers constantly face the challenge of making engineering judgments based on limited and insufficient data of ground conditions and engineering properties of geomaterials.

It was reported that under almost identical conditions, variation of pile capacities of up to 50% could be expected within a pile cap footprint under normal circumstances. For example, piles within a nine-pile group had different restruck capacities of 110, 89, 87, 96, 86, 102, 103, 74, and 117 kips (1 kip = 4.45 kN), respectively [19].

Conservatism in foundation design, however, is not necessarily always the solution. Under seismic loading, heavier and stiffer foundations may tend to attract more seismic energy and produce larger loads; therefore, massive foundations may not guarantee a safe bridge performance.

It could be advantageous that piles, steel pipes, caisson segments, or reinforcement steel bars are tailored to exact lengths. However, variation of depth and length of foundations should always be expected. Indicator programs, such as indicator piles and pilot exploratory borings, are usually a good investment.

7.4 Axial Capacity and Settlement — Individual Foundation

7.4.1 General

The axial resistance of a deep foundation includes the tip resistance (Q_{end}), side or shaft resistance (Q_{side}), and the effective weight of the foundation (W_{pile}). Tip resistance, also called end bearing, is the compressive resistance of soil near or under the tip. Side resistance consists of friction, cohesion, and keyed bearing along the shaft of the foundation. Weight of the foundation is usually ignored

under compression because it is nearly the same as the weight of the soil displaced, but is usually accounted for under uplift loading condition.

At any loading instance, the resistance of an individual deep foundation (or pile) can be expressed as follows:

$$Q = Q_{\text{end}} + \Sigma Q_{\text{side}} \pm W_{\text{pile}} \tag{7.1}$$

The contribution of each component in the above equation depends on the stress–strain behavior and stiffness of the pile and the surrounding soil and rock. The maximum capacity of a pile can be expressed as

$$Q^c{}_{\max} \le Q^c{}_{\text{end\_max}} + \Sigma Q^c{}_{\text{side\_max}} - W_{\text{pile}} \quad \text{(in compression)} \tag{7.2}$$

$$Q^t{}_{\max} \le Q^t{}_{\text{end\_max}} + \Sigma Q^t{}_{\text{side\_max}} + W_{\text{pile}} \quad \text{(in uplift)} \tag{7.3}$$

and is less than the sum of all the maximum values of resistance. The ultimate capacity of a pile undergoing a large settlement or upward movement can be expressed as

$$Q^c{}_{\text{ult}} = Q^c{}_{\text{end\_ult}} + \Sigma Q^c{}_{\text{side\_ult}} - W_{\text{pile}} \le Q^c_{\max} \tag{7.4}$$

$$Q^t{}_{\text{ult}} = Q^t{}_{\text{end\_ult}} + \Sigma Q^t{}_{\text{side\_ult}} + W_{\text{pile}} \le Q^t_{\max} \tag{7.5}$$

Side- and end-bearing resistances are related to displacement of a pile. Maximum end bearing capacity can be mobilized only after a substantial downward movement of the pile, whereas side resistance reaches its maximum capacity at a relatively smaller downward movement. Therefore, the components of the maximum capacities ($Q_{\max}$) indicated in Eqs. (7.2) and (7.3) may not be realized at the same time at the tip and along the shaft. For a drilled shaft, the end bearing is usually ignored if the bottom of the borehole is not cleared and inspected during construction. Voids or compressible materials may exist at the bottom after concrete is poured; as a result, end bearing will be activated only after a substantial displacement.

Axial displacements along a pile are larger near the top than toward the tip. Side resistance depends on the amount of displacement and is usually not uniform along the pile. If a pile is very long, maximum side resistance may not occur at the same time along the entire length of the pile. Certain types of geomaterials, such as most rocks and some stiff clay and dense sand, exhibit strain softening behavior for their side resistance, where the side resistance first increases to reach its maximum, then drops to a much smaller residual value with further displacement. Consequently, only a fixed length of the pile segment may maintain high resistance values and this segment migrates downward to behave in a pattern of a progressive failure. Therefore, the capacity of a pile or drilled shaft may not increase infinitely with its length.

For design using the permissible stress approach, allowable capacity of a pile is the design capacity under service or routine loading. The allowable capacity (Q_{all}) is obtained by dividing ultimate capacity (Q_{ult}) by a factor of safety (FS) to limit the level of settlement of the pile and to account for uncertainties involving material, installation, loads calculation, and other aspects. In many cases, the ultimate capacity (Q_{ult}) is assumed to be the maximum capacity ($Q_{\max}$). The factor of safety is usually between 2 to 3 for deep foundations depending on the reliability of the ultimate capacity estimated. With a field full-scale loading test program, the factor of safety is usually 2.

TABLE 7.5 Typical Values of Bearing Capacity Factor N_q

φ[a] (degrees)	26	28	30	31	32	33	34	35	36	37	38	39	40
N_q (driven pile displacement)	10	15	21	24	29	35	42	50	62	77	86	120	145
N_q[b] (drilled piers)	5	8	10	12	14	17	21	25	30	38	43	60	72

[a] Limit φ to 28° if jetting is used.

[b] 1. In case a bailer of grab bucket is used below the groundwater table, calculate end bearing based on φ not exceeding 28°.

2. For piers greater than 24-in. diameter, settlement rather than bearing capacity usually controls the design. For estimating settlement, take 50% of the settlement for an equivalent footing resting on the surface of comparable granular soils (Chapter 5, DM-7.01).

Source: NAVFAC [42].

7.4.2 End Bearing

End bearing is part of the axial compressive resistance provided at the bottom of a pile by the underlying soil or rock. The resistance depends on the type and strength of the soil or rock and on the stress conditions near the tip. Piles deriving their capacity mostly from end bearing are called end bearing piles. End bearing in rock and certain types of soil such as dense sand and gravel is usually large enough to support the designed loads. However, these types of soil or rock cannot be easily penetrated through driving. No or limited uplift resistance is provided from the pile tips; therefore, end-bearing piles have low resistance against uplift loading.

The end bearing of a pile can be expressed as:

$$Q_{\text{end\_max}} = \begin{cases} cN_cA_{\text{pile}} & \text{for clay} \\ \sigma'_v N_q A_{\text{pile}} & \text{for sand} \\ \dfrac{U_c}{2} N_k A_{\text{pile}} & \text{for rock} \end{cases} \tag{7.6}$$

where

$Q_{\text{end\_max}}$ = the maximum end bearing of a pile
A_{pile} = the area of the pile tip or base
N_c, N_q, N_k = the bearing capacity factors for clay, sand, and rock
c = the cohesion of clay
σ'_v = the effective overburden pressure
U_c = the unconfined compressive strength of rock and $\dfrac{U_c}{2} = S_u$, the equivalent shear strength of rock

Clay

The bearing capacity factor N_c for clay can be expressed as

$$N_c = 6.0\left(1 + 0.2\frac{L}{D}\right) \le 9 \tag{7.7}$$

where L is the embedment depth of the pile tip and D is the diameter of the pile.

Sand

The bearing capacity factor N_q generally depends on the friction angle ϕ of the sand and can be estimated by using Table 7.5 or the Meyerhof equation:

$$N_q = e^{\pi \tan \varphi} \tan^2\left(45 + \frac{\varphi}{2}\right) \tag{7.8}$$

The capacity of end bearing in sand reaches a maximum cutoff after a certain critical embedment depth. This critical depth is related to ϕ and D and for design purposes is listed as follows:

$$L_c = 7D, \qquad \phi = 30^o \text{ for loose sand}$$

$$L_c = 10D, \qquad \phi = 34^o \text{ for medium dense sand}$$

$$L_c = 14D, \qquad \phi = 38^o \text{ for dense sand}$$

$$L_c = 22D, \qquad \phi = 45^o \text{ for very dense sand}$$

The validity of the concept of critical depth has been challenged by some people; however, the practice to limit the maximum ultimate end bearing capacity in sand will result in conservative design and is often recommended.

Rock

The bearing capacity factor N_k depends on the quality of the rock mass, intact rock properties, fracture or joint properties, embedment, and other factors. Because of the complex nature of the rock mass and the usually high value for design bearing capacity, care should be taken to estimate N_k. For hard fresh massive rock without open or filled fractures, N_k can be taken as high as 6. N_k decreases with increasing presence and dominance of fractures or joints and can be as low as 1. Rock should be treated as soil when rock is highly fractured and weathered or in-fill weak materials control the behavior of the rock mass. Bearing capacity on rock also depends on the stability of the rock mass. Rock slope stability analysis should be performed where the foundation is based on a slope. A higher factor of safety, 3 to as high as 10 to 20, is usually applied in estimating allowable bearing capacity for rocks using the N_k approach.

The soil or rock parameters used in design should be taken from averaged properties of soil or rock below the pile tip within the influence zone. The influence zone is usually taken as deep as three to five diameters of the pile. Separate analyses should be conducted where weak layers exist below the tip and excessive settlement or punch failure might occur.

Empirical Methods

Empirical methods are based on information of the type of soil/rock and field tests or index properties. The standard penetration test (SPT) for sand and cone penetration test (CPT) for soil are often used.

Meyerhof [38] recommended a simple formula for piles driven into sand. The ultimate tip bearing pressure is expressed as

$$q_{\text{end\_max}} \le 4N_{\text{SPT}} \quad \text{in tsf (1 tsf = 8.9 kN)} \tag{7.9}$$

where N_{SPT} is the blow count of SPT just below the tip of the driven pile and $q_{\text{end\_max}} = Q_{\text{end\_max}} / A_{\text{pile}}$. Although the formula is developed for piles in sand, it also is used for piles in weathered rock for preliminary estimate of pile capacity.

Schmertmann [63] recommended a method to estimate pile capacity by using the CPT test:

$$q_{\text{end\_max}} = q_b = \frac{q_{c1} + q_{c2}}{2} \tag{7.10}$$

where

q_{c1} = averaged cone tip resistance over a depth of 0.7 to 4 diameters of the pile below tip of the pile
q_{c2} = the averaged cone tip resistance over a depth of 8 diameters of the pile above the tip of the pile

Chapter 6 presents recommended allowable bearing pressures for various soil and rock types for spread footing foundations and can be used as a conservative estimate of end-bearing capacity for end-bearing piles.

TABLE 7.6 Typical Values of α and f_s

Range of Shear Strength, S_u ksf	Formula to Estimate α	Range of α	Range of f_s ksf[a]	Description
0 to 0.600	$\alpha = 1.0$	1	0–0.6	Soft clay
0.600 to 3	$\alpha = 0.375\left(1+\frac{1}{S_u}\right)$,	1–0.5	0.6–1.5	Medium stiff clay to very stiff clay
3 to 11	$\alpha = 0.375\left(1+\frac{1}{S_u}\right)$,	0.5–0.41	1.5–4.5	Hard clay to very soft rock
11 to 576 (76 psi to 4000 psi)	$\alpha = \frac{5}{\sqrt{2S_u}}$, S_u in psi,	0.41–0.056	4.5–32 (31–220 psi)	Soft rock to hard rock

Note: 1 ksf = 1000 psf; 1 psi = 144 psf; 1 psf = 0.048 kPa; 1 psi = 6.9 kPa

[a] For concrete driven piles and for drilled piers without buildup of mud cakes along the shaft. (Verify if fs ≥ 3 ksf.)

7.4.3 Side Resistance

Side resistance usually consists of friction and cohesion between the pile and the surrounding soil or rock along the shaft of a pile. Piles that derive their resistance mainly from side resistance are termed *frictional piles*. Most piles in clayey soil are frictional piles, which can take substantial uplift loads.

The maximum side resistance of a pile $Q_{\text{side\_max}}$ can be expressed as

$$Q_{\text{side\_max}} = \sum f_s A_{\text{side}} \tag{7.11}$$

$$f_s = K_s \sigma'_v \tan\delta + c_a \tag{7.12}$$

$$c_a = \alpha S_u \tag{7.13}$$

where

$\sum$ = the sum for all layers of soil and rock along the pile
A_{side} = the shaft side area
f_s = the maximum frictional resistance on the side of the shaft
K_s = the lateral earth pressure factor along the shaft
σ'_v = the effective vertical stress along the side of the shaft
δ = the friction angle between the pile and the surrounding soil; for clayey soil under quick loading, δ is very small and usually omitted
c_a = the adhesion between pile and surrounding soil and rock
α = a strength factor, and
S_u = the cohesion of the soil or rock

TABLE 7.7 Typical Values Cohesion and Adhesion f_s

Pile Type	Consistency of Soil	Cohesion, S_u psf	Adhesion, f_s psf
Timber and concrete	Very soft	0–250	0–250
	Soft	250–500	250–480
	Medium stiff	500–1000	480–750
	Stiff	1000–2000	750–950
	Very stiff	2000–4000	950–1300
Steel	Very soft	0–250	0–250
	Soft	250–500	250–460
	Medium stiff	500–1000	480–700
	Stiff	1000–2000	700–720
	Very stiff	2000–4000	720–750

1 psf = 0.048 kPa.
Source: NAVFAC [42].

TABLE 7.8 Typical Values of Bond Stress of Rock Anchors for Selected Rock

Rock Type (Sound, Nondecayed)	Ultimate Bond Stresses between Rock and Anchor Plus (δ_{skin}), psi
Granite and basalt	250–450
Limestone (competent)	300–400
Dolomitic limestone	200–300
Soft limestone	150–220
Slates and hard shales	120–200
Soft shales	30–120
Sandstone	120–150
Chalk (variable properties)	30–150
Marl (stiff, friable, fissured)	25–36

Note: It is not generally recommended that design bond stresses exceed 200 psi even in the most competent rocks. 1 psi = 6.9 kPa.
Source: NAVFAC [42].

TABLE 7.9 Typical Values of earth Pressure Coefficient K_s

	Earth Pressure Coefficients K_s		
Pile Type	K_s [a] (compression)	K_s [a] (tension)	K_s [b]
Driven single H-pile	0.5–1.0	0.3–0.5	—
Driven single displacement pile	1.0–1.5	0.6–1.0	0.7–3.0
Driven single displacement tapered pile	1.5–2.0	1.0–1.3	—
Driven jetted pile	0.4–0.9	0.3–0.6	—
Drilled pile (less than 24-in. diameter)	0.7	0.4	—
Insert pile	—	—	0.7 (compression) 0.5 (tension)
Driven with predrilled hole	—	—	0.4–0.7
Drilled pier	—	—	0.1–0.4

[a] From NAVFAC [42].
[b] From Le Tirant (1979), K_s increases with OCR or D_R.

TABLE 7.10 Typical Value of Pile-Soil Friction Angles δ

Pile Type	δ, °	Alternate for δ
Concrete[a]	—	δ = ¾φ
Concrete (rough, cast-in-place)[b]	33	δ = 0.85φ
Concrete (smooth)[b]	30	δ = 0.70φ
Steel[a]	20	—
Steel (corrugated)	33	δ = φ
Steel (smooth)[c]	—	δ = φ – 5°
Timber[a]	—	δ = ¾φ

[a] NAVFAC [42].
[b] Woodward et al. [85]
[c] API [1] and de Ruiter and Beringen [13]

Typical values of α, f_s, K_s, δ are shown in Tables 7.6 through 7.10. For design purposes, side resistance f_s in sand is limited to a cutoff value at the critical depth, which is equal to about $10B$ for loose sand and $20B$ for dense sand.

Meyerhof [38] recommended a simple formula for driven piles in sand. The ultimate side adhesion is expressed as

$$f_s \le \frac{N_{\text{SPT}}}{50} \quad \text{in tsf (1 tsf = 8.9 kN)} \tag{7.14}$$

where N_{SPT} is the averaged blow count of SPT along the pile.

Meyerhof [38] also recommended a formula to calculate the ultimate side adhesion based on CPT results as shown in the following.

For full displacement piles:

$$f_s = \frac{q_c}{200} \le 1.0 \ \text{in tsf} \tag{7.15}$$

or

$$f_s = 2f_c \le 1.0 \tag{7.16}$$

For nondisplacement piles:

$$f_s = \frac{q_c}{400} \le 0.5 \ \text{in tsf} \tag{7.17}$$

or

$$f_s = f_c \le 0.5 \tag{7.18}$$

in which

q_c, f_c = the cone tip and side resistance measured from CPT; averaged values should be used along the pile

Downdrag

For piles in soft soil, another deformation-related issue should be noted. When the soil surrounding the pile settles relative to a pile, the side friction, also called the negative skin friction, should be considered when there exists underlying compressible clayey soil layers and liquefiable loose sand layers. Downdrag can also happen when ground settles because of poor construction of caissons in sand. On the other hand, updrag should also be considered in cases where heave occurs around the piles for uplift loading condition, especially during installation of piles and in expansive soils.

7.4.4 Settlement of Individual Pile, *t–z, Q–z* Curves

Besides bearing capacity, the allowable settlement is another controlling factor in determining the allowable capacity of a pile foundation, especially if layers of highly compressible soil are close to or below the tip of a pile.

Settlement of a small pile (diameter less than 350 mm) is usually kept within an acceptable range (usually less than 10 mm) when a factor of safety of 2 to 3 is applied to the ultimate capacity to obtain the allowable capacity. However, in the design of large-diameter piles or caissons, a separate settlement analysis should always be performed.

The total settlement at the top of a pile consists of immediate settlement and long-term settlement. The immediate settlement occurs during or shortly after the loads are applied, which includes elastic compression of the pile and deformation of the soil surrounding the pile under undrained loading conditions. The long-term settlement takes place during the period after the loads are applied, which includes creep deformation and consolidation deformation of the soil under drained loading conditions.

Consolidation settlement is usually significant in soft to medium stiff clayey soils. Creep settlement occurs most significantly in overconsolidated (OC) clays under large sustained loads, and can be estimated by using the method developed by Booker and Poulos (1976). In principle, however, long-term settlement can be included in the calculation of ultimate settlement if the design parameters of soil used in the calculation reflect the long-term behavior.

Presented in the following sections are three methods that are often used:

- Method of solving ultimate settlement by using special solutions from the theory of elasticity [50,85]. Settlement is estimated based on equivalent elasticity in which all deformation of soil is assumed to be linear elastic.
- Empirical method [79].
- Method using localized springs, or the so called *t–z* and *Q–z* method [52a].

Method from Elasticity Solutions

The total elastic settlement S can be separated into three components:

$$S = S_b + S_s + S_{sh} \tag{7.19}$$

where S_b is part of the settlement at the tip or bottom of a pile caused by compression of soil layers below the pile under a point load at the pile tip, and is expressed as

$$S_b = \frac{p_b D_b I_{bb}}{E_s} \tag{7.20}$$

S_s is part of the settlement at the tip of a pile caused by compression of soil layers below the pile under the loading of the distributed side friction along the shaft of the pile, and can be expressed as

$$S_s = \sum_i \frac{(f_{si} l_i \Delta z_i) I_{bs}}{E_s} \tag{7.21}$$

and S_{sh} is the shortening of the pile itself, and can be expressed as

$$S_{sh} = \sum_i \frac{(f_{si} l_i \Delta z_i) + p_b A_b (\Delta z_i)}{E_c (A_i)} \tag{7.22}$$

where

p_b = averaged loading pressure at pile tip
A_b = cross section area of a pile at pile tip; $A_b p_b$ is the total load at the tip
D_b = diameter of pile at the pile tip
i = subscript for ith segment of the pile
l = perimeter of a segment of the pile
Δz = axial length of a segment of the pile; $L = \sum_i \Delta z_i$ is the total length of the pile.
f_s = unit friction along side of shaft; $f_{si} l_i \Delta z_i$ is the side frictional force for segment i of the pile
E_s = Young's modulus of uniform and isotropic soil
E_c = Young's modulus of the pile
I_{bb} = base settlement influence factor, from load at the pile tip (Figure 7.4)
I_{bs} = base settlement influence factor, from load along the pile shaft (Figure 7.4)

Because of the assumptions of linear elasticity, uniformity, and isotropy for soil, this method is usually used for preliminary estimate purposes.

Method by Vesic [79]

The settlement S at the top of a pile can be broken down into three components, i.e.,

$$S = S_b + S_s + S_{sh} \tag{7.23}$$

Settlement due to shortening of a pile is

$$S_{sh} = (Q_p + \alpha_s Q_s) \frac{L}{AE_c} \tag{7.24}$$

where

Q_p = point load transmitted to the pile tip in the working stress range
Q_s = shaft friction load transmitted by the pile in the working stress range (in force units)
α_s = 0.5 for parabolic or uniform distribution of shaft friction, 0.67 for triangular distribution of shaft friction starting from zero friction at pile head to a maximum value at pile tip, 0.33 for triangular distribution of shaft friction starting from a maximum at pile head to zero at the pile tip
L = pile length
A = pile cross-sectional area
E_c = modulus of elasticity of the pile

Settlement of the pile tip caused by load transmitted at the pile tip is

$$S_b = \frac{C_p Q_p}{D q_o} \tag{7.25}$$

where

C_p = empirical coefficient depending on soil type and method of construction, see Table 7.11.
D = pile diameter
q_o = ultimate end bearing capacity

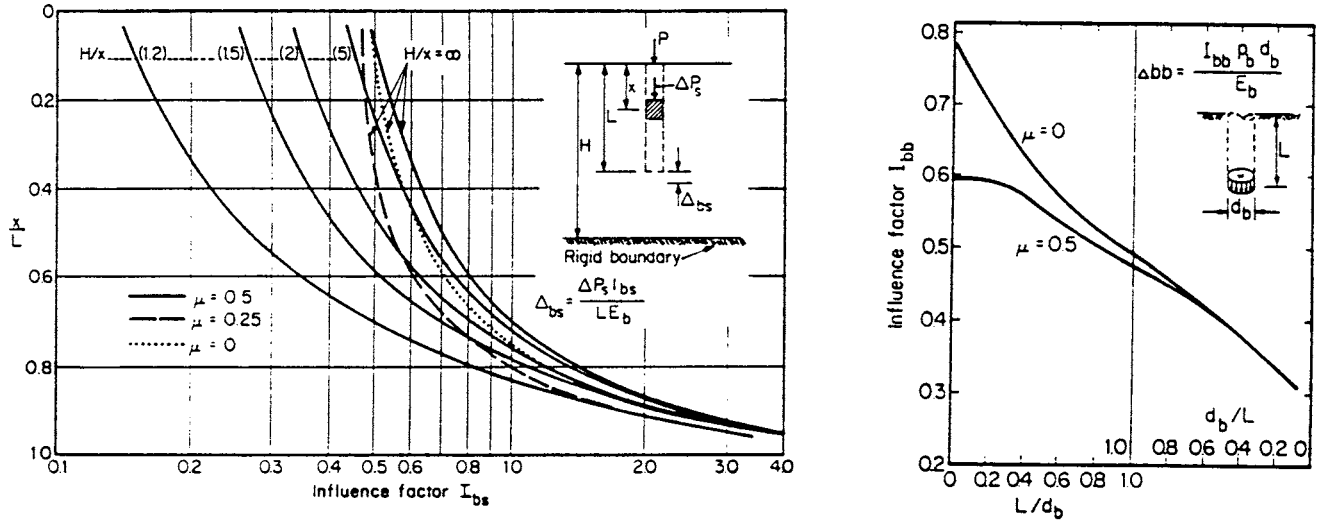

FIGURE 7.4 Influence factors I_{bb} and I_{bs} . [From Woodward, Gardner and Greer (1972).[85]

and settlement of the pile tip caused by load transmitted along the pile shaft is

$$S_s = \frac{C_s Q_s}{h q_o} \tag{7.26}$$

where
$C_s = (0.93 + 0.16\, D/B) C_p$
h = embedded length

TABLE 7.11 Typical Values of C_p for Estimating Settlement of a Single Pile

Soil Type	Driven Piles	Bored Piles
Sand (dense to loose)	0.02–0.04	0.09–0.18
Clay (stiff to soft)	0.02–0.03	0.03–0.06
Silt (dense to loose)	0.03–0.05	0.09–0.12

Note: Bearing stratum under pile tip assumed to extend at least 10 pile diameters below tip and soil below tip is of comparable or higher stiffness.

Method Using Localized Springs: The *t–z* and *Q–z* method

In this method, the reaction of soil surrounding the pile is modeled as localized springs: a series of springs along the shaft (the *t–z* curves) and the spring attached to the tip or bottom of a pile (the *Q–z* curve). *t* is the load transfer or unit friction force along the shaft, *Q* is the tip resistance of the pile, and *z* is the settlement of soil at the location of a spring. The pile itself is also represented as a series of springs for each segment. A mechanical model is shown on Figure 7.5. The procedure to obtain the settlement of a pile is as follows:

- Assume a pile tip movement *zb*_1; obtain a corresponding tip resistance *Q*_1 from the *Q–z* curve.
- Divide the pile into number of segments, and start calculation from the bottom segment. Iterations:
  1. Assume an averaged movement of the segment *zs*_1; obtain the averaged side friction along the bottom segment *ts*_1 by using the *t–z* curve at that location.
  2. Calculate the movement at middle of the segment from elastic shortening of the pile under axial loading *zs*_2. The axial load is the tip resistance *Q*_1 plus the added side friction *ts*_1.
  3. Iteration should continue until the difference between *zs*_1 and *zs*_2 is within an acceptable tolerance.

  Iteration continues for all the segments from bottom to top of the pile.
- A settlement at top of pile *zt*_1 corresponding to a top axial load *Qt*_1 is established.
- Select another pile tip movement *zb*_2 and calculate *zt*_2 and *Qt*_2 until a relationship curve of load vs. pile top settlement is found.

The *t–z* and *Q–z* curves are established from test data by many authors. Figure 7.6 shows the *t–z* and *Q–z* curves for cohesive soil and cohesionless soil by Reese and O'Neil [57].

Although the method of *t–z* and *Q–z* curves employs localized springs, the calculated settlements are usually within a reasonable range since the curves are backfitted directly from the test results. Factors of nonlinear behavior of soil, complicated stress conditions around the pile, and partial corrections to the Winkler's assumption are embedded in this methodology. Besides, settlement of a pile can be estimated for complicated conditions such as varying pile geometry, different pile materials, and different soil layers.

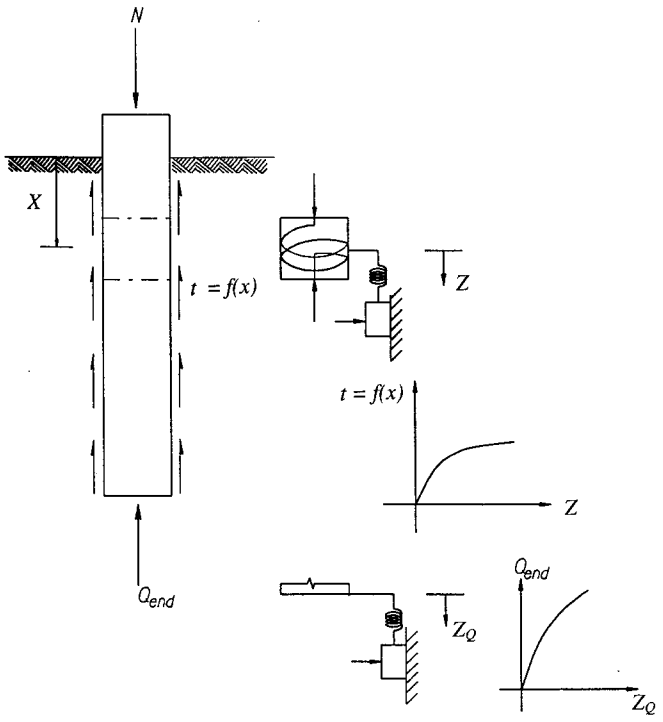

FIGURE 7.5 Analytical model for pile under axial loading with *t–z* and *Q–z* curves.

7.5 Lateral Capacity and Deflection — Individual Foundation

7.5.1 General

Lateral capacity of a foundation is the capacity to resist lateral deflection caused by horizontal forces and overturning moments acted on the top of the foundation. For an individual foundation, lateral resistance comes from three sources: lateral earth pressures, base shear, and nonuniformly distributed end-bearing pressures. Lateral earth pressure is the primary lateral resistance for long piles. Base shear and distributed end-bearing pressures are discussed in Chapter 6.

7.5.2 Broms' Method

Broms [5] developed a method to estimate the ultimate lateral capacity of a pile. The pile is assumed to be short and rigid. Only rigid translation and rotation movements are considered and only ultimate lateral capacity of a pile is calculated. The method assumes distributions of ultimate lateral pressures for cohesive and cohesionless soils; the lateral capacity of piles with different top fixity conditions are calculated based on the assumed lateral pressure as illustrated on Figures 7.7 and 7.8. Restricted by the assumptions, the Broms' method is usually used only for preliminary estimates of the ultimate lateral capacity of piles.

Ultimate Lateral Pressure

The ultimate lateral pressure $q_{h,u}$ along a pile is calculated as follows:

$$q_{h,u} = \begin{cases} 9c_u & \text{for cohesive soil} \\ 3K_p p_0' & \text{for cohesionless soil} \end{cases} \tag{7.27}$$

where

c_u = shear strength of the soil

K_p = coefficient of passive earth pressure, $K_p = \tan^2(45^o + \varphi/2)$ and φ is the friction angle of cohesionless soils (or sand and gravel)

p_0' = effective overburden pressure, $p_0' = \gamma_z'$ at a depth of z from the ground surface, where γ' is the effective unit weight of the soil

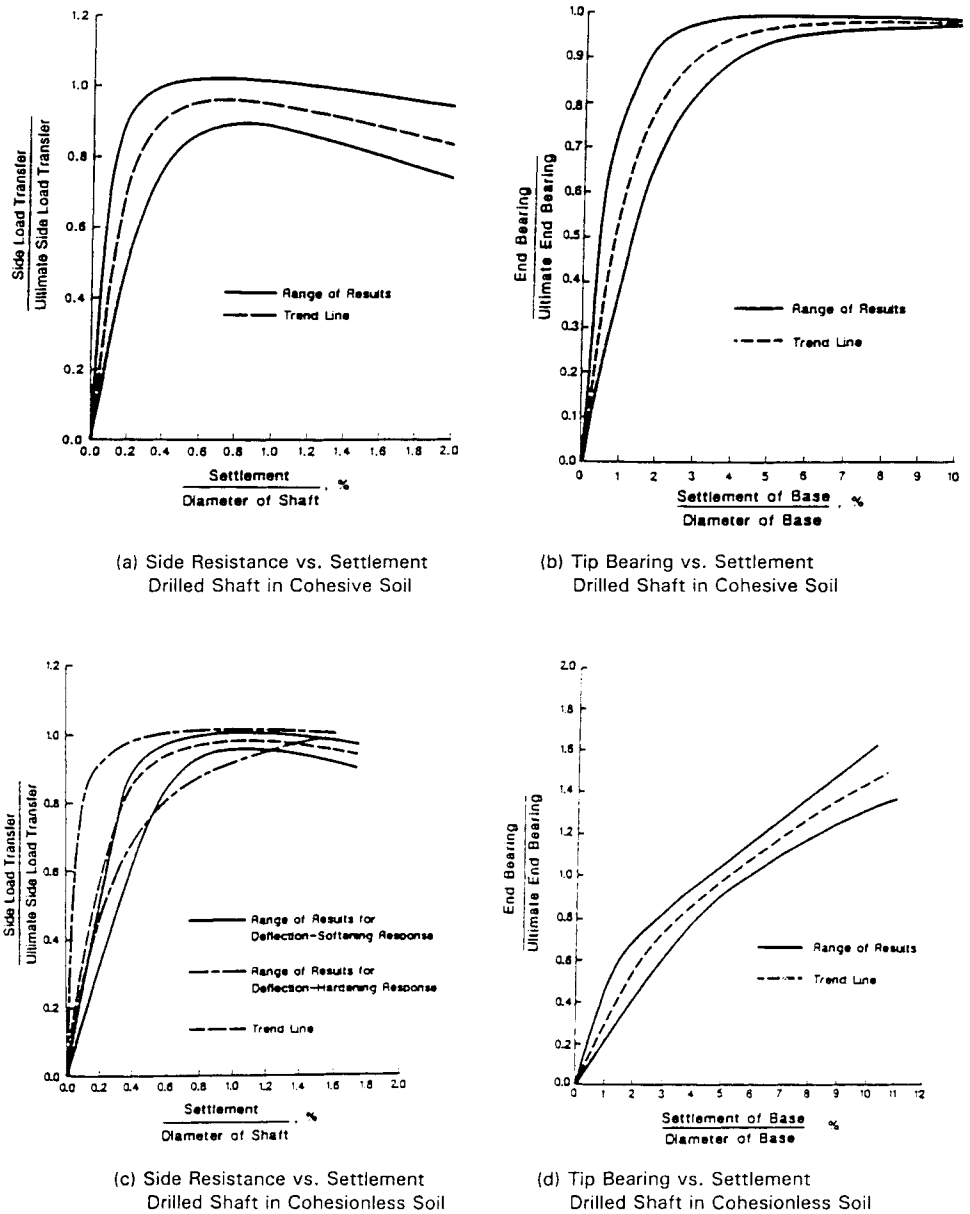

(a) Side Resistance vs. Settlement Drilled Shaft in Cohesive Soil

(b) Tip Bearing vs. Settlement Drilled Shaft in Cohesive Soil

(c) Side Resistance vs. Settlement Drilled Shaft in Cohesionless Soil

(d) Tip Bearing vs. Settlement Drilled Shaft in Cohesionless Soil

FIGURE 7.6 Load transfer for side resistance (t–z) and tip bearing (Q–z). (a) Side resistance vs. settlement, drilled shaft in cohesive soil; (b) tip bearing vs. settlement, drilled shaft in cohesive soil; (c) side resistance vs. settlement, drilled shaft in cohesionless soil; (d) tip bearing vs. settlement, drilled shaft in cohesionless soil. (From AASHTO LRFD Bridge Design Specifications, First Edition, coyyright 1996 by the American Association of State Highway and Transportation officials, Washington, D.C. Used by permission.)

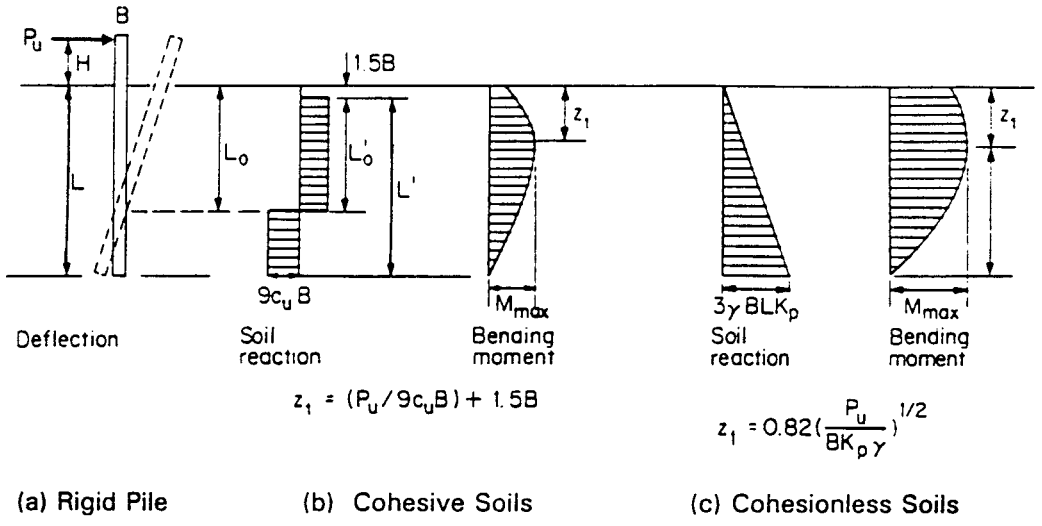

FIGURE 7.7 Free-head, short rigid piles — ultimate load conditions. (a) Rigid pile; (b) cohesive soils; (c) cohesionless soils. [After Broms (1964).[5,6]]

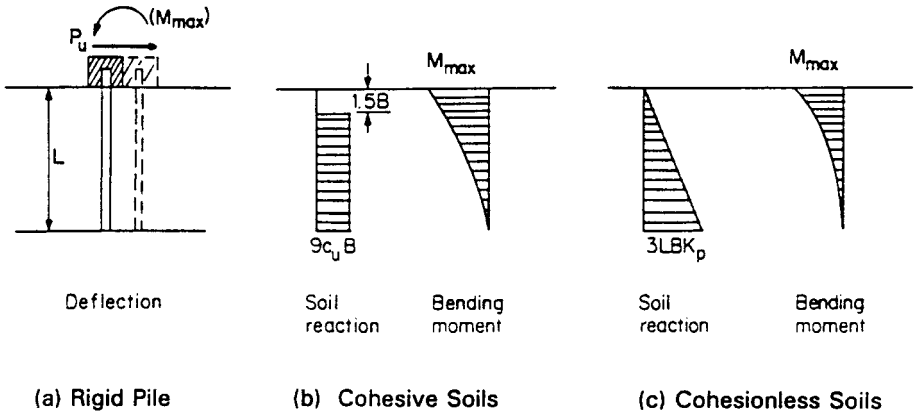

FIGURE 7.8 Fixed-head, short rigid piles — ultimate load conditions. (a) Rigid pile; (b) cohesive soils; (c) cohesionless soils. [After Broms (1964).[5,6]]

Ultimate Lateral Capacity for the Free-Head Condition

The ultimate lateral capacity P_u of a pile under the free-head condition is calculated by using the following formula:

$$P_u = \begin{cases} \left(\dfrac{L_0'^2 - 2L'L_0' + 0.5L'^2}{L' + H + 1.5B}\right)(9c_uB) & \text{for cohesive soil} \\ \dfrac{0.5BL^3K_p\gamma'}{H + L} & \text{for cohesionless soil} \end{cases} \tag{7.28}$$

where

L = embedded length of pile

H = distance of resultant lateral force above ground surface
B = pile diameter
L' = embedded pile length measured from a depth of $1.5B$ below the ground surface, or $L' = L - 1.5B$
L_0 = depth to center of rotation, and $L_0 = (H + 23L)/(2H + L)$
L_0' = depth to center of rotation measured from a depth of $1.5B$ below the ground surface, or $L_0' = L_0 - 1.5B$

Ultimate Lateral Capacity for the Fixed-Head Condition

The ultimate lateral capacity P_u of a pile under the fixed-head condition is calculated by using the following formula:

$$P_u = \begin{cases} 9c_u B(L - 1.5B) & \text{for cohesive soil} \\ 1.5\gamma' BL^2 K_p & \text{for cohesionless soil} \end{cases} \tag{7.29}$$

7.5.3 Lateral Capacity and Deflection — *p–y* Method

One of the most commonly used methods for analyzing laterally loaded piles is the *p–y* method, in which soil reactions to the lateral deflections of a pile are treated as localized nonlinear springs based on the Winkler's assumption. The pile is modeled as an elastic beam that is supported on a deformable subgrade.

The *p–y* method is versatile and can be used to solve problems including different soil types, layered soils, nonlinear soil behavior; different pile materials, cross sections; and different pile head connection conditions.

Analytical Model and Basic Equation

An analytical model for pile under lateral loading with *p–y* curves is shown on Figure 7.9. The basic equation for the beam-on-a-deformable-subgrade problem can be expressed as

$$EI\frac{d^4y}{dx^4} - P_x\frac{d^2y}{dx^2} + p + q = 0 \tag{7.30}$$

where
y = lateral deflection at point x along the pile
EI = bending stiffness or flexural rigidity of the pile
P_x = axial force in beam column
p = soil reaction per unit length, and $p = -E_s y$; where E_s is the secant modulus of soil reaction
q = lateral distributed loads

The following relationships are also used in developing boundary conditions:

$$M = -EI\frac{d^4y}{dx^4} \tag{7.31}$$

$$Q = -\frac{dM}{dx} + P_x\frac{dy}{dx} \tag{7.32}$$

$$\theta = \frac{dy}{dx} \tag{7.33}$$

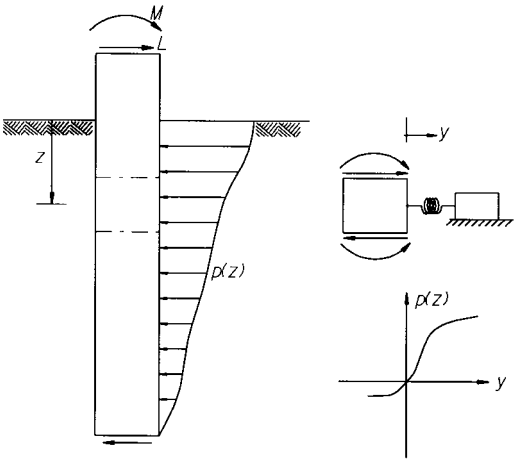

FIGURE 7.9 Analytical model for pile under lateral loading with *p–y* curves.

where M is the bending moment, Q is the shear force in the beam column, θ is the rotation of the pile.

The *p–y* method is a valuable tool in analyzing laterally loaded piles. Reasonable results are usually obtained. A computer program is usually required because of the complexity and iteration needed to solve the above equations using the finite-difference method or other methods. It should be noted that Winkler's assumption ignores the global effect of a continuum. Normally, if soil behaves like a continuum, the deflection at one point will affect the deflections at other points under loading. There is no explicit expression in the *p–y* method since localized springs are assumed. Although *p–y* curves are developed directly from results of load tests and the influence of global interaction is included implicitly, there are cases where unexpected outcomes resulted. For example, excessively large shear forces will be predicted for large piles in rock by using the *p–y* method approach, where the effects of the continuum and the shear stiffness of the surrounding rock are ignored. The accuracy of the *p–y* method depends on the number of tests and the variety of tested parameters, such as geometry and stiffness of pile, layers of soil, strength and stiffness of soil, and loading conditions. One should be careful to extrapolate *p–y* curves to conditions where tests were not yet performed in similar situations.

Generation of *p–y* Curves

A *p–y* curve, or the lateral soil resistance p expressed as a function of lateral soil movement y, is based on backcalculations from test results of laterally loaded piles. The empirical formulations of *p–y* curves are different for different types of soil. *p–y* curves also depend on the diameter of the pile, the strength and stiffness of the soil, the confining overburden pressures, and the loading conditions. The effects of layered soil, battered piles, piles on a slope, and closely spaced piles are also usually considered. Formulation for soft clay, sand, and rock is provided in the following.

p–y Curves for Soft Clay

Matlock [35] proposed a method to calculate *p–y* curves for soft clays as shown on Figure 7.10. The lateral soil resistance p is expressed as

$$p = \begin{cases} 0.5\left(\dfrac{y}{y_{50}}\right)^{1/3} p_u & y < y_p = 8y_{50} \\ p_u & y \geq y_p \end{cases} \tag{7.34}$$

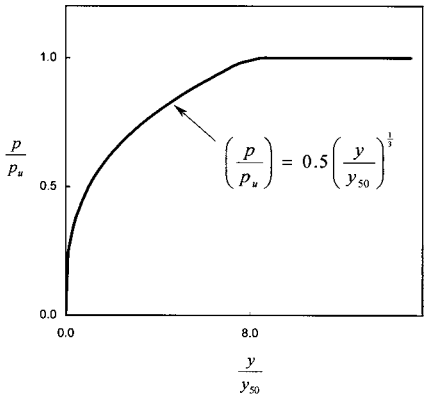

FIGURE 7.10 Characteristic shape of *p–y* curve for soft clay. [After Matlock, (1970)[35]]

in which
p_u = ultimate lateral soil resistance corresponding to ultimate shear stress of soil
y_{50} = lateral movement of soil corresponding to 50% of ultimate lateral soil resistance
y = lateral movement of soil

The ultimate lateral soil resistance p_u is calculated as

$$p_u = \begin{cases} \left(3 + \frac{\gamma' x}{c} + J\frac{x}{B}\right)cB & x < x_r = (6B)/\left(\frac{\gamma' B}{c} + J\right) \\ 9cB & x \geq x_r \end{cases} \tag{7.35}$$

where γ' is the effective unit weight, x is the depth from ground surface, c is the undrained shear strength of the clay, and J is a constant frequently taken as 0.5.

The lateral movement of soil corresponding to 50% of ultimate lateral soil resistance y_{50} is calculated as

$$y_{50} = 2.5\varepsilon_{50}B \tag{7.36}$$

where ε_{50} is the strain of soil corresponding to half of the maximum deviator stress. Table 7.12 shows the representative values of ε_{50}.

p–y Curves for Sands

Reese et al. [53] proposed a method for developing *p–y* curves for sandy materials. As shown on Figure 7.11, a typical *p–y* curve usually consists of the following four segments:

Segment	Curve type	Range of y	Range of p	p–y curve
1	Linear	0 to y_k	0 to p_k	$p = (kx)y$
2	Parabolic	y_k to y_m	p_k to p_m	$p = p_m\left(\frac{y}{y_m}\right)^n$
3	Linear	y_m to y_u	p_m to p_u	$p = p_m + \frac{p_u - p_m}{y_u - y_m}(y - y_m)$
4	Linear	$\geq y_u$	p_u	$p = p_u$

where y_m, y_u, p_m, and p_u can be determined directly from soil parameters. The parabolic form of Segment 2, and the intersection with Segment 1 (y_k and p_k) can be determined based on y_m, y_u, p_m, and p_u as shown below.

Segment 1 starts with a straight line with an initial slope of kx, where x is the depth from the ground surface to the point where the *p–y* curve is calculated. k is a parameter to be determined based on relative density and is different whether above or below water table. Representative values of k are shown in Table 7.13.

TABLE 7.12 Representative Values of ε_{50}

Consistency of Clay	Undrained Shear Strength, psf	ε_{50}
Soft	0–400	0.020
Medium stiff	400–1000	0.010
Stiff	1000–2000	0.007
Very stiff	2000–4000	0.005
Hard	4000–8000	0.004

1 psf = 0.048 kPa.

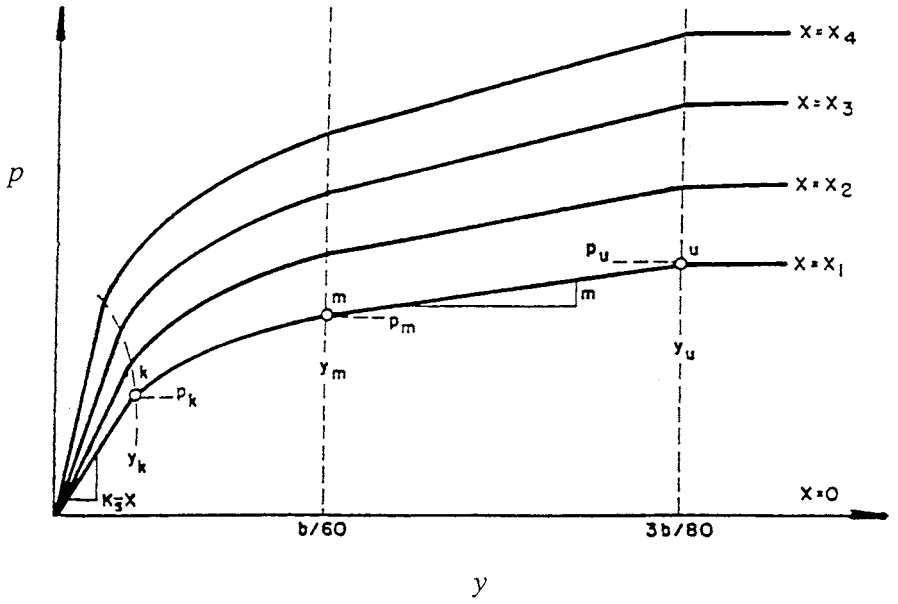

FIGURE 7.11 Characteristic shape of *p–y* curves for sand. [After Reese, et al. (1974)[53]]

TABLE 7.13 Friction Angle and Consistency

	Friction Angle and Consistency		
Relative to Water Table	29°–30° (Loose)	30°–36° (Medium Dense)	36°–40° (Dense)
Above	20 pci	60 pci	125 pci
Below	25 pci	90 pci	225 pci

1 pci = 272 kPa/m.

Segment 2 is parabolic and starts from end of Segment 1 at

$$y_k = \left[\frac{p_m / y_m}{(kx)^n}\right]^{1/(n-1)}$$

and $p_k = (kx)y_k$, the power of the parabolic

$$n = \frac{y_m}{p_m}\left(\frac{p_u - p_m}{y_u - y_m}\right)$$

Segments 3 and 4 are straight lines. y_m, y_u, p_m, and p_u are expressed as

$$y_m = \frac{b}{60} \tag{7.37}$$

$$y_u = \frac{3b}{80} \tag{7.38}$$

$$p_m = B_s p_s \tag{7.39}$$

$$p_u = A_s p_s \tag{7.40}$$

where b is the diameter of a pile; A_s and B_s are coefficients that can be determined from Figures 7.12 and 7.13, depending on either static or cyclic loading conditions; p_s is equal to the minimum of p_{st} and p_{sd}, as

$$p_{st} = \gamma x\left[\frac{K_o x \tan\varphi \sin\beta}{\tan(\beta-\varphi)\cos\alpha} + \frac{\tan\beta}{\tan(\beta-\varphi)}(b + x\tan\beta\tan\alpha) + K_o x\tan\beta(\tan\phi\tan\varphi - \tan\alpha) - K_a b\right] \tag{7.41}$$

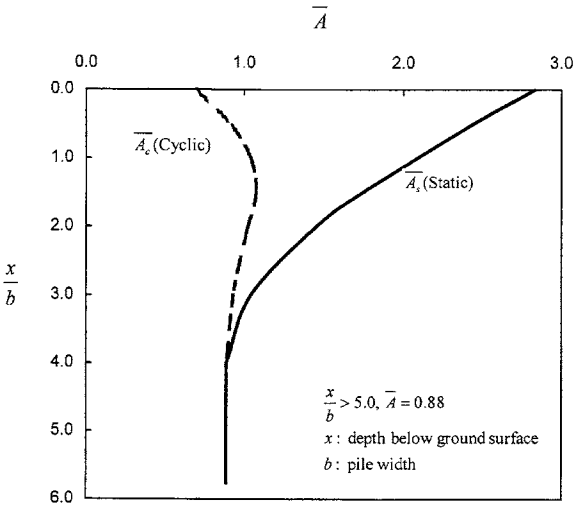

FIGURE 7.12 Variation of A_s with depth for sand. [After Reese, et al. (1974).[53]]

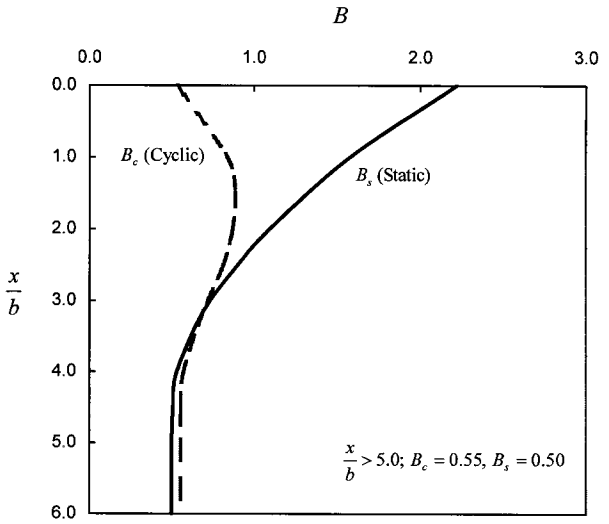

FIGURE 7.13 Variation of B_s with depth for sand. [After Reese, et al. (1974).[53]]

$$p_{sd} = K_a b x \gamma [\tan^8 \beta - 1] + K_o b \gamma x \tan\phi \tan^4 \beta \tag{7.42}$$

$$p = \min(p_{st}, p_{sd}) \tag{7.43}$$

in which φ is the friction angle of soil; α is taken as $\varphi/2$; β is equal to $45^o + \varphi/2$; K_o is the coefficient of the earth pressure at rest and is usually assumed to be 0.4; and K_a is the coefficient of the active earth pressure and equals to $\tan^2(45^o - \varphi/2)$.

7.5.4 Lateral Spring: *p–y* Curves for Rock

Reese[86] proposed a procedure to calculate *p–y* curves for rock using basic rock and rock mass properties such as compressive strength of intact rock q_{ur}, rock quality designation (RQD), and initial modulus of rock E_{ir}. A description of the procedure is presented in the following.

A *p–y* curve consists of three segments:

$$\begin{aligned}
&\text{Segment 1: } p = K_{ir} y && \text{for} \quad y \le y_a \\
&\text{Segment 2: } p = \frac{p_{ur}}{2}\left(\frac{y}{y_{rm}}\right)^{0.25} && \text{for} \quad y_a < y < 16 y_{rm} \\
&\text{Segment 3: } p = p_{ur} && \text{for} \quad y \ge 16 y_{rm}
\end{aligned} \tag{7.44}$$

where p is the lateral force per unit pile length and y is the lateral deflection.

K_{ir} is the initial slope and is expressed as

$$K_{ir} = k_{ir} E_{ir} \tag{7.45}$$

k_{ir} is a dimensionless constant and is determined by

$$k_{ir} = \begin{cases} \left(100 + \dfrac{400x_r}{3b}\right) & \text{for} \quad 0 \le x_r \le 3b \\ 500 & \text{for} \quad x_r > 3b \end{cases} \tag{7.46}$$

x_r = depth below bedrock surface, b is the width of the rock socket
E_{ir} = initial modulus of rock.

y_a is the lateral deflection separating Segment 1 and 2, and

$$y_a = \left(\frac{p_{ur}}{2y_{rm}^{0.25}K_{ir}}\right)^{1.333} \tag{7.47}$$

where

$$y_{rm} = k_{rm}b \tag{7.48}$$

k_{rm} is a constant, ranging from 0.0005 to 0.00005.
p_{ur} is the ultimate resistance and can be determined by

$$P_{ur} = \begin{cases} a_r q_{ur} b\left(1 + 1.4\dfrac{x_r}{b}\right) & \text{for} \quad 0 \le x_r \le 3b \\ 5.2 a_r q_{ur} b & \text{for} \quad x_r > 3b \end{cases} \tag{7.49}$$

where
q_{ur} = compressive strength of rock and α_r is a strength reduction factor determined by

$$\alpha_r = 1 - \frac{\text{RQD}}{150} \qquad 0 \le \text{RQD} \le 100 \tag{7.50}$$

RQD = rock quality designation for rock.

7.6 Grouped Foundations

7.6.1 General

Although a pile group is composed of a number of individual piles, the behavior of a pile group is not equivalent to the sum of all the piles as if they were separate individual piles. The behavior of a pile group is more complex than an individual pile because of the effect of the combination of piles, interactions between the piles in the group, and the effect of the pile cap. For example, stresses in soil from the loading of an individual pile will be insignificant at a certain depth below the pile tip. However, the stresses superimposed from all neighboring piles may increase the level of stress at that depth and result in considerable settlements or a bearing capacity failure, especially if there exists an underlying weak soil layer. The interaction and influence between piles usually diminish for piles spaced at approximately 7 to 8 diameters.

The axial and lateral capacity and the corresponding settlement and lateral deflection of a pile group will be discussed in the following sections.

7.6.2 Axial Capacity of Pile Group

The axial capacity of a pile group is the combination of piles in the group, with consideration of interaction between the piles. One way to account for the interaction is to use the group efficiency factor η_a, which is expressed as:

$$\eta_a = \frac{P_{\text{Group}}}{\sum_i P_{\text{Single\_Pile},i}} \tag{7.51}$$

where P_{Group} is the axial capacity of a pile group. $\sum_i P_{\text{Single\_Pile},i}$ is the sum of the axial capacity of all the individual piles. Individual piles are discussed in detail in Section 7.4. The group efficiency for axial capacity depends on many factors, such as the installation method, ground conditions, and the function of piles, which are presented in Table 7.14.

TABLE 7.14 Group Efficiency Factor for Axial Capacity

Pile Installation Method	Function	Ground Conditions	Expected Group Efficiency	Design Group Efficiency (with minimum spacing equal to 2.5 pile diameter)
Driven Pile	End bearing	Sand	1.0	1.0
	Side friction	Loose to medium dense sand	>1.0, up to 2.0	1.0, or increase with load test
	Side friction	Dense sand	May be ≧ 1.0	1.0
Drilled shaft	All	Sand	<1.0	0.67–1.0
Driven pile and drilled shaft	Side friction	Soft to medium stiff clay	<1.0	0.67–1.0
	End bearing	Soft to medium stiff clay	<1.0	0.67–1.0
	Side friction	Stiff clay	1.0	1.0
	End bearing	Stiff clay	1.0	1.0
	Side friction	Clay	<1.0	Also use "Group Block"
	End bearing	Clay, or underlying clay layers	<1.0	Also use "Group Block"

At close spacings, driven piles in loose to medium dense sand may densify the sand and consequently increase the lateral stresses and frictions along the piles. However, driven piles in dense sand may cause dilation of the sand and consequently cause heave and damage to other piles. The influence of spacing to the end bearing for sand is usually limited and the group efficiency factor η_a is taken as 1.0, under normal conditions.

For drilled piers in loose to medium dense sand, no densification of sand is made. The group efficiency factor η_a is usually less than 1.0 because of the influence of other close piles.

For driven piles in stiff to very stiff clay, the piles in a pile group tend to form a "group block" that behaves like a giant, short pile. The size of the group block is the extent of soil enclosed by the piles, including the perimeter piles as shown on Figure 7.14. The group efficiency factor η_a is usually equal to 1.0. For piles in soft to medium stiff clay, the group efficiency factor η_a is usually less than 1.0 because the shear stress levels are increased by loading from adjacent piles.

The group block method is also often used to check the bearing capacity of a pile group. The group block is treated as a large deep spread footing foundation and the assumed bottom level of the footing is different depending on whether the pile is end bearing or frictional. For end-bearing piles, the capacity of the group block is examined by assuming the bottom of the footing is at the tip of the piles. For frictional piles, the capacity of the group pile is checked by assuming that the bottom of the footing is located at ⅓ of the total embedded length above the tip. The bearing capacity of the underlying weaker layers is then estimated by using methods discussed in Chapter 6.

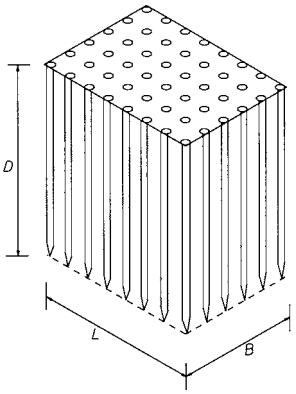

FIGURE 7.14 Block failure model for pile group in clay.

The smaller capacity, by using the group efficiency approach, the group block approach, and the group block approach with underlying weaker layers, is selected as the capacity of the pile group.

7.6.3 Settlement of a Pile Group

The superimposed stresses from neighboring piles will raise the stress level below the tip of a pile substantially, whereas the stress level is much smaller for an individual pile. The raised stress level has two effects on the settlement of a pile group. The magnitude of the settlement will be larger for a pile group and the influence zone of a pile group will be much greater. The settlement of a pile group will be much larger in the presence of underlying highly compressible layers that would not be stressed under the loading of an individual pile.

The group block method is often used to estimate the settlement of a group. The pile group is simplified to an equivalent massive spread footing foundation except that the bottom of the footing is much deeper. The plane dimensions of the equivalent footing are outlined by the perimeter piles of the pile group. The method to calculate settlement of spread footings is discussed in Chapter 6. The assumed bottom level of the footing block is different depending on either end bearing or frictional piles. For end-bearing piles, the bottom of the footing is at the tip of the piles. For frictional piles, the bottom of the footing is located at ⅓ of total embedded length above the tip. In many cases, settlement requirement also is an important factor in the design of a pile group.

Vesic [79] introduced a method to calculate settlement of a pile group in sand which is expressed as

$$S_g = S_s \sqrt{\frac{B_g}{B_s}} \tag{7.52}$$

where
S_g = the settlement of a pile group
S_s = the settlement of an individual pile
B_g = the smallest dimension of the group block
B_s = the diameter of an individual pile

7.6.4 Lateral Capacity and Deflection of a Pile Group

The behavior of a pile group under lateral loading is not well defined. As discussed in the sections above, the lateral moment capacity is greater than the sum of all the piles in a group because piles would form couples resulting from their axial resistance through the action of the pile cap. However,

the capacity of a pile group to resist lateral loads is usually smaller than the sum of separate, individual piles because of the interaction between piles.

The approach used by the University of Texas at Austin (Reese, O'Neil, and co-workers) provides a comprehensive and practical method to analyze a pile group under lateral loading. The finite-difference method is used to model the structural behavior of the foundation elements. Piles are connected through a rigid pile cap. Deformations of all the piles, in axial and lateral directions, and force and moment equilibrium are established. The reactions of soil are represented by a series of localized nonlinear axial and lateral springs. The theory and procedures to calculate axial and lateral capacity of individual piles are discussed in detail in Sections 7.4 and 7.5. A computer program is usually required to analyze a pile group because of the complexity and iteration procedure involving nonlinear soil springs.

The interaction of piles is represented by the lateral group efficiency factors, which is multiplied to the *p–y* curves for individual piles to reduce the lateral soil resistance and stiffness. Dunnavant and O'Neil [16] proposed a procedure to calculate the lateral group factors. For a particular pile *i*, the group factor is the product of influence factors from all neighboring piles *j*, as

$$\beta_i = \beta_0 \prod_{\substack{j=1 \\ j \neq i}}^{n} \beta_{ij} \tag{7.53}$$

where β_i is the group factor for pile *i*, β_0 is a total reduction factor and equals 0.85, β_{ij} is the influence factor from a neighboring pile *j*, and *n* is the total number of piles. Depending on the location of the piles *i* and *j* in relation to the direction of loading, β_{ij} is calculated as follows:

i is leading, or directly ahead of *j* ($\theta = 0°$) $\beta_l = \beta_{ij} = 0.69 + 0.5 \log_{10}\left(\frac{S_{ij}}{B}\right) \leq 1$ (7.54)

i is trailing, or directly behead of *j* ($\theta = 180°$) $\beta_t = \beta_{ij} = 0.48 + 0.6 \log_{10}\left(\frac{S_{ij}}{B}\right) \leq 1$ (7.55)

i and *j* are abreast, or side-by-side ($\theta = 90°$) $\beta_s = \beta_{ij} = 0.78 + 0.36 \log_{10}\left(\frac{S_{ij}}{B}\right) \leq 1$ (7.56)

where S_{ij} is the center-to-center distance between *i* and *j*, B is the diameter of the piles *i* and *j*, and θ is the angle between the loading direction and the connection vector from *i* to *j*. When the piles *i* and *j* are at other angles to the direction of loading, β_{ij} is computed by interpolation, as

$$0° < \theta < 90° \qquad \beta_{\theta 1} = \beta_{ij} = \beta_l + (\beta_s - \beta_l)\frac{\theta}{90} \tag{7.57}$$

$$90° < \theta < 180° \qquad \beta_{\theta 2} = \beta_{ij} = \beta_t + (\beta_s - \beta_t)\frac{\theta - 90}{90} \tag{7.58}$$

In cases that the diameters of the piles *i* and *j* are different, we propose to use the diameter of pile *j*. To avoid an abrupt change of β_0 from 0.85 to 1.0, we propose to use:

$$\beta_o = \begin{cases} 0.85 & \text{for} \quad \dfrac{S_{ij}}{B_j} \le 3 \\ 0.85 + 0.0375\left(\dfrac{S_{ij}}{B_j} - 3\right) & \text{for} \quad 3 < \dfrac{S_{ij}}{B_j} < 7 \\ 1.0 & \text{for} \quad \dfrac{S_{ij}}{B_j} \ge 7 \end{cases}$$

7.7 Seismic Design

Seismic design of deep bridge foundations is a broad issue. Design procedures and emphases vary with different types of foundations. Since pile groups, including driven piles and drilled cast-in-place shafts, are the most popular types of deep bridge foundations, following discussion will concentrate on the design issues for pile group foundations only.

In most circumstances, seismic design of pile groups is performed to satisfy one or more of the following objectives:

- Determine the capacity and deflection of the foundation under the action of the seismic lateral load;
- Provide the foundation stiffness parameters for dynamic analysis of the overall bridge structures; and
- Ensure integrity of the pile group against liquefaction and slope instability induced ground movement.

7.7.1 Seismic Lateral Capacity Design of Pile Groups

In current practice, seismic lateral capacity design of pile groups is often taken as the same as conventional lateral capacity design (see Section 7.5). The seismic lateral force and the seismic moment from the upper structure are first evaluated for each pile group foundation based on the tributary mass of the bridge structure above the foundation level, the location of the center of gravity, and the intensity of the ground surface acceleration. The seismic force and moment are then applied on the pile cap as if they were static forces, and the deflections of the piles and the maximum stresses in each pile are calculated and checked against the allowable design values. Since seismic forces are of transient nature, the factor of safety required for resistance of seismic load can be less than those required for static load. For example, in the Caltrans specification, it is stipulated that the design seismic capacity can be 33% higher than the static capacity [9].

It should be noted that, in essence, the above procedure is pseudostatic, only the seismic forces from the upper structure are considered, and the effect of seismic ground motion on the behavior of pile group is ignored. The response of a pile group during an earthquake is different from its response to a static lateral loading. As seismic waves pass through the soil layers and cause the soil layers to move laterally, the piles are forced to move along with the surrounding media. Except for the case of very short piles, the pile cap and the pile tip at any moment may move in different directions. This movement induces additional bending moments and stresses in the piles. Depending on the intensity of the seismic ground motion and the characteristics of the soil strata, this effect can be more critical to the structural integrity of the pile than the lateral load from the upper structure.

Field measurements (e.g., Tazoh et al. [70]), post-earthquake investigation (e.g., Seismic Advisory Committee, [65]), and laboratory model tests (e.g., Nomura et al., [43]) all confirm that seismic ground movements dictate the maximum responses of the piles. The more critical situation is when the soil profile consists of soft layer(s) sandwiched by stiff layers, and the modulus contrast among the layers is large. In this case, local seismic moments and stresses in the pile

section close to the soft layer/hard layer interface may very well be much higher than the moments and stresses caused by the lateral seismic loads from the upper structure. If the site investigation reveals that the underground soil profile is of this type and the bridge is of critical importance, it is desirable that a comprehensive dynamic analysis be performed using one of more sophisticated computer programs capable of modeling the dynamic interaction between the soil and the pile system, e.g., SASSI [33]. Results of such dynamic analysis can provide a better understanding of the seismic responses of a pile group.

7.7.2 Determination of Pile Group Spring Constants

An important aspect in bridge seismic design is to determine, through dynamic analysis, the magnitude and distribution of seismic forces and moments in the bridge structure. To accomplish this goal, the characteristics of the bridge foundation must be considered appropriately in an analytical model.

At the current design practice, the force–displacement relationships of a pile foundation are commonly simplified in an analytical model as a stiffness matrix, or a set of translational and rotational springs. The characteristics of the springs depend on the stiffness at pile head for individual piles and the geometric configuration of piles in the group. For a pile group consisting of vertical piles, the spring constants can be determined by the following steps:

- The vertical and lateral stiffnesses at the pile head of a single pile, K_{vv} and K_{hh}, are first evaluated based on the pile geometry and the soil profile. These values are determined by calculating the displacement at the pile head corresponding to a unit force. For many bridge foundations, a rigid pile cap can be assumed. Design charts are available for uniform soil profiles (e.g., NAVFAC [42]). For most practical soil profiles, however, it is convenient to use computer programs, such as APILE [18] and LPILE [17], to determine the single pile stiffness values. It should be noted that the force–deformation behavior of a pile is highly nonlinear. In evaluating the stiffness values, it is desirable to use the secant modulus in the calculated pile-head force–displacement relationship compatible to the level of pile-head displacement to be developed in the foundation. This is often an iterative process.

  In calculating the lateral stiffness values, it is common practice to introduce a group factor η, $\eta \leq 1.0$, to account for the effect of the other piles in the same group. The group factor depends on the relative spacing S/D in the pile group, where S is the spacing between two piles and D is the diameter of the individual pile. There are studies reported in the literature about the dynamic group factors for pile groups of different configurations. However, in the current design practice, static group factors are used in calculation of the spring constants. Two different approaches exist in determining the group factor: one is based on reduction of the subgrade reaction moduli; the other is based on the measurement of plastic deformation of the pile group. Since the foundation deformations in the analysis cases involving the spring constants are mostly in the small-strain range, the group factors based on subgrade reaction reduction should be used (e.g., NAVFAC [42]).
- The spring constants of the pile group can be calculated using the following formulas:

$$K_{G,x} = \sum_{i=1}^{N} K_{hh,i} \tag{7.59}$$

$$K_{G,y} = \sum_{i=1}^{N} K_{hh,i} \tag{7.60}$$

$$K_{G,z} = \sum_{i=1}^{N} K_{vv,i} \tag{7.61}$$

$$K_{G,yy} = \sum_{i=1}^{N} K_{vv,i} \cdot x_i^2 \tag{7.62}$$

$$K_{G,xx} = \sum_{i=1}^{N} K_{vv,i} \cdot y_i^2 \tag{7.63}$$

where $K_{G,x}$, $K_{G,y}$, $K_{G,z}$ are the group translational spring constants, $K_{G,yy}$, $K_{G,xx}$ are the group rotational spring constants with respect to the center of the pile cap. All springs are calculated at the center of the pile cap; $K_{vv,i}$ and $K_{hh,i}$ are the lateral and vertical stiffness values at pile head of the ith pile; x_i, y_i are the coordinates of the ith pile in the group; and N is the total number of piles in the group.

In the above formulas, the bending stiffness of a single pile at the pile top and the off-diagonal stiffness terms are ignored. For most bridge pile foundations, these ignored items have only minor significance. Reasonable results can be obtained using the above simplified formulas.

It should be emphasized that the behavior of the soil–pile system is greatly simplified in the concept of "spring constant." The responses of a soil–pile structure system are complicated and highly nonlinear, frequency dependent, and are affected by the inertia/stiffness distribution of the structure above ground. Therefore, for critical structures, it is advisable that analytical models including the entire soil–pile structure system should be used in the design analysis.

7.7.3 Design of Pile Foundations against Soil Liquefaction

Liquefaction of loose soil layers during an earthquake poses a serious hazard to pile group foundations. Field observations and experimental studies (e.g., Nomura et al. [43], Miyamoto et al. [40], Tazoh and Gazetas [69], Boulanger et al. [4]) indicate that soil liquefaction during an earthquake has significant impacts on the behavior of pile groups and superstructures. The impacts are largely affected by the intensity of liquefaction-inducing earthquakes and the relative locations of the liquefiable loose soil layers. If a loose layer is close to the ground surface and the earthquake intensity is moderate, the major effect of liquefaction of the loose layer is to increase the fundamental period of the foundation–structure system, causing significant lateral deflection of the pile group and superstructure. For high-intensity earthquakes, and especially if the loose soil layer is sandwiched in hard soil layers, liquefaction of the loose layer often causes cracking and breakage of the piles and complete loss of capacity of the foundation, thus the collapse of the superstructure.

There are several approaches proposed in the literature for calculation of the dynamic responses of a pile or a pile group in a liquefied soil deposit. In current engineering practice, however, more emphasis is on taking proper countermeasures to mitigate the adverse effect of the liquefaction hazard. These mitigation methods include

- Densify the loose, liquefiable soil layer. A stone column is often satisfactory if the loose layer is mostly sand. Other approaches, such as jet grouting, deep soil mixing with cementing agents, and *in situ* vibratory densification, can all be used. If the liquefiable soil layer is close to the ground surface, a complete excavation and replacement with compacted engineering fill is sometimes also feasible.
- Isolate the pile group from the surrounding soil layers. This is often accomplished by installing some types of isolation structures, such as sheet piles, diaphragm walls, soil-mixing piles,

etc., around the foundation to form an enclosure. In essence, this approach creates a huge block surrounding the piles with increased lateral stiffness and resistance to shear deformation while limiting the lateral movement of the soil close to the piles.

- Increase the number and dimension of the piles in a foundation and therefore increase the lateral resistance to withstand the forces induced by liquefied soil layers. An example is 10 ft (3.3 m) diameter cast-in-steel shell piles used in bridge seismic retrofit projects in the San Francisco Bay Area following the 1989 Loma Prieta earthquake.

References

1. API, *API Recommended Practice for Planning, Designing and Constructing Fixed Offshore Platforms,* 15th ed., API RP2A, American Petroleum Institute, 115 pp, 1984.
2. Awoshika, K. and L. C. Reese, Analysis of Foundation with Widely-Spaced Batter Piles, Research Report 117-3F, Center for Highway Research, The University of Texas at Austin, February, 1971.
3. Berezantzev, V. G., V. S. Khristoforov, and V. N. Golubkov, Load bearing capacity and deformation of piled foundations, *Proc. 5th Int. Conf. Soil Mech.,* Paris, 2, 11–15, 1961.
4. Boulanger, R. W., D. W. Wilson, B. L. Kutter, and A. Abghari, Soil–pile-structure interaction in liquefiable sand, *Transp. Res. Rec.,* 1569, April, 1997.
5. Broms, B. B., Lateral resistance of piles in cohesive soils, *Proc. ASCE, J. Soil Mech. Found. Eng. Div.,* 90(SM2), 27–64, 1964.
6. Broms, B. B., Lateral resistance of piles in cohesionless soils, *Proc. ASCE J. Soil Mech. Found. Eng. Div.,* 90(SM3), 123–156, 1964.
7. Burland, J. B., Shaft friction of piles in clay — a simple fundamental approach, *Ground Eng.,* 6(3), 30–42, 1973.
8. Bustamente, M. and L. Gianeselli, Pile bearing capacity prediction by means of static penetrometer CPT, *Proc. of Second European Symposium on Penetration Testing* (ESOPT II), Vol. 2, A. A. Balkema, Amsterdam, 493–500, 1982.
9. Caltrans, Bridge Design Specifications, California Department of Transportation, Sacramento, 1990.
10. CGS, *Canadian Foundation Engineering Manual,* 3rd ed., Canadian Geotechnical Society, BiTech Publishers, Vancouver, 512 pp, 1992.
11. Carter, J. P. and F. H. Kulhawy, Analysis and Design of Drilled Shaft Foundations Socketed into Rock, EPRI Report EI-5918, Electric Power Research Institute, Palo Alto, CA, 1988.
12. Crapps, D. K., Design, construction and inspection of drilled shafts in limerock and limestone, paper presented at the Annual Meeting of the Florida Section of ASCE, 1986.
13. De Ruiter, J. and F. L. Beringen, Pile foundations for large North Sea structures, *Marine Geotechnol.,* 3(2), 1978.
14. Dennis, N. D., Development of Correlations to Improve the Prediction of Axial Pile Capacity, Ph.D. dissertation, University of Texas at Austin, 1982.
15. Desai, C. S. and J. T. Christian, *Numerical Methods in Geotechnical Engineering,* McGraw-Hill Book, New York, 1977.
16. Dunnavant, T. W. and M. W. O'Neil, Evaluation of design-oriented methods for analysis of vertical pile groups subjected to lateral load, *Numerical Methods in Offshore Piling*, Institut Francais du Petrole, Labortoire Central des Ponts et Chausses, 303–316, 1986.
17. Ensoft Inc., Lpile Plus for Windows. Version 3.0. A Computer Program for Analysis of Laterally Loaded Piles, Austin, TX, 1997.
18. Ensoft Inc., Apile Plus. Version 3.0, Austin, TX, 1998.
19. Fellenius, B. H., in an ASCE meeting in Boston as quoted by R. E. Olson in 1991, Capacity of Individual Piles in Clay, internal report, 1986.
20. Fellenius, B. H., The critical depth — how it came into being and why it does not exist, *Proc. of the Inst. Civil Eng., Geotech. Eng.,* 108(1), 1994.

21. Focht, J. A. and K. J. Koch, Rational analysis of the lateral performance of offshore pile groups, in *Proceedings, Fifth Offshore Technology Conference,* Vol. 2, Houston, 701–708, 1973.
22. Geordiadis, M., Development of *p–y* curves for layered soils, in *Proceedings, Geotechnical Practice in Offshore Engineering,* ASCE, April, 1983, 536–545.
23. Goudreault, P. A. and B. H. Fellenius, A Program for the Design of Piles and Piles Groups Considering Capacity, Settlement, and Dragload Due to Negative Skin Friction, 1994.
24. Gupton, C. and T. Logan, Design Guidelines for Drilled Shafts in Weak Rocks in South Florida, Preprint, Annual Meeting of South Florida Branch of ASCE, 1984.
25. Horvath, R. G. and T. C. Kenney, Shaft resistance of rock-socketed drilled piers, in *Symposium on Deep Foundations,* ASCE National Convention, Atlanta, GA, 1979, 182–214.
26. Janbu, N., Static bearing capacity of friction piles, in *Proc. 6th European Conference on Soil Mech. & Found. Eng.,* Vol. 1.2, 1976, 479–488.
27. Kishida, H., Ultimate bearing capacity of piles driven into loose sand, *Soil Foundation,* 7(3), 20–29, 1967.
28. Kraft L. M., J. A. Focht, and S. F. Amerasinghe, Friction capacity of piles driven into clay, *J. Geot. Eng. Div. ASCE,* 107(GT 11), 1521–1541, 1981.
29. Kubo, K., Experimental Study of Behavior of Laterally Loaded Piles, Report, Transportation Technology Research Institute, Vol. 12, No. 2, 1962.
30. Kulhawy, F. H., Transmission Line Structures Foundations for Uplift-Compression Loading, Report No. EL-2870, Report to the Electrical Power Research Institute, Geotechnical Group, Cornell University, Ithaca, NY, 1983.
31. Kulhawy, F. H., Limiting tip and side resistance: fact or fallacy? in *Proc. of the American Society of Civil Engineers, ASCE, Symposium on Analysis and Design of Pile Foundations,* R. J. Meyer, Ed., San Francisco, 1984, 80–89.
32. Kulhawy, F. H. and K. K. Phoon, Drilled shaft side resistance in clay soil or rock, in *Geotechnical Special Publication No. 38, Design and Performance of Deep Foundations: Piles and Piers in Soil to Soft Rock,* Ed. P. P. Nelson, T. D. Smith, and E. C. Clukey, Eds., ASCE, 172–183, 1993.
33. Lysmer, J., M. Tabatabaie-Raissi, F. Tajirian, S. Vahdani, and F. Ostadan, SASSI — A System for Analysis of Soil-Structure Interaction, Report No. UCB/GT/81-02, Department of Civil Engineering, University of California, Berkeley, April, 1981.
34. McVay, M. C., F. C. Townsend, and R. C. Williams, Design of socketed drilled shafts in limestone, *J. Geotech. Eng.*, 118-GT10, 1626–1637, 1992.
35. Matlock, H., Correlations for design of laterally-loaded piles in soft clay, Paper No. OTC 1204, *Proc. 2nd Annual Offshore Tech. Conf.,* Vol. 1, Houston, TX, 1970, 577–594.
36. Menard, L. F., Interpretation and application of pressuremeter test results, *Sols-Soils,* Paris, 26, 1–23, 1975.
37. Meyerhof, G. G., Penetration tests and bearing capacity of cohesionless soils, *J. Soil Mech. Found. Div. ASCE,* 82(SM1), 1–19, 1956.
38. Meyerhof, G. G., Bearing capacity and settlement of pile foundations, *J. Geotech. Eng. Div. ASCE,* 102(GT3), 195–228, 1976.
39. Mitchell, J. K. and T. A. Lunne, Cone resistance as a measure of sand strength, *Proc. ASCE J. Geotech. Eng. Div.,* 104(GT7), 995–1012, 1978.
40. Miyamoto, Y., Y. Sako, K. Miura, R. F. Scott, and B. Hushmand, Dynamic behavior of pile group in liquefied sand deposit, *Proceedings, 10th World Conference on Earthquake Engineering,* 1992, 1749–1754.
41. Mosher, R. L., Load Transfer Criteria for Numerical Analysis of Axially Loaded Piles in Sand, U.S. Army Engineering Waterways Experimental Station, Automatic Data Processing Center, Vicksburg, MI, January, 1984.
42. NAVFAC, Design Manual DM7.02: Foundations and Earth Structures, Department of the Navy, Naval Facilities Engineering Command, Alexandra, VA, September, 1986.

43. Nomura, S., K. Tokimatsu, and Y. Shamoto, Behavior of soil-pile-structure system during liquefaction, in *Proceedings, 8th Japanese Conference on Earthquake Engineering,* Tokyo, December 12–14, Vol. 2, 1990, 1185–1190.
44. O'Neil M. W. and L. C. Reese, Load transfer in a slender drilled pier in sand, ASCE, ASCE Spring Convention and Exposition, Pittsburgh, PA, Preprint 3141, April, 1978, 30 pp.
45. O'Neil, M. W. and S. A. Sheikh, Geotechnical behavior of underrems in pleistocene clay, in *Drilled Piers and Caissons, II,* C. N. Baker, Jr., Ed., ASCE, May, 57–75, 1985.
46. O'Neil, M. W., F. C. Townsend, K. M. Hassan, A. Buller, and P. S. Chan, Load Transfer for Drilled Shafts in Intermediate Geo'materials, FHWA-RD-95-172, November, 184 pp, 1996.
47. Osterberg, J. O., New load cell testing device, in *Proc. 14th Annual Conf.,* Vol. 1, Deep Foundations Institute, 1989, 17–28.
48. Pells, P. J. N. and R. M. Turner, Elastic solutions for the design and analysis of rock-socketed piles, *Can. Geotech. J.*, 16(3), 481–487, 1979.
49. Pells, P. J. N. and R. M. Turner, End bearing on rock with particular reference to sandstone, in Structural Foundations on Rock, *Proc. Intn. Conf. on Structural Found. on Rock*, Vol. 1, Sydney, May 7–9, 1980, 181–190.
50. Poulos, H. G. and E. H. Davis, *Pile Foundation Analysis and Design,* John Wiley & Sons, New York, 1980.
51. Reese, L. C. and H. Matlock, Behavior of a two-dimensional pile group under inclined and eccentric loading, in *Proc. Offshore Exploration Conf.,* Long Beach, CA, February, 1966.
52. Reese, L. C. and M. W. O'Neil, The analysis of three-dimensional pile foundations subjected to inclined and eccentric loads, *Proc. ASCE Conf.,* September, 1967, 245–276.
53. Reese, L. C., W. R. Cox, and F. D. Koop, Analysis of laterally loaded piles in sand, paper OTC 2080, *Proc. Fifth Offshore Tech. Conf.,* Houston, TX, 1974.
54. Reese, L. C., W. R. Cox, and F. D. Koop, Field testing and analysis of laterally loaded piles in stiff clay, paper OTC 2313, in *Proc. Seventh Offshore Tech. Conf.,* Houston, TX, 1975.
55. Reese, L. C. and S. J. Wright, Drilled Shafts: Design and Construction, Guideline Manual, Vol. 1; Construction Procedures and Design for Axial Load, U.S. Department of Transportation, Federal Highway Administration, July, 1977.
56. Reese, L. C., Behavior of Piles and Pile Groups under Lateral Load, a report submitted to the Federal Highway Administration, Washington, D.C., July, 1983, 404 pp.
57. Reese, L. C. and M. W. O'Neil, Drilled Shafts: Construction Procedures and Design Methods, U.S. Department of Transportation, Federal Highway Administration, McLean, VA, 1988.
58. Reynolds, R. T. and T. J. Kaderabek, Miami Limestone Foundation Design and Construction, Preprint No. 80-546, South Florida Convention, ASCE, 1980.
59. Robertson, P. K., R. G. Campanella, et al., Axial Capacity of Driven Piles in Deltaic Soils Using CPT, Penetration Testing 1988, ISOPT-1, De Ruite, Ed., 1988.
60. Rosenberg, P. and N. L. Journeaux, Friction and end bearing tests on bedrock for high capacity socket design, *Can. Geotech. J.*, 13(3), 324–333, 1976.
61. Rowe, R. K. and H. H. Armitage, Theoretical solutions for axial deformation of drilled shafts in rock, *Can. Geotech. J.*, Vol. 24(1), 114–125, 1987.
62. Rowe, R. K. and H. H. Armitage, A design method for drilled piers in soft rock, *Can. Geotech. J.*, 24(1), 126–142, 1987.
63. Schmertmann, J. H., Guidelines for Cone Penetration Test: Performance and Design, FHWA-TS-78-209, Federal Highway Administration, Office of Research and Development, Washington, D.C., 1978.
64. Seed, H. B. and L. C. Reese, The action of soft clay along friction piles, *Trans. Am. Soc. Civil Eng.,* Paper No. 2882, 122, 731–754, 1957.
65. Seismic Advisory Committee on Bridge Damage, Investigation Report on Highway Bridge Damage Caused by the Hyogo-ken Nanbu Earthquake, Japan Ministry of Construction, 1995.

66. Skempton, A. W., The bearing capacity of clay, *Proc. Building Research Congress*, Vol. 1, 1951, 180–189.
67. Skempton, A. W., Cast-*in situ* bored piles in London clay, *Geotechnique*, 9, 153–173, 1959.
68. Sörensen, T. and B. Hansen, Pile driving formulae — an investigation based on dimensional considerations and a statistical analysis, *Proc. 4th Int. Conf. Soil Mech.,* London, 2, 61–65, 1957.
69. Tazoh, T. and G. Gazetas, Pile foundations subjected to large ground deformations: lessons from kobe and research needs, *Proceedings, 11th World Conference on Earthquake Engineering,* Paper No. 2081, 1996.
70. Tazoh, T., K. Shimizu, and T. Wakahara, Seismic Observations and Analysis of Grouped Piles, Dynamic Response of Pile Foundations — Experiment, Analysis and Observation, ASCE Geotechnical Special Publication No. 11, 1987.
71. Terzaghi, K., *Theoretical Soil Mechanics,* John Wiley & Sons, New York, 510 pp, 1943.
72. Tomlinson, M. J., The adhesion of piles in clay soils, *Proc., Fourth Int. Conf. Soil Mech. Found. Eng.,* 2, 66–71, 1957.
73. Tomlinson, M. J., Some effects of pile driving on skin friction, in *Behavior of Piles,* Institution of Civil Engineers, London, 107–114, and response to discussion, 149–152, 1971.
74. Touma, F. T. and L. C. Reese, Load Tests of Instrumented Drilled Shafts Constructed by the Slurry Displacement Method. Research report conducted under Interagency contract 108 for the Texas Highway Department, Center for Highway Research, the University of Texas at Austin, January, 1972, 79 pp.
75. Townsend, F. C., Comparison of deep foundation load test method, in *FHWA 25th Annual Southeastern Transportation Geotechnical Engineering Conference*, Natchez, MS, October 4–8, 1993.
76. Vesic, A. S., Ultimate loads and settlements of deep foundations in sand, in *Proc. Symp. on Bearing Capacity and Settlement of Foundations*, Duke University, Durham, NC, 1967.
77. Vesic, A. S., Load transfer in pile-soil system, in *Design and Installation of Pile Foundations and Cellar Structures,* Fang and Dismuke, Eds., Envo, Lehigh, PA, 47–74, 1970.
78. Vesic, A. S., Expansion of cavities in infinite soil mass, *Proc. ASCE J. Soil Mech. Found. Eng. Div.,* 98(SM3), 1972.
79. Vesic, A. S., Design of Pile Foundations, National Cooperative Highway Research Program Synthesis 42, Transportation Research Board, 1977.
80. Vijayvergiya, V. N. and J. A. Focht, A new way to predict the capacity of piles in clay, *Offshore Technology Conference,* Vol. 2, Houston, TX, 1972, 965–874.
81. Vijayvergiya, V. N., Load-movement characteristics of piles, *Proc. of Ports '77 Conf.,* Long Beach, CA, 1977.
82. Welsh, R. C. and Reese, L. C., Laterally Loaded Behavior of Drilled Shafts, Research Report No. 3-5-65-89, conducted for Texas Highway Department and U.S. Department of Transportation, Federal Highway Administration, Bureau of Public Roads, by Center for Highway Research, the University of Texas at Austin, May, 1972.
83. Weltman, A. J. and P. R. Healy, Piling in boulder clay and other glacial tills, *Construction Industry Research and Information Association,* Report PG5, 1978.
84. Williams, A. F., I. W. Johnson, and I. B. Donald, The Design of Socketed Piles in Weak Rock, *Structural Foundations on Rock, Proc. Int. Conf. on Structural Found. on Rock*, Vol. 1, Sydney, May 7–9, 1980, 327–347.
85. Woodward, R. J., W. S. Gardner, and D. M. Greer, *Drilled Pier Foundations,* McGraw-Hill, New York, 1972.
86. Reese, L. C., Analysis of Laterally Loaded Piles in Weak Rock, *J. of Geotech & Geoenvironmental Engr.*, Vol. 123, No., 11, 1010–1017, 1997.

8

Effective Length of Compression Members*

Lian Duan
California Department of Transportation

Wai-Fah Chen
University of Hawaii at Manoa

8.1 Introduction

The concept of *effective length factor* or *K factor* plays an important role in compression member design. Although great efforts have been made in the past years to eliminate the *K* factor in column design, *K* factors are still popularly used in practice for routine design [1].

Mathematically, the effective length factor or the *elastic K* factor is defined as

$$K = \sqrt{\frac{P_e}{P_{cr}}} = \sqrt{\frac{\pi^2 E I}{L^2 P_{cr}}} \tag{8.1}$$

where P_e is Euler load, elastic buckling load of a pin-ended column, P_{cr} is elastic buckling load of an end-restrained framed column, E is modulus of elasticity, I is moment of inertia in the flexural buckling plane, and L is unsupported length of column.

*Much of the material of this chapter was taken from Duan, L. and Chen, W. F., Chapter 17: Effective length factors of compression members, in *Handbook of Structural Engineering,* Chen, W. F., Ed., CRC Press, Boca Raton, FL, 1997.

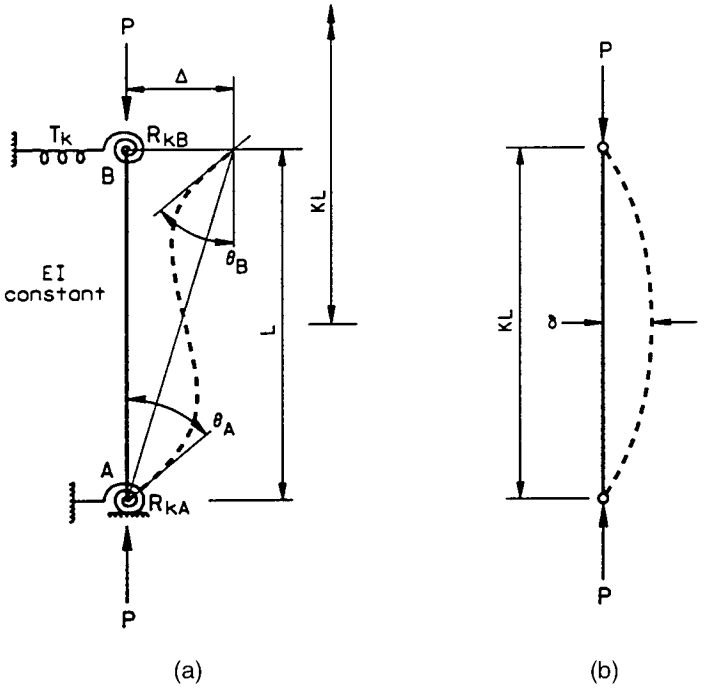

FIGURE 8.1 Isolated columns. (a) End-restrained columns; (b) pin-ended columns.

Physically, the *K* factor is a factor that, when multiplied by actual length of the end-restrained column (Figure 8.1a), gives the length of an equivalent pin-ended column (Figure 8.1b) whose buckling load is the same as that of the end-restrained column. It follows that the *effective length KL* of an end-restrained column is the length between adjacent inflection points of its pure flexural buckling shape.

Practically, design specifications provide the resistance equations for pin-ended columns, while the resistance of framed columns can be estimated through the *K* factor to the pin-ended column strength equations. Theoretical *K* factor is determined from an elastic eigenvalue analysis of the entire structural system, while practical methods for the *K* factor are based on an elastic eigenvalue analysis of selected subassemblages. This chapter presents the state-of-the-art engineering practice of the effective length factor for the design of columns in bridge structures.

8.2 Isolated Columns

From an eigenvalue analysis, the general *K* factor equation of an end-restrained column as shown in Figure 8.1 is obtained as

$$\det \begin{vmatrix} C+\dfrac{R_{kA}L}{EI} & S & -(C+S) \\ S & C+\dfrac{R_{kB}L}{EI} & -(C+S) \\ -(C+S) & -(C+S) & 2(C+S)-\left(\dfrac{\pi}{K}\right)^2+\dfrac{T_k L^3}{EI} \end{vmatrix} = 0 \tag{8.2}$$

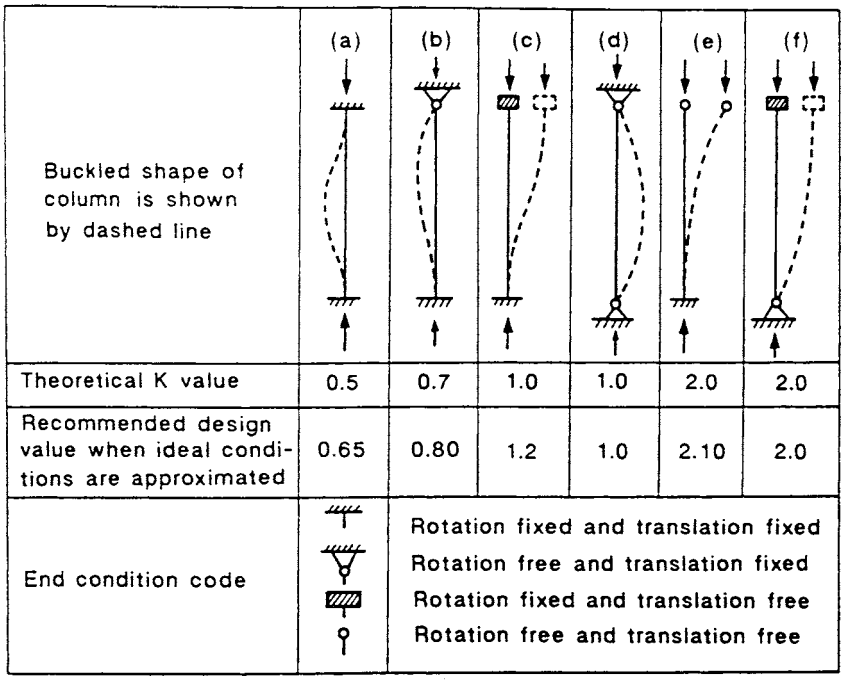

FIGURE 8.2 Theoretical and recommended *K* factors for isolated columns with idealized end conditions. (*Source:* American Institute of Steel Construction. *Load and Resistance Factor Design Specification for Structural Steel Buildings,* 2nd ed., Chicago, IL, 1993. With permission. Also from Johnston, B. G., Ed., Structural Stability Research Council, *Guide to Stability Design Criteria for Metal Structures,* 3rd ed., John Wiley & Sons, New York, 1976. With permission.)

where the stability function C and S are defined as

$$C = \frac{(\pi / K)\sin(\pi / K) - (\pi / K)^2 \cos(\pi / K)}{2 - 2\cos(\pi / K) - (\pi / K)\sin(\pi / K)} \tag{8.3}$$

$$S = \frac{(\pi / K)^2 - (\pi / K)\sin(\pi / K)}{2 - 2\cos(\pi / K) - (\pi / K)\sin(\pi / K)} \tag{8.4}$$

The largest value of K satisfying Eq. (8.2) gives the elastic buckling load of an end-retrained column.

Figure 8.2 summarizes the theoretical K factors for columns with some idealized end conditions [2,3]. The recommended K factors are also shown in Figure 8.2 for practical design applications. Since actual column conditions seldom comply fully with idealized conditions used in buckling analysis, the recommended K factors are always equal or greater than their theoretical counterparts.

8.3 Framed Columns — Alignment Chart Method

In theory, the effective length factor K for any columns in a framed structure can be determined from a stability analysis of the entire structural analysis — eigenvalue analysis. Methods available for stability analysis include slope–deflection method [4], three-moment equation method [5], and energy methods [6]. In practice, however, such analysis is not practical, and simple models are often used to determine the effective length factors for framed columns [7~10]. One such practical procedure that provides an approximate value of the elastic K factor is the alignment chart method [11]. This procedure has been adopted by the AASHTO [2] and AISC [3]. Specifications and the

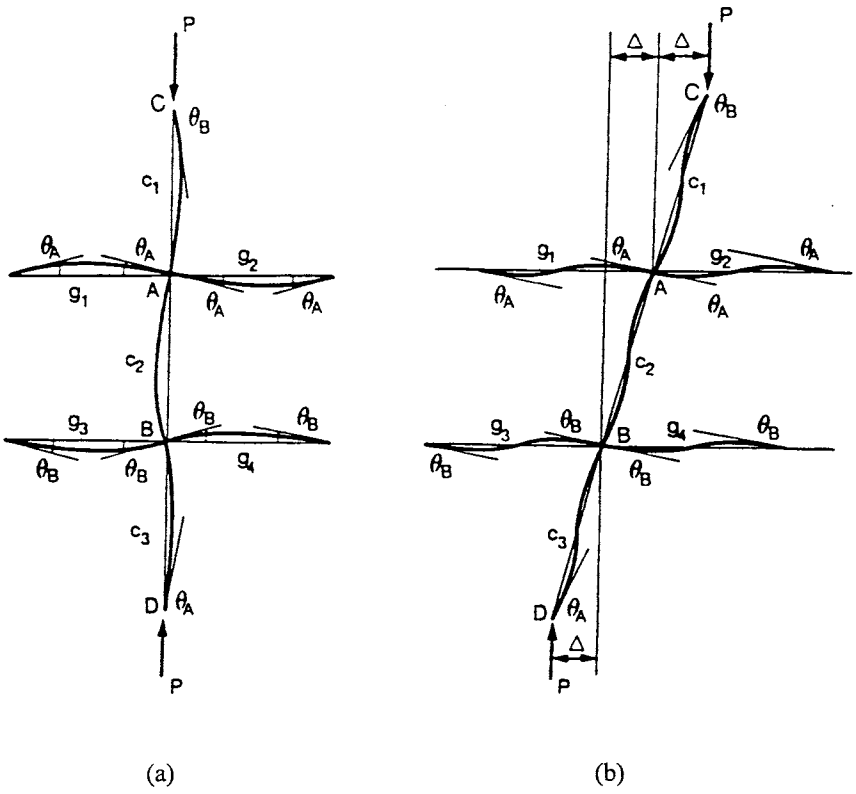

FIGURE 8.3 Subassemblage models for *K* factors of framed columns. (a) Braced frames; (b) unbraced frames.

ACI-318-95 Code [12], among others. At present, most engineers use the alignment chart method in lieu of an actual stability analysis.

8.3.1 Alignment Chart Method

The structural models employed for determination of *K* factors for framed columns in the alignment chart method are shown in Figure 8.3 The assumptions [2,4] used in these models are:

1. All members have constant cross section and behave elastically.
2. Axial forces in the girders are negligible.
3. All joints are rigid.
4. For braced frames, the rotations at near and far ends of the girders are equal in magnitude and opposite in direction (i.e., girders are bent in single curvature).
5. For unbraced frames, the rotations at near and far ends of the girders are equal in magnitude and direction (i.e., girders are bent in double curvature).
6. The stiffness parameters, $L\sqrt{P/EI}$, of all columns are equal.
7. All columns buckle simultaneously.

By using the slope–deflection equation method and stability functions, the effective length factor equations of framed columns are obtained as follows:

For columns in braced frames:

$$\frac{G_A G_B}{4}(\pi/K)^2+\left(\frac{G_A+G_B}{2}\right)\left(1-\frac{\pi/K}{\tan(\pi/K)}\right)+\frac{2\tan(\pi/2K)}{\pi/K}-1=0 \tag{8.5}$$

For columns in unbraced frames:

$$\frac{G_A G_B(\pi / K)^2 - 36}{6(G_A + G_B)} - \frac{\pi / K}{\tan(\pi / K)} = 0 \tag{8.6}$$

where G is stiffness ratios of columns and girders, subscripts A and B refer to joints at the two ends of the column section being considered, and G is defined as

$$G = \frac{\sum (E_c I_c / L_c)}{\sum (E_g I_g / L_g)} \tag{8.7}$$

where Σ indicates a summation of all members rigidly connected to the joint and lying in the plane in which buckling of the column is being considered; subscripts c and g represent columns and girders, respectively.

Eqs. (8.5) and (8.6) can be expressed in form of alignment charts as shown in Figure 8.4. It is noted that for columns in braced frames, the range of K is $0.5 \le K \le 1.0$; for columns in unbraced frames, the range is $1.0 \le K \le \infty$. For column ends supported by but not rigidly connected to a footing or foundations, G is theoretically infinity, but, unless actually designed as a true friction-free pin, may be taken as 10 for practical design. If the column end is rigidly attached to a properly designed footing, G may be taken as 1.0.

Example 8.1

Given

A four-span reinforced concrete bridge is shown in Figure 8.5. Using the alignment chart, determine the K factor for Column DC. $E = 25{,}000$ MPa.

Section properties are

Superstructure:	$I = 3.14\ (10^{12})$ mm^4	$A = 5.86\ (10^6)$ mm^2
Columns:	$I = 3.22\ (10^{11})$ mm^4	$A = 2.01\ (10^6)$ mm^2

Solution

1. **Calculate *G* factor for Column DC.**

$$G_D = \frac{\sum_D (E_c I_c / L_c)}{\sum_D (E_g I_g / L_g)} = \frac{3.22(10^{12}) / 12{,}000}{2(3.14)(10^{12}) / 55{,}000} = 0.235$$

$$G_D = 1.0 \quad \text{(Ref. [3])}$$

2. **From the alignment chart in Figure 8.4b, $K = 1.21$ is obtained.**

8.3.2 Requirements for Braced Frames

In stability design, one of the major decisions engineers have to make is the determination of whether a frame is braced or unbraced. The AISC-LRFD [3] states that a frame is braced when "lateral stability is provided by diagonal bracing, shear walls or equivalent means." However, there is no specific provision for the "amount of stiffness required to prevent sidesway buckling" in the AISC, AASHTO, and other specifications. In actual structures, a completely braced frame seldom exists.

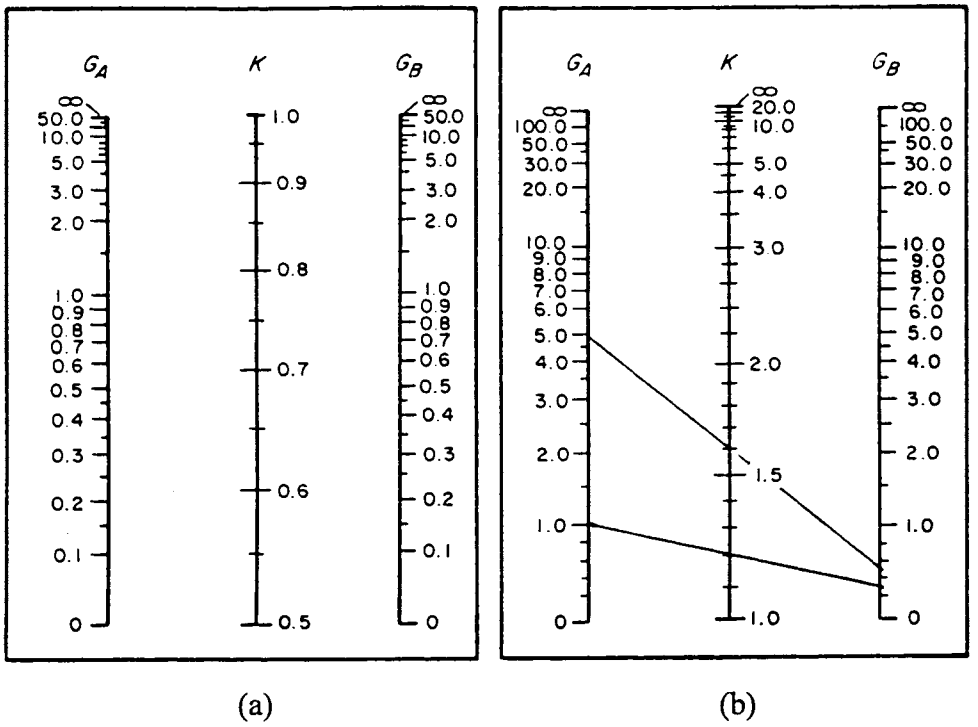

FIGURE 8.4 Alignment charts for effective length factors of framed columns. (a) Braced frames; (b) unbraced frames. (*Source:* American Institute of Steel Construction, *Load and Resistance Factor Design Specifications for Structural Steel Buildings,* 2nd ed., Chicago, IL, 1993. With permission. Also from Johnston, B. G., Ed., Structural Stability Research Council, *Guide to Stability Design Criteria for Metal Structures,* 3rd ed., John Wiley & Sons, New York, 1976. With permission.)

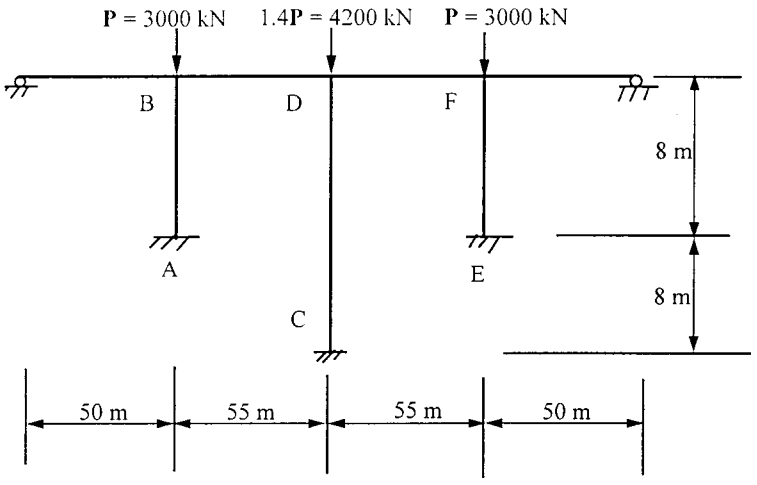

FIGURE 8.5 A four-span reinforced concrete bridge.

But in practice, some structures can be analyzed as braced frames as long as the lateral stiffness provided by bracing system is large enough. The following brief discussion may provide engineers with the tools to make engineering decisions regarding the basic requirements for a braced frame.

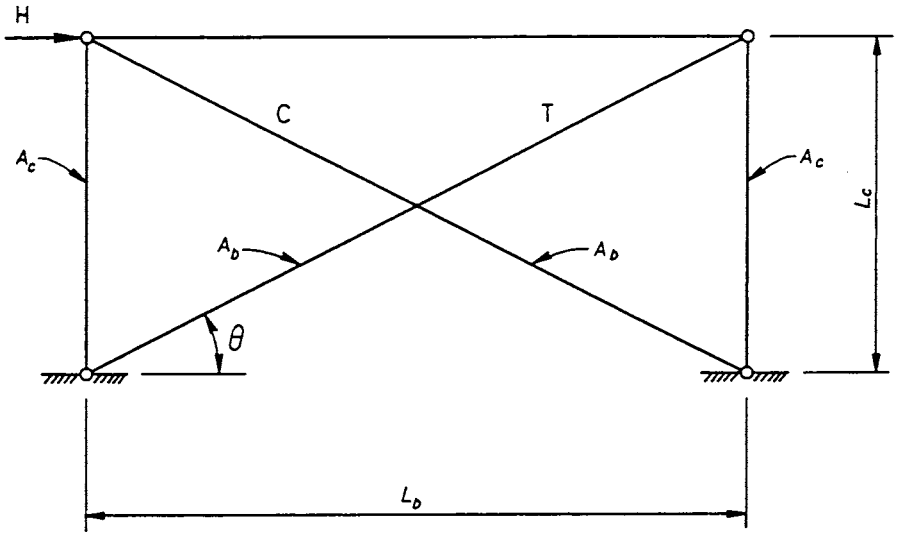

FIGURE 8.6 Diagonal cross-bracing system.

8.3.2.1 Lateral Stiffness Requirement

Galambos [13] presented a simple conservative procedure to estimate the minimum lateral stiffness provided by a bracing system so that the frame is considered braced.

$$\text{Required Lateral Stiffness } T_k = \frac{\sum P_n}{L_c} \tag{8.8}$$

where $\sum$ represents summation of all columns in one story, P_n is nominal axial compression strength of column using the effective length factor $K = 1$, and L_c is unsupported length of the column.

8.3.2.2 Bracing Size Requirement

Galambos [13] employed Eq. (8.8) to a diagonal bracing (Figure 8.6) and obtained minimum requirements of diagonal bracing for a braced frame as

$$A_b = \frac{\left[1 + (L_b / L_c)^2\right]^{3/2} \sum P_n}{(L_b / L_c)^2 E} \tag{8.9}$$

where A_b is cross-sectional area of diagonal bracing and L_b is span length of beam.

A recent study by Aristizabal-Ochoa [14] indicates that the size of diagonal bracing required for a totally braced frame is about 4.9 and 5.1% of the column cross section for "rigid frame" and "simple farming," respectively, and increases with the moment inertia of the column, the beam span, and with beam to column span ratio L_b/L_c.

8.3.3 Simplified Equations to Alignment Charts

8.3.3.1. Duan–King–Chen Equations

A graphical alignment chart determination of the K factor is easy to perform, while solving the chart Eqs. (8.5) and (8.6) always involves iteration. To achieve both accuracy and simplicity for design purpose, the following alternative K factor equations were proposed by Duan, King, and Chen [15].

For braced frames:

$$K = 1 - \frac{1}{5 + 9G_A} - \frac{1}{5 + 9G_B} - \frac{1}{10 + G_A G_B} \tag{8.10}$$

For unbraced frames:

$$\text{For } K < 2 \qquad K = 4 - \frac{1}{1 + 0.2G_A} - \frac{1}{1 + 0.2G_B} - \frac{1}{1 + 0.01G_A G_B} \tag{8.11}$$

$$\text{For } K \geq 2 \qquad K = \frac{2\pi a}{0.9 + \sqrt{0.81 + 4ab}} \tag{8.12}$$

where

$$a = \frac{G_A G_B}{G_A + G_B} + 3 \tag{8.13}$$

$$b = \frac{36}{G_A + G_B} + 6 \tag{8.14}$$

8.3.3.2 French Equations

For braced frames:

$$K = \frac{3G_A G_B + 1.4(G_A + G_B) + 0.64}{3G_A G_B + 2.0(G_A + G_B) + 1.28} \tag{8.15}$$

For unbraced frames:

$$K = \sqrt{\frac{1.6G_A G_B + 4.0(G_A + G_B) + 7.5}{G_A + G_B + 7.5}} \tag{8.16}$$

Eqs. (8.15) and (8.16) first appeared in the French Design Rules for Steel Structure [16] in 1966, and were later incorporated into the *European Recommendations for Steel Construction*[17]. They provide a good approximation to the alignment charts [18].

8.4 Modifications to Alignment Charts

In using the alignment charts in Figure 8.4 and Eqs. (8.5) and (8.6), engineers must always be aware of the assumptions used in the development of these charts. When actual structural conditions differ from these assumptions, unrealistic design may result [3,19,20]. SSRC Guide [19] provides methods enabling engineers to make simple modifications of the charts for some special conditions, such as, for example, unsymmetrical frames, column base conditions, girder far-end conditions, and flexible conditions. A procedure that can be used to account for far ends of restraining columns being hinged or fixed was proposed by Duan and Chen [21~23], and Essa [24]. Consideration of effects of material inelasticity on the K factor for steel members was developed originally by Yura

[25] and expanded by Disque [26]. LeMessurier [27] presented an overview of unbraced frames with or without leaning columns. An approximate procedure is also suggested by AISC-LRFD [3]. Several commonly used modifications for bridge columns are summarized in this section.

8.4.1 Different Restraining Girder End Conditions

When the end conditions of restraining girders are not rigidly jointed to columns, the girder stiffness (I_g/L_g) used in the calculation of G factor in Eq. (8.7) should be multiplied by a modification factor α_k given below:

For a braced frame:

$$\alpha_k = \begin{Bmatrix} 1.0 & \text{rigid far end} \\ 2.0 & \text{fixed far end} \\ 1.5 & \text{hinged far end} \end{Bmatrix} \tag{8.17}$$

For a unbraced frame:

$$\alpha_k = \begin{Bmatrix} 1.0 & \text{rigid far end} \\ 2/3 & \text{fixed far end} \\ 0.5 & \text{hinged far end} \end{Bmatrix} \tag{8.18}$$

8.4.2 Consideration of Partial Column Base Fixity

In computing the K factor for monolithic connections, it is important to evaluate properly the degree of fixity in foundation. The following two approaches can be used to account for foundation fixity.

8.4.2.1. Fictitious Restraining Beam Approach

Galambos [28] proposed that the effect of partial base fixity can be modeled as a fictitious beam. The approximate expression for the stiffness of the fictitious beam accounting for rotation of foundation in the soil has the form:

$$\frac{I_s}{L_B} = \frac{q\,BH^3}{72\,E_{\text{steel}}} \tag{8.19}$$

where q is modulus of subgrade reaction (varies from 50 to 400 lb/in.^{3}, 0.014 to 0.109 N/mm^3); B and H are width and length (in bending plane) of foundation, and E_{steel} is modulus of elasticity of steel.

Based on Salmon et al. [29] studies, the approximate expression for the stiffness of the fictitious beam accounting for the rotations between column ends and footing due to deformation of base plate, anchor bolts, and concrete can be written as

$$\frac{I_s}{L_B} = \frac{b\,d^2}{72\,E_{\text{steel}} / E_{\text{concrete}}} \tag{8.20}$$

where b and d are width and length of the base plate, subscripts concrete and steel represent concrete and steel, respectively. Galambos [28] suggested that the smaller of the stiffness calculated by Eqs. (8.25) and (8.26) be used in determining K factors.

8.4.2.2 AASHTO-LRFD Approach

The following values are suggested by AASHTO-LRFD [2]:

$G = 1.5$ footing anchored on rock
$G = 3.0$ footing not anchored on rock
$G = 5.0$ footing on soil
$G = 1.0$ footing on multiple rows of end bearing piles

Example 8.2

Given
Determine K factor for the Column AB as shown in Figure 8.5 by using the alignment chart with the necessary modifications. Section and material properties are given in Example 8.1 and spread footings are on soil.

Solution

1. **Calculate G factor with Modification for Column AB.**
   Since the far end of restraining girders are hinged, girder stiffness should be multiplied by 0.5. Using section properties in Example 8.1, we obtain:

$$G_B = \frac{\sum_B (E_c I_c / L_c)}{\sum_B \alpha_k (E_g I_g / L_g)}$$

$$= \frac{3.22(10^{12})/8{,}000}{(3.14)(10^{12})/55{,}000 + 0.5(3.14)(10^{12})/50{,}000} = 0.454$$

$$G = 5.0_A \quad \text{(Ref. [2])}$$

2. **From the alignment chart in Figure 8.4b, $K = 1.60$ is obtained.**

8.4.3 Column Restrained by Tapered Rectangular Girders

A modification factor α_T was developed by King et al. [30] for those framed columns restrained by tapered rectangular girders with different far-end conditions. The following modified G factor is introduced in connection with the use of alignment charts:

$$G = \frac{\sum (E_c I_c / L_c)}{\sum \alpha_T (E_g I_g / L_g)} \tag{8.21}$$

where I_g is moment of inertia of the girder at the near end. Both closed-form and approximate solutions for modification factor α_T were derived. It is found that the following two-parameter power-function can describe the closed-form solutions very well:

$$\alpha_T = \alpha_k (1 - r)^{\beta} \tag{8.22}$$

in which the parameter α_k is a constant (Eqs. 8.17 and 8.18) depending on the far-end conditions, and β is a function of far-end conditions and tapering factor a and r as defined in Figure 8.7.

1. For a linearly tapered rectangular girder (Figure 8.7a):

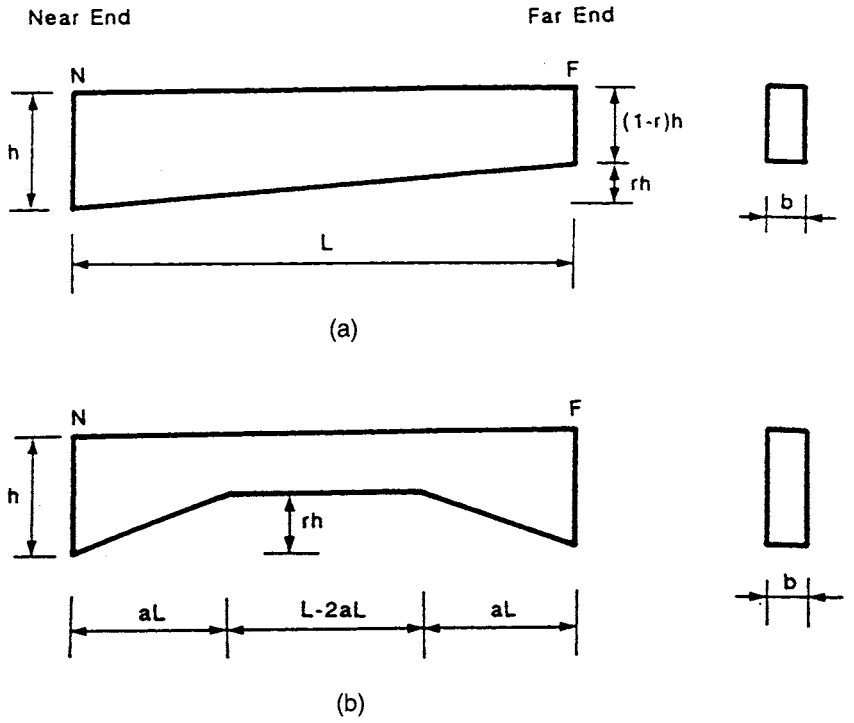

FIGURE 8.7 Tapered rectangular girders: (a) linearly tapered girder. (b) symmetrically tapered girder.

For a braced frame:

$$\beta = \begin{Bmatrix} 0.02 + 0.4r & \text{rigid far end} \\ 0.75 - 0.1r & \text{fixed far end} \\ 0.75 - 0.1r & \text{hinged far end} \end{Bmatrix} \tag{8.23}$$

For an unbraced frame:

$$\beta = \begin{Bmatrix} 0.95 & \text{rigid far end} \\ 0.70 & \text{fixed far end} \\ 0.70 & \text{hinged far end} \end{Bmatrix} \tag{8.24}$$

2. For a symmetrically tapered rectangular girder (Figure 8.7b)
For a braced frame:

$$\beta = \begin{Bmatrix} 3 - 1.7a^2 - 2a & \text{rigid far end} \\ 3 + 2.5a^2 - 5.55a & \text{fixed far end} \\ 3 - a^2 - 2.7a & \text{hinged far end} \end{Bmatrix} \tag{8.25}$$

For an unbraced frame:

$$\beta = \begin{Bmatrix} 3 + 3.8a^2 - 6.5a & \text{rigid far end} \\ 3 + 2.3a^2 - 5.45a & \text{fixed far end} \\ 3 - 0.3a & \text{hinged far end} \end{Bmatrix} \tag{8.26}$$

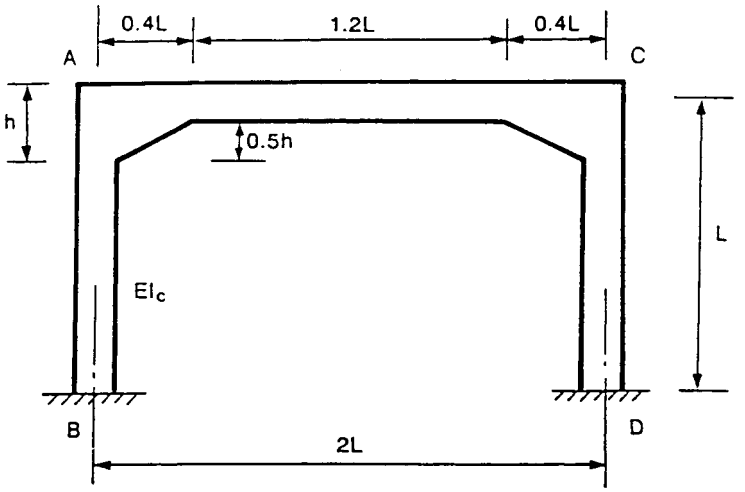

FIGURE 8.8 A simple frame with rectangular sections.

Example 8.3

Given
A one-story frame with a symmetrically tapered rectangular girder is shown in Figure 8.8. Assuming $r = 0.5$, $a = 0.2$, and $I_g = 2I_c = 2I$, determine K factor for Column AB.

Solution

1. **Use the Alignment Chart with Modification**
   For joint A, since the far end of girder is rigid, use Eqs. (8.26) and (8.22)

$$\beta = 3 + 3.8(0.2)^2 - 6.5(0.2) = 1.852$$

$$\alpha_T = (1 - 0.5)^{1.852} = 0.277$$

$$G_A = \frac{\sum E_c I_c / L_c}{\sum \alpha_T E_g I_g / L_g} = \frac{EI/L}{0.277\ E(2I)/2L} = 3.61$$

$$G_B = 1.0 \quad \text{(Ref. [3])}$$

   From the alignment chart in Figure 8.4b, $K = 1.59$ is obtained

2. **Use the Alignment Chart without Modification**
   A direct use of Eq. (8.7) with an average section $(0.75h)$ results in

$$I_g = 0.75^3\,(2\,I) = 0.844\,I$$

$$G_A = \frac{EI\,/\,L}{0.844\,EI\,/\,2L} = 2.37$$

$$G_B = 1.0$$

   From the alignment chart in Figure 8.4b, $K = 1.50$, *or* $(1.50 - 1.59)/1.59 = -6\%$ in error on the less conservative side.

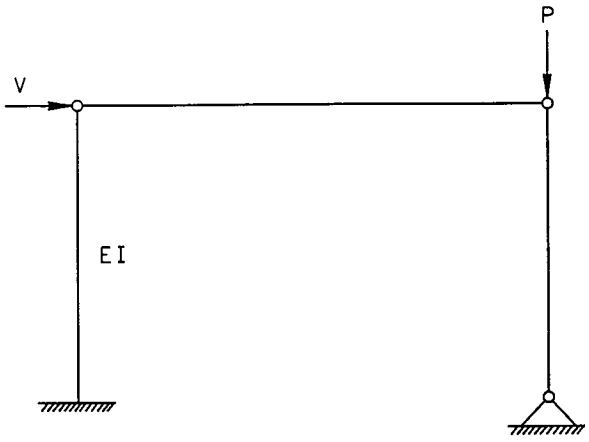

FIGURE 8.9 Subassemblage of LeMessurier method.

8.5 Framed Columns — Alternative Methods

8.5.1 LeMessurier Method

Considering that all columns in a story buckle simultaneously and strong columns will brace weak columns (Figure 8.9), a more accurate approach to calculate K factors for columns in a side-sway frame was developed by LeMessurier [27]. The K_i value for the ith column in a story can be obtained by the following expression:

$$K_i = \sqrt{\frac{\pi^2 EI_i}{L_i^2 P_i}\left(\frac{\sum P + \sum C_L P}{\sum P_L}\right)} \tag{8.27}$$

where P_i is axial compressive force for member i, and subscript i represents the ith column and ΣP is the sum of axial force of all columns in a story.

$$P_L = \frac{\beta EI}{L^2} \tag{8.28}$$

$$\beta = \frac{6(G_A + G_B) + 36}{2(G_A + G_B) + G_A G_B + 3} \tag{8.29}$$

$$C_L = \left(\beta \frac{K_o^2}{\pi^2} - 1\right) \tag{8.30}$$

in which K_o is the effective length factor obtained by the alignment chart for unbraced frames and P_L is only for those columns that provide side-sway stiffness.

Example 8.4

Given
Determine K factors for bridge columns shown in Figure 8.5 by using the LeMessurier method. Section and material properties are given in Example 8.1.

TABLE 8.1 Example 8.4 — Detailed Calculations by LeMessurier Method

Members	AB and EF	CD	Sum	Notes
I (mm$^4 \times 10^{11}$)	3.217	3.217	—	
L (mm)	8,000	12,000	—	
G_{top}	0.454	0.235	—	Eq. (8.7)
G_{bottom}	0.0	0.0	—	Eq. (8.7)
β	9.91	10.78	—	Eq. (8.29)
K_{io}	1.082	1.045	—	Alignment chart
C_L	0.176	0.193	—	Eq. (8.30)
P_L	50,813E	24,083E	123,709E	Eq. (8.28)
P	P	1.4P	3.4P	P = 3,000 kN
C_LP	0.176P	0.270P	0.622P	P = 3,000 kN

Solutions
The detailed calculations are listed in Table 8.1 By using Eq. (8.32), we obtain:

$$K_{AB} = \sqrt{\frac{\pi^2 EI_{AB}}{L_{AB}^2 P_{AB}}\left(\frac{\sum P + \sum C_L P}{\sum P_L}\right)}$$

$$= \sqrt{\frac{\pi^2 E(3.217)(10^{11})}{(8.000)^2 (P)}\left(\frac{3.4P + 0.622P}{123,709\,E}\right)} = 1.270$$

$$K_{CD} = \sqrt{\frac{\pi^2 EI_{CD}}{L_{CD}^2 P_{CD}}\left(\frac{\sum P + \sum C_L P}{\sum P_L}\right)}$$

$$= \sqrt{\frac{\pi^2 E(3.217)(10^{11})}{(12,000)^2 (1.4P)}\left(\frac{3.4P + 0.622P}{123,709\,E}\right)} = 0.715$$

8.5.2 Lui Method

A simple and straightforward approach for determining the effective length factors for framed columns without the use of alignment charts and other charts was proposed by Lui [31]. The formulas take into account both the member instability and frame instability effects explicitly. The K factor for the ith column in a story was obtained in a simple form:

$$K_i = \sqrt{\left(\frac{\pi^2 E I_i}{P_i L_i^2}\right)\left[\left(\sum \frac{P}{L}\right)\left(\frac{1}{5\sum \eta} + \frac{\Delta_1}{\sum H}\right)\right]} \tag{8.31}$$

where $\Sigma(P/L)$ represents the sum of axial-force-to-length ratio of all members in a story; ΣH is the story lateral load producing Δ_1, Δ_1 is the first-order interstory deflection; η is member stiffness index and can be calculated by

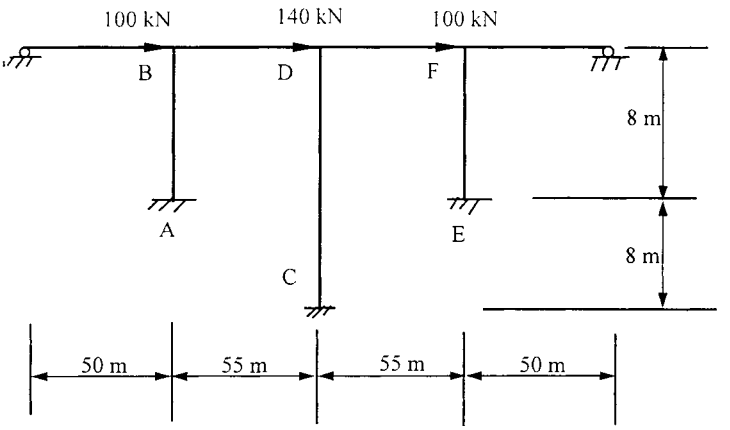

FIGURE 8.10 A bridge structure subjected to fictitious lateral loads.

TABLE 8.2 Example 8.5 — Detailed Calculations by Lui Method

Members	AB and EF	CD	Sum	Notes
I (mm$^4 \times 10^{11}$)	3.217	3.217	—	
L (mm)	8,000	12,000	—	
H (kN)	150	210	510	
Δ_I (mm)	0.00144	0.00146	—	
$\Delta_I / \Sigma H$ (mm/kN)	—	—	2.843 (10^{-6})	Average
M_{top} (kN-m)	–476.9	–785.5	—	
M_{bottom} (kN-m)	–483.3	–934.4	—	
m	0.986	0.841	—	
η (kN/mm)	185,606	46,577	417,789	Eq. (8.32)
P/L (kN/mm)	P/8,000	1.4 P/12,000	1.1P/3,000	P = 3,000 kN

$$\eta = \frac{(3 + 4.8m + 4.2m^2)EI}{L^3} \tag{8.32}$$

in which m is the ratio of the smaller to larger end moments of the member; it is taken as positive if the member bends in reverse curvature, and negative for single curvature.

It is important to note that the term ΣH used in Eq. (8.36) is not the actual applied lateral load. Rather, it is a small disturbing or fictitious force (taken as a fraction of the story gravity loads) to be applied to each story of the frame. This fictitious force is applied in a direction such that the deformed configuration of the frame will resemble its buckled shape.

Example 8.5

Given

Determine the K factors for bridge columns shown in Figure 8.5 by using the Lui method. Section and material properties are given in Example 8.1.

Solutions

Apply fictitious lateral forces at B, D, and F (Figure 8.10) and perform a first-order analysis. Detailed calculation is shown in Table 8.2.

By using Eq. (8.31), we obtain

$$K_{AB} = \sqrt{\left(\frac{\pi^2 E I_{AB}}{P_{AB} L_{AB}^2}\right)\left[\left(\sum \frac{P}{L}\right)\left(\frac{1}{5\sum \eta} + \frac{\Delta_1}{\sum H}\right)\right]}$$

$$= \sqrt{\left(\frac{\pi^2 (25{,}000)(3.217)(10^{11})}{P(8{,}000)^2}\right)\left[\left(\frac{1.1P}{3{,}000}\right)\left(\frac{1}{5(417{,}789)} + 2.843(10^{-6})\right)\right]}$$

$$= 1.229$$

$$K_{CD} = \sqrt{\left(\frac{\pi^2 E I_{CD}}{P_{CD} L_{CD}^2}\right)\left[\left(\sum \frac{P}{L}\right)\left(\frac{1}{5\sum \eta} + \frac{\Delta_1}{\sum H}\right)\right]}$$

$$= \sqrt{\left(\frac{\pi^2 (25{,}000)(3.217)(10^{11})}{1.4P(12{,}000)^2}\right)\left[\left(\frac{1.1P}{3{,}000}\right)\left(\frac{1}{5(417{,}789)} + 2.843(10^{-6})\right)\right]}$$

$$= 0.693$$

8.5.3 Remarks

For a comparison, Table 8.3 summarizes the *K* factors for the bridge columns shown in Figure 8.5 obtained from the alignment chart, LeMessurier and Lui methods, as well as an eigenvalue analysis. It is seen that errors of alignment chart results are rather significant in this case. Although the *K* factors predicted by Lui's formulas and LeMessurier's formulas are almost the same in most cases, the simplicity and independence of any chart in the case of Lui's formula make it more desirable for design office use [32].

TABLE 8.3 Comparison of *K* Factors for Frame in Figure 8.5

Columns	Theoretical	Alignment Chart	Lui Eq. (8.31)	LeMessurier Eq. (8.27)
AB	1.232	1.082	1.229	1.270
CD	0.694	1.045	0.693	0.715

8.6 Crossing Bracing Systems

Picard and Beaulieu [33,34] reported theoretical and experimental studies on double diagonal cross-bracings (Figure 8.6) and found that

1. A general effective length factor equation is given as

$$K = \sqrt{0.523 - \frac{0.428}{C/T}} \geq 0.50 \tag{8.33}$$

where *C* and *T* represent compression and tension forces obtained from an elastic analysis, respectively.

2. When the double diagonals are continuous and attached at an intersection point, the *effective length* of the compression diagonal is 0.5 times the diagonal length, i.e., $K = 0.5$, because the C/T ratio is usually smaller than 1.6.

El-Tayem and Goel [35] reported a theoretical and experimental study about the X-bracing system made from single equal-leg angles. They concluded that

1. Design of X-bracing system should be based on an exclusive consideration of one half diagonal only.
2. For X-bracing systems made from single equal-leg angles, an effective length of 0.85 times the half-diagonal length is reasonable, i.e., $K = 0.425$.

8.7 Latticed and Built-Up Members

It is a common practice that when a buckling model involves relative deformation produced by shear forces in the connectors, such as lacing bars and batten plates, between individual components, a modified effective length factor K_m or effective slenderness ratio $(KL/r)_m$ is used in determining the compressive strength. K_m is defined as

$$K_m = \alpha_v K \tag{8.34}$$

in which K is the usual effective length factor of a latticed member acting as a unit obtained from a structural analysis and α_v is the shear factor to account for the effect of shear deformation on the buckling strength. Details of the development of the shear factor α_v can be found in textbooks by Bleich [5] and Timoshenko and Gere [36]. The following section briefly summarizes α_v formulas for various latticed members.

8.7.1 Latticed Members

By considering the effect of shear deformation in the latticed panel on buckling load, shear factor α_v of the following form has been introduced:

Laced Compression Members (Figures 8.11a and b)

$$\alpha_v = \sqrt{1 + \frac{\pi^2 EI}{(KL)^2} \frac{d^3}{A_d E_d a b^2}} \tag{8.35}$$

Compression Members with Battens (Figure 8.11c)

$$\alpha_v = \sqrt{1 + \frac{\pi^2 EI}{(KL)^2} \left(\frac{ab}{12 E_b I_b} + \frac{a^2}{24 EI_f} \right)} \tag{8.36}$$

Laced-Battened Compression Members (Figure 8.11d)

$$\alpha_v = \sqrt{1 + \frac{\pi^2 E I}{(KL)^2} \left(\frac{d^3}{A_d E_d a b^2} + \frac{b}{a A_b E_b} \right)} \tag{8.37}$$

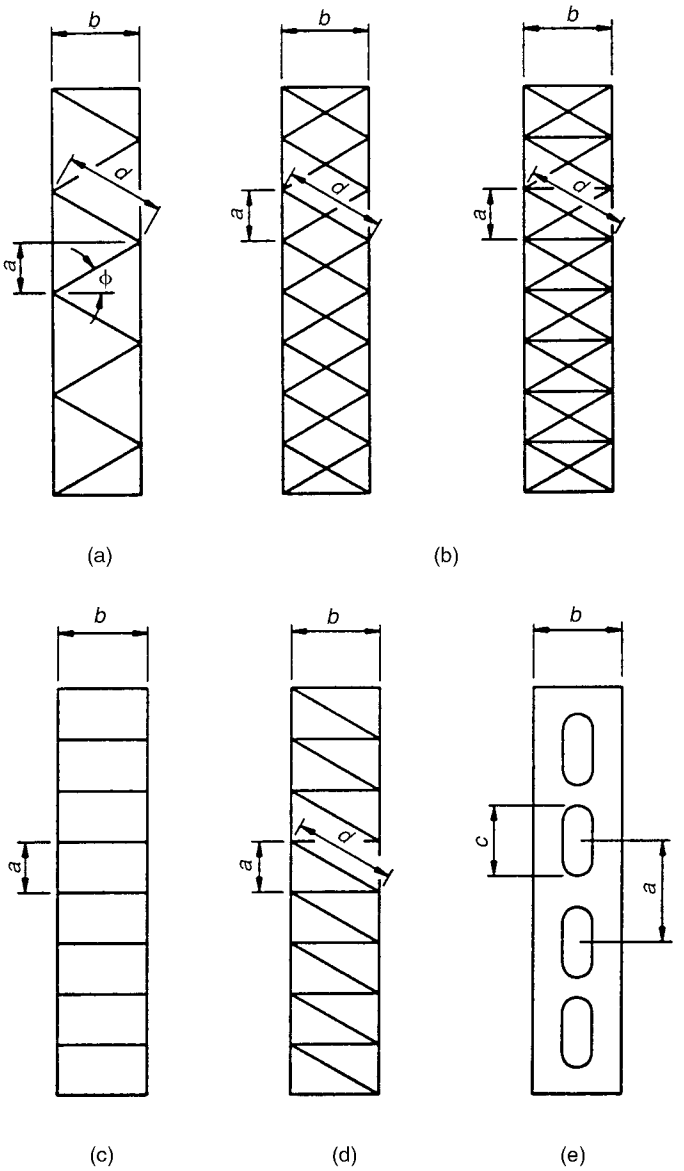

FIGURE 8.11 Typical configurations of latticed members: (a) single lacing; (b) double lacing; (c) battens; (d) lacing-battens; (e) perforated cover plates.

Compression Members with Perforated Cover Plates (Figure 8.11e)

$$\alpha_v = \sqrt{1 + \frac{\pi^2 EI}{(KL)^2}\left(\frac{9c^3}{64aEI_f}\right)} \tag{8.38}$$

where E_d is modulus of elasticity of materials for lacing bars; E_b is modulus of elasticity of materials for batten plates; A_d is cross-sectional area of all diagonals in one panel; I_b is moment inertia of all

battens in one panel in the buckling plane and I_f is moment inertia of one side of main components taken about the centroid axis of the flange in the buckling plane; *a, b, d* are height of panel, depth of member, and length of diagonal, respectively; and *c* is the length of a perforation.

The Structural Stability Research Council [37] suggested that a conservative estimating of the influence of 60° or 45° lacing, as generally specified in bridge design practice, can be made by modifying the overall effective length factor *K* by multiplying a factor α_v, originally developed by Bleich [5] as follows:

$$\text{For } \frac{KL}{r} > 40, \quad \alpha_v = \sqrt{1 + 300/(KL/r)^2} \tag{8.39}$$

$$\text{For } \frac{KL}{r} \le 40, \quad \alpha_v = 1.1 \tag{8.40}$$

It should be pointed out that the usual *K* factor based on a solid member analysis is included in Eqs. (8.35) through (8.38). However, since the latticed members studied previously have pin-ended conditions, the *K* factor of the member in the frame was not included in the second terms of the square root of the above equations in their original derivations [5,36].

8.7.5 Built-Up Members

AISC-LRFD [3] specifies that if the buckling of a built-up member produces shear forces in the connectors between individual component members, the usual slenderness ratio *KL*/*r* for compression members must be replaced by the modified slenderness ratio $(KL/r)_m$ in determining the compressive strength.

1. *For snug-tight bolted connectors*:

$$\left(\frac{KL}{r}\right)_m = \sqrt{\left(\frac{KL}{r}\right)_o^2 + \left(\frac{a}{r_i}\right)^2} \tag{8.41}$$

2. *For welded connectors and for fully tightened bolted connectors*:

$$\left(\frac{KL}{r}\right)_m = \sqrt{\left(\frac{KL}{r}\right)_o^2 + 0.82\frac{\alpha^2}{(1+\alpha^2)}\left(\frac{a}{r_{ib}}\right)^2} \tag{8.42}$$

where $(KL/r)_o$ is the slenderness ratio of built-up member acting as a unit, $(KL/r)_m$ is modified slenderness ratio of built-up member, a/r_i is the largest slenderness ratio of the individual components, a/r_{ib} is the slenderness ratio of the individual components relative to its centroidal axis parallel to axis of buckling, a is the distance between connectors, r_i is the minimum radius of gyration of individual components, r_{ib} is the radius of gyration of individual components relative to its centroidal axis parallel to member axis of buckling, α is the separation ratio = $h/2r_{ib}$, and h is the distance between centroids of individual components perpendicular to the member axis of buckling.

Eq. (8.41) is the same as that used in the current Italian code, as well as in other European specifications, based on test results [38]. In this equation, the bending effect is considered in the first term in square root, and shear force effect is taken into account in the second term. Eq. (8.42) was derived from elastic stability theory and verified by test data [39]. In both cases, the end connectors must be welded or slip-critical-bolted.

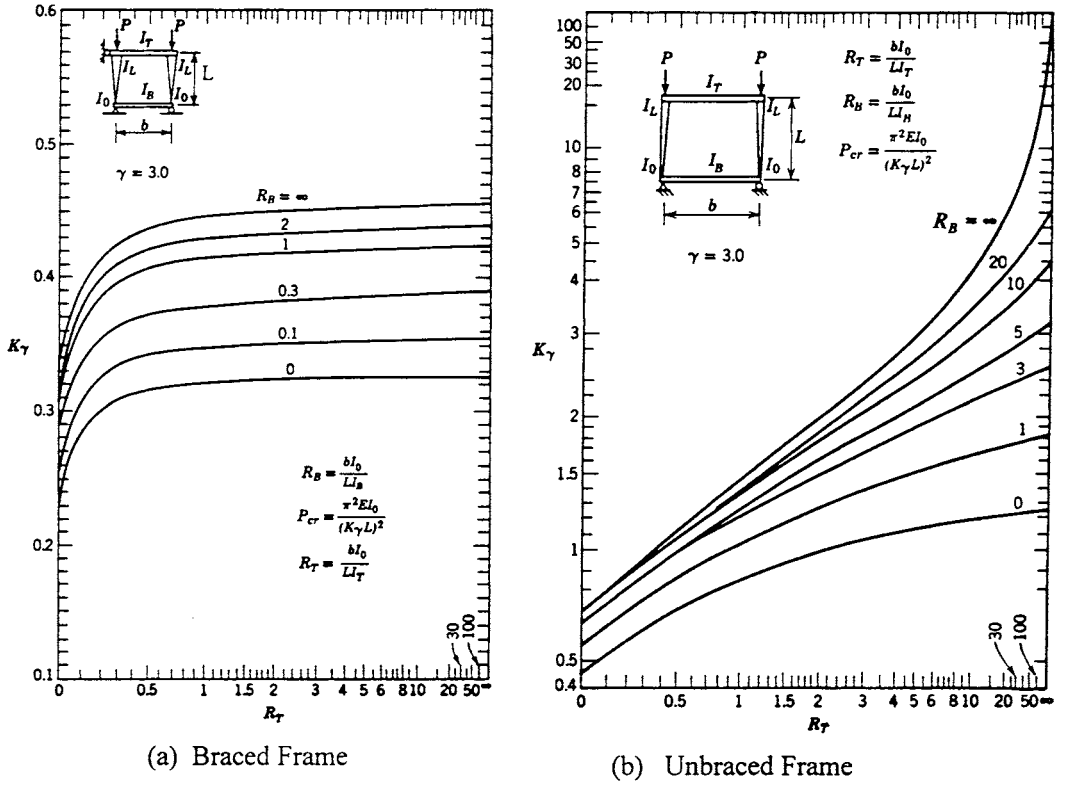

FIGURE 8.12 Effective length factor for tapered columns. (a) Braced frame; (b) unbraced frame. (*Source:* Galambos, T. V., Ed., *Structural Stability Research Council Guide to Stability Design Criteria for Metal Structures,* 4th ed., John Wiley & Sons, New York, 1988. With permission.)

8.8 Tapered Columns

The state-of-the-art design for tapered structural members was provided in the SSRC guide [37]. The charts as shown in Figure 8.12 can be used to evaluate the effective length factors for tapered column restrained by prismatic beams [37]. In these figures, I_T and I_B are the moment of inertia of top and bottom beam, respectively; b and L are length of beam and column, respectively; and γ is tapering factor as defined by

$$\gamma = \frac{d_1 - d_o}{d_o} \tag{8.43}$$

where d_o and d_1 are the section depth of column at the smaller and larger end, respectively.

8.9 Summary

This chapter summarizes the state-of-the-art practice of the effective length factors for isolated columns, framed columns, diagonal bracing systems, latticed and built-up members, and tapered columns. Design implementation with formulas, charts, tables, and various modification factors adopted in current codes and specifications, as well as those used in bridge structures, are

described. Several examples are given to illustrate the steps of practical applications of these methods.

References

1. McGuire, W., Computers and steel design, *Modern Steel Constr.*, 32(7), 39, 1992.
2. AASHTO, *LRFD Bridge Design Specifications*, American Association of State Highway and Transportation Officials, Washington, D.C., 1994.
3. AISC, *Load and Resistance Factor Design Specification for Structural Steel Buildings*, 2nd ed., American Institute of Steel Construction, Chicago, IL, 1993.
4. Chen, W. F. and Lui, E. M., *Stability Design of Steel Frames*, CRC Press, Boca Raton, FL, 1991.
5. Bleich, F., *Buckling Strength of Metal Structures*, McGraw-Hill, New York, 1952.
6. Johnson, D. E., Lateral stability of frames by energy method, *J. Eng. Mech. ASCE,* 95(4), 23, 1960.
7. Lu, L. W., A survey of literature on the stability of frames, *Weld. Res. Counc. Bull.*, New York, 1962.
8. Kavanagh, T. C., Effective length of framed column, *Trans. ASCE,* 127(II) 81, 1962.
9. Gurfinkel, G. and Robinson, A. R., Buckling of elasticity restrained column, *J. Struct. Div. ASCE,* 91(ST6), 159, 1965.
10. Wood, R. H., Effective lengths of columns in multi-storey buildings, *Struct. Eng.*, 50(7–9), 234, 295, 341, 1974.
11. Julian, O. G. and Lawrence, L. S., Notes on J and L Nomograms for Determination of Effective Lengths, unpublished report, 1959.
12. ACI, *Building Code Requirements for Structural Concrete* (ACI 318-95) and Commentary (ACI 318R-95), American Concrete Institute, Farmington Hills, MI, 1995.
13. Galambos, T. V., Lateral support for tier building frames, *AISC Eng. J.*, 1(1), 16, 1964.
14. Aristizabal-Ochoa, J. D., K-factors for columns in any type of construction: nonparadoxical approach, *J. Struct. Eng. ASCE,* 120(4), 1272, 1994.
15. Duan, L., King, W. S., and Chen, W. F., *K* factor equation to alignment charts for column design, *ACI Struct. J.*, 90(3), 242, 1993.
16. *Regles de Cacul des Constructions en acier,* CM66, Eyrolles, Paris, 1975.
17. ECCS, *European Recommendations for Steel Construction*, European Convention for Construction Steelworks, 1978.
18. Dumonteil, P., Simple equations for effective length factors, *AISC Eng. J.*, 29(3), 111, 1992.
19. Johnston, B. G., Ed., Structural Stability Research Council, *Guide to Stability Design Criteria for Metal Structures*, 3rd ed., John Wiley & Sons, New York, 1976.
20. Liew, J. Y. R., White, D. W., and Chen, W. F., Beam-column design in steel frameworks — insight on current methods and trends, *J. Constr. Steel. Res.,* 18, 269, 1991.
21. Duan, L. and Chen, W. F., Effective length factor for columns in braced frames, *J. Struct. Eng. ASCE,* 114(10), 2357, 1988.
22. Duan, L. and Chen, W. F., Effective length factor for columns in unbraced frames, *J. Struct. Eng. ASCE,* 115(1), 150, 1989.
23. Duan, L. and Chen, W. F., 1996. Errata of paper: effective length factor for columns in unbraced frames, *J. Struct. Eng. ASCE,* 122(1), 224, 1996.
24. Essa, H. S., Stability of columns in unbraced frames, *J. Struct. Eng., ASCE,* 123(7), 952, 1997.
25. Yura, J. A., The effective length of columns in unbraced frames, *AISC Eng. J.*, 8(2), 37, 1971.
26. Disque, R. O., Inelastic *K* factor in design, *AISC Eng. J.*, 10(2), 33, 1973.
27. LeMessurier, W. J., A practical method of second order analysis, part 2 — rigid frames, *AISC Eng. J.*, 14(2), 50, 1977.
28. Galambos, T. V., Influence of partial base fixity on frame instability, *J. Struct. Div.* ASCE, 86(ST5), 85, 1960.

29. Salmon, C. G., Schenker, L., and Johnston, B. G., Moment-rotation characteristics of column anchorage, *Trans. ASCE,* 122, 132, 1957.
30. King, W. S., Duan, L., Zhou, R. G., Hu, Y. X., and Chen, W. F., *K* factors of framed columns restrained by tapered girders in U.S. codes, *Eng. Struct.*, 15(5), 369, 1993.
31. Lui, E. M., A novel approach for K-factor determination. *AISC Eng. J.*, 29(4), 150, 1992.
32. Shanmugam, N. E. and Chen, W. F., An assessment of K factor formulas, *AISC Eng. J.*, 32(3), 3, 1995.
33. Picard, A. and Beaulieu, D., Design of diagonal cross bracings, part 1: theoretical study, *AISC Eng. J.*, 24(3), 122, 1987.
34. Picard, A. and Beaulieu, D., Design of diagonal cross bracings, part 2: experimental study, *AISC Eng. J.*, 25(4), 156, 1988.
35. El-Tayem, A. A. and Goel, S. C., Effective length factor for the design of X-bracing systems, *AISC Eng. J.*, 23(4), 41, 1986.
36. Timoshenko, S. P. and Gere, J. M., *Theory of Elastic Stability*, 2nd ed., McGraw-Hill, New York, 1961.
37. Galambos, T. V., Ed., *Structural Stability Research Council, Guide to Stability Design Criteria for Metal Structures*, 4th ed., John Wiley & Sons, New York, 1988.
38. Zandonini, R., Stability of compact built-up struts: experimental investigation and numerical simulation, *Constr. Met.*, 4, 1985 [in Italian].
39. Aslani, F. and Goel, S. C., An analytical criteria for buckling strength of built-up compression members, *AISC Eng. J.*, 28(4), 159, 1991.

9

Vessel Collision Design of Bridges

Michael Knott
Moffatt & Nichol Engineers

Zolan Prucz
Modjeski and Masters, Inc.

Notations

The following symbols are used in this chapter. The section number in parentheses after definition of a symbol refers to the section or figure number where the symbol first appears or is identified.

AF annual frequency of bridge element collapse (Section 9.5.2)
B_M beam (width) of vessel (Figure 9.2)
B_P width of bridge pier (Figure 9.2)
DWT size of vessel based on deadweight tonnage (one tonne = 2205 lbs = 9.80 kN) (Section 9.4.1)
H ultimate bridge element strength (Section 9.5.2)
N number of one-way vessel passages through the bridge (Section 9.5.2)
P vessel collision impact force (Section 9.5.2)
P_{BH} ship collision impact force for head-on collision between ship bow and a rigid object (Section 9.6.1)
P_{DH} ship collision impact force between ship deckhouse and a rigid superstructure (Section 9.6.1)

P_{MT} ship collision impact force between ship mast and a rigid superstructure (Section 9.6.1)
P_S ship collision impact force for head-on collision between ship bow and a rigid object (Section 9.6.1)
PA probability of vessel aberrancy (Section 9.5.2)
PC probability of bridge collapse (Section 9.5.2)
PG geometric probability of vessel collision with bridge element (Section 9.5.2)
R_{BH} ratio of exposed superstructure depth to the total ship bow depth (Section 9.6.1)
R_{DH} reduction factor for ship deckhouse collision force (Section 9.6.1)
V design impact speed of vessel (Section 9.6.1)
x distance to bridge element from the centerline of vessel transit path (Figure 9.2)
ϕ angle between channel and bridge centerlines (Figure 9.2)

9.1 Introduction

9.1.1 Background

It was only after a marked increase in the frequency and severity of vessel collisions with bridges that studies of the vessel collision problem have been initiated in recent years. In the period from 1960 to 1998, there have been 30 major bridge collapses worldwide due to ship or barge collision, with a total loss of life of 321 people. The greatest loss of life occurred in 1983 when a passenger ship collided with a railroad bridge on the Volga River, Russia; 176 were killed when the aberrant vessel attempted to transit through a side span of the massive bridge. Most of the deaths occurred when a packed movie theater on the top deck of the passenger ship was sheared off by the low vertical clearance of the bridge superstructure.

Of the bridge catastrophes mentioned above, 15 have occurred in the United States, including the 1980 collapse of the Sunshine Skyway Bridge crossing Tampa Bay, Florida, in which 396 m of the main span collapsed and 35 lives were lost as a result of the collision by an empty 35,000 DWT (deadweight tonnage) bulk carrier (Figure 9.1).

One of the more publicized tragedies in the United States involved the 1993 collapse of a CSX Railroad Bridge across Bayou Canot near Mobile, Alabama. During dense fog, a barge tow became lost and entered a side channel of the Mobile River where it struck a railroad bridge causing a large displacement of the structure. The bridge collapsed a few minutes later when a fully loaded Amtrak passenger train attempted to cross the damaged structure; 47 fatalities occurred as a result of the collapse and the train derailment.

It should be noted that there are numerous vessel collision accidents with bridges which cause significant damage, but do not necessarily result in collapse of the structure. A study of river towboat collisions with bridges located on the U.S. inland waterway system during the short period from 1970 to 1974 revealed that there were 811 accidents with bridges costing $23 million in damages and 14 fatalities. On the average, some 35 vessel collision incidents are reported every day to U.S. Coast Guard Headquarters in Washington, D.C.

A recent accident on a major waterway bridge occurred in Portland, Maine in September 1996 when a loaded tanker ship (171 m in length and 25.9 m wide) rammed the guide pile fender system of the existing Million Dollar Bridge over the Fore River. A large portion of the fender was destroyed; the flair of the ship's bow caused significant damage to one of the bascule leafs of the movable structure (causing closure of the bridge until repairs were made); and 170,000 gallons of fuel oil were spilled in the river due to a 9-m hole ripped in the vessel hull by an underwater protrusion of the concrete support pier (a small step in the footing). Although the main cause of the accident was attributed to pilot error, a contributing factor was certainly the limited horizontal clearance of the navigation opening through the bridge (only 29 m).

The 1980 collapse of the Sunshine Skyway Bridge was a major turning point in awareness and increased concern for the safety of bridges crossing navigable waterways. Important steps in the development of modern ship collision design principles and specifications include:

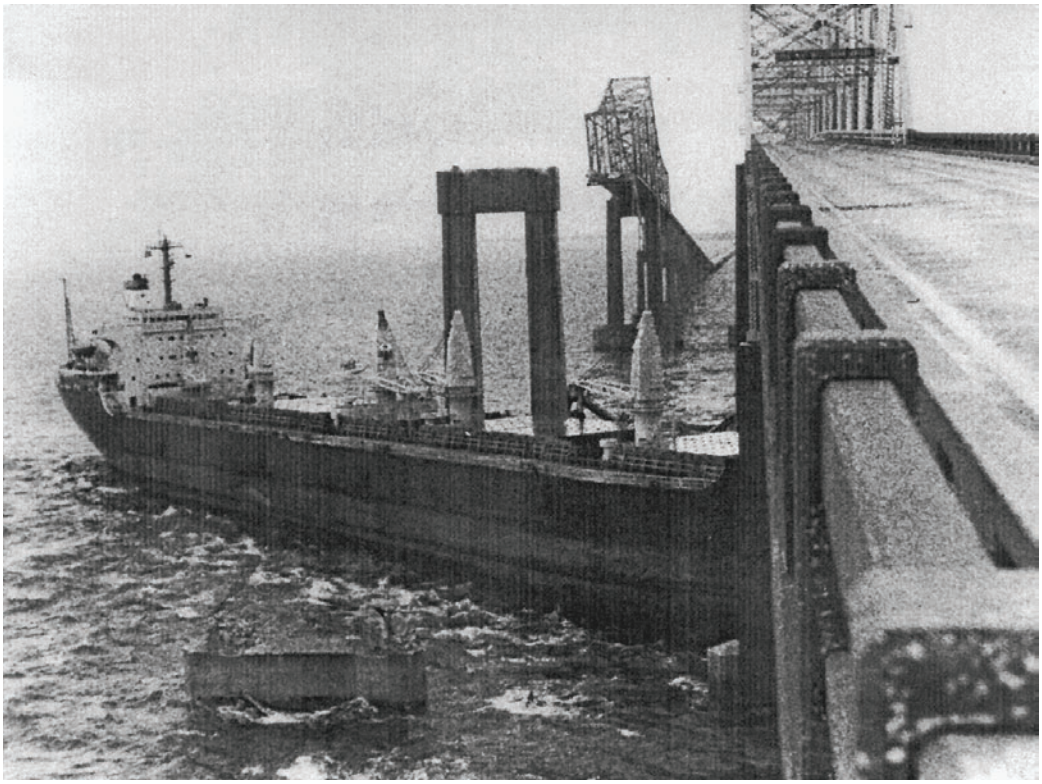

FIGURE 9.1 Sunshine Skyway Bridge, May 9, 1980 after being struck by the M/V *Summit Venture.*

- In 1983, a "Committee on Ship/Barge Collision," appointed by the Marine Board of the National Research Council in Washington, D.C., completed a study on the risk and consequences of ship collisions with bridges crossing navigable coastal waters in the United States [1].
- In June 1983, a colloquium on "Ship Collision with Bridges and Offshore Structures" was held in Copenhagen, Denmark under the auspices of the International Association for Bridge and Structural Engineering (IABSE), to bring together and disseminate the latest developments on the subject [2].
- In 1984, the Louisiana Department of Transportation and Development incorporated criteria for the design of bridge piers with respect to vessel collision for structures crossing waterways in the state of Louisiana [3,4].
- In 1988, a pooled-fund research project was sponsored by 11 states and the Federal Highway Administration to develop vessel collision design provisions applicable to all of the United States. The final report of this project [5] was adopted by AASHTO as a Vessel Collision Design Guide Specification in February, 1991 [6].
- In 1993, the International Association for Bridge and Structural Engineering (IABSE) published a comprehensive document that included a review of past and recent developments in the study of ship collisions and the interaction between vessel traffic and bridges [7].
- In 1994, AASHTO adopted the recently developed LRFD bridge design specifications [8], which incorporate the vessel collision provisions developed in Reference [6] as an integral part of the bridge design criteria.
- In December 1996, the Federal Highway Administration sponsored a conference on "The Design of Bridges for Extreme Events" in Atlanta, Georgia to discuss developments in design

loads (vessel collision, earthquake, and scour) and issues related to the load combinations of extreme events [9].

- In May 1998, an international symposium on "Advances in Bridge Aerodynamics, Ship Collision Analysis, and Operation & Maintenance" was held in Copenhagen, Denmark in conjunction with the opening of the record-setting Great Belt Bridge to disseminate the latest developments on the vessel collision subject [10].

Current highway bridge design practices in the United States follow the AASHTO specifications [6,8]. The design of railroad bridge protection systems against vessel collision is addressed in the American Railway Engineering and Maintenance-of-Way Association (AREMA) Manual for Railway Engineering [11]. Research and development work in the area of vessel collision with bridges continues. Several aspects, such as the magnitude of the collision loads to be used in design, and the appropriate combination of extreme events (such as collision plus scour) are not yet well established and understood. As further research results become available, appropriate code changes and updates can be expected.

9.1.2 Basic Concepts

The vulnerability of a bridge to vessel collision is affected by a variety of factors, including:

- Waterway geometry, water stage fluctuations, current speeds, and weather conditions;
- Vessel characteristics and navigation conditions, including vessel types and size distributions, speed and loading conditions, navigation procedures, and hazards to navigation;
- Bridge size, location, horizontal and vertical geometry, resistance to vessel impact, structural redundancy, and effectiveness of existing bridge protection systems;
- Serious vessel collisions with bridges are extreme events associated with a great amount of uncertainty, especially with respect to the impact loads involved. Since designing for the worst-case scenario could be overly conservative and economically undesirable, a certain amount of risk must be considered as acceptable. The commonly accepted design objective is to minimize (in a cost-effective manner) the risk of catastrophic failure of a bridge component, and at the same time reduce the risk of vessel damage and environmental pollution.

The intent of vessel collision provisions is to provide bridge components with a "reasonable" resistance capacity against ship and barge collisions. In navigable waterway areas where collision by merchant vessels may be anticipated, bridge structures should be designed to prevent collapse of the superstructure by considering the size and type of vessel, available water depth, vessel speed, structure response, the risk of collision, and the importance classification of the bridge. It should be noted that damage to the bridge (even failure of secondary structural members) is usually permitted as long as the bridge deck carrying motorist traffic does not collapse (i.e., sufficient redundancy and alternate load paths exist in the remaining structure to prevent collapse of the superstructure).

9.1.3 Application

The vessel collision design recommendations provided in this chapter are consistent with the AASHTO specifications [6,8] and they apply to all bridge components in navigable waterways with water depths over 2.0 ft (0.6 m). The vessels considered include merchant ships larger than 1000 DWT and typical inland barges.

9.2 Initial Planning

It is very important to consider vessel collision aspects as early as possible in the planning process for a new bridge, since they can have a significant effect on the total cost of the bridge. Decisions related to the bridge type, location, and layout should take into account the waterway geometry, the navigation channel layout, and the vessel traffic characteristics.

9.2.1 Selection of Bridge Site

The location of a bridge structure over a waterway is usually predetermined based on a variety of other considerations, such as environmental impacts, right-of-way, costs, roadway geometry, and political considerations. However, to the extent possible, the following vessel collision guidelines should be followed:

- Bridges should be located away from turns in the channel. The distance to the bridge should be such that vessels can line up before passing the bridge, usually at least eight times the length of the vessel. An even larger distance is preferable when high currents and winds are likely to occur at the site.
- Bridges should be designed to cross the navigation channel at right angles and should be symmetrical with respect to the channel.
- An adequate distance should exist between bridge locations and areas with congested navigation, port facilities, vessel berthing maneuvers, or other navigation problems.
- Locations where the waterway is shallow or narrow so that bridge piers could be located out of vessel reach are preferable.

9.2.2 Selection of Bridge Type, Configuration, and Layout

The selection of the type and configuration of a bridge crossing should consider the characteristics of the waterway and the vessel traffic, so that the bridge would not be an unnecessary hazard to navigation. The layout of the bridge should maximize the horizontal and vertical clearances for navigation, and the bridge piers should be placed away from the reach of vessels. Finding the optimum bridge configuration and layout for different bridge types and degrees of protection is an iterative process which weighs the costs involved in risk reduction, including political and social aspects.

9.2.3 Horizontal and Vertical Clearance

The horizontal clearance of the navigation span can have a significant impact on the risk of vessel collision with the main piers. Analysis of past collision accidents has shown that bridges with a main span less than two to three times the design vessel length or less than two times the channel width are particularly vulnerable to vessel collision.

The vertical clearance provided in the navigation span is usually based on the highest vessel that uses the waterway in a ballasted condition and during periods of high water level. The vertical clearance requirements need to consider site-specific data on actual and projected vessels, and must be coordinated with the Coast Guard in the United States. General data on vessel height characteristics are included in References [6,7].

9.2.4 Approach Spans

The initial planning of the bridge layout should also consider the vulnerability of the approach spans to vessel collision. Historical vessel collisions have shown that bridge approach spans were damaged in over 60% of the total number of accidents. Therefore, the number of approach piers exposed to vessel collision should be minimized, and horizontal and vertical clearance considerations should also be applied to the approach spans.

9.2.5 Protection Systems

Bridge protection alternatives should be considered during the initial planning phase, since the cost of bridge protection systems can be a significant portion of the total bridge cost. Bridge protection systems include fender systems, dolphins, protective islands, or other structures designed to redirect, withstand, or absorb the impact force and energy, as described in Section 9.8.

9.3 Waterway Characteristics

The characteristics of the waterway in the vicinity of the bridge site such as the width and depth of the navigation channel, the current speed and direction, the channel alignment and cross section, the water elevation, and the hydraulic conditions, have a great influence on the risk of vessel collision and must be taken into account.

9.3.1 Channel Layout and Geometry

The channel layout and geometry can affect the navigation conditions, the largest vessel size that can use the waterway, and the loading condition and speed of vessels.

The presence of bends and intersections with other waterways near the bridge increases the probability of vessels losing control and become aberrant. The navigation of downstream barge tows through bends is especially difficult.

The vessel transit paths in the waterway in relation to the navigation channel and the bridge piers can affect the risk of aberrant vessels hitting the substructure.

9.3.2 Water Depth and Fluctuations

The design water depth for the channel limits the size and draft of vessels using the waterway. In addition, the water depth plays a critical role in the accessibility of vessels to piers outside the navigation channel. The vessel collision analysis must include the possibility of ships and barges transiting ballasted or empty in the waterway. For example, a loaded barge with a 6 m draft would run aground before it could strike a pier in 4 m of water, but the same barge empty with a 1 m draft could potentially strike the pier.

The water level along with the loading condition of vessels influences the location on the pier where vessel impact loads are applied, and the susceptibility of the superstructure to vessel hits. The annual mean high water elevation is usually the minimum water level used in design. In waterways with large water stage fluctuations, the water level used can have a significant effect on the structural requirements for the pier and/or pier protection design. In these cases, a closer review of the water stage statistics at the bridge site is necessary in order to select an appropriate design water level.

9.3.3 Current Speed and Direction

Water currents at the location of the bridge can have a significant effect on navigation and on the probability of vessel aberrancy. The design water currents commonly used represent annual average values rather than the occasional extreme values that occur only a few times per year, and during which vessel traffic restrictions may also apply.

9.4 Vessel Traffic Characteristics

9.4.1 Physical and Operating Characteristics

General knowledge on the operation of vessels and their characteristics is essential for safe bridge design. The types of commercial vessels encountered in navigable waterways may be divided into ships and barge tows.

9.4.1.1 Ships

Ships are self-propelled vessels using deep-draft waterways. Their size may be determined based on the DWT. The DWT is the weight in metric tonnes (1 tonne = 2205 lbs = 9.80 kN) of cargo, stores, fuel, passenger, and crew carried by the ship when fully loaded. There are three main classes of merchant ships: bulk carriers, product carriers/tankers, and freighter/containers. General information on ship

profiles, dimensions, and sizes as a function of the class of ship and its DWT is provided in References [6,7]. The dimensions given in References [6,7] are typical values, and due to the large variety of existing vessels, they should be regarded as general approximations.

The steering of ships in coastal waterways is a difficult process. It involves constant communications between the shipmaster, the helmsman, and the engine room. There is a time delay before a ship starts responding to an order to change speed or course, and the response of the ship itself is relatively slow. Therefore, the shipmaster has to be familiar with the waterway and be aware of obstructions and navigation and weather conditions in advance. Very often local pilots are used to navigate the ships through a given portion of a coastal waterway. When the navigation conditions are difficult, tugboats are used to assist ships in making turns. Ships need speed to be able to steer and maintain rudder control. A minimum vessel speed of about 5 knots (8 km/h) is usually needed to maintain steering. Fully loaded ships are more maneuverable, and in deep water they are directionally stable and can make turns with a radius equal to one to two times the length of the ship. However, as the underkeel clearance decreases to less than half the draft of the ship, many ships tend to become directionally unstable, which means that they require constant steering to keep them traveling in a straight line. In the coastal waterways of the United States, the underkeel clearance of many laden ships may be far less than this limit, in some cases as small as 5% of the draft of the ship. Ships riding in ballast with shallow draft are less maneuverable than loaded ships, and, in addition, they can be greatly affected by winds and currents. Historical accident data indicate that most bridge accidents involve empty or ballasted vessels.

9.4.1.2 Barge Tows

Barge tows use both deep-draft and shallow-draft waterways. The majority of the existing bridges cross shallow draft waterways where the vessel fleet comprises barge tows only. The size of barges in the United States is usually defined in terms of the cargo-carrying capacity in short tons (1 ton = 2000 lbs = 8.90 kN). The types of inland barges include open and covered hoppers, tank barges, and deck barges. They are rectangular in shape and their dimensions are quite standard so they can travel in tows. The number of barges per tow can vary from one to over 20 and their configuration is affected by the conditions of the waterway. In most cases barges are pushed by a towboat. Information on barge dimensions and capacity, as well as on barge tow configurations, is included in References [6,7]. A statistical analysis of barge tow types, configurations, and dimensions, which utilizes barge traffic data from the Ohio River, is reported in Reference [12].

It is very difficult to control and steer barge tows, especially in waterways with high stream velocities and cross currents. Taking a turn in a fast waterway with high current is a serious undertaking. In maneuvering a bend, tows experience a sliding effect in a direction opposite to the direction of the turn, due to inertial forces, which are often coupled with the current flow. Sometimes, bridge piers and fenders are used to line up the tow before the turn. Bridges located in a high-velocity waterway near a bend in the channel will probably be hit by barges numerous times during their lifetime. In general, there is a high likelihood that any bridge element that can be reached by a barge will be hit during the life of the bridge.

9.4.2 Vessel Fleet Characteristics

The vessel data required for bridge design include types of vessels and size distributions, transit frequencies, typical vessel speeds, and loading conditions. In order to determine the vessel size distribution at the bridge site, detailed information on both present and projected future vessel traffic is needed. Collecting data on the vessel fleet characteristics for the waterway is an important and often time-consuming process.

Some of the sources in the United States for collecting vessel traffic data are listed below:

- U.S. Army Corps of Engineers, District Offices
- Port authorities and industries along the waterway

- Local pilot associations and merchant marine organizations
- U.S. Coast Guard, Marine Safety & Bridge Administration Offices
- U.S. Army Corps of Engineers, "Products and Services Available to the Public," Water Resources Support Center, Navigation Data Center, Fort Belvoir, Virginia, NDC Report 89-N-1, August 1989
- U.S. Army Corps of Engineers, "Waterborne Commerce of the United States (WCUS), Parts 1 thru 5," Water Resources Support Center (WRSC), Fort Belvoir, Virginia
- U.S. Army Corps of Engineers, "Lock Performance Monitoring (LPM) Reports," Water Resources Support Center (WRSC), Fort Belvoir, Virginia
- Shipping registers (American Bureau of Shipping Register, New York; and Lloyd's Register of Shipping, London)
- Bridge tender reports for movable bridges

Projections for anticipated vessel traffic during the service life of the bridge should address both changes in the volume of traffic and in the size of vessels. Factors that need to be considered include:

- Changes in regional economics;
- Plans for deepening or widening the navigation channel;
- Planned changes in alternate waterway routes and in navigation patterns;
- Plans for increasing the size and capacity of locks leading to the bridge;
- Port development plans.

Vessel traffic projections that are made by the Maritime Administration of the U.S. Department of Transportation, Port Authorities, and U.S. Army Corps of Engineers in conjunction with planned channel-deepening projects or lock replacements are also good sources of information for bridge design. Since a very large number of factors can affect the vessel traffic in the future, it is important to review and update the projected traffic during the life of the bridge.

9.5 Collision Risk Analysis

9.5.1 Risk Acceptance Criteria

Bridge components exposed to vessel collision could be subjected to a very wide range of impact loads. Due to economic and structural constraints, bridge design for vessel collision is not based on the worst-case scenario, and a certain amount of risk is considered acceptable.

The risk acceptance criteria consider both the probability of occurrence of a vessel collision and the consequences of the collision. The probability of occurrence of a vessel collision is affected by factors related to the waterway, vessel traffic, and bridge characteristics. The consequences of a collision depend on the magnitude of the collision loads and the bridge strength, ductility, and redundancy characteristics. In addition to the potential for loss of life, the consequences of a collision can include damage to the bridge, disruption of motorist and marine traffic, damage to the vessel and cargo, regional economic losses, and environmental pollution.

Acceptable risk levels have been established by various codes and for individual bridge projects [2–10]. The acceptable annual frequencies of bridge collapse values used generally range from 0.001 to 0.0001. These values were usually determined in conjunction with the risk analysis procedure recommended, and should be used accordingly.

The AASHTO provisions [6,8] specify an annual frequency of bridge collapse of 0.0001 for critical bridges and an annual frequency of bridge collapse of 0.001 for regular bridges. These annual frequencies correspond to return periods of bridge collapse equal to 1 in 10,000 years, and 1 in 1000 years, respectively. Critical bridges are defined as those bridges that are expected to continue to function after a major impact, because of social/survival or security/defense requirements.

9.5.2 Collision Risk Models

9.5.2.1 General Approach

Various collision risk models have been developed to achieve design acceptance criteria [2–10]. In general, the occurrence of a collision is separated into three events: (1) a vessel approaching the bridge becomes aberrant, (2) the aberrant vessel hits a bridge element, and (3) the bridge element that is hit fails. Collision risk models consider the effects of the vessel traffic, the navigation conditions, the bridge geometry with respect to the waterway, and the bridge element strength with respect to the impact loads. They are commonly expressed in the following form [6,8]:

$$AF = (N)\ (PA)\ (PG)\ (PC) \tag{9.1}$$

where AF is the annual frequency of collapse of a bridge element; N is the annual number of vessel transits (classified by type, size, and loading condition) which can strike a bridge element; PA is the probability of vessel aberrancy; PG is the geometric probability of a collision between an aberrant vessel and a bridge pier or span; PC is the probability of bridge collapse due to a collision with an aberrant vessel.

9.5.2.2 Vessel Traffic Distribution, *N*

The number of vessels, N, passing the bridge based on size, type, and loading condition and available water depth has to be developed for each pier and span component to be evaluated. All vessels of a given type and loading condition have to be divided into discrete groupings of vessel size by DWT to determine the contribution of each group to the annual frequency of bridge element collapse. Once the vessels are grouped and their frequency distribution is established, information on typical vessel characteristics may be obtained from site-specific data, or from published general data such as References [6,7].

9.5.2.3 Probability of Aberrancy, *PA*

The probability of vessel aberrancy reflects the likelihood that a vessel is out of control in the vicinity of a bridge. Loss of control may occur as a result of pilot error, mechanical failure, or adverse environmental conditions. The probability of aberrancy is mainly related to the navigation conditions at the bridge site. Vessel traffic regulations, vessel traffic management systems, and aids to navigation can improve the navigation conditions and reduce the probability of aberrancy.

The probability of vessel aberrancy may be evaluated based on site-specific information that includes historical data on vessel collisions, rammings, and groundings in the waterway, vessel traffic, navigation conditions, and bridge/waterway geometry. This has been done for various bridge design provisions and specific bridge projects worldwide [2,3,7,9,12]. The probability of aberrancy values determined range from 0.5×10^{-4} to over 7.0×10^{-4}.

As an alternative, the AASHTO provisions [6,8] recommend base rates for the probability of vessel aberrancy that are multiplied by correction factors for bridge location relative to bends in the waterway, currents acting parallel to vessel transit path, crosscurrents acting perpendicular to vessel transit path, and the traffic density of vessels using the waterway. The recommended base rates are 0.6×10^{-4} for ships, and 1.2×10^{-4} for barges.

9.5.2.4 Geometric Probability, *PG*

The geometric probability is the probability that a vessel will hit a particular bridge pier given that it has lost control (i.e., is aberrant) in the vicinity of the bridge. It is mainly a function of the geometry of the bridge in relation to the waterway. Other factors that can affect the likelihood that an aberrant vessel will strike a bridge element include the original vessel transit path, course, rudder position, velocity at the time of failure, vessel type, size, draft and maneuvering characteristics, and the hydraulic and environmental conditions at the bridge site. Various geometric probability models, some based on simulation studies, have been recommended and used on different bridge projects

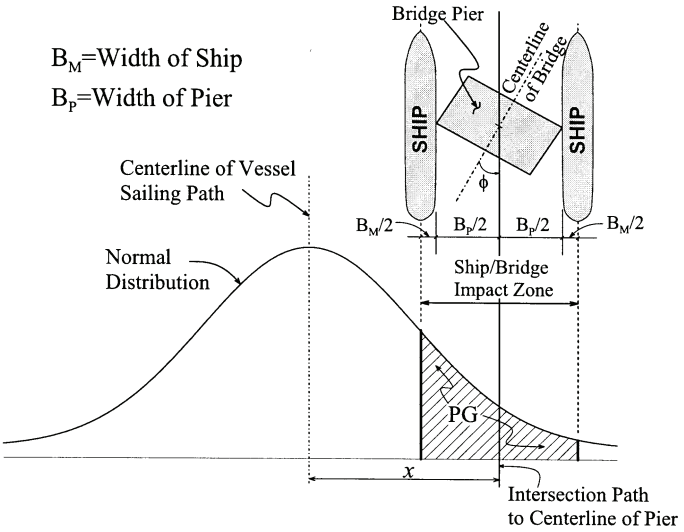

FIGURE 9.2 Geometric probability of pier collision.

[2,3,7]. The AASHTO provisions [6,8] use a normal probability density function about the centerline of the vessel transit path for estimating the likelihood of an aberrant vessel being within a certain impact zone along the bridge axis. Using a normal distribution accounts for the fact that aberrant vessels are more likely to pass under the bridge closer to the navigation channel than farther away from it. The standard deviation of the distribution equals the length of the design vessel considered. The probability that an aberrant vessel is located within a certain zone is the area under the normal probability density function within that zone (Figure 9.2).

Bridge elements beyond three times the standard deviation from the centerline of vessel transit path are designed for specified minimum impact load requirements, which are usually associated with an empty vessel drifting with the current.

9.5.2.5 Probability of Collapse, *PC*

The probability of collapse, *PC*, is a function of many variables, including vessel size, type, forepeak ballast and shape, speed, direction of impact, and mass. It is also dependent on the ultimate lateral load strength of the bridge pier (particularly the local portion of the pier impacted by the bow of the vessel). Based on collision damages observed from numerous ship–ship collision accidents which have been correlated to the bridge–ship collision situation [2], an empirical relationship has been developed based on the ratio of the ultimate pier strength, *H*, to the vessel impact force, *P*. As shown in Figure 9.3, for *H*/*P* ratios less than 0.1, *PC* varies linearly from 0.1 at *H*/*P* = 0.1 to 1.0 at *H*/*P* = 0.0. For *H*/*P* ratios greater than 0.1, *PC* varies linearly from 0.1 at *H*/*P* = 0.1 to 0.0 at *H*/*P* = 1.0.

9.6 Vessel Impact Loads

9.6.1 Ship Impact

The estimation of the load on a bridge pier during a ship collision is a very complex problem. The actual force is time dependent, and varies depending on the type, size, and construction of the vessel; its velocity; the degree of water ballast in the forepeak of the bow; the geometry of the collision; and the geometry and strength characteristics of the bridge. There is a very large scatter among the collision force values recommended in various vessel collision guidelines or used in various bridge projects [2–10].

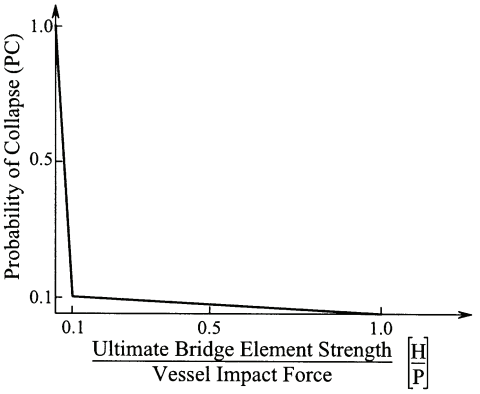

FIGURE 9.3 Probability of collapse distribution.

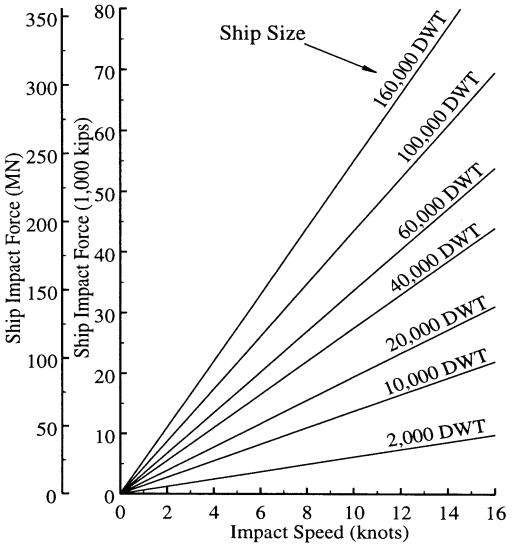

FIGURE 9.4 Ship impact force.

Ship collision forces are commonly applied as equivalent static loads. Procedures for evaluating dynamic effects when the vessel force indentation behavior is known are included in References [3,4,10,13,14]. The AASHTO provisions [6,8] use the following formula for estimating the static head-on ship collision force, P_S, on a rigid pier:

$$P_s = 0.98(DWT)^{1/2}(V/16) \tag{9.2}$$

where P_S is the equivalent static vessel impact force (MN); DWT is the ship deadweight tonnage in tonnes; and V is the vessel impact velocity in knots (Figure 9.4). This formulation was primarily developed from research conducted by Woisin in West Germany during 1967 to 1976 on physical ship models to generate data for protecting the reactors of nuclear power ships from collisions with other ships. A schematic representation of a typical impact force time history is shown in Figure 9.6 based on Woisin's test data. The scatter in the results of these tests is of the order of ±50%. The formula recommended (Eq. 9.2) uses a 70% fractile of an assumed triangular distribution with zero values at 0% and 100% and a maximum value at the 50% level (Figure 9.7).

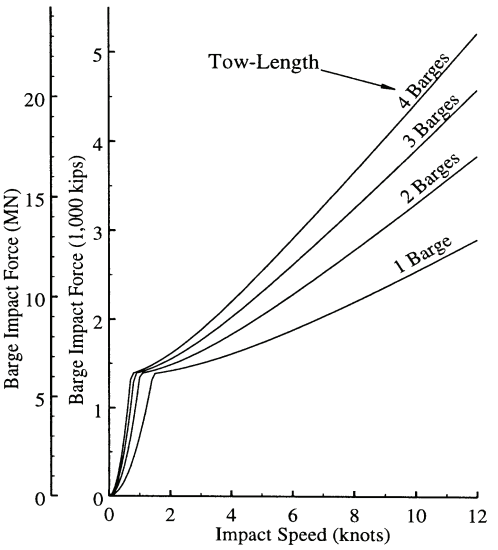

FIGURE 9.5 Barge impact force.

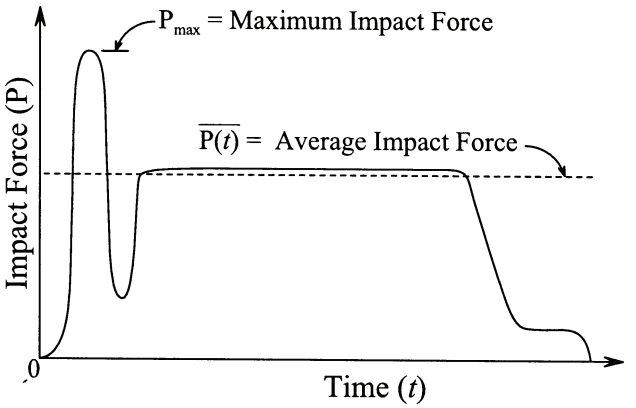

FIGURE 9.6 Typical ship impact force time history by Woisin.

Formulas for computing design ship collision loads on a bridge superstructure are given in the AASHTO provisions [6,8] as a function of the design ship impact force, P_S, as follows:

- Ship Bow Impact Force, P_{BH}:

$$P_{BH} = (R_{BH})\ (P_S) \tag{9.3}$$

  where R_{BH} is a reduction coefficient equal to the ratio of exposed superstructure depth to the total bow depth.

- Ship Deckhouse Impact Force, P_{DH}:

$$P_{DH} = (R_{DH})\ (P_S) \tag{9.4}$$

  where R_{DH} is a reduction coefficient equal to 0.10 for ships larger than 100,000 DWT, and

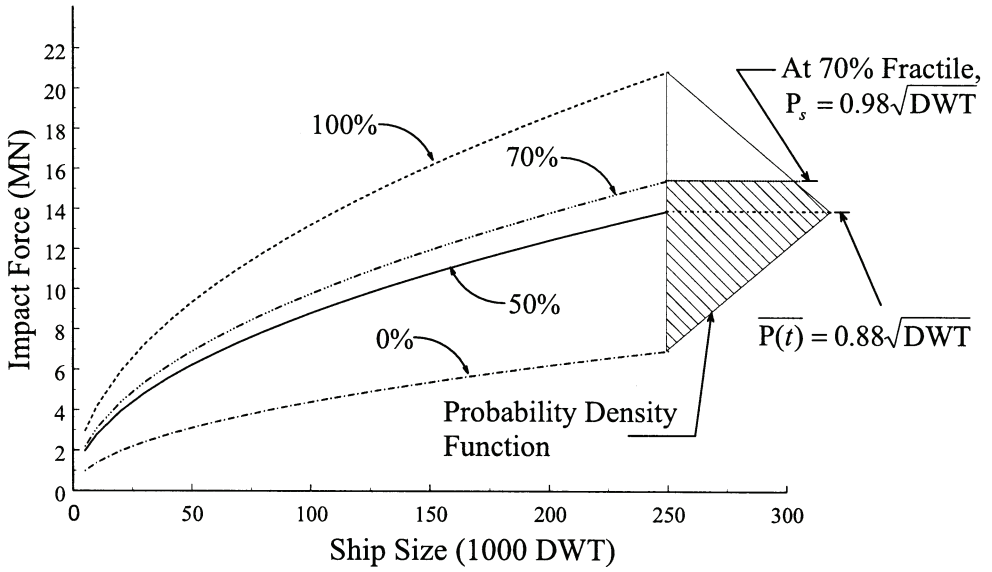

FIGURE 9.7 Probability density function of ship impact force.

$$0.2 - \frac{DWT}{100{,}000}(0.10)$$

for ships under 100,000 DWT.

- Ship Mast Impact Force, P_{MT}:

$$P_{MT} = 0.10\ P_{DH} \tag{9.5}$$

where P_{DH} is the ship deckhouse impact force.

The magnitude of the impact loads computed for ship bow and deckhouse collisions are quite high relative to the strength of most bridge superstructure designs. Also, there is great uncertainty associated with predicting ship collision loads on superstructures because of the limited data available and the ship–superstructure load interaction effects. It is therefore suggested that superstructures, and also weak or slender parts of the substructure, be located out of the reach of a ship's hull or bow.

9.6.2 Barge Impact

The barge collision loads recommended by AASHTO for the design of piers are shown in Figure 9.5 as a function of the tow length and the impact speed. Numerical formulations for deriving these relationships may be found in References [6,8].

The loads in Figure 9.5 were computed using a standard 59.5 × 10.7 m hopper barge. The impact force recommended for barges larger than the standard hopper barge is determined by increasing the standard barge impact force by the ratio of the width of the wider barge to the width of the standard hopper barge.

9.6.3 Application of Impact Forces

Collision forces on bridge substructures are commonly applied as follows:

- 100% of the design impact force in a direction parallel to the navigation channel (i.e., head-on);
- 50% of the design impact force in the direction normal to the channel (but not simultaneous with the head-on force);
- For overall stability, the design impact force is applied as a concentrated force at the mean high water level;
- For local collision forces, the design impact force is applied as a vertical line load equally distributed along the ship's bow depth for ships, and along head log depth for barges;
- For superstructure design the impact forces are applied transversely to the superstructure component in a direction parallel to the navigation channel.

When determining the bridge components exposed to physical contact by any portion of the hull or bow of the vessel considered, the bow overhang, rake, or flair distance of vessels have to be taken into account. The bow overhang of ships and barges is particularly dangerous for bridge columns and for movable bridges with relatively small navigation clearances.

9.7 Bridge Analysis and Design

Vessel collisions are extreme events with a very low probability of occurrence; therefore the limit state considered is usually structural survival. Depending on the importance of the bridge, various degrees of damage are allowed — provided that the structure maintains its integrity, hazards to traffic are minimized, and repairs can be made in a relatively short period of time. When the design is based on more frequent but less severe collisions, structural damage and traffic interruptions are not allowed.

Designing for vessel collision is commonly based on equivalent static loads that include global forces for checking overall capacity and local forces for checking local strength of bridge components. A clear load path from the location of the vessel impact to the bridge foundation needs to be established and the components and connections within the load path must be adequately designed and detailed. The design of individual bridge components is based on strength and stability criteria. Overall stability, redundancy, and ductility are important criteria for structural survival.

The contribution of the superstructure to the transfer of loads to adjacent substructure units depends on the capacity of the connection of the superstructure to substructure and the relative stiffness of the substructure at the location of the impact. Analysis guidelines for determining the distribution of collision loads to adjacent piers are included in Reference [15]. To find out how much of the transverse impact force is taken by the pier and how much is transferred to the superstructure, two analytical models are typically used. One is a two-dimensional or a three-dimensional model of the complete pier, and the other is a two-dimensional model of the superstructure projected on a horizontal plane. The projected superstructure may be modeled as a beam with the moment of inertia referred to a vertical axis through the center of the roadway, and with hinges at expansion joint locations. The beam is supported at pier locations by elastic horizontal springs representing the flexibility of each pier. The flexibility of the piers is obtained from pier models using virtual forces. The superstructure model is loaded with a transverse virtual force acting at the place where the pier under consideration is located. The spring in the model at that place is omitted to obtain a flexibility coefficient of the superstructure at the location of the top of the pier under consideration. Thus, the horizontal displacement of the top of the pier due to the impact force on the pier (usually applied at mean high water level) is equal to the true displacement of the superstructure due to the transmitted part of the impact force. The magnitude of the force transmitted to the superstructure is obtained by equating the total true displacement of the top of the pier from the pier model to the displacement of the superstructure. However, in order to consider partial transfer of lateral forces to the superstructure, positive steel or concrete connections of superstructure to substructure, such as shear keys must be provided. Similarly, for partial transfer to the superstructure of the longitudinal component of the impact force the shear capacity of the

bearings must be adequate. When elastomeric bearings are used, their longitudinal flexibility may be added to the longitudinal flexibility of the piers. If the ultimate capacity of the bearings is exceeded, then the pier must take the total longitudinal force and be treated as a cantilever.

The modeling of pile foundations could vary from the simple assumption of a point of fixity to nonlinear soil–structure interaction models, depending on the limit state considered and the sensitivity of the response to the soil conditions. Lateral load capacity analysis methods for pile groups that include nonlinear behavior are recommended in References [15,16] and the features of a finite-element analysis computer program developed for bridge piers composed of pier columns and cap supported on a pile cap and nonlinear piles and soil are presented in Reference [17]. Transient foundation uplift or rocking involving separation from the subsoil of an end bearing foundation pile group or the contact area of a foundation footing could be allowed under impact loading provided sufficient consideration is given to the structural stability of the substructure.

9.8 Bridge Protection Measures

The cost associated with protecting a bridge from catastrophic vessel collision can be a significant portion of the total bridge cost, and must be included as one of the key planning elements in establishing a bridge's type, location, and geometry. The alternatives listed below are usually evaluated in order to develop a cost-effective solution for a new bridge project:

- Design the bridge piers, foundations, and superstructure to withstand directly the vessel collision forces and impact energies;
- Design a pier fender system to reduce the impact loads to a level below the capacity of the pier and foundation;
- Increase span lengths and locate piers in shallow water out of reach of large vessels in order to reduce the impact design loads; and
- Protect piers from vessel collision by means of physical protection systems.

9.8.1 Physical Protection Systems

Piers exposed to vessel collision can be protected by special structures designed to absorb the impact loads (forces or energies), or redirect the aberrant vessel away from the pier. Because of the large forces and energies involved in a vessel collision, protection structures are usually designed for plastic deformation under impact (i.e., they are essentially destroyed during the head-on design collision and must be replaced). General types of physical protection systems include:

Fender Systems. These usually consist of timber, rubber, steel, or concrete elements attached to a pier to fully, or partially, absorb vessel impact loads. The load and energy absorbing characteristics of such fenders is relatively low compared with typical vessel impact design loads.

Pile-Supported Systems. These usually consist of pile groups connected by either flexible or rigid caps to absorb vessel impact forces. The piles may be vertical (plumb) or battered depending on the design approach followed, and may incorporate relatively large-diameter steel pipe or concrete pile sizes. The pile-supported protection structure may be either freestanding away from the pier, or attached to the pier itself. Fender systems may be attached to the pile structure to help resist a portion of the impact loads.

Dolphin Protection Systems. These usually consist of large-diameter circular cells constructed of driven steel sheet piles, filled with rock or sand, and topped by a thick concrete cap. Vessel collision loads are absorbed by rotation and lateral deformation of the cell during impact.

Island Protection Systems. These usually consist of protective islands built of a sand or quarry-run rock core and protected by outer layers of heavy rock riprap for wave, current, and ice protection. The island geometry is developed to stop an aberrant vessel from hitting a pier

by forcing it to run aground. Although extremely effective as protection systems, islands are often difficult to use due to adverse environmental impacts on river bottoms (dredge and fill permits) and river currents (increase due to blockage), as well as impacts due to settlement and downdrag forces on the bridge piers.

Floating Protection Systems. These usually consist of cable net systems suspended across the waterway to engage and capture the bow of an aberrant vessel, or floating pontoons anchored in front of the piers. Floating protection systems have a number of serious drawbacks (environmental, effectiveness, maintenance, cost, etc.) and are usually only considered for extremely deep water situations where other protection options are not practicable.

The AASHTO Guide Specification [6] provides examples and contains a relatively extensive discussion of various types of physical protection systems, such as fenders, pile-supported structures, dolphins, protective islands, and floating structures. However, the code does not include specific procedures and recommendations on the actual design of such protection structures. Further research is needed to establish consistent analysis and design methodologies for protection structures, particularly since these structures undergo large plastic deformations during the collision.

9.8.2 Aids to Navigation Alternatives

Since 60 to 85% of all vessel collisions are caused by pilot error, it is important that all aspects of the bridge design, siting, and aids to navigation with respect to the navigation channel be carefully evaluated with the purpose of improving or maintaining safe navigation in the waterway near the bridge. Traditional aids include buoys, range markers, navigation lighting, and radar reflectors, as well as standard operating procedures and regulations specifically developed for the waterway by government agencies and pilot associations. Modern aids include advanced vessel traffic control systems (VTS) using shore-based radar surveillance and radio-telephone communication systems; special electronic transmitters known as Raycon devices mounted to bridge spans for improved radar images indicating the centerline of the channel; and advanced navigation positioning systems based on shipboard global positioning satellite (GPS) receivers using differential signal techniques to improve location accuracy.

Studies have indicated that improvements in the aids to navigation near a bridge can provide extremely cost-effective solutions to reducing the risk of collisions to acceptable levels. The cost of such aid to navigation improvements and shipboard electronic navigation systems is usually a fraction of the cost associated with expensive physical protection alternatives. However, few electronic navigation systems have ever been implemented (worldwide) due to legal complications arising from liability concerns; impacts on international laws governing trade on the high seas; and resistance by maritime users.

It should be noted that the traditional isolation of the maritime community must come to an end. In addition to the bridge costs, motorist inconvenience, and loss of life associated with a catastrophic vessel collision, significant environmental damage can also occur due to spilled hazardous or noxious cargoes in the waterway. The days when the primary losses associated with an accident rested with the vessel and her crew are over. The \$13 million value of the *M/V Summit Venture* was far below the \$250 million replacement cost of the Sunshine Skyway Bridge which the vessel destroyed. The losses associated with the 11 million gallons of crude oil spilled from the *M/V Exxon Valdez* accident off the coast of Alaska in 1989 are over \$3.5 billion. Both of these accidents could have been prevented using shipboard advanced electronic navigation systems.

9.9 Conclusions

Experience to date has shown that the use of the vessel impact and bridge protection requirements (such as the AASHTO specifications [6,8]) for planning and design of new bridges has resulted in a significant change in proposed structure types over navigable waterways. Incorporation of the risk

of vessel collision and cost of protection in the total bridge cost has almost always resulted in longer-span bridges being more economical than traditional shorter span structures, since the design goal for developing the bridge pier and span layout is the least cost of the total structure (including the protection costs). Typical costs for incorporating vessel collision and protection issues in the planning stages of a new bridge have ranged from 5% to 50% of the basic structure cost without protection.

Experience has also shown that it is less expensive to include the cost of protection in the planning stages of a proposed bridge than to add it after the basic span configuration has been established without considering vessel collision concerns. Typical costs for adding protection, or for retrofitting an existing bridge for vessel collision, have ranged from 25% to over 100% of the existing bridge costs.

It is recognized that vessel collision is but one of a multitude of factors involved in the planning process for a new bridge. The designer must balance a variety of needs including political, social, and economic in arriving at an optimal bridge solution for a proposed highway crossing. Because of the relatively high bridge costs associated with vessel collision design for most waterway crossings, it is important that additional research be conducted to improve our understanding of vessel impact mechanics, the response of the structure, and the development of cost-effective protection systems.

References

1. National Research Council, *Ship Collisions with Bridges — The Nature of the Accidents, Their Prevention and Mitigation,* National Academy Press, Washington, D.C., 1983.
2. IABSE, *Ship Collision with Bridges and Offshore Structures*, International Association for Bridge and Structural Engineering, Colloquium Proceedings, Copenhagen, Denmark, 3 vols. (Introductory, Preliminary, and Final Reports), 1983.
3. Modjeski and Masters, Criteria for the Design of Bridge Piers with Respect to Vessel Collision in Louisiana Waterways, Report prepared for Louisiana Department of Transportation and Development and the Federal Highway Administration, 1984.
4. Prucz, Z. and Conway, W. B., Design of bridge piers against ship collision, in *Bridges and Transmission Line Structures,* L. Tall, Ed., ASCE, New York, 1987, 209–223.
5. Knott, M. A. and Larsen, O. D. 1990. *Guide Specification and Commentary for Vessel Collision Design of Highway Bridges*, U.S. Department of Transportation, Federal Highway Administration, Report No. FHWA-RD-91-006.
6. AASHTO, *Guide Specification and Commentary for Vessel Collision Design of Highway Bridges*, American Association of State Highway and Transportation Officials, Washington, D.C., 1991.
7. Larsen, O. D., Ship Collision with Bridges: The Interaction between Vessel Traffic and Bridge Structures, IABSE Structural Engineering Document 4, IABSE-AIPC-IVBH, Zürich, Switzerland, 1993.
8. AASHTO, *LRFD Bridge Design Specifications and Commentary*, American Association of State Highway and Transportation Officials, Washington, D.C., 1994.
9. FHWA, *The Design of Bridges for Extreme Events,* Proceedings of Conference in Atlanta, Georgia, December 3–6, 1996.
10. *International Symposium on Advances in Bridge Aerodynamics, Ship Collision Analysis, and Operation & Maintenance*, Copenhagen, Denmark, May 10–13, Balkema Publishers, Rotterdam, Netherlands, 1998.
11. AREMA, *Manual for Railway Engineering*, Chapter 8, Part 23, American Railway Engineering Association, Washington, D.C., 1999.
12. Whitney, M. W., Harik, I. E., Griffin, J. J., and Allen, D. L., Barge collision design of highway bridges, *J. Bridge Eng. ASCE,* 1(2), 47–58, 1996.
13. Prucz, Z. and Conway, W. B., Ship Collision with Bridge Piers — Dynamic Effects, Transportation Research Board Paper 890712, Transportation Research Board, Washington, D.C., 1989.

14. Grob, B. and Hajdin, N., Ship impact on inland waterways, *Struct. Eng. Int.,* IABSE, Zürich, Switzerland, 4, 230–235, 1996.
15. Kuzmanovic, B. O. and Sanchez, M. R., Design of bridge pier pile foundations for ship impact, *J. Struct. Eng. ASCE,* 118(8), 2151–2167, 1992.
16. Brown, D. A. and Bollmann, H. T., Pile supported bridge foundations designed for impact loading, Transportation Research Record 1331, TRB, National Research Council, Washington, D.C., 87–91, 1992.
17. Hoit, M., McVay, M., and Hays, C., Florida Pier Computer Program for Bridge Substructure Analysis: Models and Methods, Conference Proceedings, Design of Bridges for Extreme Events, FHWA, Washington, D.C., 1996.

10 Bridge Hydraulics

Jim Springer
California Department of Transportation

Ke Zhou
California Department of Transportation

10.1 Introduction

This chapter presents bridge engineers basic concepts, methods, and procedures used in bridge hydraulic analysis and design. It involves hydrology study, hydraulic analysis, on-site drainage design, and bridge scour evaluation.

Hydrology study for bridge design mainly deals with the properties, distribution, and circulation of water on and above the land surface. The primary objective is to determine either the peak discharge or the flood hydrograph, in some cases both, at the highway stream crossings. Hydraulic analysis provides essential methods to determine runoff discharges, water profiles, and velocity distribution. The on-site drainage design part of this chapter is presented with the basic procedures and references for bridge engineers to design bridge drainage.

Bridge scour is a big part of this chapter. Bridge engineers are systematically introduced to concepts of various scour types, presented with procedures and methodology to calculate and evaluate bridge scour depths, provided with guidelines to conduct bridge scour investigation and to design scour preventive measures.

10.2 Bridge Hydrology and Hydraulics

10.2.1 Hydrology

10.2.1.1 Collection of Data

Hydraulic data for the hydrology study may be obtained from the following sources: as-built plans, site investigations and field surveys, bridge maintenance books, hydraulic files from experienced report writers, files of government agencies such as the U.S. Corps of Engineers studies, U.S. Geological Survey (USGS), Soil Conservation Service, and FEMA studies, rainfall data from local water agencies, stream gauge data, USGS and state water agency reservoir regulation, aerial photographs, and floodways, etc.

Site investigations should always be conducted except in the simplest cases. Field surveys are very important because they can reveal conditions that are not readily apparent from maps, aerial

photographs and previous studies. The typical data collected during a field survey include high water marks, scour potential, stream stability, nearby drainage structures, changes in land use not indicated on maps, debris potential, and nearby physical features. See HEC-19, Attachment D [16] for a typical Survey Data Report Form.

10.2.1.2 Drainage Basin

The area of the drainage basin above a given point on a stream is a major contributing factor to the amount of flow past that point. For given conditions, the peak flow at the proposed site is approximately proportional to the drainage area.

The shape of a basin affects the peak discharge. Long, narrow basins generally give lower peak discharges than pear-shaped basins. The slope of the basin is a major factor in the calculation of the time of concentration of a basin. Steep slopes tend to result in shorter times of concentration and flatter slopes tend to increase the time of concentration. The mean elevation of a drainage basin is an important characteristic affecting runoff. Higher elevation basins can receive a significant amount of precipitation as snow. A basin orientation with respect to the direction of storm movement can affect peak discharge. Storms moving upstream tend to produce lower peaks than those moving downstream.

10.2.1.3 Discharge

There are several hydrologic methods to determine discharge. Most of the methods for estimating flood flows are based on statistical analyses of rainfall and runoff records and involve preliminary or trial selections of alternative designs that are judged to meet the site conditions and to accommodate the flood flows selected for analysis.

Flood flow frequencies are usually calculated for discharges of 2.33 years through the overtopping flood. The frequency flow of 2.33 years is considered to be the mean annual discharge. The base flood is the 100-year discharge (1% frequency). The design discharge is the 50-year discharge (2% frequency) or the greatest of record, if practical. Many times, the historical flood is so large that a structure to handle the flow becomes uneconomical and is not warranted. It is the engineer's responsibility to determine the design discharge. The overtopping discharge is calculated at the site, but may overtop the roadway some distance away from the site.

Changes in land use can increase the surface water runoff. Future land-use changes that can be reasonably anticipated to occur in the design life should be used in the hydrology study. The type of surface soil is a major factor in the peak discharge calculation. Rock formations underlying the surface and other geophysical characteristics such as volcanic, glacial, and river deposits can have a significant effect on runoff. In the United States, the major source of soil information is the Soil Conservation Service (SCS). Detention storage can have a significant effect on reducing the peak discharge from a basin, depending upon its size and location in the basin.

The most commonly used methods to determine discharges are

1. Rational method
2. Statistical Gauge Analysis Methods
3. Discharge comparison of adjacent basins from gauge analysis
4. Regional flood-frequency equations
5. Design hydrograph

The results from various methods of determining discharge should be compared, not averaged.

10.2.1.3.1 Rational Method

The rational method is one of the oldest flood calculation methods and was first employed in Ireland in urban engineering in 1847. This method is based on the following assumptions:

1. Drainage area is smaller than 300 acres.
2. Peak flow occurs when all of the watershed is contributing.

TABLE 10.1 Runoff Coefficients for Developed Areas

Type of Drainage Area	Runoff Coefficient
Business	
Downtown areas	0.70–0.95
Neighborhood areas	0.50–0.70
Residential areas	
Single-family areas	0.30–0.50
Multiunits, detached	0.40–0.60
Multiunits, attached	0.60–0.75
Suburban	0.25–0.40
Apartment dwelling areas	0.50–0.70
Industrial	
Light areas	0.50–0.80
Heavy areas	0.60–0.90
Parks, cemeteries	0.10–0.25
Playgrounds	0.20–0.40
Railroad yard areas	0.20–0.40
Unimproved areas	0.10–0.30
Lawns	
Sandy soil, flat, 2%	0.05–0.10
Sandy soil, average, 2–7%	0.10–0.15
Sandy soil, steep, 7%	0.15–0.20
Heavy soil, flat, 2%	0.13–0.17
Heavy soil, average, 2–7%	0.18–0.25
Heavy soil, steep, 7%	0.25–0.35
Streets	
Asphaltic	0.70–0.95
Concrete	0.80–0.95
Brick	0.70–0.85
Drives and walks	0.75–0.85
Roofs	0.75–0.95

3. The rainfall intensity is uniform over a duration equal to or greater than the time of concentration, T_c.
4. The frequency of the peak flow is equal to the frequency of the rainfall intensity.

$$Q = C\,i\,A \tag{10.1}$$

where
Q = discharge, in cubic foot per second
C = runoff coefficient (in %) can be determined in the field and from Tables 10.1 and 10.2 [5,16] or a weighted C value is used when the basin has varying amounts of different cover. The weighted C value is determined as follows:

$$C = \frac{\sum C_j A_j}{\sum A_j} \tag{10.2}$$

i = rainfall intensity (in inches per hour) can be determined from either regional IDF maps or individual IDF curves
A = drainage basin area (in acres) is determined from topographic map

(*Note*: 1 sq. mile = 640 acres = 0.386 sq. kilometer)

TABLE 10.2 Runoff Coefficients for Undeveloped Area Watershed Types

Soil	0.12–0.16 No effective soil cover, either rock or thin soil mantle of negligible infiltration capacity	0.08–0.12 Slow to take up water, clay or shallow loam soils of low infiltration capacity, imperfectly or poorly drained	0.06–0.08 Normal, well-drained light or medium-textured soils, sandy loams, silt and silt loams	0.04–0.06 High, deep sand or other soil that takes up water readily, very light well-drained soils
Vegetal Cover	0.12–0.16 No effective plant cover, bare or very sparse cover	0.08–0.12 Poor to fair; clean cultivation crops, or poor natural cover, less than 20% of drainage area over good cover	0.06–0.08 Fair to good; about 50% of area in good grassland or woodland, not more than 50% of area in cultivated crops	0.04–0.06 Good to excellent; about 90% of drainage area in good grassland, woodland or equivalent cover
Surface Storage	0.10–0.12 Negligible surface depression few and shallow, drainageways steep and small, no marshes	0.08–0.10 Low, well-defined system of small drainageways; no ponds or marshes	0.06–0.08 Normal; considerable surface depression storage; lakes and pond marshes	0.04–0.06 High; surface storage, high; drainage system not sharply defined; large floodplain storage or large number of ponds or marshes

The time of concentration for a pear-shaped drainage basin can be determined using a combined overland and channel flow equation, the Kirpich equation:

$$T_c = 0.0195(L / S^{0.5})^{0.77} \tag{10.3}$$

where
T_c = Time of concentration in minutes
L = Horizontally projected length of watershed in meters
S = H/L (H = difference in elevation between the most remote point in the basin and the outlet in meters)

10.2.1.3.2 Statistical Gauge Analysis Methods

The following two methods are the major statistical analysis methods which are used with stream gauge records in the hydrological analysis.

1. Log Pearson Type III method
2. Gumbel extreme value method

The use of stream gauge records is a preferred method of estimating discharge/frequencies since they reflect actual climatology and runoff. Discharge records, if available, may be obtained from a state department of water resources in the United States. A good record set should contain at least 25 years of continuous records.

It is important, however, to review each individual stream gauge record carefully to ensure that the database is consistent with good statistical analysis practice. For example, a drainage basin with a large storage facility will result in a skewed or inconsistent database since smaller basin discharges will be influenced to a much greater extent than large discharges.

The most current published stream gauge description page should be reviewed to obtain a complete idea of the background for that record. A note should be given to changes in basin area over time, diversions, revisions, etc. All reliable historical data outside of the recorded period should

be included. The adjacent gauge records for supplemental information should be checked and utilized to extend the record if it is possible. Natural runoff data should be separated from later controlled data. It is known that high-altitude basin snowmelt discharges are not compatible with rain flood discharges. The zero years must also be accounted for by adjusting the final plot positions, not by inclusion as minor flows. The generalized skew number can be obtained from the chart in Bulletin No.17 B [8].

Quite often the database requires modification for use in a Log Pearson III analysis. Occasionally, a high outlier, but more often low outliers, will need to be removed from the database to avoid skewing results. This need is determined for high outliers by using $Q_H = \bar{Q}_H + K S_H$, and low outliers by using $Q_L = \bar{Q}_L + K S_L$, where K is a factor determined by the sample size, $\bar{Q}_H$ and $\bar{Q}_L$ are the high and low mean logarithm of systematic peaks, Q_H and Q_L are the high and low outlier thresholds in log units, S_H and S_L are the high and low standard deviations of the logarithmic distribution. Refer to FHWA HEC-19, Hydrology [16] or USGS Bulletin 17B [8] for this method and to find the values of K.

The data to be plotted are "PEAK DISCHARGE, Q (CFS)" vs. "PROBABILITY, Pr" as shown in the example in Figure 10.1. This plot usually results in a very flat curve with a reasonably straight center portion. An extension of this center portion gives a line for interpolation of the various needed discharges and frequencies.

The engineer should use an adjusted skew, which is calculated from the generalized and station skews. Generalized skews should be developed from at least 40 stations with each station having at least 25 years of record.

The equation for the adjusted skew is

$$G_w = \frac{MSE_{G_S}(G_L) + MSE_{G_L}(G_S)}{MSE_{G_S} + MSE_{G_L}} \tag{10.4}$$

where

G_w = weighted skew coefficient
G_S = station skew
G_L = generalized skew
MSE_{G_S} = mean square error of station skew
MSE_{G_L} = mean square error of generalized skew

The entire Log Pearson type III procedure is covered by Bulletin No. 17B, "Guidelines for Determining Flood Flow Frequency" [8].

The Gumbel extreme value method, sometimes called the double-exponential distribution of extreme values, has also been used to describe the distribution of hydrological variables, especially the peak discharges. It is based on the assumption that the cumulative frequency distribution of the largest values of samples drawn from a large population can be described by the following equation:

$$f(Q) = e^{-e^{a(Q-b)}} \tag{10.5}$$

where

$a = \dfrac{1.281}{S}$

$b = \overline{Q} - 0.450\,S$

S = standard deviation
$\overline{Q}$ = mean annual flow

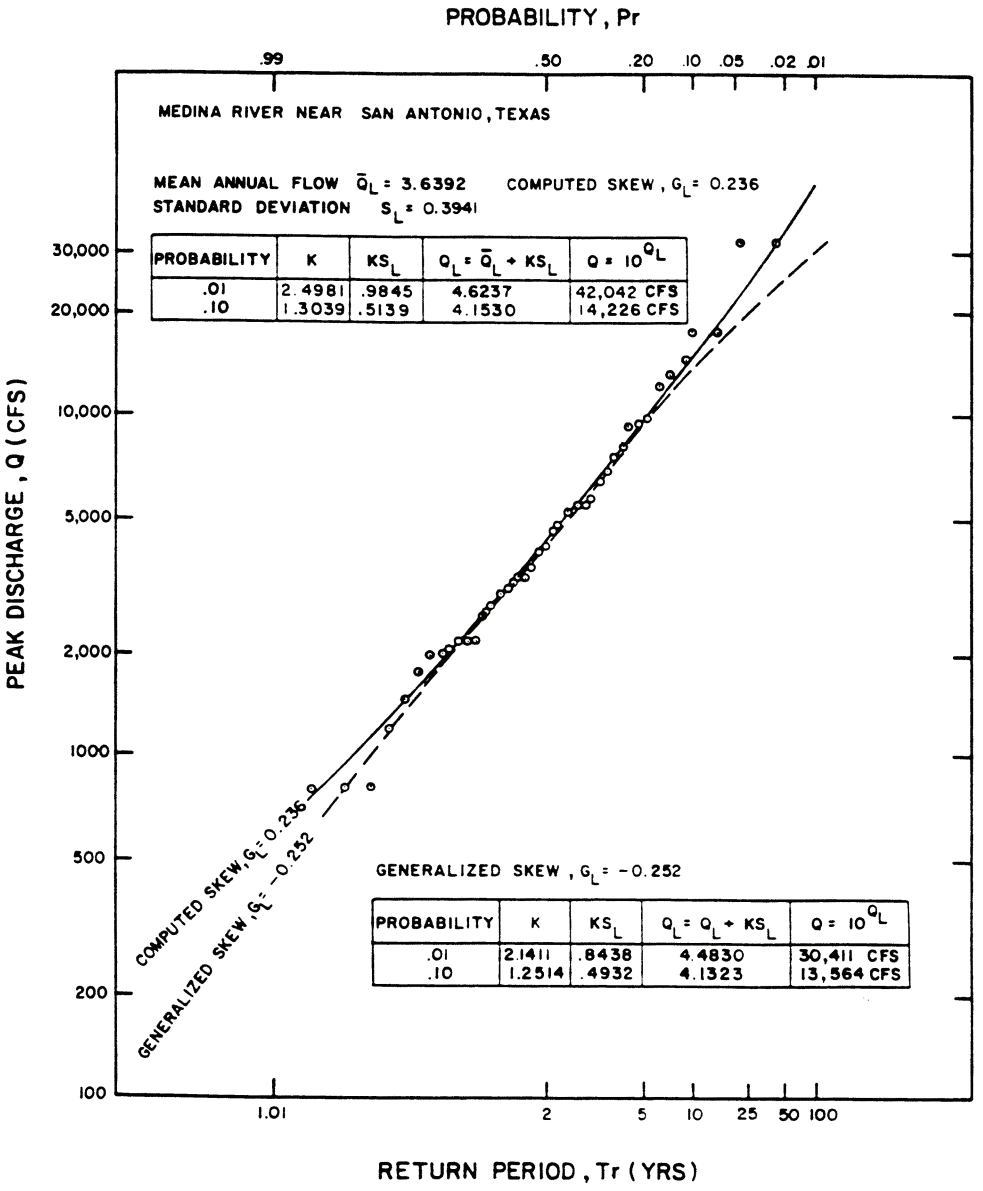

FIGURE 10.1 Log Pearson type III distribution analysis, Medina River, TX.

Values of this distribution function can be computed from Eq. (10.5). Characteristics of the Gumbel extreme value distribution are that the mean flow, $\overline{Q}$, occurs at the return period of $T_r = 2.33$ years and that it is skewed toward the high flows or extreme values as shown in the example of Figure 10.2. Even though it does not account directly for the computed skew of the data, it does predict the high flows reasonably well. For this method and additional techniques, please refer to USGS Water Supply Paper 1543-A, Flood-Frequency Analysis, and Manual of Hydrology Part 3.

The Gumbel extreme value distribution is given in "Statistics of Extremes" by E.J. Gumbel and is also found in HEC-19, p.73. Results from this method should be plotted on special Gumbel paper as shown in Figure 10.2.

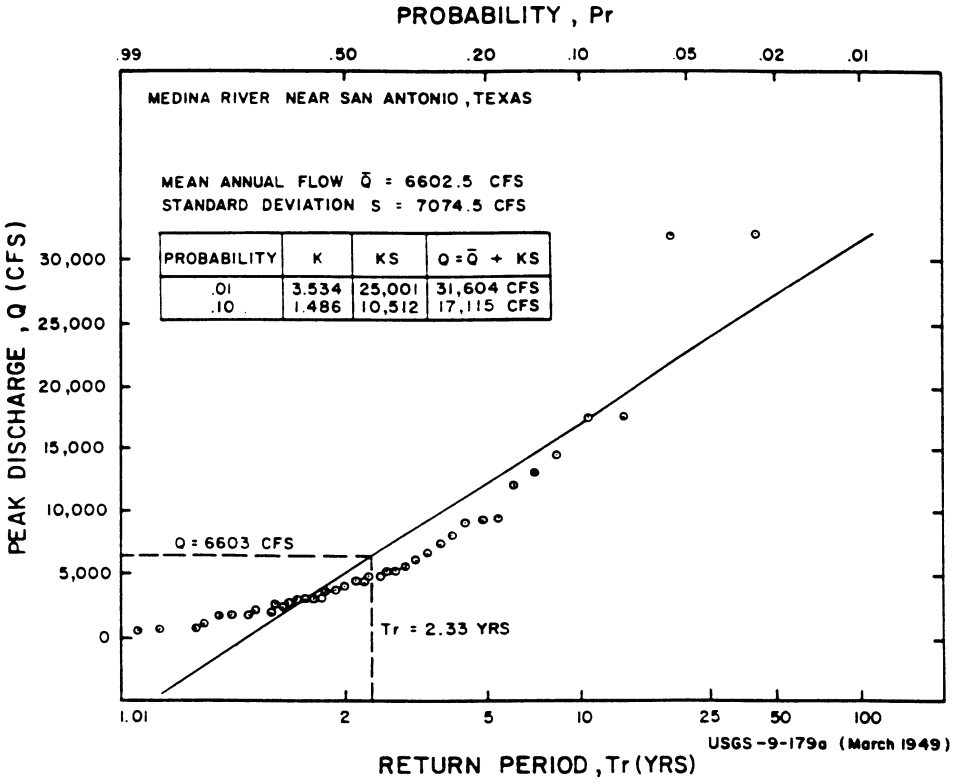

FIGURE 10.2 Gumbel extreme value frequency distribution analysis, Medina River, TX.

10.2.1.3.3 Discharge Comparison of Adjacent Basins

HEC 19, Appendix D [16] contains a list of reports for various states in the United States that have discharges at gauges that have been determined for frequencies from 2-year through 100-year frequencies. The discharges were determined by the Log Pearson III method. The discharge frequency at the gauges should be updated by the engineer using Log Pearson III and the Gumbel extreme value method.

The gauge data can be used directly as equivalent if the drainage areas are about the same (within less than 5%). Otherwise, the discharge determination can be obtained by the formula:

$$Q_u = Q_g (A_u / A_g)^b \tag{10.6}$$

where

Q_u = discharge at ungauged site

Q_g = discharge at gauged site

A_u = area of ungauged site

A_g = area of gauged site

b = exponent of drainage area

10.2.1.3.4 Regional Flood-Frequency Equations

If no gauged site is reasonably nearby, or if the record for the gauge is too short, then the discharge can be computed using the applicable regional flood-frequency equations. Statewide regional regression equations have been established in the United States. These equations permit peak flows to be

estimated for return periods varying between 2 and 100 years. The discharges were determined by the Log Pearson III method. See HEC-19, Appendix D [16] for references to the studies that were conducted for the various states.

10.2.1.3.5 Design Hydrographs

Design hydrographs [9] give a complete time history of the passage of a flood at a particular site. This would include the peak flow. A runoff hydrograph is a plot of the response of a watershed to a particular rainfall event. A unit hydrograph is defined as the direct runoff hydrograph resulting from a rainfall event that lasts for a unit duration of time. The ordinates of the unit hydrograph are such that the volume of direct runoff represented by the area under the hydrograph is equal to 1 in. of runoff from the drainage area. Data on low water discharges and dates should be given as it will control methods and procedures of pier excavation and construction. The low water discharges and dates can be found in the USGS Water Resources Data Reports published each year. One procedure is to review the past 5 or 6 years of records to determine this.

10.2.1.4 Remarks

Before arriving at a final discharge, the existing channel capacity should be checked using the velocity as calculated times the channel waterway area. It may be that a portion of the discharge overflows the banks and never reaches the site.

The proposed design discharge should also be checked to see that it is reasonable and practicable. As a rule of thumb, the unit runoff should be 300 to 600 s-ft per square mile for small basins (to 20 square miles), 100 to 300 s-ft per square mile for median areas (to 50 square miles) and 25 to 150 s-ft for large basins (above 50 square miles). The best results will depend on rational engineering judgment.

10.2.2 Bridge Deck Drainage Design (On-Site Drainage Design)

10.2.2.1 Runoff and Capacity Analysis

The preferred on-site hydrology method is the rational method. The rational method, as discussed in Section 10.2.1.3.1, for on-site hydrology has a minimum time of concentration of 10 min. Many times, the time of concentration for the contributing on-site pavement runoff is less than 10 min. The initial time of concentration can be determined using an *overland flow* method until the runoff is concentrated in a curbed section. Channel flow using the roadway-curb cross section should be used to determine velocity and subsequently the time of flow to the first inlet. The channel flow velocity and flooded width is calculated using Manning's formula:

$$V = \frac{1.486}{n} A R^{2/3} S_f^{1/2} \tag{10.7}$$

where
V = velocity
A = cross-sectional area of flow
R = hydraulic radius
S_f = slope of channel
n = Manning's roughness value [11]

The intercepted flow is subtracted from the initial flow and the bypass is combined with runoff from the subsequent drainage area to determine the placement of the next inlet. The placement of inlets is determined by the allowable flooded width on the roadway.

Oftentimes, bridges are in sump areas, or the lowest spot on the roadway profile. This necessitates the interception of most of the flow before reaching the bridge deck. Two overland flow equations are as follows.

1. **Kinematic Wave Equation:**

$$t_o = \frac{6.92 L^{0.6} n^{0.6}}{i^{0.4} S^{0.3}} \tag{10.8}$$

2. **Overland Equation:**

$$t_o = \frac{3.3(1.1 - C)(L)^{1/2}}{(100\,S)^{1/3}} \tag{10.9}$$

where
t_o = overland flow travel time in minutes
L = length of overland flow path in meters
S = slope of overland flow in meters
n = Manning's roughness coefficient [12]
i = design storm rainfall intensity in mm/h
C = runoff coefficient (Tables 10.1 and 10.2)

10.2.2.2 Select and Size Drainage Facilities

The selection of inlets is based upon the allowable flooded width. The allowable flooded width is usually outside the traveled way. The type of inlet leading up to the bridge deck can vary depending upon the flooded width and the velocity. Grate inlets are very common and, in areas with curbs, curb opening inlets are another alternative. There are various monographs associated with the type of grate and curb opening inlet. These monographs are used to determine interception and therefore the bypass [5].

10.2.3 Stage Hydraulics

High water (HW) stage is a very important item in the control of the bridge design. All available information should be obtained from the field and the Bridge Hydrology Report regarding HW marks, HW on upstream and downstream sides of the existing bridges, high drift profiles, and possible backwater due to existing or proposed construction.

Remember, observed high drift and HW marks are not always what they seem. Drift in trees and brush that could have been bent down by the flow of the water will be extremely higher than the actual conditions. In addition, drift may be pushed up on objects or slopes above actual HW elevation by the velocity of the water or wave action. Painted HW marks on the bridge should be searched carefully. Some flood insurance rate maps and flood insurance study reports may show stages for various discharges. Backwater stages caused by other structures should be included or streams should be noted.

Duration of high stages should be given, along with the base flood stage and HW for the design discharge. It should be calculated for existing and proposed conditions that may restrict the channel producing a higher stage. Elevation and season of low water should be given, as this may control design of tremie seals for foundations and other possible methods of construction. Elevation of overtopping flow and its location should be given. Normally, overtopping occurs at the bridge site, but overtopping may occur at a low sag in the roadway away from the bridge site.

10.2.3.1 Waterway Analysis

When determining the required waterway at the proposed bridge, the engineers must consider all adjacent bridges if these bridges are reasonably close. The waterway section of these bridges should be tied into the stream profile of the proposed structure. Structures that are upstream or downstream of the proposed bridge may have an impact on the water surface profile. When calculating the

effective waterway area, adjustments must be made for the skew and piers and bents. The required waterway should be below the 50-year design HW stage.

If stream velocities, scour, and erosive forces are high, then abutments with wingwall construction may be necessary. Drift will affect the horizontal clearance and the minimum vertical clearance line of the proposed structure. Field surveys should note the size and type of drift found in the channel. Designs based on the 50-year design discharge will require drift clearance. On major streams and rivers, drift clearance of 2 to 5 m above the 50-year discharge is needed. On smaller streams 0.3 to 1 m may be adequate. A formula for calculating freeboard is

$$\text{Freeboard} = 0.1Q^{0.3} + 0.008V^2 \tag{10.10}$$

where
Q = discharge
V = velocity

10.2.3.2 Water Surface Profile Calculation

There are three prominent water surface profile calculation programs available [1,2]. The first one is HEC-2 which takes stream cross sections perpendicular to the flow. WSPRO is similar to HEC-2 with some improvements. SMS is a new program that uses finite-element analysis for its calculations. SMS can utilize digital elevation models to represent the streambeds.

10.2.2.3 Flow Velocity and Distribution

Mean channel, overflow velocities at peak stage, and localized velocity at obstructions such as piers should be calculated or estimated for anticipated high stages. Mean velocities may be calculated from known stream discharges at known channel section areas or known waterway areas of bridge, using the correct high water stage.

Surface water velocities should be measured roughly, by use of floats, during field surveys for sites where the stream is flowing. Stream velocities may be calculated along a uniform section of the channel using Manning's formula Eq. (10.7) if the slope, channel section (area and wetted perimeter), and roughness coefficient (n) are known.

At least three profiles should be obtained, when surveying for the channel slope, if possible. These three slopes are bottom of the channel, the existing water surface, and the HW surface based on drift or HW marks. The top of low bank, if overflow is allowed, should also be obtained. In addition, note some tops of high banks to prove flows fall within the channel. These profiles should be plotted showing existing and proposed bridges or other obstructions in the channel, the change of HW slope due to these obstructions, and possible backwater slopes.

The channel section used in calculating stream velocities should be typical for a relatively long section of uniform channel. Since this theoretical condition is not always available, however, the nearest to uniform conditions should be used with any necessary adjustments made for irregularities.

Velocities may be calculated from PC programs, or calculator programs, if the hydraulic radius, roughness factor, and slope of the channel are known for a section of channel, either natural or artificial, where uniform stream flow conditions exist. The hydraulic radius is the waterway area divided by the wetted perimeter of an average section of the uniform channel. A section under a bridge whose piers, abutments, or approach fills obstruct the uniformity of the channel cannot be used as there will not be uniform flow under the structure. If no part of the bridge structure seriously obstructs or restricts the channel, however, the section at the bridge could be used in the above uniform flow calculations.

The roughness coefficient n for the channel will vary along the length of the channel for various locations and conditions. Various values for n can be found in the References [1,5,12,17].

At the time of a field survey the party chief should estimate the value of n to be used for the channel section under consideration. Experience is required for field determination of a relatively

close to actual *n* value. In general, values for natural streams will vary between 0.030 and 0.070. Consider both low and HW *n* value. The water surface slope should be used in this plot and the slope should be adjusted for obstructions such as bridges, check dams, falls, turbulence, etc.

The results as obtained from this plot may be inaccurate unless considerable thought is given to the various values of slope, hydraulic radius, and *n*. High velocities between 15 and 20 ft/s (4.57) and 6.10 m/s through a bridge opening may be undesirable and may require special design considerations. Velocities over 20/ 6.10 m/s should not be used unless special design features are incorporated or if the stream is mostly confined in rock or an artificial channel.

10.3 Bridge Scour

10.3.1 Bridge Scour Analysis

10.3.1.1 Basic Scour Concepts

Scour is the result of the erosive action of flowing water, excavating and carrying away material from the bed and banks of streams. Determining the magnitude of scour is complicated by the cyclic nature of the scour process. Designers and inspectors need to study site-specific subsurface information carefully in evaluating scour potential at bridges. In this section, we present bridge engineers with the basic procedures and methods to analyze scour at bridges.

Scour should be investigated closely in the field when designing a bridge. The designer usually places the top of footings at or below the total potential scour depth; therefore, determining the depth of scour is very important. The total potential scour at a highway crossing usually comprises the following components [11]: aggradation and degradation, stream contraction scour, local scour, and sometimes with lateral stream migration.

10.3.1.1.1 Long-Term Aggradation and Degradation

When natural or human activities cause streambed elevation changes over a long period of time, aggradation or degradation occurs. Aggradation involves the deposition of material eroded from the channel or watershed upstream of the bridge, whereas degradation involves the lowering or scouring of the streambed due to a deficit in sediment supply from upstream.

Long-term streambed elevation changes may be caused by the changing natural trend of the stream or may be the result of some anthropogenic modification to the stream or watershed. Factors that affect long-term bed elevation changes are dams and reservoirs up- or downstream of the bridge, changes in watershed land use, channelization, cutoffs of meandering river bends, changes in the downstream channel base level, gravel mining from the streambed, diversion of water into or out of the stream, natural lowering of the fluvial system, movement of a bend, bridge location with respect to stream planform, and stream movement in relation to the crossing. Tidal ebb and flood may degrade a coastal stream, whereas littoral drift may cause aggradation. The problem for the bridge engineer is to estimate the long-term bed elevation changes that will occur during the lifetime of the bridge.

10.3.1.1.2 Stream Contraction Scour

Contraction scour usually occurs when the flow area of a stream at flood stage is reduced, either by a natural contraction or an anthropogenic contraction (like a bridge). It can also be caused by the overbank flow which is forced back by structural embankments at the approaches to a bridge. There are some other causes that can lead to a contraction scour at a bridge crossing [11]. The decreased flow area causes an increase in average velocity in the stream and bed shear stress through the contraction reach. This in turn triggers an increase in erosive forces in the contraction. Hence, more bed material is removed from the contracted reach than is transported into the reach. The natural streambed elevation is lowered by this contraction phenomenon until relative equilibrium is reached in the contracted stream reach.

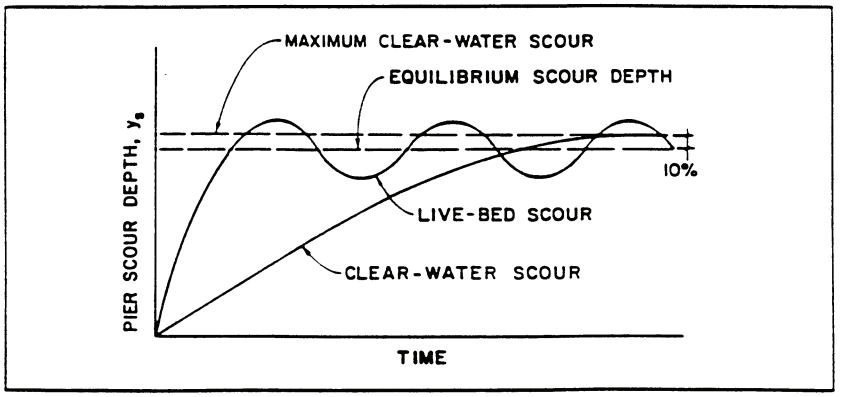

FIGURE 10.3 Illustrative pier scour depth in a sand-bed stream as a function of time.

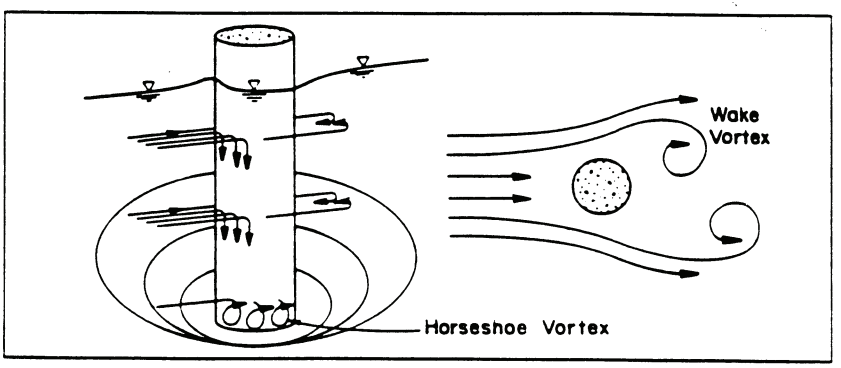

FIGURE 10.4 Schematic representation of local scour at a cylindrical pier.

There are two forms of contraction scour: live-bed and clear-water scours. Live-bed scour occurs when there is sediment being transported into the contracted reach from upstream. In this case, the equilibrium state is reached when the transported bed material out of the scour hole is equal to that transported into the scour hole from upstream. Clear-water scour occurs when the bed sediment transport in the uncontracted approach flow is negligible or the material being transported in the upstream reach is transported through the downstream at less than the capacity of the flow. The equilibrium state of the scour is reached when the average bed shear stress is less than that required for incipient motion of the bed material in this case (Figure 10.3).

10.3.1.1.3 Local Scour

When upstream flow is obstructed by obstruction such as piers, abutments, spurs, and embankments, flow vortices are formed at their base as shown in Figure 10.4 (known as horseshoe vortex). This vortex action removes bed material from around the base of the obstruction. A scour hole eventually develops around the base. Local scour can also be either clear-water or live-bed scour. In considering local scour, a bridge engineer needs to look into the following factors: flow velocity, flow depth, flow attack angle to the obstruction, obstruction width and shape, projected length of the obstruction, bed material characteristics, bed configuration of the stream channel, and also potential ice and debris effects [11, 13].

10.3.1.1.4 Lateral Stream Migration

Streams are dynamic. The lateral migration of the main channel within a floodplain may increase pier scour, embankment or approach road erosion, or change the total scour depth by altering the

flow angle of attack at piers. Lateral stream movements are affected mainly by the geomorphology of the stream, location of the crossing on the stream, flood characteristics, and the characteristics of the bed and bank materials [11,13].

10.3.1.2 Designing Bridges to Resist Scour

It is obvious that all scour problems cannot be covered in this special topic section of bridge scour. A more-detailed study can be found in HEC-18, "Evaluating Scour at Bridges" and HEC-20, "Stream Stability at Highway Structures" [11,18]. As described above, the three most important components of bridge scour are long-term aggradation or degradation, contraction scour, and local scour. The total potential scour is a combination of the three components. To design a bridge to resist scour, a bridge engineer needs to follow the following observation and investigation steps in the design process.

1. **Field Observation** — Main purposes of field observation are as follows:
   - Observe conditions around piers, columns, and abutments (Is the hydraulic skew correct?),
   - Observe scour holes at bends in the stream,
   - Determine streambed material,
   - Estimate depth of scour, and
   - Complete geomorphic factor analysis.

   There is usually no fail-safe method to protect bridges from scour except possibly keeping piers and abutments out of the HW area; however, proper hydraulic bridge design can minimize bridge scour and its potential negative impacts.
2. **Historic Scour Investigation** — Structures that have experienced scour in the past are likely to continue displaying scour problems in the future. The bridges that we are most concerned with include those currently experiencing scour problems and exhibiting a history of local scour problems.
3. **Problem Location Investigation** — Problem locations include "unsteady stream" locations, such as near the confluence of two streams, at the crossing of stream bends, and at alluvial fan deposits.
4. **Problem Stream Investigation** — Problem streams are those that have the following characteristics of aggressive tendencies: indication of active degradation or aggradation; migration of the stream or lateral channel movement; streams with a steep lateral slope and/or high velocity; current, past, or potential in-stream aggregate mining operations; and loss of bank protection in the areas adjacent to the structure.
5. **Design Feature Considerations** — The following features, which increase the susceptibility to local scour, should be considered:
   - Inadequate waterway opening leads to inadequate clearance to pass large drift during heavy runoff.
   - Debris/drift problem: Light drift or debris may cause significant scour problems, moderate drift or debris may cause significant scour but will not create severe lateral forces on the structure, and heavy drift can cause strong lateral forces or impact damage as well as severe scour.
   - Lack of overtopping relief: Water may rise above deck level. This may not cause scour problems but does increase vulnerability to severe damage from impact by heavy drift.
   - Incorrect pier skew: When the bridge pier does not match the channel alignment, it may cause scour at bridge piers and abutments.
6. **Traffic Considerations** — The amount of traffic such as average daily traffic (ADT), type of traffic, the length of detour, the importance of crossings, and availability of other crossings should be taken into consideration.

7. **Potential for Unacceptable Damage** — Potential for collapse during flood, safety of traveling public and neighbors, effect on regional transportation system, and safety of other facilities (other bridges, properties) need to be evaluated.
8. **Susceptibility of Combined Hazard of Scour and Seismic** — The earthquake prioritization list and the scour-critical list are usually combined for bridge design use.

10.3.1.3 Scour Rating

In the engineering practice of the California Department of Transportation, the rating of each structure is based upon the following:

1. **Letter grading** — The letter grade is related to the potential for scour-related problems at this location.
2. **Numerical grading** — The numerical rating associated with each structure is a determination of the severity for the potential scour:

A-1 No problem anticipated
A-2 No problem anticipated/new bridge — no history
A-3 Very remote possibility of problems
B-1 Slight possibility of problems
B-2 Moderate possibility of problems
B-3 Strong possibility of problems
C-1 Some probability of problems
C-2 Moderate probability of problems
C-3 Very strong probability of problems

Scour effect of storms is usually greater than design frequency, say, 500-year frequency. FHWA specifies 500-year frequency as 1.7 times 100-year frequency. Most calculations indicate 500-year frequency is 1.25 to 1.33 times greater than the 100-year frequency [3,8]; the 1.7 multiplier should be a maximum. Consider the amount of scour that would occur at overtopping stages and also pressure flows. Be aware that storms of lesser frequency may cause larger scour stress on the bridge.

10.3.2 Bridge Scour Calculation

All the equations for estimating contraction and local scour are based on laboratory experiments with limited field verification [11]. However, the equations recommended in this section are considered to be the most applicable for estimating scour depths. Designers also need to give different considerations to clear-water scour and live-bed scour at highway crossings and encroachments.

Prior to applying the bridge scour estimating methods, it is necessary to (1) obtain the fixed-bed channel hydraulics, (2) determine the long-term impact of degradation or aggradation on the bed profile, (3) adjust the fixed-bed hydraulics to reflect either degradation or aggradation impact, and (4) compute the bridge hydraulics accordingly.

10.3.2.1 Specific Design Approach

Following are the recommended steps for determining scour depth at bridges:

Step 1: Analyze long-term bed elevation change.
Step 2: Compute the magnitude of contraction scour.
Step 3: Compute the magnitude of local scour at abutments.
Step 4: Compute the magnitude of local scour at piers.
Step 5: Estimate and evaluate the total potential scour depths.

The bridge engineers should evaluate if the individual estimates of contraction and local scour depths from Step 2 to 4 are reasonable and evaluate the total scour derived from Step 5.

10.3.2.2 Detailed Procedures

1. **Analyze Long-Term Bed Elevation Change** — The face of bridge sections showing bed elevation are available in the maintenance bridge books, old preliminary reports, and sometimes in FEMA studies and U.S. Corps of Engineers studies. Use this information to estimate aggradation or degradation.
2. **Compute the Magnitude of Contraction Scour** — It is best to keep the bridge out of the normal channel width. However, if any of the following conditions are present, calculate contraction scour.
   a. Structure over channel in floodplain where the flows are forced through the structure due to bridge approaches
   b. Structure over channel where river width becomes narrow
   c. Relief structure in overbank area with little or no bed material transport
   d. Relief structure in overbank area with bed material transport

   The general equation for determining contraction scour is

$$y_s = y_2 - y_1 \tag{10.11}$$

   where
   y_s = depth of scour
   y_1 = average water depth in the main channel
   y_2 = average water depth in the contracted section

   Other contraction scour formulas are given in the November 1995 HEC-18 publication — also refer to the workbook or HEC-18 for the various conditions listed above [11]. The detailed scour calculation procedures can be referenced from this circular for either live-bed or clear-water contraction scour.
3. **Compute the Magnitude of Local Scour at Abutments** — Again, it is best to keep the abutments out of the main channel flow. Refer to publication HEC-18 from FHWA [13]. The scour formulas in the publication tend to give excessive scour depths.
4. **Compute the Magnitude of Local Scour at Piers** — The pier alignment is the most critical factor in determining scour depth. Piers should align with stream flow. When flow direction changes with stages, cylindrical piers or some variation may be the best alternative. Be cautious, since large-diameter cylindrical piers can cause considerable scour. Pier width and pier nose are also critical elements in causing excessive scour depth.

Assuming a sand bed channel, an acceptable method to determine the maximum possible scour depth for both live-bed and clear-water channel proposed by the Colorado State University [11] is as follows:

$$\frac{y_s}{y_1} = 2.0\,K_1K_2K_3\left(\frac{a}{y_1}\right)^{0.65} F_r^{0.43} l \tag{10.12}$$

where
y_s = scour depth
y_1 = flow depth just upstream of the pier
K_1 = correction for pier shape from Figure 10.5 and Table 10.3
K_2 = correction for angle of attack of flow from Table 10.4
K_3 = correction for bed condition from Table 10.5
a = pier width
l = pier length
F_r = Froude number = $\dfrac{V}{(gy)}$ (just upstream from bridge)

Drift retention should be considered when calculating pier width/type.

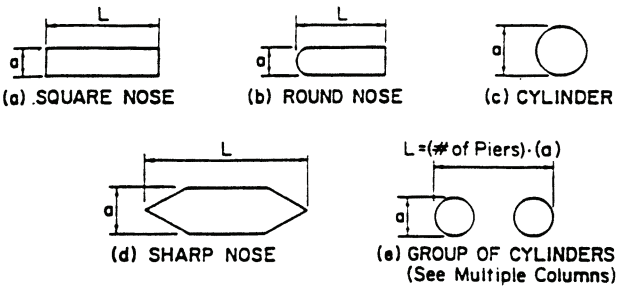

FIGURE 10.5 Common pier shapes.

TABLE 10.3 Correction Factor, K_1, for Pier Nose Shape

Shape of Pier Nose	K_1
Square nose	1.1
Round nose	1.0
Circular cylinder	1.0
Sharp nose	0.9
Group of cylinders	l.0

TABLE 10.4 Correction Factor, K_2, for Flow Angle of Attack

Angle	$L/a = 4$	$L/a = 8$	$L/a = 12$
0	1.0	1.0	1.0
15	1.5	2.0	2.5
30	2.0	2.75	3.5
45	2.3	3.3	4.3
90	2.5	3.9	5

TABLE 10.5 Increase in Equilibrium Pier Scour Depths K_3 for Bed Conditions

Bed Conditions	Dune Height H, ft	K_3
Clear-water scour	N/A	1.1
Plane bed and antidune flow	N/A	1.1
Small dunes	$10 > H > 2$	1.1
Medium dunes	$30 > H > 10$	1.1–1.2
Large dunes	$H > 30$	1.3

10.3.2.3 Estimate and Evaluate Total Potential Scour Depths

Total potential scour depths is usually the sum of long-term bed elevation change (only degradation is usually considered in scour computation), contraction scour, and local scour. Historical scour depths and depths of scourable material are determined by geology. When estimated depths from the above methods are in conflict with geology, the conflict should be resolved by the hydraulic engineer and the geotechnical engineer; based on economics and experience, it is best to provide for maximum anticipated problems.

10.3.3 Bridge Scour Investigation and Prevention

10.3.3.1 Steps to Evaluate Bridge Scour

It is recommended that an interdisciplinary team of hydraulic, geotechnical, and bridge engineers should conduct the evaluation of bridge scour. The following approach is recommended for evaluating the vulnerability of existing bridges to scour [11]:

Step 1. Screen all bridges over waterways into five categories: (1) low risk, (2) scour-susceptible, (3) scour-critical, (4) unknown foundations, or (5) tidal. Bridges that are particularly vulnerable to scour failure should be identified immediately and the associated scour problem addressed. These particularly vulnerable bridges are:

1. Bridges currently experiencing scour or that have a history of scour problems during past floods as identified from maintenance records, experience, and bridge inspection records
2. Bridges over erodible streambeds with design features that make them vulnerable to scour
3. Bridges on aggressive streams and waterways
4. Bridges located on stream reaches with adverse flow characteristics

Step 2. Prioritize the scour-susceptible bridges and bridges with unknown foundations by conducting a preliminary office and field examination of the list of structures compiled in Step 1 using the following factors as a guide:

1. The potential for bridge collapse or for damage to the bridge in the event of a major flood
2. The functional classification of the highway on which the bridge is located
3. The effect of a bridge collapse on the safety of the traveling public and on the operation of the overall transportation system for the area or region

Step 3. Conduct office and field scour evaluations of the bridges on the prioritized list in Step 2 using an interdisciplinary team of hydraulic, geotechnical, and bridge engineers:

1. In the United States, FHWA recommends using 500-year flood or a flow 1.7 times the 100-year flood where the 500-year flood is unknown to estimate scour [3,6]. Then analyze the foundations for vertical and lateral stability for this condition of scour. The maximum scour depths that the existing foundation can withstand are compared with the total scour depth estimated. An engineering assessment must be then made whether the bridge should be classified as a scour-critical bridge.
2. Enter the results of the evaluation study in the inventory in accordance with the instructions in the FHWA "Bridge Recording and Coding Guide" [7].

Step 4. For bridges identified as scour critical from the office and field review in Steps 2 and 3, determine a plan of action for correcting the scour problem (see Section 10.3.3.3).

10.3.3.2 Introduction to Bridge Scour Inspection

The bridge scour inspection is one of the most important parts of preventing bridge scour from endangering bridges. Two main objectives to be accomplished in inspecting bridges for scour are:

1. To record the present condition of the bridge and the stream accurately; and
2. To identify conditions that are indicative of potential problems with scour and stream stability for further review and evaluation by other experts.

In this section, the bridge inspection practice recommended by U.S. FHWA [6,10] is presented for engineers to follow as guidance.

10.3.3.2.1 Office Review

It is highly recommended that an office review of bridge plans and previous inspection reports be conducted prior to making the bridge inspection. Information obtained from the office review

provides a better foundation for inspecting the bridge and the stream. The following questions should be answered in the office review:

- Has an engineering scour evaluation been conducted? If so, is the bridge scour critical?
- If the bridge is scour-critical, has a plan of action been made for monitoring the bridge and/or installing scour prevention measures?
- What do comparisons of stream-bed cross sections taken during successive inspections reveal about the stream bed? Is it stable? Degrading? Aggrading? Moving laterally? Are there scour holes around piers and abutments?
- What equipment is needed to obtain stream-bed cross sections?
- Are there sketches and aerial photographs to indicate the planform locations of the stream and whether the main channel is changing direction at the bridge?
- What type of bridge foundation was constructed? Do the foundations appear to be vulnerable to scour?
- Do special conditions exist requiring particular methods and equipment for underwater inspections?
- Are there special items that should be looked at including damaged riprap, stream channel at adverse angle of flow, problems with debris, etc.?

10.3.3.2.2 Bridge Scour Inspection Guidance

The condition of the bridge waterway opening, substructure, channel protection, and scour prevention measures should be evaluated along with the condition of the stream during the bridge inspection. The following approaches are presented for inspecting and evaluating the present condition of the bridge foundation for scour and the overall scour potential at the bridge.

Substructure is the key item for rating the bridge foundations for vulnerability to scour damage. Both existing and potential problems with scour should be reported so that an interdisciplinary team can make a scour evaluation when a bridge inspection finds that a scour problem has already occurred. If the bridge is determined to be scour critical, the rating of the substructures should be evaluated to ensure that existing scour problems have been considered. The following items should be considered in inspecting the present condition of bridge foundations:

- Evidence of movement of piers and abutments such as rotational movement and settlement;
- Damage to scour countermeasures protecting the foundations such as riprap, guide banks, sheet piling, sills, etc.;
- Changes in streambed elevation at foundations, such as undermining of footings, exposure of piles; and
- Changes in streambed cross section at the bridge, including location and depth of scour holes.

In order to evaluate the conditions of the foundations, the inspectors should take cross sections of the stream and measure scour holes at piers and abutments. If equipment or conditions do not permit measurement of the stream bottom, it should be noted for further investigation.

To take and plot measurement of stream bottom elevations in relation to the bridge foundations is considered the single most important aspect of inspecting the bridge for actual or potential damage from scour. When the stream bottom cannot be accurately measured by conventional means, there are other special measures that need to be taken to determine the condition of the substructures or foundations such as using divers and using electronic scour detection equipment. For the purposes of evaluating resistance to scour of the substructures, the questions remain essentially the same for foundations in deep water as for foundations in shallow water [7] as follows:

- How does the stream cross section look at the bridge?

- Have there been any changes as compared with previous cross section measurements? If so, does this indicate that (1) the stream is aggrading or degrading or (2) is local or contraction scour occurring around piers and abutments?
- What are the shapes and depths of scour holes?
- Is the foundation footing, pile cap, or the piling exposed to the stream flow, and, if so, what is the extent and probable consequences of this condition?
- Has riprap around a pier been moved or removed?

Any condition that a bridge inspector considers to be an emergency or of a potentially hazardous nature should be reported immediately. This information as well as other conditions, which do not pose an immediate hazard but still warrant further investigation, should be conveyed to the interdisciplinary team for further review.

10.3.3.3 Introduction to Bridge Scour Prevention

Scour prevention measures are generally incorporated after the initial construction of a bridge to make it less vulnerable to damage or failure from scour. A plan of preventive action usually has three major components [11]:

1. Timely installation of temporary scour prevention measures;
2. Development and implementation of a monitoring program;
3. A schedule for timely design and construction of permanent scour prevention measures.

For new bridges [11], the following is a summary of the best solutions for minimizing scour damage:

1. Locating the bridge to avoid adverse flood flow patterns;
2. Streamlining bridge elements to minimize obstructions to the flow;
3. Designing foundations safe from scour;
4. Founding bridge pier foundations sufficiently deep to not require riprap or other prevention measures; and
5. Founding abutment foundations above the estimated local scour depth when the abutment is protected by well-designed riprap or other suitable measures.

For existing bridges, the available scour prevention alternatives are summarized as follows:

1. Monitoring scour depths and closing the bridge if excessive bridge scour exists;
2. Providing riprap at piers and/or abutments and monitoring the scour conditions;
3. Constructing guide banks or spur dikes;
4. Constructing channel improvements;
5. Strengthening the bridge foundations;
6. Constructing sills or drop structures; and
7. Constructing relief bridges or lengthening existing bridges.

These scour prevention measures should be evaluated using sound hydraulic engineering practice. For detailed bridge scour prevention measures and types of prevention measures, refer to "Evaluating Scour at Bridges" from FHWA. [10,11,18,19]

References

1. AASHTO, *Model Drainage Manual,* American Association of State Highway and Transportation Officials, Washington, D.C., 1991.
2. AASHTO, *Highway Drainage Guidelines,* American Association of State Highway and Transportation Officials, Washington, D.C., 1992.
3. California State Department of Transportation, *Bridge Hydraulics Guidelines,* Caltrans, Sacramento.

4. California State Department of Transportation, *Highway Design Manual,* Caltrans, Sacramento.
5. Kings, *Handbook of Hydraulics,* Chapter 7 (*n* factors).
6. U.S. Department of the Interior, Geological Survey (USGS), Magnitude and Frequency of Floods in California, Water-Resources Investigation 77–21.
7. U.S. Department of Transportation, Recording and Coding Guide for the Structure Inventory and Appraisal of the Nation's Bridges, FHWA, Washington D.C., 1988.
8. U.S. Geological Survey, Bulletin No. 17B, Guidelines for Determining Flood Flow Frequency.
9. U.S. Federal Highway Administration, Debris-Control Structures, Hydraulic Engineering Circular No. 9, 1971.
10. U.S. Federal Highway Administration, Design of Riprap Revetments, Hydraulic Engineering Circular No. 11, 1989.
11. U.S. Federal Highway Administration, Evaluating Scour at Bridges, Hydraulic Engineering Circular No. 18, Nov. 1995.
12. U.S. Federal Highway Administration, Guide for Selecting Manning's Roughness Coefficient (*n* factors) for Natural Channels and Flood Plains, Implementation Report, 1984.
13. U.S. Federal Highway Administration, Highways in the River Environment, Hydraulic and Environmental Design Considerations, Training & Design Manual, May 1975.
14. U.S. Federal Highway Administration, Hydraulics in the River Environment, Spur Dikes, Sect. VI-13, May 1975.
15. U.S. Federal Highway Administration, Hydraulics of Bridge Waterways, Highway Design Series No. 1, 1978.
16. U.S. Federal Highway Administration, Hydrology, Hydraulic Engineering Circular No. 19, 1984.
17. U.S. Federal Highway Administration, Local Design Storm, Vol. I–IV (*n* factor) by Yen and Chow.
18. U.S. Federal Highway Administration, Stream Stability at Highway Structures, Hydraulic Engineering Circular No. 20, Nov. 1990.
19. U.S. Federal Highway Administration, Use of Riprap for Bank Protection, Implementation Report, 1986.